

Institut für Bodenökologie
GSF – Forschungszentrum für Umwelt und Gesundheit

**Environmental fate of the herbicide glyphosate
in the soil-plant system:
Monitoring and modelling using large-scale weighing lysimeters**

Christine Klier

Vollständiger Abdruck der von der Fakultät Wissenschaftszentrum Weihenstephan für Ernährung, Landnutzung und Umwelt der Technischen Universität München zur Erlangung des akademischen Grades eines

Doktors der Naturwissenschaften (Dr. rer. nat.)

genehmigten Dissertation.

Vorsitzender: Univ.-Prof. Dr. K.-J. Hülsbergen
Prüfer der Dissertation: 1. Univ.-Prof. Dr. Dr. J.C. Munch
2. Univ.-Prof. Dr. O. Richter,
Technische Universität Braunschweig
3. Univ.-Prof. Dr. M. Matthies,
Universität Osnabrück

Die Dissertation wurde am 5. Dezember 2006 bei der Technischen Universität München eingereicht und durch die Fakultät Wissenschaftszentrum Weihenstephan für Ernährung, Landnutzung und Umwelt am 30. Juli 2007 angenommen.

Acknowledgements

In particular I thank Prof. Dr. Jean Charles Munch, Institute of Soil Ecology, GSF-National Research Centre for Environment and Health, Neuherberg, for giving me the opportunity to work on the research project, for the excellent research facilities, his support and moreover for his valuable suggestions and critical comments.

Furthermore, I declaim my special thanks to Prof. Dr. Otto Richter, Institute of Geocology, Technical University Braunschweig, for his interest to review the work as the co-examiner and the most valuable guidance by his book “Environmental fate modelling of pesticides”.

I also thank Prof. Dr. Michael Matthies, Institute of Environmental Systems Research, University Osnabrück for his willingness to be co-examiner and Prof. Dr. Kurt-Jürgen Hülsbergen, Department of Plant Sciences, Centre of Life and Food Sciences, Weihenstephan, for accepting the position as chairman of the examination board.

Particularly, I want to express my gratitude to my supervisor, Dr. Eckart Priesack, Institute of Soil Ecology, GSF, for his constant advice and valuable guidance on all aspects of my work, his confidence and his support.

Moreover, many friends, colleagues and external collaborators helped to promote and realize my ideas and often introduced new aspects in my work.

I express my gratitude to Dr. Sebastian Gayler for his excellent support with *Expert-N*, his constructive criticism and creative suggestions and his steady encouragement.

Furthermore, I thank Dr. Sabine Grundmann and Dr. Reiner Schroll for the access to their extensive data set from the field lysimeter study prior to publication.

For technical and experimental support I thank Willibald Stichler (tracer and precipitation measurements), Dr. Bernhard Ruth (capacitance water content measurements), Oliver Gefke and Dr. Sascha Reth (lysimeter facility), Dr. Babro Winkler (LAI measurements) and Heinz Lösslein (Meteorological Institute, University of Munich; climate data). Dr. Tobias Wagner, Heidrun Karl and other collaborators in the project I thank for their friendship, cooperation and help. I also thank my room mate Xiaohong Duan and Walkiria Levy for the interesting scientific discussions but also on being good friends.

Most importantly my family deserves my deepest gratitude for providing unconditional support whenever I needed them and finally, I thank my husband Mathias.

Table of Contents

List of Figures	V
List of Tables	XI
Abbreviations	XV
1 Introduction	1
1.1 Genetically modified crops in modern agriculture	2
1.1.1 The glyphosate resistant soybean system	3
1.1.2 Risk assessment research for glyphosate resistant soybean	4
1.2 Aim and structure of the work.....	4
2 Degradation and sorption experiments with the herbicide glyphosate under controlled laboratory conditions	7
2.1 Introduction.....	7
2.2 Materials and Methods	8
2.2.1 Soils	8
2.2.2 Chemicals	9
2.2.3 Biodegradation experiments	10
2.2.4 Microbial biomass measurement	11
2.2.5 Batch adsorption-desorption studies	12
2.3 Results and Discussion	13
2.3.1 Microbial biomass and biodegradation of glyphosate in batch experiments	13
2.3.2 Sorption and desorption of glyphosate in batch experiments	19
2.3.3 Mass balance	22
2.4 Conclusions	23
3 Water flow and assessment of water balance on four undisturbed field soil lysimeters	25
3.1 Introduction.....	25
3.2 Materials and Methods	26
3.2.1 The dataset	26
3.2.1.1 GSF-lysimeter facility	26
3.2.1.2 Soil properties and planting	28
3.2.1.3 Methods to obtain water storage changes	29
3.2.2 Water transport models.....	30
3.2.2.1 Model configuration	30
3.2.2.2 Water retention and hydraulic conductivity functions	30
3.2.2.3 Models of potential and actual evapotranspiration	33

3.2.2.4	Statistical analysis	36
3.3	Results and Discussion	37
3.3.1	Direct and indirect evaluation of evapotranspiration	37
3.3.2	Percolation and water flow simulations	39
3.3.2.1	Soil hydraulic properties	39
3.3.2.2	Detailed analysis of infiltration and drying cycles	42
3.3.2.3	Evapotranspiration for the year 2001.....	45
3.3.2.3.1	Sandy and loamy soil type	45
3.3.2.3.2	Transferability to other soils	47
3.3.2.4	Evapotranspiration for the years 1999 to 2003.....	50
3.3.3	Direct evaluation of daily evapotranspiration fluxes in the year 2004	53
3.4	Conclusions	55
4	Environmental fate of the herbicide glyphosate in the presence of genetically modified soybean	57
4.1	Introduction.....	57
4.2	Materials and Methods	61
4.2.1	The dataset	61
4.2.1.1	Pesticide degradation and plant uptake monitoring.....	61
4.2.1.2	Measurement of plant growth parameters	62
4.2.1.3	Soil properties.....	62
4.2.1.4	Tracer experiment and ¹⁴ C-radioactivity in the leachate.....	63
4.2.2	Solute transport model	64
4.2.2.1	Model configuration and modelling strategy	64
4.2.2.2	Governing equations.....	65
4.2.2.3	Sorption processes ϕ_{sorb}	70
4.2.2.4	Surface volatilisation ϕ_v	71
4.2.2.5	Microbial degradation ϕ_{deg}	72
4.2.2.6	Plant uptake of pesticides ϕ_{plant}	76
4.2.2.7	Statistical analysis	81
4.3	Results and Discussion	82
4.3.1	Model calibration and model input parameters	82
4.3.1.1	Calibration of degradation parameters with laboratory results	83
4.3.1.1.1	First-order degradation including humidity and temperature dependencies.....	83
4.3.1.1.2	Parameter estimation problems in Monod degradation characteristics.....	87
4.3.1.2	Water flow and soil hydraulic properties	94
4.3.1.3	Determination of the dispersivity coefficient	101

4.3.2	Model choice by comparison of deterministic modelling approaches	103
4.3.2.1	Microbial degradation of glyphosate in the field lysimeters	103
4.3.2.1.1	First-order degradation influenced by water flow simulations	103
4.3.2.1.2	Microbial growth kinetics and microbial communities	108
4.3.2.2	Adsorption of glyphosate to soil matrix.....	114
4.3.2.3	Movement and leaching of glyphosate in the lysimeters.....	117
4.3.3	Modelling approach considering probability distribution of substrate availability, sorption and dispersivity.....	121
4.3.4	Uptake and translocation of glyphosate in transgene soybeans.....	128
4.4	Conclusions.....	136
5	Technical note: Solute transport model implementation in <i>Expert-N</i>	141
5.1	Introduction to <i>Expert-N</i>	141
5.2	Description of the DLL system components.....	142
5.3	Process functions and calling order	142
5.4	Function parameters and C-data structures.....	144
5.5	Input/Output files	145
6	Conclusions.....	147
7	Summary.....	151
	References	155
	Appendix A – List of Symbols.....	167
	Appendix B – List of Variables.....	173
	Appendix C – Pesticide input file.....	179
	Appendix D – Input file for variable selection.....	183
	Appendix E – Pesticide output file.....	185

List of Figures

Fig. 1.1:	Adoption of GM soybean 1997 to 2006 in the USA (2006 forecasted, National Agricultural Statistics Service, 2006).....	3
Fig. 1.2:	Mathematical modelling of water flow and solute transport in the soil-plant-atmosphere system.....	5
Fig. 2.1:	Glyphosate mineralization in the five soils through the 41 days incubation period at a water content of 60 % of max. WHC.....	13
Fig. 2.2:	Glyphosate mineralization in LM 3 and LM 5 through the 41 days incubation period at a water content of 60 % of max. WHC (treatments: (4+1) = 4 times non-labelled + 1 time labelled glyphosate application and controls).	14
Fig. 2.3:	Glyphosate mineralization in LM 2 and LM 5 through the 41 days incubation period at a water content of 60 % of max. WHC (treatments: inoculation with 5 % of soil of LM 3 and controls).....	15
Fig. 2.4:	Glyphosate mineralization in LM 5 in dependence of soil water content in % of max. WHC.	16
Fig. 2.5:	Scatter plot of microbial biomass and cumulative evolved $^{14}\text{CO}_2$ from ^{14}C -glyphosate in the biodegradation experiment (grey symbol LM 2, not included in the regression equation).....	18
Fig. 2.6:	Microbial biomass in the control soils (not treated with glyphosate) and in the soils after repeated application of non-labelled glyphosate.....	18
Fig. 2.7:	Glyphosate mineralization in the upper soil horizon of LM 5 in the sorption kinetic experiment (soil to solution ratio 1:5).	20
Fig. 2.8:	Freundlich sorption isotherm for glyphosate in the upper soil horizon of LM 5. .	21
Fig. 2.9:	Desorption of glyphosate from the soil material of the upper soil horizon of LM 5.	21
Fig. 3.1:	Sensor positions of tensiometer and TDR probes in the lysimeters.	26
Fig. 3.2:	An example of data from measurements of TDR-sensors and tensiometers, graphical displayed by <i>LysiVisu</i>	28
Fig. 3.3:	Changes in lysimeter weight ΔW (kg) of LM 1 in the year 2001 and 2004 in hourly resolution.....	37
Fig. 3.4:	Water retention curves estimated and measured for LM 1 and LM 2 in the year 2001; closed symbols: period of bare soil; open symbols: vegetation period ; solid line: simulated with ptf Scheinost; dotted line: simulated with ptf Campbell.....	40
Fig. 3.5:	Water content (a) measured (symbols; TDR, daily values) and simulated (lines) and percolation amounts (b) measured (symbols; daily values) and simulated (lines) for LM 2 in 2001; soil hydraulic characteristics are calculated by	

	approaches of Brutsaert-Gardner (thick lines) and Hutson & Cass-Burdine (thin lines) (ET_p by PM grass).	41
Fig. 3.6:	Water content simulated in 30 cm depth with ET_p calculated by PM grass (dotted line) and Haude (mrH; solid line) and measured (symbols) lysimeter weight (LM 1, 2001).	43
Fig. 3.7:	Water content simulated in 30 cm depth with ET_p calculated by PM grass (dotted line) and Haude (mrH; solid line) and measured (symbols) lysimeter weight (LM 2, 2001).	43
Fig. 3.8:	Daily percolation amounts measured (symbols) and simulated with ET_p calculated by a) PM grass b) PM crop and c) Haude (mrH) approach (LM 1, 2001; hydraulic characteristics by Brutsaert-Gardner).	46
Fig. 3.9:	Weekly percolation amounts measured (with standard deviation; symbols) and simulated (line) with ET_p calculated by Haude (mrH); weekly measurements were available for three replications of the soil type of a) LM 1 and b) LM 2 in the year 2001 (hydraulic characteristics by Brutsaert-Gardner).	48
Fig. 3.10:	Daily percolation amounts measured (symbols) and simulated (line) in the years 1999 to 2003 for LM 2 (ET_p by Haude (mrH); hydraulic characteristics by Brutsaert-Gardner).	52
Fig. 3.11:	Daily actual evapotranspiration measured (symbols) and simulated (solid line: ET_p by PM grass; dashed line: ET_p by Haude (mrH); hydraulic characteristics by Brutsaert-Gardner; LM 1, 2004).	53
Fig. 4.1:	The uncertainty iceberg. Although uncertainty in pesticide fate modelling has been ignored in the past (a), there have been a number of attempts to quantify uncertainty over the last 10 years (b). The challenge is now to ascertain whether the uncertainty, which is accounted for, represents a large (c) or small (d) proportion of the overall uncertainty in pesticide fate modelling (Dubus et al., 2003).	59
Fig. 4.2:	Definition of nodes in the original LEACHP version compared to HYDRUS and water flux direction (arrows: water fluxes; red-black points: specific nodal concentrations; red point: nodal concentration $(C_l)_i^{j+1/2}$; $i = 1, \dots, k$ soil layer; $j = t_0, \dots, t_e$ simulation time, β see Eq. (4.10)).	67
Fig. 4.3:	Schematic representation of biodegradation capacities.	72
Fig. 4.4:	Schematic representation of the pesticide degradation pathway.....	73
Fig. 4.5:	Schematic representation of pesticide uptake by plants; the open arrows represent the so far not included diffusive exchange between air and plant leaves.	76
Fig. 4.6:	Concentration of glyphosate in the liquid phase in the batch degradation study at a water content of 40 % of max. WHC (LM 5; part a) symbols: measurement, line: fitted model simulation with $k_{mic} = 2.31 \text{ d}^{-1}$ and part b) sensitivity analysis for k_{mic} with $2.31 \text{ d}^{-1} \pm 100 \%$ with step size 0.4 d^{-1}).	84

Fig. 4.7:	Humidity response functions for k_{mic} (symbols: measurements, line: part a) Gauss type function with $\theta_{crit} = 0.12 \text{ m}^3 \text{ m}^{-3}$, $b_w = 1.71$, $k_{max} = 2.31 \text{ d}^{-1}$ and part b) Weibull type function $\theta_{crit1} = 0.055 \text{ m}^3 \text{ m}^{-3}$, $\theta_{crit2} = 0.23 \text{ m}^3 \text{ m}^{-3}$, $b1 = 3$ and $b2 = 15$).....	85
Fig. 4.8:	Liquid concentration of glyphosate in the batch degradation studies at water contents of 10, 20, 30 and 40 % of max. WHC (symbols: measurements at 10 (diamonds), 20 (stars), 30 (squares) and 40 (triangles) % of max. WHC; line: model simulation with humidity response according to a) Gauss type and b) Weibull type function; LM 5).....	86
Fig. 4.9:	k_{mic} in dependence of temperature (part a: O'Neill function with $T_{opt} = 23 \text{ }^\circ\text{C}$, $T_{max} = 50 \text{ }^\circ\text{C}$, $x = 8$) and of the combination of humidity and temperature (part b: Weibull type (parameters as in Fig. 4.8 b) and O'Neill function).....	86
Fig. 4.10:	Matrix scatter plot of μ (range 1-10 d^{-1} , step size 1 d^{-1}), C_{MBmax} (range 3-30 mg-C dm^{-3} , step size 3 mg-C dm^{-3}) and resulting C_l concentration at 1, 4, 8 and 15 days after application date; graphics predetermined in <i>Mathematica</i> ®.	89
Fig. 4.11:	Matrix scatter plot of μ (range 1-10 d^{-1} , step size 1 d^{-1}), σ (range 1-10 d^{-1} , step size 1 d^{-1}) and resulting C_l concentration at 1 and 15 days after application date; graphics predetermined in <i>Mathematica</i> ®.	90
Fig. 4.12:	Matrix scatter plot of γ (range 0.1-1.0 $\text{mg-C mg}^{-1}\text{-C}_{\text{substrate}}$, step size 0.1 mg mg^{-1}), K_M (range 0.4-3.6 mg dm^{-3} , step size 0.4 mg dm^{-3}) and resulting C_l concentration at 1 and 15 days after application date; graphics predetermined in <i>Mathematica</i> ®.	90
Fig. 4.13:	Degradation of glyphosate in soil solution by a specialized microbial community in the batch degradation study at a water content of 40 % of max. WHC (part a: symbols – measurement, line – fitted model simulation; part b: simulated microbial biomass concentration; $r^2 = 0.966$).....	91
Fig. 4.14:	Degradation of glyphosate in soil solution by total microbial community in the batch degradation study at a water content of 40 % of WHC (part a: symbols – measurement, line – fitted model simulation; part b: simulated microbial biomass concentration; $r^2 = 0.940$).	93
Fig. 4.15:	Water retention curve measured (symbols) and fitted (line) for LM 5.2 in the year 2004 ($\theta_{sat} = 0.25 \text{ m}^3 \text{ m}^{-3}$, $\theta_{res} = 0.0 \text{ m}^3 \text{ m}^{-3}$, fitted van Genuchten parameters: $\alpha = 0.004$, $n = 1.404$).....	94
Fig. 4.16:	Percolation amounts (line with symbols) and lysimeter weight measurements (line) for LM 5.2 (black) and LM 5.3 (red) in the year 2004.	95
Fig. 4.17:	Measured daily ET_a amounts for LM 5.2 and LM 5.3 in the year 2004.....	96
Fig. 4.18:	Scatter plot of measured daily ET_a amounts for LM 5.2 and LM 5.3 in the year 2004.	96
Fig. 4.19:	Scatter plot of modelled and measured daily ET_a amounts for the year 2004.....	97

Fig. 4.20:	Weekly percolation amounts measured (symbols, LM 5.1 to LM 5.4) and simulated with ET_p calculated by Haude (mrH) approach and hydraulic characteristics by Hutson & Cass-Burdine and van Genuchten-Mualem for the period 2003 to 2005.	98
Fig. 4.21:	Water content measured (symbols) and simulated (lines) at 30 cm depth in the year 2004 to 2005 (ET_p calculated by Haude (mrH) approach).....	99
Fig. 4.22:	Water content measured (line with symbols) and simulated (lines) at 1 cm and 5 cm depth in the year 2005 (ET_p calculated by Haude (mrH) approach).....	100
Fig. 4.23:	Deuterium (LM 5.2 and 5.3) and radioactivity (LM 5.1 and 5.4) loads in the weekly leachate from July 2004 to the end of 2005.....	101
Fig. 4.24:	Fitted deuterium breakthrough curve by the inverse analytical solution.	102
Fig. 4.25:	Cumulative degradation curve measured (symbols, bars denote standard deviation between soil chambers) and simulated (dashed line: Hutson & Cass-Burdine, solid line: van Genuchten-Mualem parameterisation, red lines: response surface Gauss type, black lines: response surface Weibull type) in the years a) 2004 and b) 2005 ($k_{mic} = 2.31 \text{ d}^{-1}$).	105
Fig. 4.26:	Measured (symbols; bars denote standard deviation) and simulated (lines) degradation rates obtained by using the environmental response surface of the Weibull type and two different hydraulic parameterisations for the years a) 2004 and b) 2005; grey bars document rain events ($k_{mic} = 2.31 \text{ d}^{-1}$).	106
Fig. 4.27:	Water content measured (humidity capacitance sensor; dashed line with symbols) and simulated (line) at 1 cm depth in the year 2005 (ET_p calculated by Haude (mrH) approach).....	107
Fig. 4.28:	Measurement (symbols; bars denote standard deviation) and simulation of cumulative amounts of degraded pesticide (black line) and simulated biomass concentration of specialized microbes (red line) ($C_{MB}(t_0) = C_{MBmin} = 0.15 \text{ mg-C dm}^{-3}$, $C_{MBmax} = 15.0 \text{ mg-C dm}^{-3}$, $\mu_{max} = 4.76 \text{ d}^{-1}$, $\sigma = 4.11 \text{ d}^{-1}$, $\gamma = 0.2$, $K_m = 1.80 \text{ mg dm}^{-3}$).	110
Fig. 4.29:	Simulation of concentration of total microbial biomass (a) and of cumulative amounts of degraded pesticide (b) ($C_{MB}(t_0) = C_{MBmin} = 303 \text{ mg-C dm}^{-3}$, $C_{MBmax} = 3030 \text{ mg-C dm}^{-3}$, $\sigma = 0.080 \text{ d}^{-1}$, $\gamma = 0.23$, $K_m = 1.87 \text{ mg dm}^{-3}$).	111
Fig. 4.30:	Simulations of concentration of total microbial biomass and CO_2 emission from soil.	112
Fig. 4.31:	Measurement (symbols, bars denote standard deviation) and simulation of cumulative amounts of degraded pesticide (black lines) and biomass concentration of total microbial biomass (red lines) ($C_{MB}(t_0) = C_{MBmin} = 303 \text{ mg-C dm}^{-3}$, $C_{MBmax} = 3030 \text{ mg-C dm}^{-3}$, $\mu_{max} = 0.207 \text{ d}^{-1}$, $\sigma = 0.080 \text{ d}^{-1}$, $\gamma = 0.23$, $K_m = 1.87 \text{ mg dm}^{-3}$ and $C_{org} = 145.50$ or $43.65 \text{ mg-C dm}^{-3}$).	113
Fig. 4.32:	Simulated profiles of glyphosate movement with linear equilibrium (black solid lines) and non-linear equilibrium (red solid lines) approach and two-site kinetic sorption model (black dashed lines) at 4, 14 and 60 days after application.....	115

Fig. 4.33: Simulated profiles of glyphosate movement with two different parameterisations of the hydraulic characteristics and two different dispersivities (Hutson & Cass-Burdine (red lines) and van Genuchten-Mualem (black lines); λ_{50} solid lines, λ_{10} dashed lines) at 4, 14 and 60 days after application. 118

Fig. 4.34: Weekly measured ^{14}C -radioactivity amounts and simulated glyphosate leaching. 119

Fig. 4.35: Simulation of cumulative amounts of degraded pesticide following variation ($N = 25$) of pesticide input parameters K_d , available carbon substrate and dispersivity (top line: maximum, bottom line: minimum, black line and grey bars: mean of 25 simulation runs with standard deviation, red line: reference run with average parameters). 122

Fig. 4.36: Simulation of concentration of total microbial biomass following variation ($N = 25$) of pesticide input parameters K_d , available carbon substrate and dispersivity (top line: maximum, bottom line: minimum, black line and grey bars: mean of 25 simulation runs with standard deviation, red line: reference run with average parameters). 122

Fig. 4.37: Box-and-whisker plots for cumulative amounts of degradation and leachate amounts at the end of the simulation period 2003-2005 and maximum microbial biomass (day 572) for variation ($N = 25$) of pesticide input parameters (dashed lines: median, “whiskers” lines: full data, boxes: values between 25th and 75th percentile). 123

Fig. 4.38: Box-and-whisker plots for glyphosate movement in 2 cm depth at 4, 14 and 60 days after application in 2004 for variation ($N = 25$) of pesticide input parameters (dashed lines: median, “whiskers” lines: full data, boxes: values between 25th and 75th percentile). 124

Fig. 4.39: Measured profile (grey bars) of glyphosate movement and model simulation following variation ($N = 25$) of pesticide input parameters K_d , available carbon substrate, and dispersivity (dashed lines: maximum and minimum, black line with bars: mean of 25 simulation runs with standard deviation) in 2004. Note the different amount scale from day 29. 125

Fig. 4.40: Measured profile (grey bars) of glyphosate movement and model simulation following variation ($N = 25$) of pesticide input parameters K_d , available carbon substrate and dispersivity (dashed lines: maximum and minimum, black line with bars: mean of 25 simulation runs with standard deviation) in 2005. Note the different amount scale from day 57. 126

Fig. 4.41: Soybean biomass and glyphosate concentrations simulated and measured in respective plant tissues in the growing seasons 2004 and 2005 on lysimeters (for the year 2004 glyphosate was only measured in a mixed sample of leaf and stem material denoted as ‘above concentration’). 129

Fig. 4.42: Glyphosate concentration in plant tissues (above = leaf and stem) measurement in 2004 and simulation with different application scenarios (see Table 4.19). 132

Fig. 4.43: Simulated soil cover factor (a) and above ground biomass (b) in dependence of LAI at 4, 7, 8 and 11 weeks after sowing in 2004. 132

Fig. 4.44: Simulated plant biomass (a) and simulated glyphosate concentration in above ground biomass (plant) and beans and maximum residue level (MRL) (b) of glyphosate in GR beans with different permeances ($P_l =$ a) $2.10 \cdot 10^{-6}$ b) $1.01 \cdot 10^{-5}$ c) $2.1 \cdot 10^{-5} \text{ m d}^{-1}$) in the year 2003.....	135
Fig. 5.1: The modular modelling system <i>Expert-N</i>	141
Fig. 5.2: Calling order of functions in the main program source code.....	143
Fig. 5.3: Organisation of the superordinate data structure PXENO of the solute transport module.....	144

List of Tables

Table 2.1: Soil properties of the first soil horizon of lysimeter monoliths (LM 1 – LM 4) and soil cores (LM 5.1 to 5.4)	9
Table 2.2: Glyphosate biodegradation experiments in soils of LM 1 - 5	11
Table 2.3: Glyphosate mineralization after 41 days in LM 2 and LM 5 in control experiment and after inoculation with soil of LM 5	15
Table 2.4: Basal microbial activity and microbial biomass with standard deviations (Std) for soils of LM 1 to LM 5	17
Table 2.5: Statistical results for the ANOVA test between control (not treated with glyphosate) and repeated herbicide treatments concerning biomass contents.....	19
Table 2.6: Adsorption in percentage of applied amount and adsorption coefficients of glyphosate to soil matrix measured by the OECD laboratory batch sorption procedure for the upper soil horizon of LM 5 taking into consideration microbial degradation	19
Table 2.7: Glyphosate mineralization and volatilization, formation of extractable and non extractable residues and mass balance in the biodegradation experiments in percent of applied ¹⁴ C	22
Table 3.1: Soil properties and hydraulic characteristics for soil monoliths in LM 1 – LM 4	29
Table 3.2: Crop growth stages and differentiation categories	34
Table 3.3: Difference (Δ , mm) between simulated and measured percolation (DR), cumulative evapotranspiration (ET _a) and water storage (W) amounts from April to November 2004 with different ET _p modules (hydraulic characteristics by Brutsaert-Gardner).....	38
Table 3.4: Percolation amounts measured as well as simulated with different hydraulic characteristics in percentages of measured amounts in the year 2001 (ET _p by PM grass approach)	42
Table 3.5: Lysimeter storage changes measured and simulated in the top 30 cm at infiltration and drying cycles for the sandy (LM 1) and loamy soil type (LM 2); time periods are described in Figs. 3.6 and 3.7 in further detail	44
Table 3.6: Data of percolation amounts simulated with different ET _p modules in percentages of measured amounts in the year 2001 (hydraulic characteristics by Brutsaert-Gardner).....	47
Table 3.7: Precipitation and measured percolation amounts in the years 1999 to 2003 for LM 1 – LM 4	50
Table 3.8: Modelling efficiency (EF), correlation coefficient (r) and mean and standard deviation (Std) of yearly simulated percolation amounts in percentages of measured amounts in the years 1999-2003 for LM 1 – LM 4 (hydraulic characteristics by Brutsaert-Gardner).....	51

List of Tables

Table 3.9: Modelling efficiency (EF), correlation coefficient (r) and cumulative percolation and evapotranspiration amounts in percentages of measured amounts in the period March to November 2004 for LM 1 (hydraulic characteristics by Brutsaert-Gardner)	54
Table 4.1: Experimental design of the project	61
Table 4.2: Sampling scheme for pesticide measurements of soil and plant samples.....	62
Table 4.3: Soil properties and some hydraulic characteristics of LM 5.1 to LM 5.4.....	63
Table 4.4: Main model input parameters for the glyphosate study.....	82
Table 4.5: Soybean input parameters for the plant uptake model (Penning de Vries et al., 1989; Trapp, 1992).....	82
Table 4.6: Haude factors calibrated for soybean in 2004 in the lysimeter study	83
Table 4.7: Parameter values in the laboratory experiment for calculation of the initial concentration of glyphosate in the liquid phase.....	84
Table 4.8: Partial correlation coefficients in the Monod degradation approach	88
Table 4.9: Multiple correlation coefficients in the Monod degradation approach.....	88
Table 4.10: Microbial community settings for glyphosate degradation at optimum soil moisture content.....	92
Table 4.11: Parameter settings in the Monod approach with growth linked and co-metabolic biodegradation at optimum soil moisture content.....	92
Table 4.12: Parameter settings in the Monod approach accounting for the additional indigenous carbon source of glyphosate degradation at optimum soil moisture content.....	93
Table 4.13: Modelling efficiency (EF), correlation coefficient (r) and cumulative evapotranspiration amount in percentage of measured amount in the period March to April 2004 from the mean of LM 5.2 and 5.3.....	97
Table 4.14: Correlation coefficients (r) between simulated (with various model combinations) and measured weekly percolation amounts in 2003 to 2005	98
Table 4.15: Modelling efficiency (EF) for weekly leachate amounts in 2003 to 2005.....	98
Table 4.16: RMSE for the simulation of the degradation rates with different hydraulic characteristics and environmental response surface of the Weibull type	107
Table 4.17: RMSE values for the simulation of degradation rates with microbial growth kinetics of different degradation community approaches and parameterisation.	109
Table 4.18: Statistical criterion (RMSE) for model performance of the movement of glyphosate in the lysimeters.....	119
Table 4.19: Herbicide application scenarios	131

Table 4.20: Plant parameters of soybean growth at the date of the assumed herbicide applications in 2004.....	131
Table 4.21: Rain in 2004 within five days after the assumed application date and with more than 5 mm amount	131
Table 4.22: Cuticular permeance in dependence of cuticular thickness for GR soybean leaves at the first day after application and afterwards.....	134
Table 5.1: DLLs called from the <i>Expert-N</i> program.....	142
Table 5.2: Information contained in the subsidiary data structures in the solute transport model	144

Abbreviations

a.i.	active ingredient
AMPA	aminomethylphosphonic acid
ANOVA	analysis of variance
BTC	breakthrough curve
CDE	convection-dispersion equation
C_{org}	organic carbon content
CV	coefficient of variation
DLL	dynamic link library
DNA	deoxyribonucleic acid
DOC	dissolved organic carbon
DOM	dissolved organic matter
DT ₅₀	50 % disappearance time (half life)
EF	model efficiency
EPSPS	enzyme 5-enolpyruvylshikimic acid-3-phosphate synthase
ET	evapotranspiration
ET _a	actual evapotranspiration
ET _p	potential evapotranspiration
EV _a	actual evaporation
GM	genetically modified
GR	glyphosate resistant
Haude (mrH)	modified Haude approach (mean relative humidity)
HGT	horizontal gene transfer
IPA	isoproplamine
LAI	leaf area index
LHS	latin hypercube sampling
LM	lysimeter
MRL	maximum residue level
PM crop	Penman-Monteith dual crop coefficient method
PM grass	Penman-Monteith grass reference method
ptf	pedotransfer function
r	correlation coefficient
RMSE	root mean square error
Std	standard deviation
TDR	time domain reflectometry
TR _a	actual transpiration
WC	volumetric water content
WHC	water holding capacity

1 Introduction

Contaminants, which are dispersed at the land surface by accepted management practices or due to accidents, migrate through the vadose zone and influence the long-term quality of groundwater. Leaching through soil has been identified as a major cause for the occurrence of agrochemicals in groundwater (Flury, 1996). The wide range of factors that influence pesticide fate such as soil type, hydrogeology, climate, agricultural land use and physico-chemical pesticide properties makes experimental assessments highly complex and labour-intensive. The use of models allows extrapolation in time and space of data from leaching experiments and monitoring campaigns (Vanderborght et al., 2005). Mathematical modelling is an accepted scientific practice, providing a mechanism for comprehensively integrating basic processes and describing a system beyond what can be accomplished using subjective human judgments (Hutson and Wagenet, 1992).

Frequently, pesticide loads exceed the drinking water limit set by the European Union at $0.1 \mu\text{g L}^{-1}$ (Vanclouster et al., 2000). Thus, the use of pesticides needs to be regulated to protect aquifers from contamination. Pesticide fate models are increasingly used as tools for risk assessment and registration purposes (Herbst et al., 2005). Because comparative estimates regarding exposure, accumulation and leaching of pesticides to assess their ecological risk are especially important for new plant protection products for which no monitoring data exist (FOCUS, 2000), the use of simulation models is suggested by legislation in the registration procedure of new pesticides since 1997 (e.g., Council directive 91/414/EEC; Council of the European Union, 1997). Quantitative information of uncertainties associated with modelling predictions is unavoidable for applications, where pesticide leaching models are used for the legislative decision-making process. Besides differences in model concepts, definition of upper and lower boundary conditions, and parameterization of models, their use by different modellers may also lead to essential differences in simulation results (Diekkrüger et al., 1995; FOCUS, 2000; Klein et al., 2000; Vanclouster et al., 2000). An extensive review of the different sources of uncertainty in pesticide fate modelling was given by Dubus et al. (2003).

Precise environmental fate modelling of agrochemicals goes along with a correctly simulated water balance and water flow in soil (Loos et al., 2007). Field lysimeter studies represent a suitable tool for the determination of water balance components in the soil-plant-atmosphere continuum. Various problems indeed exist in the data surveyed in lysimeter studies e.g. sidewall flow effects, disturbing effects of measurements, microclimatic effects (Bergström, 1990; Flury et al., 1999; Corwin, 2000), but up to now lysimeter studies are the most precise

tool to reproduce real field conditions. Leachate amounts and composition resulting from pesticide and fertiliser applications can be exactly measured in lysimeters (Vink et al., 1997; Schierholz et al., 2000; Vanclooster et al., 2000; Beulke et al., 2004a). Thus, they are also used to assess environmental behaviour of agrochemicals and large undisturbed lysimeters are applied for pesticide registration purposes. Large weighing lysimeters (1 m diameter, 2 m depth) are an appropriate tool for water balance and pesticide transport assessment as they are a closed system in a natural environment.

1.1 Genetically modified crops in modern agriculture

The use of genetically modified (GM) plants has become an integral part of modern agriculture similar to the use of pesticides (Fresco, 2001). The term GM crops or transgenic crops refers to crop cultivars that were developed using recombinant DNA techniques without classic crossing and that contain genetic material from another organism. Especially genetically modified varieties of soybean (*Glycine max*), maize (*Zea mays*), cotton (*Gossypium* spp.) and oilseed rape (*Brassica napus*) are of great importance in the global agricultural production. Herbicide and insecticide resistance are the main applications of the technology.

In the European Union rules are put in place with the objective of consumer protection concerning GM crops. The labelling of foodstuffs enables European consumers to get comprehensive information on the contents and the composition of food products including genetic modification. A threshold of 1% was established for the adventitious presence of (authorised) GM material in food and food ingredients in respect of labelling under Commission Regulation No. 49/2000. Threshold values for technologically unavoidable and coincidental additions of raw material of GM organisms are discussed for agricultural products. For food and animal feed a threshold value of 1% and for seed phased threshold values of 0%, 0.3%, 0.5% and 0.7% are under discussion (DFG Senate commission, 2001). Modelling of pollen dispersal and cross-pollination is of great importance for the ongoing discussion on thresholds for the adventitious presence of genetically modified material in food and feed (Loos et al., 2003). However, beneath the widely discussed direct effects of transgenic plants, e.g. ecological and economical consequences of the release, the indirect effects like modified agricultural practices must be discussed as well. The EU-Directive 2001/18/EC on the deliberate release of genetically modified organisms demands monitoring programs to detect potential unanticipated long-term effects on the environment.

1.1.1 The glyphosate resistant soybean system

Nowadays GM soybean cultivars have become the predominant cultivars marketed in the USA (Fig. 1.1). In 2005 they occupied 60 % of the global GM crops cultivation area (James, 2005). In soybean, the dominant transgenic technology currently in use is the Roundup Ready system (Raymer and Grey, 2003). Roundup Ready soybean cultivars contain a bacterial transgene, commonly known as CP4-EPSPS, from an *Agrobacterium* strain that confers resistance to glyphosate the active ingredient in the herbicide Roundup.

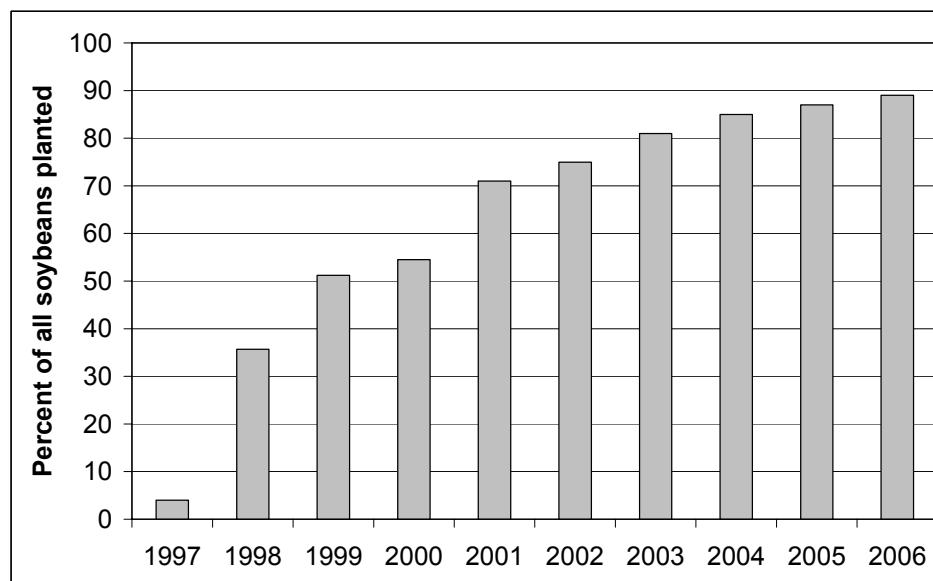


Fig. 1.1: Adoption of GM soybean 1997 to 2006 in the USA (2006 forecasted, National Agricultural Statistics Service, 2006).

New risks of this technology may arise from gene flow in the environment by cross-pollination or by horizontal gene transfer (HGT). The impact of the cultivation of GM crops on the microbial biodiversity in soil must be regarded and the risk of an increased occurrence of the herbicide glyphosate in groundwater due to misapplication of the technology must be addressed. Additionally, the nutritional quality of GM crops concerning herbicide residues must be evaluated.

The glyphosate resistant (GR) soybean technology dramatically changed weed management strategies in the USA (Raymer and Grey, 2003). The rapid adoption rate of the GR soybean system worldwide can be mainly explained by the prospects of an easier weed control and pesticide cost reduction. Although four years (1997 – 2000) of official U.S. Department of Agriculture data show that GR weed management systems require a modest to moderate increase in per-acre herbicide use. Moreover, use rates are trending upward because of shifts in the composition of weeds towards species less responsive to glyphosate, of loss of susceptibility or of the emergence of resistance in some weed species (Benbrook, 2001).

1.1.2 Risk assessment research for glyphosate resistant soybean

The present work was part of the project “Effects of transgenic, glyphosate tolerant soybean in combination with the herbicide glyphosate on the soil ecosystem – A risk assessment study using lysimeters” of the GSF - National Research Centre for Environment and Health. The working hypothesis of the GSF-project was that the cultivation of herbicide-resistant, genetically modified plants can result in a repeated annual and perennial application of the non-selective, systemic herbicide glyphosate that controls a wide range of weeds, as the herbicide can be also applied post-emergence. The potential increase of glyphosate applications includes several risks such as increased loading of the leachate with herbicide residues. As a consequence of herbicide accumulation in the upper soil horizon an increased selection pressure on microorganisms can occur. Thus, microbial transformation processes of the herbicide as well as microbial population dynamics may change. The possibility of a HGT from plants to bacteria based on homologous recombination must be evaluated. Genetically modified plants like GR soybeans have different glyphosate retention. In the plants the herbicide is transported in the phloem. Since there is no evidence of metabolic degradation of glyphosate in the GR soybean (personal communication Norbert Mülleder, Monsanto, Düsseldorf), glyphosate is transported to and accumulated in metabolic sinks given as nodules and beans.

Topics of the risk assessment research that were included in the project up to now are listed as follows:

- environmental fate of glyphosate after repeated application over several years in presence of GR soybean,
- HGT by homologous recombination under normal conditions and under increased selection pressure (repeated glyphosate application) in the rhizosphere as well as during litter degradation,
- accumulation of glyphosate in GR soybean nodules and beans.

1.2 Aim and structure of the work

Purpose of this research work was to assess and describe the environmental fate of the herbicide glyphosate in the presence of genetically modified soybean by mathematical modelling using the named experiment and the modular modelling system *Expert-N*. Therefore, in *Expert-N* which was developed to simulate N cycles in agroecosystems (Priesack, 2006), a submodel based on the solute transport model LEACHP (Hutson and Wagenet, 1992) was implemented. The newly implemented modelling system should be also

able to assess the behaviour of various xenobiotics in different soils and plants under environmental conditions.

In the soil-plant-atmosphere system (Fig. 1.2) the pesticide, e.g. glyphosate, may be photodecomposed or volatilised after spraying and it may be adsorbed by plant leaves before it reaches the soil. In soil the pesticide transport is mainly determined by water flow. Water transport and outflow strongly depend on available water amounts, which are determined by precipitation and evapotranspiration processes. Preferential flow in macropores contributes to hydromechanical dispersion and enhances pesticide transport and leaching. Further on, pesticide movement through the vadose zone is strongly affected by the sorption capacity of the soil matrix. The bioavailable pesticide fraction can be degraded by microbial communities and uptake by plant roots is possible.

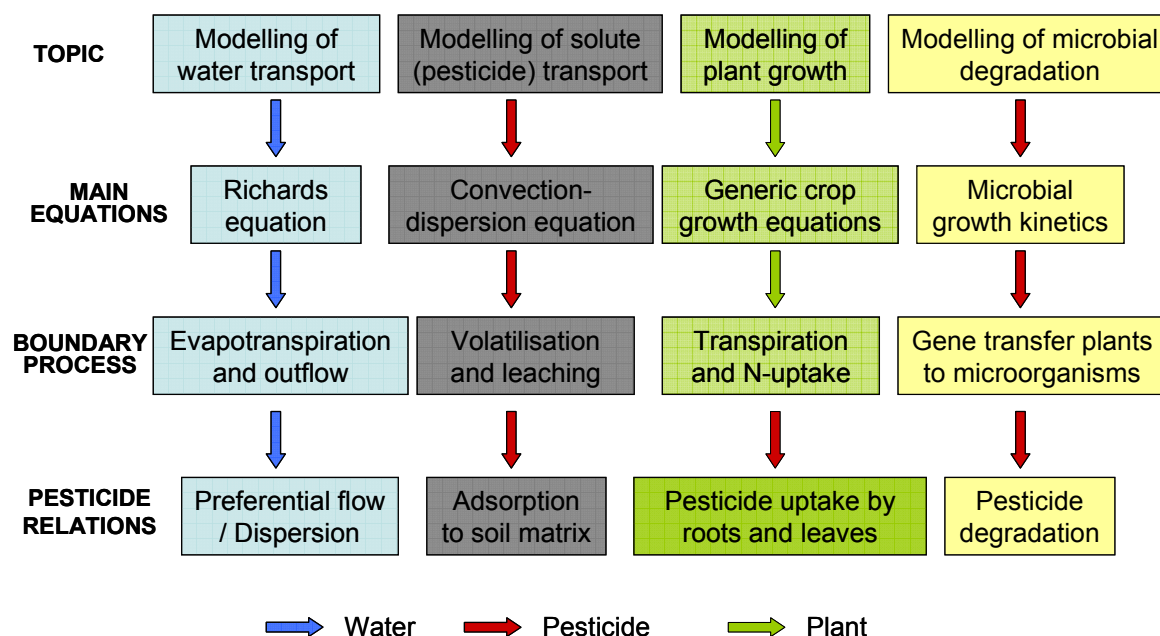


Fig. 1.2: Mathematical modelling of water flow and solute transport in the soil-plant-atmosphere system.

Modelling the effects of gene exchange from plants to microorganisms as suggested in the right column of Fig. 1.2 is strongly hindered (Soulas and Lagacherie, 2001) due to the lack of appropriate measurement techniques to detect HGT (Nielsen and Townsend, 2004). Up to now, monitoring efforts have failed to identify HGT events occurring from transgenic plants into bacterial communities in soil in the GSF-project.

The presented work is composed of four discrete chapters. In **chapter 2** the laboratory experimental background is illustrated. Detailed results of degradation and sorption experiments are explained, which were necessary for calibration of the mathematical model system and as model input parameters.

As already pointed out, precise environmental fate modelling of pesticides depends on a correctly simulated water flow in soil. Therefore, water flow and assessment of water balance are discussed in **chapter 3**. Lysimeter data from four cropped, undisturbed field lysimeters representing four different soil types were evaluated over five years. This chapter includes a detailed description of the GSF-lysimeter facility.

The environmental behaviour of glyphosate is described concerning data from four re-packed field lysimeters filled with the same soil type and cropped with transgene soybean over two years. The conceptual structure of **chapter 4** results mainly from the process interactions described in Fig. 1.2. Microbial degradation of glyphosate and microbial growth are studied first (section 4.3.2.1). Adsorption of glyphosate to soil matrix is analysed in section 4.3.2.2 and the influence of dispersion on movement and leaching of glyphosate is shown afterwards (section 4.3.2.3). Finally, special attention was given to the glyphosate uptake by plant leaves and translocation in the plants (section 4.3.4).

The modelling of pesticide behaviour in the soil-plant-atmosphere system is based on the pesticide transport model LEACHP (Hutson and Wagenet, 1992) and the model PLANTX of Trapp (1992) to simulate the pesticide uptake by plants. The implementation of these modules in *Expert-N* was realized using the concept of dynamic link libraries (DLLs) of the *Microsoft C* programming environment (*Visual Studio .NET 2003*®). This is described as technical note in **chapter 5**.

2 Degradation and sorption experiments with the herbicide glyphosate under controlled laboratory conditions

2.1 Introduction

The non-selective systemic herbicide glyphosate [N-(phosphonomethyl)glycine] is classified among the less persistent pesticides. It is one of the most widely applied herbicides worldwide and was introduced by Monsanto in the year 1974. It is a foliar-applied herbicide, which is taken up by leaves and shoots and is then translocated with the assimilation stream in the whole plant. The systemic herbicide controls most annual and perennial weeds by inhibiting the synthesis of aromatic amino acids needed for protein formation. This mechanism of action is unique since glyphosate is the only herbicide that specifically inhibits the enzyme 5-enolpyruvylshikimic acid-3-phosphate synthase (EPSPS), which catalyzes the condensation of shikimic acid and phosphoenolpyruvate (Zablotowicz and Reddy, 2004). Beneath the use in agricultural fields and silviculture, it is widely used for weed control on the wayside and on railways. In agricultural practice it is used especially in no-till agriculture to prepare fields for planting, to control weeds during crop development, or to control perennial weeds after crop harvest (Battaglin et al., 2005) and is thus commonly applied throughout the season. Persistence and degradation of glyphosate vary greatly between soils (von Wieren-Lehr et al., 1997) and depend strongly on soil microbial factors (Rueppel et al., 1977; Vereecken, 2005). Two pathways of the degradation of glyphosate have been documented (citations in Liu et al., 1991). The main way is to cleave the C-N bond which results in the metabolite aminomethylphosphonic acid (AMPA). A few microbial populations can use glyphosate as a sole source of phosphorus (Penaloza-Vazquez et al., 1995). This results in the second pathway which is via initial cleavage of the C-P bond to give the metabolite sarcosine. Glyphosate and AMPA are both negatively charged at neutral pH and degradation in microbial cells can only take place if the transport problem across the lipid bilayer of the plasma membrane of cells has solved (Jacob et al., 1988). The transport problem can be circumvented if external degradation via membrane bound or periplasmic enzymes occurs. Partitioning of glyphosate between the two degradative pathways would naturally favour breakdown to AMPA (Jacob et al., 1988). Thus, degradation rates of glyphosate can be strongly influenced by the microbial communities in the soils and the enzymatic degradation pathway used. Soil microbial activity and microbial community structure themselves are mainly governed by environmental conditions like temperature, moisture, and substrate availability in the soil microhabitats and are therefore closely linked to water and heat transport in soil profiles. Thus, the variability in

soil microbial factors is found to be higher than the variability in soil physical and chemical parameters (Stenrød et al., 2006). This results in a high variability in the rates of biodegradation of glyphosate in different soils under various environmental conditions.

A major factor governing pesticide leaching potential is the mobility of the pesticide in soil (Jury et al., 1987). The mobility can be mainly described by adsorption parameters like the soil distribution coefficient K_d and the soil organic carbon distribution coefficient K_{oc} (Wauchope et al., 2002). The relation between biodegradation and sorption is a complex process and already discussed in several works (see section 4.3.2.2, Soulas and Lagacherie, 2001; Beulke et al., 2004b). Several studies show that glyphosate is strongly adsorbed by soil matrices (de Jonge et al., 2000) and is considered to be almost immobile on the basis of its sorption properties. A detailed review concerning adsorption of glyphosate to the different soil constituents like clay minerals, organic matter, oxides, and hydroxides was recently given by Vereecken (2005).

For the assessment of field lysimeter studies various laboratory experiments were necessary concerning the biodegradation and sorption of glyphosate under controlled environmental conditions. The aim of this part of the work was therefore the conduction of biodegradation studies, the determination of active microbial biomass in soil, and the determination of adsorption coefficients by the usage of batch sorption studies.

2.2 Materials and Methods

2.2.1 Soils

The biodegradation of glyphosate in soils under laboratory conditions was examined in five different soil types (Table 2.1). They represent soil types of Southern Bavaria which are available as lysimeter soils at the GSF-lysimeter facility for further experiments. The full description of the lysimeter soils is given in the respective sections (LM 1 – LM 4 section 3.2.1.2 and LM 5.1 – 5.4 section 4.2.1.3) in the following main chapters 3 and 4. The soils of the lysimeter (LM) monoliths LM 1 to LM 4 were well examined as they were already subject of various laboratory and field lysimeter experiments concerning the behaviour of isoproturon in soils (Kühn, 2004; Dörfler et al., 2006). Soil samples for LM 1 to LM 4 were taken in the tillage zone from a field storage container preserved at the lysimeter facility. For the soil cores of LM 5 (with four identical lysimeter cores LM 5.1 to 5.4) soil samples (tillage zone) were obtained from the field site near to where the soil of the re-packed lysimeters was taken. Only the top soil was examined as this horizon has the highest microbial biomass and organic matter content and it is the critical zone for pesticide biodegradation, sorption and retention.

Table 2.1: Soil properties of the first soil horizon of lysimeter monoliths (LM 1 – LM 4) and soil cores (LM 5.1 to 5.4)

Lysimeter	Soil type ¹⁾	Horizon (cm)	C _{org} ²⁾ (% dry matter)	N _{total} (% dry matter)	Phosphorous (P2O5-CAL mg/100g)	pH CaCl ₂	Clay (%)	Silt (%)	Sand (%)
LM 1	HC	0-30	1.09	0.10	38	6.9	11	19	70
LM 2	MG	0-40	1.50	0.17	15	5.4	22	60	18
LM 3	CR	0-50	2.70	0.27	33	7.2	33	34	33
LM 4	AA	0-30	0.95	0.11	22	6.7	13	19	68
LM 5.1 to LM 5.4	HA	0-30	0.95	0.10	15	5.5	4	8	88

1) HC = Humic Cambisol, MG = Mollic Gleysol, CR = Calcaric Regosol, AA = Aric Anthrosol, HA = Haplic Arenosol

2) organic carbon content

All soil samples were sieved to ≤ 2 mm grain size. Additionally, the microbial biomass was determined in all soils. They were equilibrated at $20 \text{ }^\circ\text{C} \pm 3 \text{ }^\circ\text{C}$ and the respective moisture contents (given in Table 2.2) for minimum one week prior to analysis. Or they were first stored at $4 \text{ }^\circ\text{C}$ in the dark prior to the equilibration time. The soil of LM 5 was examined in more detail, because this soil was used for the field lysimeter study with glyphosate. The maximum water holding capacity (max. WHC) for the upper soil of LM 5 was determined according to Nehring (1960) and also batch adsorption-desorption studies were conducted (see section 2.2.5).

2.2.2 Chemicals

Glyphosate [*N*-(phosphonomethyl)glycine] radiolabelled with carbon-14 (^{14}C) at the phosphonomethylene position was obtained in a residue amount (1 mCi) from PerkinElmer (Köln, Germany) with a denoted purity of 99 % at time of production (21 month before first experiments were conducted) and specific activity of $51.2 \text{ mCi mmol}^{-1}$. The ^{14}C -glyphosate was dissolved in autoclaved and distilled water and mixed with the commercially available glyphosate formulation Roundup LBplus (Scotts Celaflor, Ingelheim am Rhein, Germany) to a stock solution with a concentration of the active ingredient (a.i.) of $3.63 \text{ } \mu\text{g } \mu\text{L}^{-1}$ and a specific radioactivity of $481.05 \text{ Bq } \mu\text{L}^{-1}$. In the LBplus formulation glyphosate is formulated as Isoproylamine (IPA) salt. Usually, there is an excess of approximately 10-20 % of IPA in the formulation (personal communication Marie Reding, Monsanto, Brussel). The added ^{14}C -glyphosate amount was 16.9 %. Therefore, it was not necessary to add IPA to the stock

solution. It was proved that the ^{14}C -glyphosate aqueous solution was not volatile at temperatures of up to 45 °C.

Pure, non labelled glyphosate and AMPA were purchased from Dr. Ehrenstorfer (purity > 98 %, Augsburg, Germany). The scintillation cocktails for radioactivity measurements were purchased from Packard (Dreieich, Germany) and the solvents of analytical grade from Merck (Darmstadt, Germany).

2.2.3 Biodegradation experiments

Biodegradation studies with ^{14}C -labelled compounds allow the characterisation of the fate of pesticides in soils and to distinguish between mineralization, volatilization and formation of extractable and non extractable residues. For the biodegradation experiments 0.1 mL of the ^{14}C -glyphosate stock solution (363 μg non labelled and 3.3 μg ^{14}C -labelled a.i.) was applied on an amount of 3.5 g oven dried (105 °C, 24 h) and pulverised soil sample with a Hamilton syringe. The spiked soil aliquots were further mixed with soil portions (dry equivalent 46.5 g) equilibrated at 60 % of max. WHC, transferred to glass flasks and adjusted to the designated moisture content. The flasks were incubated for 41 days in the dark at 20 °C \pm 1 ° C in the incubation system for biodegradation studies described in more detail at Dörfler et al. (1996) and Schroll et al. (2004). The closed incubation system consisted of a discontinuously aerated laboratory system where humidified air (1.0 L h⁻¹) passed through three times per week for one hour. After passage through the soil incubation flasks air was trapped in three subsequent absorption tubes, the first filled with 10 mL ethyleneglycolmonomethylether to absorb ^{14}C -volatile compounds and the other two filled with 10 mL 0.1 n NaOH to absorb $^{14}\text{CO}_2$ (Schroll et al., 2006). At each sampling the adsorption liquid of the first tube was mixed with 3 mL scintillation cocktail (Ultima Gold XR). A 3 mL aliquot of the NaOH solution in the following two tubes was mixed with 2 mL scintillation cocktail (Ultima Flo AF) and given in the liquid scintillation counter (Tricarb 1900 TR, Packard, Dreieich, Germany). At the end of the incubation time, aliquots of 1 g moisture soil were combusted (Sample-Oxidizer 306, Canberra-Packard, Dreieich, Germany) and the evolved $^{14}\text{CO}_2$ was quantified to establish the ^{14}C mass balance.

Further experiments were performed with modified test conditions to examine

- a) whether microorganisms can adapt to glyphosate in a short time period and if microbial degradation can be enhanced by repeated pesticide applications. The soils of LM 3 and LM 5 were treated with inactive glyphosate (3 L ha⁻¹ Roundup equivalent to 1080 g ha⁻¹ glyphosate) four times with intervals of four weeks between the single applications.

- b) whether degradation is influenced by the composition of the microbial community. For LM 2 and LM 5 the soil samples were additionally inoculated with 5 % soil (dry weight) of LM 3 to survey the transferability of the specific soil function for glyphosate mineralization of the soil community of LM 3 to the communities of LM 2 and LM 5. The soil of LM 3 was used, because it showed the highest glyphosate mineralization capability,
- c) whether initial pesticide concentration and soil moisture content are of great influence for degradation. For LM 5 the applied pesticide concentration was also halved and the soil was adjusted to further moisture contents.

After these additional modifications were accomplished the biodegradation experiments were conducted with soil samples of the essays with ^{14}C -glyphosate as described before. All biodegradation experiments consisted of minimum three replicates and are summarised in Table 2.2.

Table 2.2: Glyphosate biodegradation experiments in soils of LM 1 - 5

Soil	Moisture content (% of max. WHC)	Applied amount (μg a.i. in 50 g dry soil)	Treatments	Inoculation
LM 1	60	366.3	1	no
LM 2	60	366.3	1	yes/no ²⁾
LM 3	60	366.3	1or (4+1) ¹⁾	no
LM 4	60	366.3	1	no
LM 5	30/40/50/60	183.2/366.3	1or (4+1)	yes/no

¹⁾ (4+1) = 4 times non-labelled + 1 time labelled glyphosate application

²⁾ yes = soil inoculated with 5 % of soil LM 3, no = no soil inoculum

2.2.4 Microbial biomass measurement

The degradation of pesticides in general and in particular the degradation of glyphosate in soils is mainly controlled by the microbial activity (Rueppel et al., 1977; von Wiren-Lehr et al., 1997). The soil microbial biomass and the microbial activity were measured by the microcalorimetric method (Sparling, 1981; 1983). With the microcalorimetric method the actual (basal) and also the substrate induced (potential) microbial activity are quantified by measuring the heat production of the microbes. For the measurement of the substrate induced activity 0.4 % (dry equivalent) of an easy utilizable substrate (yeast) was added to 1 g fresh soil with a moisture content of 35-40 and 45-50 % of the max. WHC. The soil samples were then incubated for 6 h in the microcalorimeter (Thermal Activity Monitor 2277,

Thermometric, Järfälla, Sweden). The basal activity was measured in the same way without substrate addition.

According to the regression equation of Sparling (1981) the heat production E_H ($\mu\text{W g}^{-1}$ dry soil) of the substrate induced microbial activity can be converted by

$$C_{bio-C} = X \cdot E_H \quad (2.1)$$

to the biomass-C concentration C_{bio-C} ($\mu\text{g-C g}^{-1}$ dry soil) with $X = 5.544 \mu\text{g-C } \mu\text{W}^{-1}$. For the estimation of the substrate induced heat production at the point where the substrate induced microbial growth begins, see Sparling (1983).

2.2.5 Batch adsorption-desorption studies

The adsorption-desorption kinetics of glyphosate in the upper soil of LM 5 were investigated using the OECD laboratory batch sorption procedure (OECD, 1981). A ^{14}C -labelled pesticide solution with a concentration of 5 mg L^{-1} and a specific radioactivity of 0.042 MBq L^{-1} was prepared from a mixture of the stock solution with an aqueous Roundup LBplus solution (0.01 M CaCl_2 background electrolyte).

In the adsorption batch experiment ($n = 3$) 35 mL of the ^{14}C -glyphosate solution were added to 7 g air dried soil sample (1:5 soil to solution ratio) and shaken in an end-over-end rotary shaker (REAX 2, Heidolph, Schwabach, Germany) at 2, 4, 6 and 16 h incubation time at $20 \text{ }^\circ\text{C} \pm 3 \text{ }^\circ\text{C}$ for the determination of the sorption equilibrium. At the end of the respective incubation times the samples were centrifuged (centrifuge J2-21 with rotor JA-14, Beckman, Munich, Germany) at 10 000 rotations per min for 25 min. Then 2 mL aliquots of the accumulated supernatant were mixed with 3 mL scintillation cocktail (Ultima Gold XR) and given in the liquid scintillation counter. Because the biodegradation of glyphosate starts without lag phase the degradation rate in the soil suspensions was determined in a parallel conducted biodegradation experiment under the same conditions as for the adsorption experiment and at the respective incubation times.

For the desorption batch experiment ($n = 3$) the samples were prepared in the same way as described for the adsorption experiment, shaken in the end-over-end rotary shaker until the previously determined sorption equilibrium was reached and then centrifuged as described before. Afterwards 75 % of the supernatant in the centrifuged samples were substituted with 0.01 M CaCl_2 solution. The refilled samples were attached to the rotary shaker, centrifuged and 75 % of the supernatant were substituted again. The desorption procedure was repeated three times in succession. The radioactivity in the supernatant was measured as described before.

For the determination of an adsorption isotherm ($n = 3$) further working solutions of concentrations of 1 mg L^{-1} (0.008 MBq L^{-1}), 0.2 mg L^{-1} (0.002 MBq L^{-1}) and 0.04 mg L^{-1} ($0.0003 \text{ MBq L}^{-1}$) were prepared and adsorption was measured at sorption equilibrium. Sorption parameters were estimated from a linear isotherm and from the linearized Freundlich equation (cp. non linearized form Eq. (4.14)):

$$\log C_s = \log K_f + n_f \log C_l \quad (2.2)$$

where C_s (mg kg^{-1}) is the sorbed concentration and C_l (mg L^{-1}) the concentration in solution, K_f (L kg^{-1}) the Freundlich coefficient and n_f (-) the Freundlich exponent.

2.3 Results and Discussion

2.3.1 Microbial biomass and biodegradation of glyphosate in batch experiments

The biodegradation studies show that after 41 days between 12.8 to 56.6 % of the applied ^{14}C -glyphosate was mineralized to $^{14}\text{CO}_2$ at a water content of 60 % of the max. WHC in the five different soils (Fig. 2.1). High variability in the rate of degradation in laboratory studies was also reported in the Review Report Glyphosate of the European Union (Bruno and Schaper, 2002), were $\text{DT}_{50\text{lab}}$ values (time it takes to reach 50 % of the original concentration) between 4 to 180 d (mean 49 d) at $20 \text{ }^\circ\text{C}$ were listed. A direct correlation between other conceivable soil properties like adsorption capacity and C_{org} content (cp. Table 2.1 and see also Stenrød et al.(2006)) of the soils and the degradation rates could not be observed.

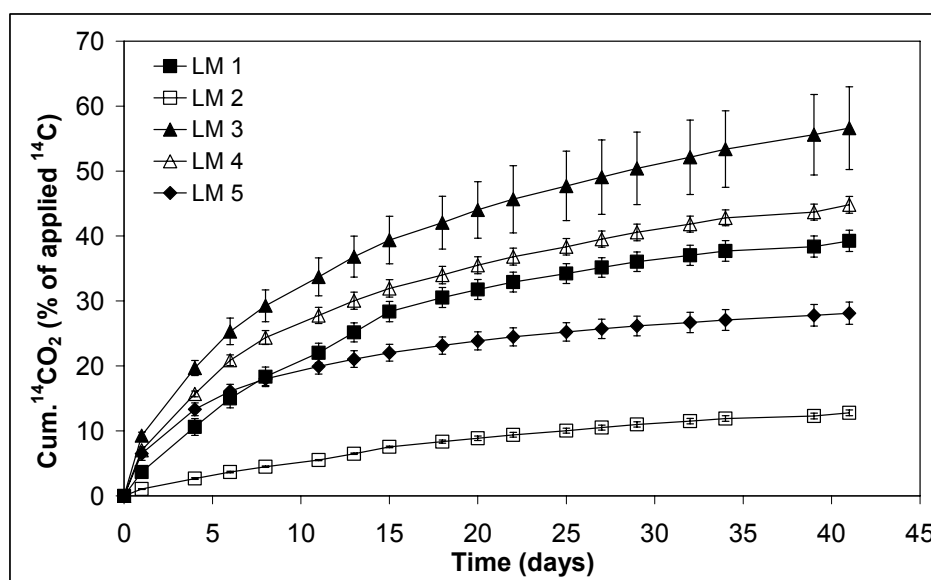


Fig. 2.1: Glyphosate mineralization in the five soils through the 41 days incubation period at a water content of 60 % of max. WHC.

Although microbial activity in the soil of LM 2 is similar to that of the other soils glyphosate degradation in LM 2 is very low (Fig. 2.1). The soil of LM 2 has a high silt and clay content and sorption capacity seems to be high. Mineralization studies of Scow and Hutson (1992) and Scow and Alexander (1992) showed that degradation of organic compounds was strongly influenced by the presence of porous aggregates (e.g. clay) compared to pure buffer-salts solutions. At low substrate concentrations, not only the rates of degradation were reduced in the presence of aggregates but also the shapes of the biodegradation curves differ, and a shift of first-order to zero-order or sigmoidal shapes occurs. In contrast to the other mineralization kinetics for the soil of LM 2 mineralization follows a curve that gradually changes from a first-order to a zero-order curve in the observed time interval. This indicates that solute diffusion out of the soil aggregates may be the main rate-limiting process of degradation in this soil with high clay content.

Fig. 2.2 shows additionally the results of the conducted biodegradation experiments after repeated applications of inactive glyphosate. Differences in degradation curves between multiple and single glyphosate treatments are small. No adaptation or inhibition of the microorganisms could be observed after repeated applications of glyphosate for the soil (LM 3) with the highest degradation rates and also no adaptation for a less degrading soil (LM 5).

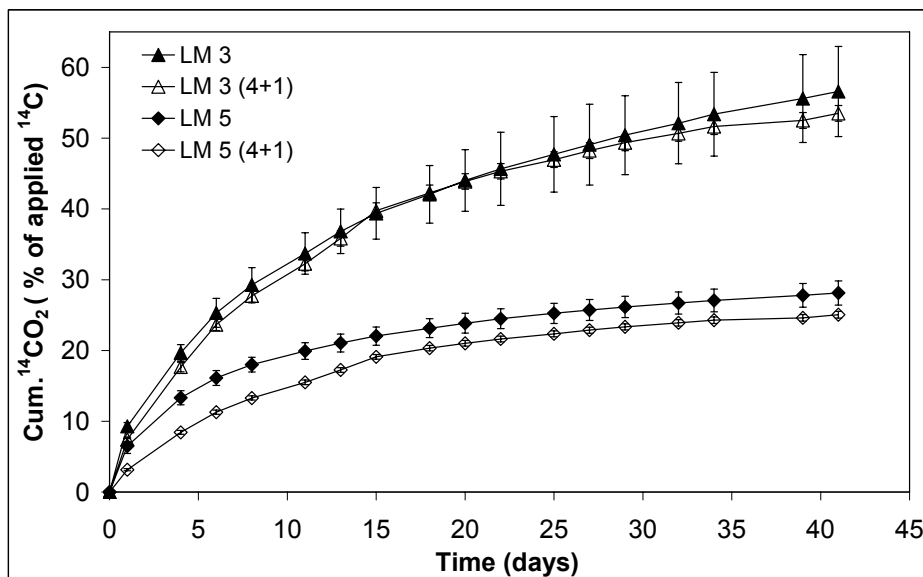


Fig. 2.2: Glyphosate mineralization in LM 3 and LM 5 through the 41 days incubation period at a water content of 60 % of max. WHC (treatments: (4+1) = 4 times non-labelled + 1 time labelled glyphosate application and controls).

Rueppel et al. (1977) reported also a minimal and not pronounced effect of glyphosate on microorganisms. In soil of LM 5 even slightly decreased degradation rates could be observed at the first eight days of the experiment. As reported by Forlani et al. (1999) the rate of

utilization of glyphosate was not enhanced following repeated treatment of the soil even with increasing herbicide doses. An influence of the applied amount was also not measurable in the experiment conducted with halved herbicide dose (results not shown).

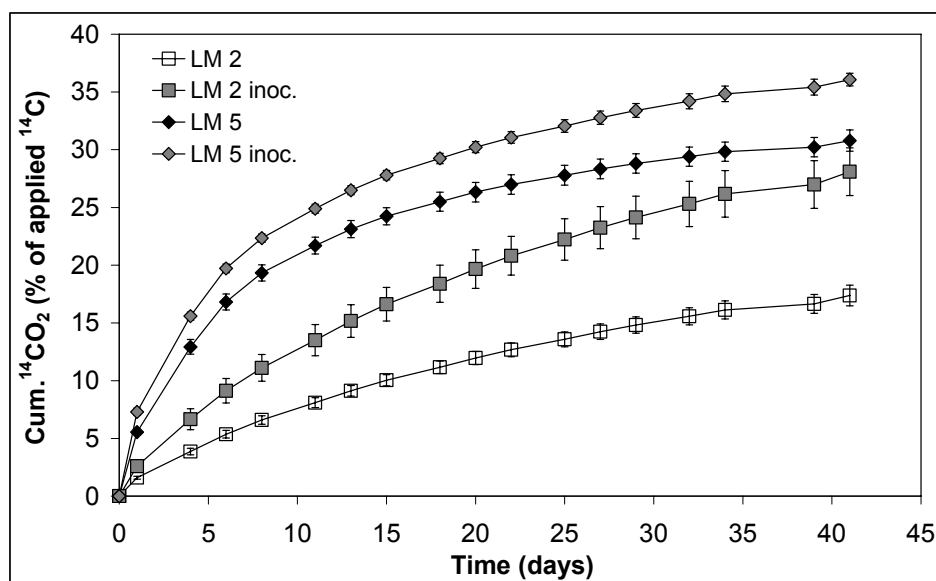


Fig. 2.3: Glyphosate mineralization in LM 2 and LM 5 through the 41 days incubation period at a water content of 60 % of max. WHC (treatments: inoculation with 5 % of soil of LM 3 and controls).

The transfer of the soil community of the soil with the highest degradation rate (LM 3) to the soils of LM 2 and LM 5 results in an accelerated degradation in both soils, which gets obvious from Fig. 2.3. The inoculated soils degrade 28.1 % (LM 2) and 36.1 % (LM 5) of the applied glyphosate. In both soils the transfer of the microbial community leads to a significant increase (61.7 % in LM 2 and 17.2 % in LM 5) of the mineralization rates. The degradation rate of the soil of LM 3 alone was 56.6 % after 41 days (cp. Fig. 2.1). If 5 % of this rate (accordant to the added soil amount) are summed to the measured mineralization rates of the controls of LM 2 and LM 5 the calculated cumulative mineralization amount would be lower than the measured means of the inoculated soils (see Table 2.3).

Table 2.3: Glyphosate mineralization after 41 days in LM 2 and LM 5 in control experiment and after inoculation with soil of LM 5

Cumulative $^{14}\text{CO}_2$ amounts of degraded pesticide	LM 2 (%)	LM 5 (%)
Control	17.4	30.8
Inoculated		
Calculated (control + 5 % of LM 5)	20.2	33.6
Measured	28.1	36.1

This shows that the degradation behaviour of the inoculated soil could not be explained only by a greater amount of adapted microorganisms in the samples, and indicates that degradation is also influenced to a great part by the composition of the microbial community and may reflect shifts in species distribution of the degrading community. This also shows that solute diffusion out of the soil aggregates is not the only rate-limiting process of degradation in the soil of LM 2.

The variability in water content observed in field experiments and its influence on degradation rates was also studied in laboratory experiments for the soil of LM 5. Fig. 2.4 shows the biodegradation results for soil moisture contents between 30 to 60 % of the max. WHC. A water content variability in the range of 40 to 60 % max. WHC has no influence on the degradation rates. Primal, at a water content of 30 % of the max. WHC a clear reduced degradation (7.8 %) could be observed. Further mineralization studies with glyphosate in the soil of LM 5 of Schroll et al. (2006) indicate that the analysed soil moisture contents in the present experiments lie in the range of optimum moisture for glyphosate degradation.

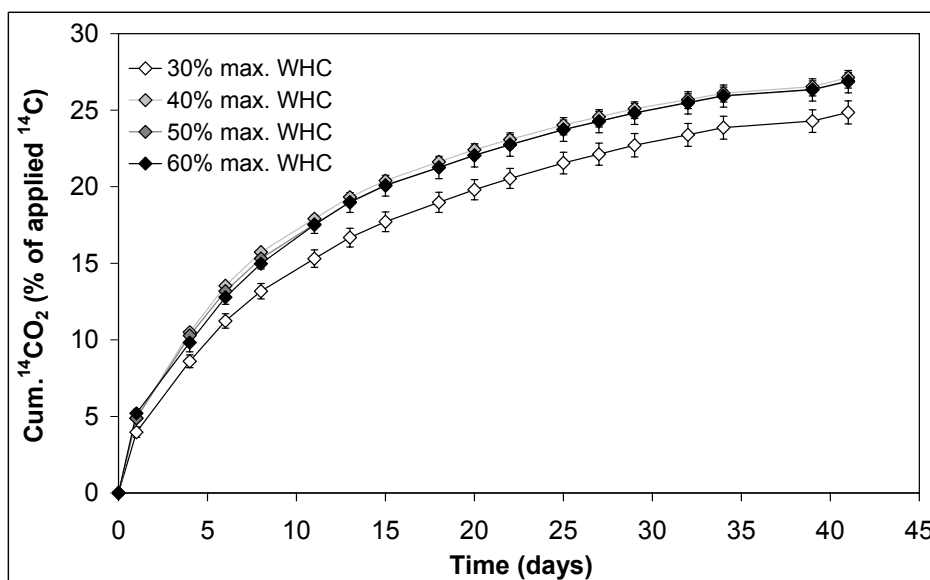


Fig. 2.4: Glyphosate mineralization in LM 5 in dependence of soil water content in % of max. WHC.

The soil microbial biomass and the potential microbial activity were analysed to investigate the influence of microbial activity and growth on the degradation of glyphosate. In Table 2.4 the actual (basal) and the substrate induced (potential) microbial activity are shown for the five soils. These soils exhibit high differences in these properties.

Table 2.4: Basal microbial activity and microbial biomass with standard deviations (Std) for soils of LM 1 to LM 5

Soil	Basal ($\mu\text{W g}^{-1}$ dry weight)	Std ($\mu\text{W g}^{-1}$)	Biomass ($\mu\text{g-C g}^{-1}$ dry weight)	Std ($\mu\text{g-C g}^{-1}$)
LM 1	4.25	0.84	406.49	21.89
LM 2	3.52	0.35	349.82	4.33
LM 3	3.61	0.19	646.32	14.33
LM 4	4.58	0.68	547.04	17.99
LM 5	2.80	0.74	202.53	15.38

A one-way Analysis of Variance (ANOVA)¹ verifies that there was a significant difference of microbial biomass between the soils. Appropriate post-hoc tests were subsequently performed to elucidate any differences found. The conventional five-percent level was specified as the significance threshold. For the biomass a significant difference could be found between all soils. The post-hoc test showed that a significant difference for the basal activity can only be found between the soils of LM 1 – LM 5 and LM 4 – LM 5. A correlation between organic carbon content and microbial activity is not obvious (cp. Tables 2.1 and 2.4).

Fig. 2.5 shows a clear positive correlation between microbial biomass and degradation rate of glyphosate in the laboratory batch experiments with exception for LM 2 where the mineralization of glyphosate was least. Because the adsorption of glyphosate by soils is related to the clay content and the cation-exchange capacities of the soils (Glass, 1987), the minor degradation in soil of LM 2 may be explained by the high silt and clay content (cp. Table 2.1) and the high sorption capacity of the soil as has been already discussed. The relation between degradation and sorption coefficients was not further investigated for the soils in the present work. The biodegradation experiments provide the basis for the analysis of the relation between microbial activity and degradation of glyphosate and it was assumed that only the bioavailable and therefore not sorbed glyphosate fractions can be degraded. The positive correlation between microbial biomass and degradation rate of glyphosate indicates that a great amount of microbial communities in soil is responsible for the mineralization and not only a small community of highly specialized species. The degradation curves without lag phase support this argument.

¹ The software package *Mathematica*® (version 5.0) was employed for all statistical analyses.

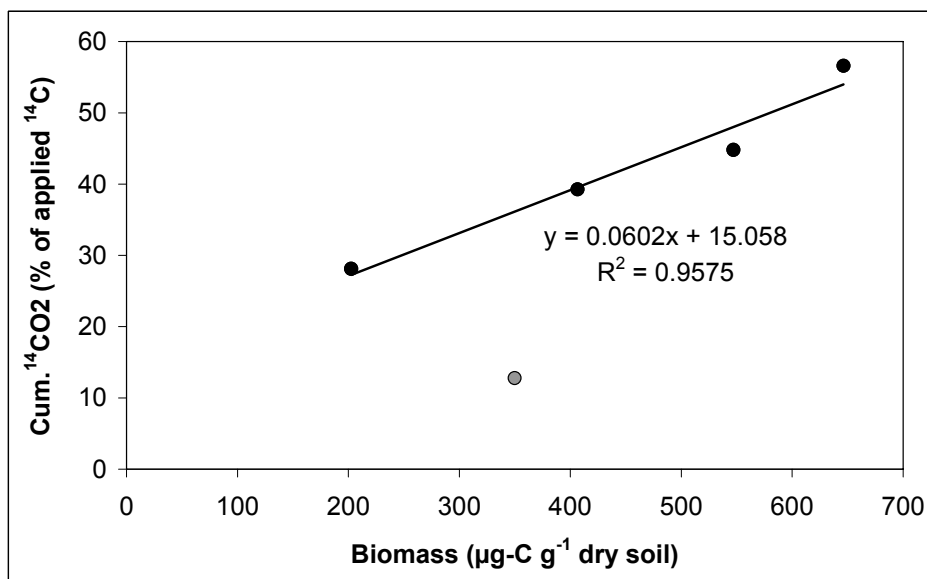


Fig. 2.5: Scatter plot of microbial biomass and cumulative evolved ¹⁴CO₂ from ¹⁴C-glyphosate in the biodegradation experiment (grey symbol LM 2, not included in the regression equation).

Fig. 2.6 shows that the repeated application of glyphosate on the soils has an influence on the microbial biomass which is measurable in the substrate induced microbial activity although no enhanced degradation was observed (cp. Fig. 2.2) in the biodegradation experiments. With exception of soil LM 4 where a reduction of biomass could be observed, for all other soils the repeated herbicide treatments resulted in an increased microbial biomass in all the other soils.

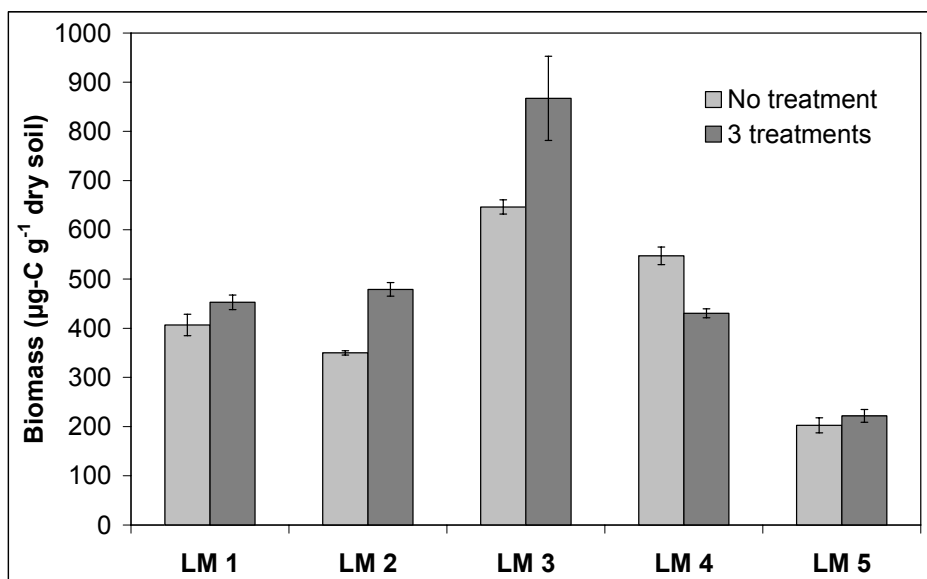


Fig. 2.6: Microbial biomass in the control soils (not treated with glyphosate) and in the soils after repeated application of non-labelled glyphosate.

A second ANOVA test was performed to determine whether the influence of repeated applications on the microbial biomass is statistically firm (Table 2.5).

Table 2.5: Statistical results for the ANOVA test between control (not treated with glyphosate) and repeated herbicide treatments concerning biomass contents

Soil	F-ratio	P-value
LM 1	3.471	0.099
LM 2	54.466	0.000
LM 3	6.052	0.049
LM 4	128.880	0.000
LM 5	3.117	0.094

For LM 1 and LM 5 only a weak (ten percent level) significant difference could be observed between treated soil and untreated control. For LM 2 and LM 3 the ANOVA results show that there is a significant relationship between glyphosate applications and increased microbial biomass in the soils. For LM 4 a significant decrease of microbial biomass was observed which cannot be explained by the available information.

2.3.2 Sorption and desorption of glyphosate in batch experiments

Different results are cited in the literature concerning the pH dependence of glyphosate sorption. No pH dependence was listed in the Review Report Glyphosate (Bruno and Schaper, 2002) while de Jonge et al. (2000) cited literature where a pH dependence of sorption was reported. In the present work it was assumed that glyphosate sorption is independent of the pH value. Sorption kinetic studies showed that glyphosate was rapidly and strongly sorbed to soil materials (Miles and Moye, 1988; de Jonge et al., 2000). The same results were found for the soil sample of the upper soil horizon of LM 5: rapid equilibrium adjustment and a high adsorption to soil matrix (Table 2.6).

Table 2.6: Adsorption in percentage of applied amount and adsorption coefficients of glyphosate to soil matrix measured by the OECD laboratory batch sorption procedure for the upper soil horizon of LM 5 taking into consideration microbial degradation

Time (h)	Adsorption (%)	Std (%)	K_d -value ($\text{dm}^3 \text{kg}^{-1}$)	K_{oc} -value ($\text{dm}^3 \text{kg}^{-1}$)
2	71.0	0.1	12.2	1287.4
4	72.5	0.1	13.2	1385.0
6	74.2	0.4	14.4	1516.9
16	77.2	0.6	17.0	1786.9

As discussed by Wauchope et al. (2002) it is often assumed that high values of K_d indicate that a pesticide will be immobile in soil and also resistant to microbial degradation. In the present study it was shown that this statement is not entirely correct as glyphosate has high K_d values and also shows high microbial degradation rates. Therefore, the desorption process must be taken into account as well. Microbial degradation (cp. Fig. 2.7) during the sorption experiment was taken into consideration in the listed K_d values of the linear sorption isotherm. Fig. 2.7 states that after 2 h one percent of the applied ^{14}C -glyphosate was already mineralized in the liquid soil suspension.

In the Review Report Glyphosate (Bruno and Schaper, 2002) a K_{OC} value for glyphosate of $884 \text{ dm}^3 \text{ kg}^{-1}$ was documented for a loamy sand. This value is in good accordance with the value of $1287.4 \text{ dm}^3 \text{ kg}^{-1}$ measured after 2 h in the present study for linear sorption (Table 2.6) since a typical confidence value among reported K_{OC} is 40 – 60 % (Wauchope et al., 2002). Because K_{OC} values are used as measures for the relative potential mobility of pesticides, the K_d values for the subjacent soil horizons of the lysimeter study (soil LM 5) were calculated from the K_{OC} values of the upper soil horizon.

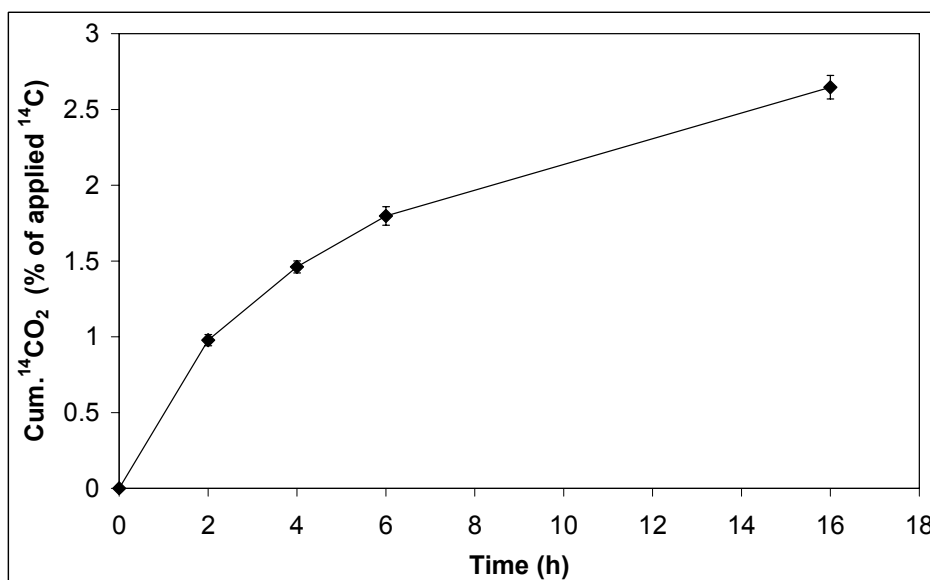


Fig. 2.7: Glyphosate mineralization in the upper soil horizon of LM 5 in the sorption kinetic experiment (soil to solution ratio 1:5).

For the sorption of glyphosate to the soil matrix different mechanisms were stated in the literature at disposal. Cation-exchange reactions (Glass, 1987) and the relation to phosphate binding sites (Wauchope et al., 2002) were reported as well as the importance of the interactions with humic substances by multiple hydrogen bindings (Piccolo et al., 1996). Additionally, soil organic matter seems to have an indirect effect by blockage of sorption sites (Vereecken, 2005). This shows that the transferability of the measured K_{OC} value to other

soils must be seen critical, but seems to be justified for different soil horizons of one soil profile with the same soil genesis.

The sorption isotherm was also well fitted with a Freundlich isotherm (Fig. 2.8) with values for the Freundlich adsorption coefficient K_f and the Freundlich exponent n_f of 24.7 L kg⁻¹ and 0.943. Values for K_f and n_f of 59.0 L kg⁻¹ and 0.787 were reported by de Jonge et al. (2000) for a coarse sand.

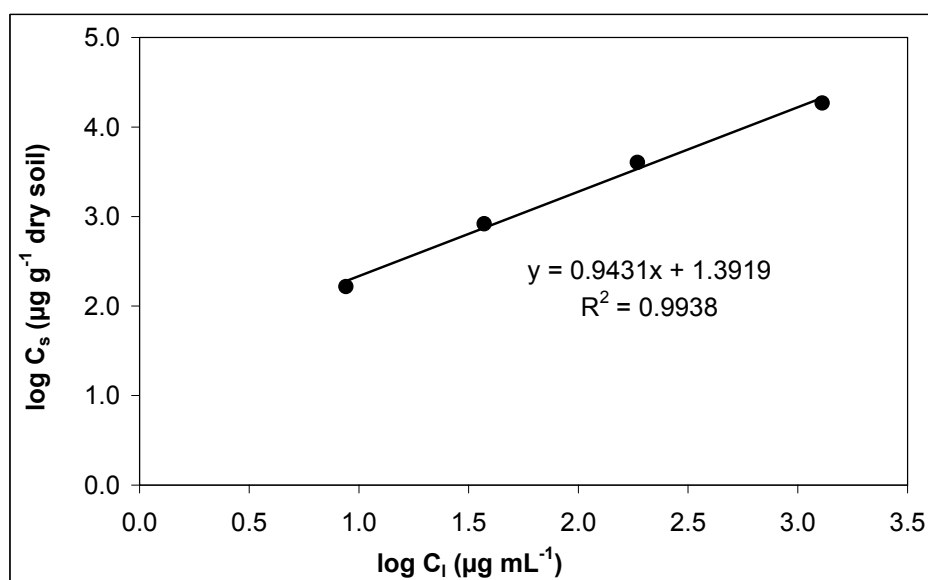


Fig. 2.8: Freundlich sorption isotherm for glyphosate in the upper soil horizon of LM 5.

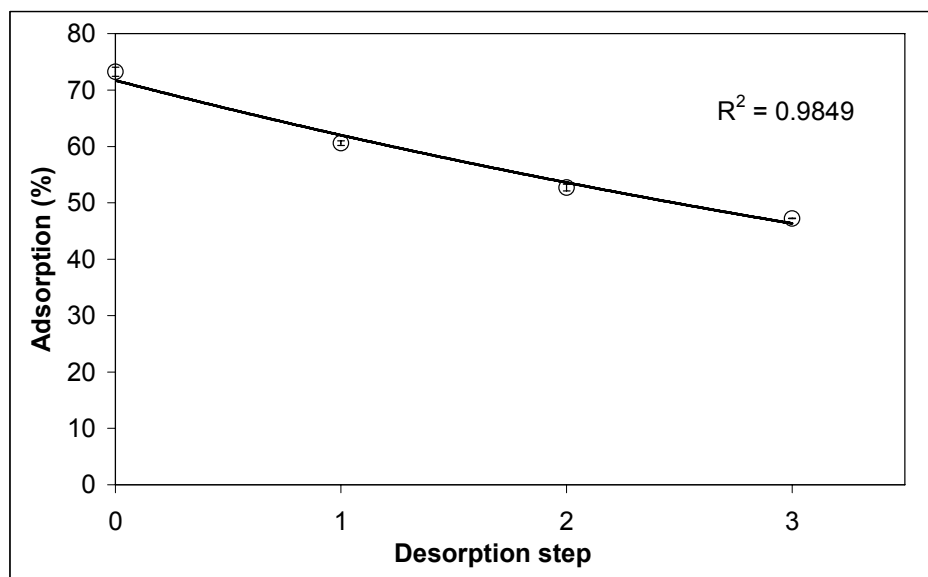


Fig. 2.9: Desorption of glyphosate from the soil material of the upper soil horizon of LM 5.

The desorption process is also important since it determines the potential mobility (Boivin et al., 2005) and the amount of pesticide available for the degradation process. Taking into account that the desorption occurs with a limited degree of reversibility the desorption of

glyphosate from the soil material of LM 5 (Fig. 2.9) can be described by an exponential function ($dC_s/dt = -K_{f-de}C_t$ with K_{f-de} ($L\ kg^{-1}$) the Freundlich desorption coefficient).

2.3.3 Mass balance

As already discussed, biodegradation studies with ^{14}C -labelled glyphosate allow the characterisation of the mass balance of the herbicide in the soil and the distinction between mineralization, volatilization and formation of extractable and non extractable residues under controlled test conditions. An estimation of the mass balance was done at the end of the biodegradation experiments by combustion of the soil samples and quantification of the evolved $^{14}CO_2$ (Table 2.7).

Table 2.7: Glyphosate mineralization and volatilization, formation of extractable and non extractable residues and mass balance in the biodegradation experiments in percent of applied ^{14}C

soil and test conditions	mineralization (%)	volatilization (%)	extr. and non-extr. residues (%)	balance (%)	n*
LM 1	39.29 (\pm 2.01)	0.114 (\pm 0.026)	45.13 (\pm 1.81)	84.53 (\pm 3.36)	4
LM 2	12.67 (\pm 0.45)	0.044 (\pm 0.013)	71.37 (\pm 6.90)	84.08 (\pm 6.49)	7
LM 2 inoc.	28.09 (\pm 2.07)	0.019 (\pm 0.007)	60.75 (\pm 1.06)	88.86 (\pm 1.22)	3
LM 3 (60,(1+4))	53.64 (\pm 1.32)	0.105 (\pm 0.011)	32.51 (\pm 0.47)	86.25 (\pm 1.15)	8
LM 4	44.96 (\pm 1.53)	0.034 (\pm 0.021)	40.68 (\pm 0.73)	85.67 (\pm 1.29)	4
LM 5 (30)	24.86 (\pm 0.75)	0.006 (\pm 0.005)	65.35 (\pm 1.14)	90.21 (\pm 1.46)	3
LM 5 (40,50,60,(1+4))	27.39 (\pm 1.96)	0.024 (\pm 0.046)	60.66 (\pm 3.78)	88.07 (\pm 3.37)	20
LM 5 inoc.	36.06 (\pm 0.54)	0.010 (\pm 0.005)	45.53 (\pm 0.73)	81.60 (\pm 0.18)	3

* n: number of samples

Because the laboratory biodegradation experiments were only used for the calibration of the degradation model, the differentiation between extractable and non extractable residues and the quantification of glyphosate and AMPA in the extracts was not done. Mean recovery reached in the biodegradation experiments was 86.87 % (\pm 3.89) (Table 2.7). The amount of volatile organic ^{14}C -compounds evolved was negligibly small ($<$ 0.12 %) for all soils as reported by others (von Wiren-Lehr et al., 1997). Variability of mineralization was high and ranged between 12.67 % (LM 2) and 53.64 % (LM 3) of the applied ^{14}C -glyphosate, while glyphosate residues amounted 32.51 % to 71.37 % for all experiments.

In the work of Stenrød et al. (2006) a small mean recovery of 87 % (\pm 4) was also documented. A possible explanation for these suboptimal recovery rates would be the

formation of volatile formaldehyde in the degradation process. But as reported by Monsanto (2005) formaldehyde is not a major degradate of glyphosate in the environment, although glyphosate can be selectively oxidized under certain laboratory conditions to form aqueous formaldehyde.

2.4 Conclusions

In the biodegradation experiments a large variability for glyphosate mineralization was observed between the five different soils. After 41 days 12.8 to 56.6 % of the applied ¹⁴C-glyphosate were mineralized. The results indicate that the variability in degradation was linked to the variability in soil microbial biomass, as a clear positive correlation between microbial biomass and degradation of glyphosate in the laboratory batch experiments was deduced. After multiple applications of glyphosate no adaptation or inhibition of the degrading microbial community could be noticed. An acceleration of degradation in soils with low degradation rates could be observed after inoculation of the soil samples with soil material of another soil with high mineralization capacity. The variation of soil moisture contents in the biodegradation experiments between 40 to 60 % of the max. WHC had no influence on the degradation rates. Primal, at a water content of 30 % of the max. WHC a clear reduced degradation (7.8 %) could be observed. Glyphosate shows a relatively rapid degradation in soil and high adsorption to soil matrix ($K_{OC} = 1287.4 \text{ dm}^3 \text{ kg}^{-1}$). The recovery of glyphosate in the biodegradation experiments was lower than expected and further research to explain this discrepancy in mass balance is necessary.

Pesticide fate models are highly sensitive to parameters controlling biodegradation and sorption. The conducted experiments are therefore useful to generate appropriate input values in dependence on environmental conditions for the subsequent fate modelling of glyphosate in chapter 4.

3 Water flow and assessment of water balance on four undisturbed field soil lysimeters

3.1 Introduction

A challenge of water transport modelling in soil is the assessment of various uncertainties resulting from input data, from parameterisation of soil hydraulic characteristics and from estimation of sink terms like plant water uptake and soil evaporation. In the mathematical modelling of water transport the characterisation of soil water retention and hydraulic conductivity curves did receive much attention (Cornelis et al., 2001; Acutis and Donatelli, 2003; Givi et al., 2004). Because soil water transport strongly depends on available water amounts, the influence of water retention characteristics on water balance simulations must be studied together with the influence of evapotranspiration models.

Evapotranspiration is one of the most critical parameters and the one with the greatest impact on water losses (Rana and Katerji, 2000; Eitzinger et al., 2004). Evapotranspiration model estimates and field measurements vary widely. For the estimation of evapotranspiration usually the potential evapotranspiration (ET_p) is calculated using methods driven by meteorological data and vegetation characteristics. These estimates are scaled down to actual evapotranspiration (ET_a) based on limitations in available soil water (Fisher et al., 2005). ET_p is defined as the evapotranspiration flux from the soil-plant system under well-watered soil conditions (i.e. soil at or close to field capacity). Following Fisher et al. (2005) two types of ET_p modelling approaches can be distinguished: reference-surface ET_p that would occur from a land surface specified as a reference crop (e.g. grass) and surface-dependent ET_p that would occur from any of a variety of designated land surfaces.

Soil water transport models combined with plant-growth models enable a reasonable partitioning of calculated ET_a into actual evaporation (EV_a) and actual transpiration (TR_a). This part of the work describes the simulation of actual evapotranspiration and leaching by the modular modelling system *Expert-N* (Engel and Priesack, 1993; Stenger et al., 1999; Priesack et al., 2001; Priesack, 2006), which allows the combination of different ET_p models with various simulation models of water transport and plant growth. Within the present work the Penman-Monteith dual crop coefficient approach (Allen, 2000) was additionally implemented in *Expert-N*.

The objective is to evaluate different modelling approaches for the estimation of soil hydraulic characteristics and evapotranspiration and to assess their influence on percolation simulations. A dataset from a lysimeter facility in South-Germany with rotative crop

vegetations over five years was used to perform the analysis. Additionally, a direct and an indirect approach for the evaluation of daily evapotranspiration fluxes were compared using a dataset of a further year.

3.2 Materials and Methods

3.2.1 The dataset

3.2.1.1 GSF-lysimeter facility

The lysimeter facility of the GSF-National Research Centre of Environment and Health is located in Neuherberg, Munich (latitude 48° 13' N, longitude 11° 35' E and altitude 484 m NN). The mean annual sum (1961-1990) of precipitation is 804 mm and the mean annual temperature is 7.8 °C. 48 field lysimeters (stainless steel) with 2 m depth and 1 m² surface can be installed on the facility, which is surrounded by an agricultural field of size 1 ha. Each lysimeter is equipped with 48 sampling ports (Fig. 3.1) for soil solution samplers, tensiometers and time domain reflectometry (TDR).

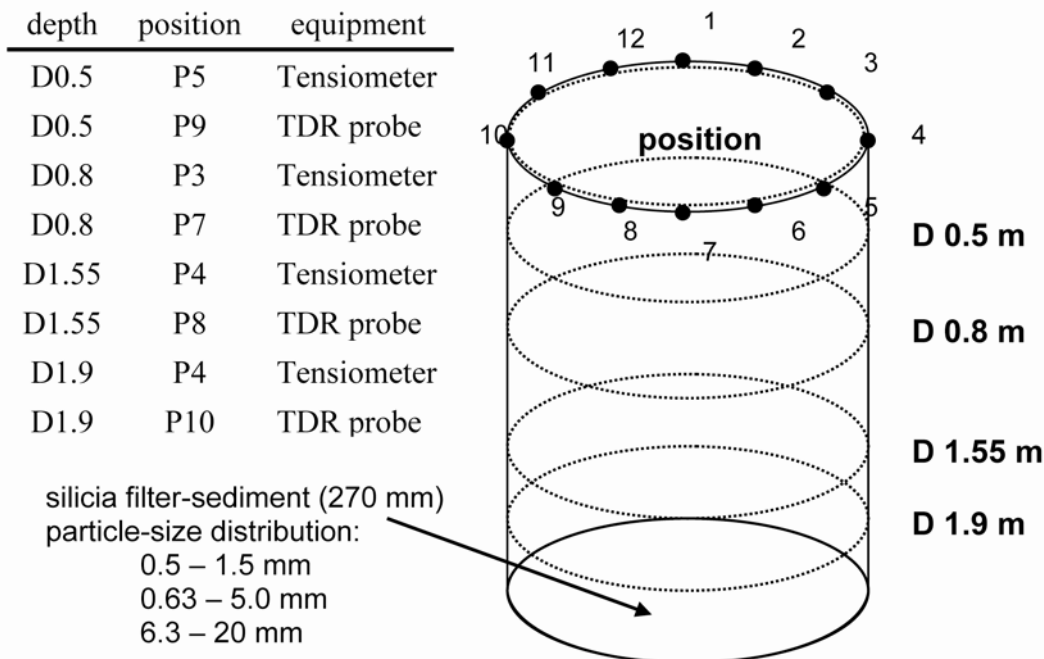


Fig. 3.1: Sensor positions of tensiometer and TDR probes in the lysimeters.

The scales of the lysimeters have a capacity of 6 Mg (UMS GmbH, Munich, Germany) and can detect a mass change of ± 100 g, equivalent to ± 0.1 mm of water on the surface. Three electronic load cells (type TEDEA 3510-C3) are installed in angles of 120° on each lysimeter basement. The single measurements of each load cell are summed to the total lysimeter

weight. Until the middle of the year 2002 the data logger system of the lysimeter scales was working event dependent, which means that 10 min values were only recorded, if a change in value was registered. This method resulted in the problems described in section 3.3.1. From September 2002 on the data logger system was changed and the weight values were logged continuously every 10 minutes. The scales of the leachate catchment tanks (tank size 60 L) consist of one load cell and can detect a mass change of ± 10 g. Generally, both TDR probes (type TRIME-MUX6, distance between rods 20 mm, length 110 mm; IMKO GmbH, Ettlingen, Germany) and tensiometers (type T6-ti, \varnothing 24 mm, length 60 mm; UMS GmbH, Munich, Germany) are horizontally installed at 0.5, 0.8, 1.55 and 1.90 m depth (Fig. 3.1). Additionally, a diagonal TDR probe and a tensiometer are placed at 0.3 m.

Until November 2002 no climate station was installed on the lysimeter facility. From July 2003 on the first time continuous, reliable climate data were available. This fact makes the generation of reliable model input parameters difficult and water balance calculations on a daily basis until July 2003 impracticable.

Therefore, diurnal climate data (maximum, minimum and mean air temperature, mean relative humidity, mean wind speed, total global radiation) measured at the local station of the German National Meteorological Service (DWD) in 10 km distance from the lysimeter facility were used for the years 1999 to 2003. In addition precipitation was measured in immediate vicinity to the facility by the GSF-Institute of Hydrology. The meteorological station of the University of Munich (LMU; in 7 km distance) provided data of temperature and relative humidity in resolution of hours for this period.

In the water balance equation the actual evapotranspiration ET_a (mm) within a given period can be then calculated from the lysimeter measurements by

$$ET_a = PR - DR - \Delta W \quad (3.1)$$

considering in this way that ET_a includes evaporation from soil and plant transpiration and also evaporation from the interception reservoir. PR (mm) denotes the precipitation (including irrigation), DR (mm) the percolation amount and ΔW (mm) the change in lysimeter weight during this period, which corresponds to the change in soil water and interception storage. Run-off can be neglected for the lysimeter construction applied for the experiments of the present work.

The measurements of lysimeter weight, weight of the leachate catchment tank, TDR-sensors, tensiometer, and of the climate station are available as uncontrolled and uncorrected hourly values in the lysimeter database *LysiVisu*. In Fig. 3.2 measurements of TDR-sensors and tensiometers graphical displayed by *LysiVisu* are exemplarily shown for LM 5.1 (equivalent

to lysimeter 41 in the graphic) and LM 2 (equivalent to lysimeter 46) in 50 cm depth. It is shown a decreasing water content (volumetric) and the related increasing water potential. In the following chapters the description water content (WC) always denotes the volumetric water content.

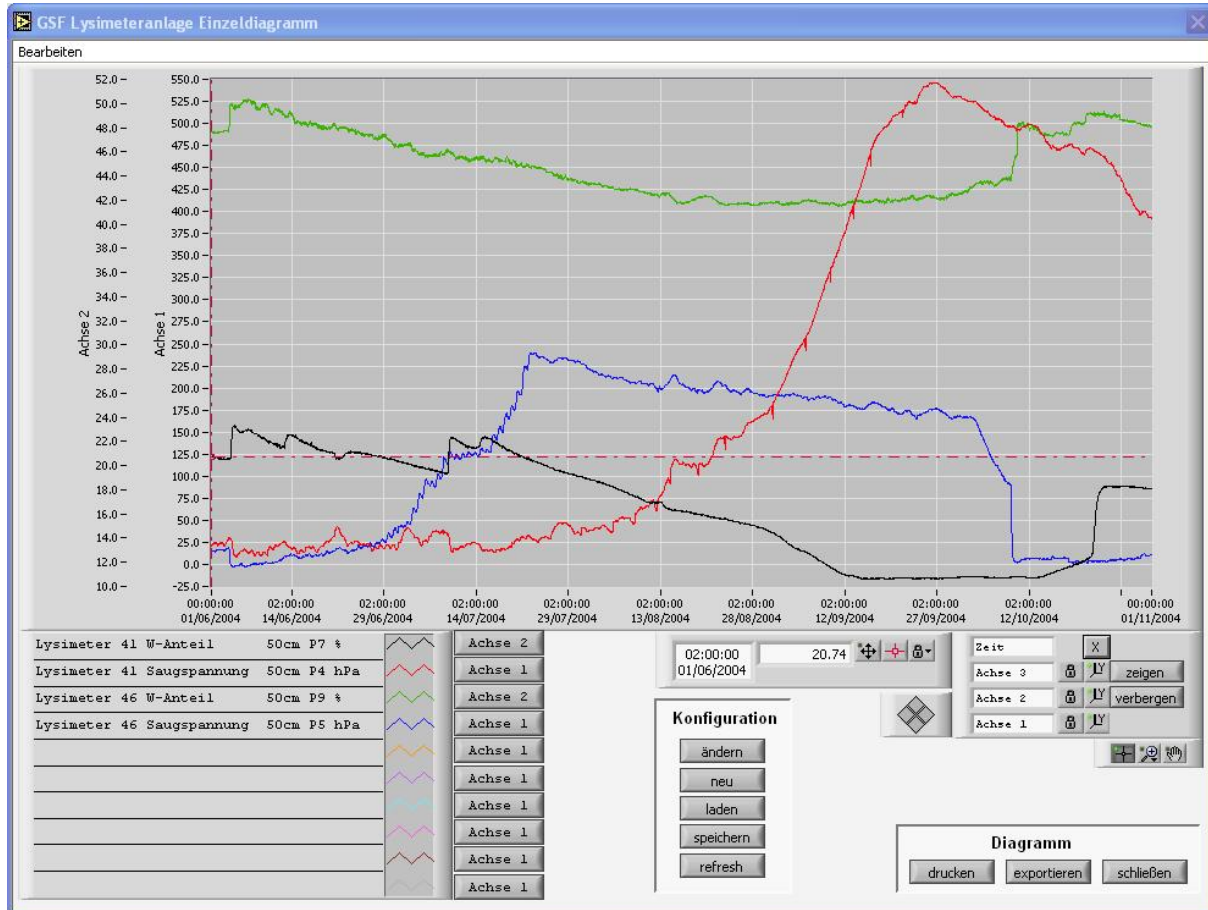


Fig. 3.2: An example of data from measurements of TDR-sensors and tensiometers, graphical displayed by *LysiVisu*.

3.2.1.2 Soil properties and planting

Daily percolation data from four lysimeters (LM 1 – LM 4) that were filled with undisturbed soils (since 1996) representing four different soil types of Southern Bavaria (the regional provenance of the soils is given in (Table 3.1) were investigated. For each soil type of LM 1 and LM 2, two other lysimeters provided weekly percolation measurements, which resulted in three replicates of weekly measurements. Until 1999 the data were deficient and were therefore not analysed.

From 1999 to 2003 a three-course crop rotation (maize, winter and summer wheat, summer barley, plus mustard as green manure after wheat and barley) was grown on the lysimeters. Crop and fertilization management were the same as on the surrounding agricultural field. The soil properties and some hydraulic characteristics are described in Table 3.1.

Table 3.1: Soil properties and hydraulic characteristics for soil monoliths in LM 1 – LM 4

Soil Type Site	Horizon depth (cm)	Bulk density (kg dm ⁻³)	Clay (%)	Silt (%)	Sand (%)	θ_{sat} (mm ³ mm ⁻³)	K_{sat} (mm d ⁻¹)
LM 1	0-30	1.55	11	19	70	0.37	102
Humic Cambisol	30-80	1.49	12	13	75	0.39	381
Kelheim	80-200	1.62	6	46	48	0.40	308
LM 2	0-40	1.58	22	60	18	0.38	94
Mollic Gleysol	40-90	1.32	29	61	10	0.48	1604
Scheyern	90-200	1.46	28	65	7	0.43	777
LM 3	0-50	1.62	33	34	33	0.36	232
Calcaric Regosol	50-200*	1.80	0	0	0	0.15	3548
Feldkirchen							
LM 4	0-30	1.55	13	19	68	0.37	101
Aric Anthrosol	30-70	1.65	9	21	70	0.32	64
Hohenwart	70-100	1.85	5	14	81	0.15	47
	100-200	1.60	1	4	95	0.33	2260

* no analysis were carried out for particle size distribution, because of gravel content > 75 %

θ_{sat} saturated vol. water content

K_{sat} saturated hydraulic conductivity calculated by Brutsaert-Gardner approach (Vereecken et al., 1990)

3.2.1.3 Methods to obtain water storage changes

For the reason that until September 2002 evapotranspiration on the lysimeters could not be evaluated directly from the lysimeter weight by water balance calculations, single infiltration and drying cycles were studied in detail to support data analysis. For the infiltration dynamics the water storage change in mm per time sequence in the top 30 cm was calculated by multiplying the horizon thickness (mm) by the first derivative of the water content with respect to time as proposed by Evett et al. (1993). Estimates of infiltration rates in the lysimeters were obtained by water content changes measured by TDR in 30 cm. For the modelled storage change the same method was applied as for the calculated water contents. This method implies that for the top 30 cm the infiltration process proceeds as homogenous wetting front. For the reason that the assumption of a homogenous drying front in the top 30 cm does not hold true, evapotranspiration dynamic was calculated by the water balance method and by considering changes in the lysimeter weight. The simulated evapotranspiration amounts were given by the sum of calculated EV_a and TR_a .

3.2.2 Water transport models

The combination of water flow and water balance considerations of an infinitely small soil volume results in the well known Richards equation. Thereby it is assumed that water flow through an unsaturated soil volume can be described by the product of a hydraulic gradient and a water content-dependent hydraulic conductivity i.e. by Darcy-Buckingham's law:

$$C_w(h) \frac{\partial h}{\partial t} = \frac{\partial}{\partial z} \left[K(h) \left(\frac{\partial h}{\partial z} + 1 \right) \right] - \phi_w \quad (3.2)$$

where C_w (mm^{-1}) is the water capacity ($C_w(h) = \partial\theta/\partial h$ with θ ($\text{mm}^3 \text{mm}^{-3}$) the volumetric water content and h (mm) the matric potential). K (mm d^{-1}) is the unsaturated hydraulic conductivity, z (mm) the vertical coordinate taken positively upward, t (d) time and ϕ_w ($\text{mm}^3 \text{mm}^{-3} \text{d}^{-1}$) the soil water extraction rate by plant roots.

3.2.2.1 Model configuration

The *Expert-N* model system comprises a number of modules that provide various simulation approaches (see section 5.1). In the present study soil water flow simulations are based on Richards equation using the numerical solution according to the model HYDRUS 6.0 (Simunek et al., 1998). Run-off is not considered. Snow processes are regarded according to Schulla and Jasper (2000). At the lower boundary free drainage is assumed according to Hutson and Wagenet (1992). In a freely draining profile the hydraulic potential gradient is approximately unity. The effect of the lower boundary condition on water and solute transport in lysimeters is discussed in further detail by Flury et al. (1999). The estimation of ET_a is described below. Heat transfer, N-transport and N-turnover are simulated following the approaches of the model LEACHM (Hutson and Wagenet, 1992). For the simulation of crop development and crop growth the generic plant model CERES (Jones and Kiniry, 1986; Ritchie, 1991) is applied. The phenological parameters needed by the crop growth model were adapted to field data collected at the FAM research station near Munich, South Germany (Schröder et al., 2002) and were not further calibrated for the present lysimeter study.

3.2.2.2 Water retention and hydraulic conductivity functions

The simulation of water transport by means of the Richards equation needs information on the retention and the hydraulic conductivity curve. For the GSF-lysimeters only reliable measurements of the retention curves were available. Jarvis et al. (2002) pointed out that predicting near-saturated hydraulic conductivity by pedotransfer-functions (ptfs) remains difficult and uncertain, because of high variation in the pore structure of arable soils due to

loosening by tillage, subsequent consolidation and the formation of surface seals. However, in the absence of any direct measurements ptf's were used to calculate the hydraulic conductivity function.

As expected a large variability in the field measured retention curves was found (given later in section 3.3.2.1 in Fig. 3.4). This variability was probably caused by hysteresis effects, soil heterogeneity and especially for the silty loam (LM 2) by various shrink- and swelling processes during the year. Therefore, the measured curves were only used to estimate the saturated volumetric water content θ_{sat} (cp. Table 3.1), all other parameters of the retention and unsaturated hydraulic conductivity curves were estimated using ptf's.

Field capacity is the volumetric water content of the soil after wetting and initial (1 - 3 days) redistribution and is usually defined as the volumetric water content at a soil moisture suction of 10 kPa. Permanent wilting point (or simply wilting point) is usually reached if plants do not recover at night and wilt permanently and if the soil moisture suction has a value of about 1600 kPa (van Laar et al., 1997). Field capacity and wilting point which are necessary input parameters for the plant growth model were estimated by the predicted water retention curve. This seems useful since in the case of the wilting point the correlation between observed and simulated values was satisfactory for most of the tested ptf's. The same held true for the field capacity if organic matter was also included as input for the ptf's and if the ptf's were applied to soils that have similar characteristics as the soils from which the functions were derived (Givi et al., 2004). Two approaches for the parameterisation of the soil hydraulic characteristics were compared.

Hutson & Cass – Burdine approach

Following the approach of Hutson & Cass (1987) the water retention function can be written as

$$\theta(h) = \begin{cases} \theta_{sat} (h/a)^{-1/b} & \text{if } h < h_i \\ \theta_{sat} \left[1 - (h/a)^2 (2b)^{-1} (h_i/a)^{-2-1/b} \right] & \text{if } 0 \geq h \geq h_i \end{cases} \quad (3.3)$$

with the matric potential $h_i = a[2b/(1+2b)]^{-b}$ (mm) at the inflexion point and where θ_{sat} ($\text{mm}^3 \text{mm}^{-3}$) denotes the saturated water content. The variables a (mm) and b (-) are empirical parameters, where a is the matric potential at the air entry value.

The model of Burdine (1953) was applied to predict the unsaturated soil hydraulic conductivity from the retention function, resulting in the following equation for the conductivity function:

$$K = \begin{cases} K(h) = K_{sat} (h/a)^{-2-3/b} & \text{if } h < h_i \\ K(\theta) = K_{sat} (\theta/\theta_{sat})^{2b+3} & \text{if } \theta \geq \theta_i, \text{ i.e. } h \geq h_i \end{cases} \quad (3.4)$$

where a and b are parameters as in Eq. (3.3) and K_{sat} (mm d^{-1}) is the saturated hydraulic conductivity.

K_{sat} and the parameters a and b can be estimated by the following ptf (Campbell, 1985):

$$K_{sat} = 3.9 \cdot 10^{-5} (1.3/\rho_s)^{1.3b} \exp(-6.9f_{clay} - 3.7f_{silt}) \quad (3.5)$$

$$a = -0.5 d_g^{-1/2} (\rho_s/1.3)^{0.67b} \quad (3.6)$$

$$b = d_g^{-1/2} + 0.2\sigma_g \quad (3.7)$$

where f_{clay} (-) and f_{silt} (-) are the fraction of clay and silt and ρ_s (mg mm^{-3}) is the soil bulk density. For a detailed description of the geometric mean particle diameter d_g (mm) and its standard deviation σ_g (mm), see Shirazi and Boersma (1984).

Brutsaert – Gardner approach

In the second approach for the water retention function the model of Brutsaert (1966) was used, which is a previous version and a special case ($m = 1$) of the van Genuchten (1980) function

$$\theta(h) = \theta_{res} + (\theta_{sat} - \theta_{res}) [1 + (\alpha_w |h|)^n]^{-m} \quad (3.8)$$

where θ_{res} ($\text{mm}^3 \text{mm}^{-3}$) denotes the residual water content and α_w (mm^{-1}), n (-) and m (-) are empirical parameters. For the unsaturated hydraulic conductivity Gardner (1958) proposed a parameterisation depending on the soil pressure head (Vereecken et al., 1990):

$$K(h) = K_{sat} \frac{1}{1 + A|h|^B} \quad (3.9)$$

with the empirical parameters A (mm^{-1}) and B (-).

Similar to the ptf of Campbell, Scheinost et al. (1997) have used information on particle-size distribution, bulk density and organic carbon content to develop a ptf for Brutsaert's (1966) parameterisation of the retention function.

$$\theta_{res} = 0.52 f_{clay} + 1.6 f_{Corg} \quad (3.10)$$

$$\alpha_w = 0.00025 + 0.0043 d_g \quad (3.11)$$

$$n = 0.39 + 2.2 \sigma_g^{-1} \quad (3.12)$$

where f_{Corg} (-) is the fraction of organic carbon and d_g (mm) the geometric mean particle diameter and its standard deviation σ_g (mm), in this case according to Shirazi and Boersma (1988). The ptf of Scheinost is based on experimental data from the FAM research station near Munich, from where the loamy soil for LM 2 was taken.

Saturated hydraulic conductivity and parameters A and B (K_{sat} here in (cm d⁻¹)! and A in (cm⁻¹)!) for the hydraulic conductivity function according to Gardner (1958) were obtained using the following ptf of Vereecken et al. (1990):

$$\log(K_{sat}) = 11.04 - 0.96 \log(f_{clay}) - 0.66 \log(f_{sand}) - 0.46 \log(f_{Corg}) - 8.43 \rho_s \quad (3.13)$$

$$\log(A) = -2.64 - 1.90 f_{sand} + 5.0 f_{clay} + 0.51 \log(K_{sat}) \quad (3.14)$$

$$\log(B) = 0.07 - 0.19 \log(f_{clay}) - 0.05 \log(f_{silt}) \quad (3.15)$$

where f_{sand} (-) is the fraction of sand. The calculated values for K_{sat} are listed in Table 3.1.

3.2.2.3 Models of potential and actual evapotranspiration

For the estimation of reference-surface ET_p the Penman and Penman-Monteith grass reference method (denoted as PM grass) and for the estimation of surface-dependent ET_p the Penman-Monteith dual crop coefficient (denoted as PM crop) and the empirical approach of Haude were compared.

Reference-surface ET_p methods

According to Penman (Penman, 1948; VDI, 1993) the daily potential evapotranspiration ET_p^{day} (mm d⁻¹) was calculated by:

$$ET_p^{day} = \frac{1}{L} \frac{\Delta(R_{ns} - R_{nl})}{\Delta + \Gamma} + \frac{\Gamma(e_s(T) - e_a) f(v)}{\Delta + \Gamma} \quad (3.16)$$

where L (MJ m⁻² mm⁻¹) is the specific heat of evaporation, Δ (hPa K⁻¹) the derivative of saturated vapour pressure versus temperature, R_{ns} and R_{nl} (MJ m⁻² d⁻¹) are short- and long-wave radiation. Γ (hPa K⁻¹) denotes the psychrometric constant and e_s and e_a (hPa) denote

saturated and actual vapour pressure. The function $f(v)$ ($\text{mm d}^{-1} \text{ hPa}^{-1}$) describes the dependency of evaporation on wind (VDI, 1993).

The Penman-Monteith equation (Allen et al., 1998; Allen, 2000) for predicting ET_p for a hypothetical grass reference crop with crop height of 0.12 m, a fixed surface resistance of 70 s m^{-1} and an albedo of 0.23 has the form:

$$ET_p^{day} = \frac{0.408\Delta(R_n - G) + \Gamma \frac{900}{T + 273} u_2 (e_s(T) - e_a)}{\Delta + \Gamma(1 + 0.34u_2)} \quad (3.17)$$

where R_n ($\text{MJ m}^{-2} \text{ d}^{-1}$) is the net radiation at the crop surface, G ($\text{MJ m}^{-2} \text{ d}^{-1}$) the soil heat flux density and u_2 the wind speed at 2 m height (m d^{-1}).

Surface-dependent ET_p methods

For the calculation of the newly implemented Penman-Monteith dual crop coefficient method the daily potential evapotranspiration (here denoted as ET_{p0} , see Eq. 3.17) was multiplied by a specific crop coefficient K_c (-):

$$ET_{pC}^{day} = K_C ET_{p0}^{day} \quad (3.18)$$

The K_C -coefficient is the sum of the basal crop coefficient K_{Cb} (-) and the soil water evaporation coefficient K_e (-), which represents the evaporation from wet soil. Because of energy limitations the sum of K_{Cb} and K_e cannot exceed the value of the maximum coefficient K_{Cmax} (-). For the calculation of the basal crop coefficient the different growth stages of the plants must be specified (Table 3.2). It was decided to realise the differentiation of the crop growth stages in *Expert-N* in the following way:

Table 3.2: Crop growth stages and differentiation categories

Crop growth stage	Differentiation scheme
Initial stage	planting date to 10 % ground cover equivalent to $LAI^* = 0.25$
Crop development stage	$LAI = 0.25$ to full ground cover equivalent to $LAI = 3.0$
Mid season stage	$LAI = 3.0$ to plant development stage “start of senescence”
Late season stage	“start of senescence” to plant stage “harvest”

* LAI denotes Leaf Area Index

For a detailed description of the basal crop coefficient considering the different growth stages of the plants and related coefficients K_e and K_{Cmax} , see the FAO-56 publication (Allen et al.,

1998; Allen, 2000). When the soil is wet, the daily potential evaporation EV_p^{day} (mm d⁻¹) can be described by

$$EV_p^{day} = \min\left\{\left(K_{C_{max}} - K_{C_b}\right)(1 - f_{sc})K_{C_{max}}\right\}ET_{p0}^{day} \quad (3.19)$$

and the daily potential transpiration TR_p^{day} (mm d⁻¹) by

$$TR_p^{day} = \max\left\{K_{C_b}, f_{sc}K_{C_{max}}\right\}ET_{p0}^{day} \quad (3.20)$$

where f_{sc} (-) denotes the soil cover fraction.

In the approach of Haude, which is the most popular in Germany (Bormann et al., 1996), the ET_p^{day} is calculated from the atmospheric vapour pressure deficit at 14³⁰ CET. The deficit was derived from the relative humidity and the air temperature in 2 m height:

$$ET_p^{day} = f_{Haude}[e_s(T) - e_a]_{1430} \quad (3.21)$$

where f_{Haude} (mm d⁻¹ hPa⁻¹) is a monthly, crop dependent factor. In this study the factor f_{Haude} was chosen for wheat, barley, maize and for the fallow periods (bare soil: $f_{Haude} = 0.11$ mm d⁻¹ hPa⁻¹) according to the German VDI guideline (1993). For mustard the same values are used as for wheat. Instead of taking the vapour pressure deficit at 14³⁰ CET, the maximum temperature and the mean daily humidity, in a second approach, were used in the simulations (denoted as Haude (mrH)). This resulted in a lower potential daily evapotranspiration compared to the original approach according to Haude (1955), because the mean daily humidity is generally lower than that at 14³⁰ CET.

With exception of PM crop method (see Eq. 3.19 and 3.20), for all approaches the daily ET_p^{day} was partitioned into EV_p^{day} and TR_p^{day} according to a modification of the approach of Droogers (2000):

$$EV_p^{day} = (1 - f_{sc})ET_p^{day} \quad (3.22)$$

$$TR_p^{day} = f_{sc}ET_p^{day} \quad (3.23)$$

The actual evaporation was simulated by limiting the potential evaporation by the maximal water flux q_{max} (mm d⁻¹) at time t (d) from the top soil segment (Hutson and Wagenet, 1992).

The actual evapotranspiration EV_a was then calculated by

$$EV_a = \min(EV_p; q_{max}\Delta t). \quad (3.24)$$

According to the plant model CERES (Ritchie, 1991) the actual transpiration was simulated by

$$TR_a^{day} = \min(TR_p^{day}, R_p^{day}) \quad (3.25)$$

with R_p^{day} (mm d⁻¹) being the daily potential root water uptake which results from actual soil water content and maximum water uptake rate per unit root length (Jones and Kiniry, 1986).

3.2.2.4 Statistical analysis

In order to assess adequacy of model simulations in relation to measurements, the statistical measures model efficiency (EF), correlation coefficient (r) and root mean square error (RMSE) were used, as suggested by Loague and Green (1991). The maximum and ideal value for EF is 1.0, while a negative value indicates that model predictions are worse than using the observed mean as an estimate of the data points. In addition to statistical measures graphical displays can be useful for showing trends, types of errors, and distribution patterns (Loague and Green, 1991). Analysis was focused on daily percolation values, because they represent the most reliable factor in water balance measurements in the present work. For the examination of percolation dynamics especially time dependent distribution patterns are of importance. For this reason graphical presentations and total percolation and evapotranspiration amounts per year were emphasised. The goodness-of-fit for the water retention curves was supplementarily compared by RMSE values. Modelling efficiency and correlation coefficient were used to evaluate the accuracy of simulations for longer periods of more than one year.

3.3 Results and Discussion

3.3.1 Direct and indirect evaluation of evapotranspiration

Lysimeter weight measurements are often exposed to external disturbances. A daily and direct evapotranspiration measurement by water balance calculation as described in Eq. (3.1) is only feasible if weight measurements are continuously provided with high time resolution.

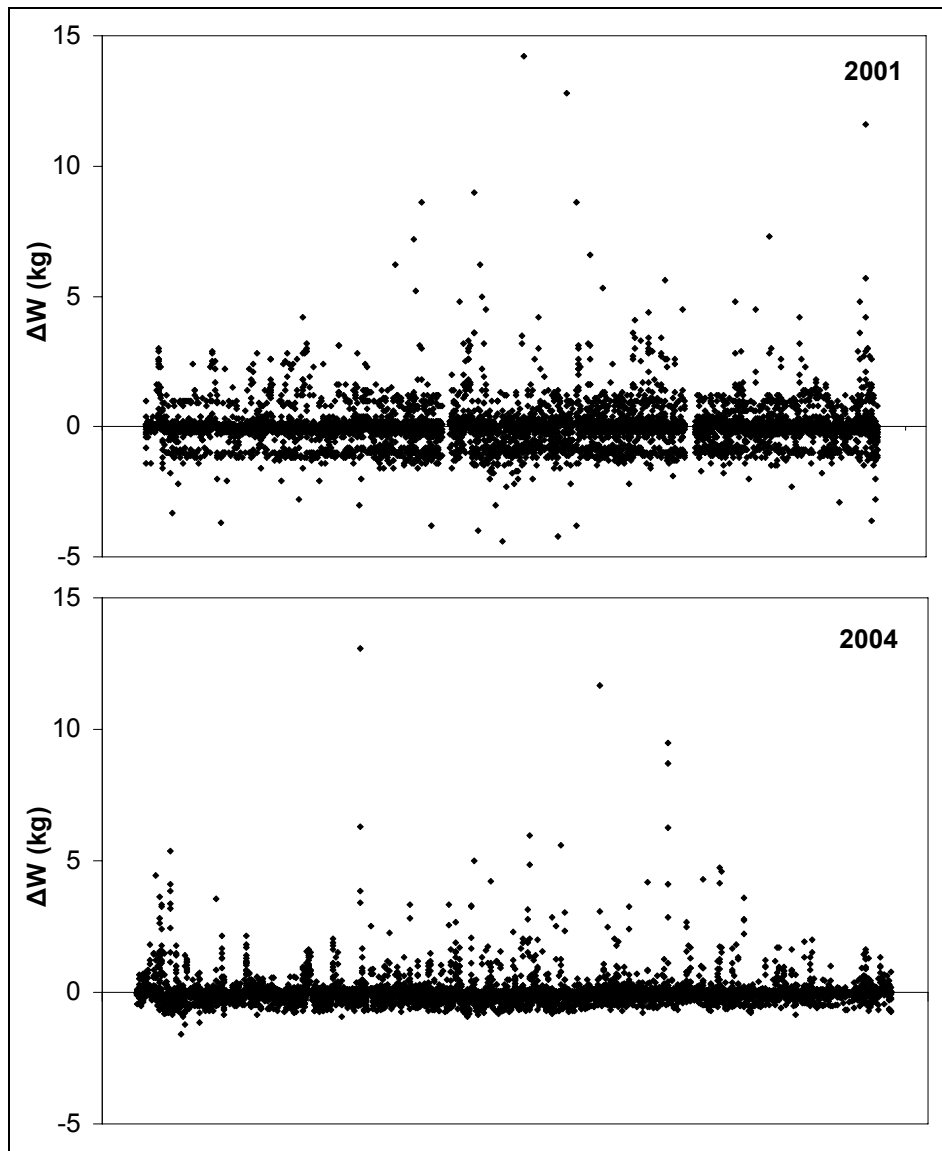


Fig. 3.3: Changes in lysimeter weight ΔW (kg) of LM 1 in the year 2001 and 2004 in hourly resolution.

Fig. 3.3 shows the effects of the event dependent and continuous data logging systems for the lysimeter weight registration in hourly resolution. In the year 2001 precipitation was 944 mm and the sum of the positive weight changes in hourly resolution for LM 1 was 1632 kg which is equivalent to 1632 mm, while in the year 2004 precipitation was 849 mm and the positive change in the lysimeter weight was 869 mm. This small error in 2004 can be explained by

single disturbances that can be corrected. In 2001 the great error can be explained by the system of data registration at the lysimeter facility. Until the year 2001 the data logger registered six values per hour, but only when changes occurred the value was logged. This result in a different mean value per hour compared to a system where all six values were registered. Since the year 2004 six values per hour were constantly registered without event dependency. Thus, the technical requirements of a precise water balance calculation for the GSF-lysimeter facility were fulfilled in the year 2004 for the first time. Precipitation measurements in hourly resolution essentially improve water balance calculations. In Table 3.3 all differences between modelled and measured amounts of relevant water balance terms (according to Eq. (3.1)) between April and November 2004 are shown. The precipitation term cancels out, because precipitation acts as input value.

Table 3.3: Difference (Δ , mm) between simulated and measured percolation (DR), cumulative evapotranspiration (ET_a) and water storage (W) amounts from April to November 2004 with different ET_p modules (hydraulic characteristics by Brutsaert-Gardner)

Model - Measurement	PM grass	Haude (mrH)
LM 1: Δ DR (mm)	-68.67	-17.02
LM 1: Δ ET_a (mm)	48.84	21.05
LM 1: Δ W (mm)	22.99	-0.68
LM 2: Δ DR (mm)	30.92	73.93
LM 2: Δ ET_a (mm)	-36.62	-58.38
LM 2: Δ W (mm)	7.17	-14.01
LM 3: Δ DR (mm)	-3.11	51.18
LM 3: Δ ET_a (mm)	5.82	-40.65
LM 3: Δ W (mm)	-1.28	-9.11
LM 4: Δ DR (mm)	22.74	68.53
LM 4: Δ ET_a (mm)	-58.35	-83.14
LM 4: Δ W (mm)	36.92	16.12

Table 3.3 shows that ΔET_a (Δ is the difference between simulated and measured amounts) corresponds to ΔDR for all four lysimeters. Evapotranspiration is the driving force in the water balance and determines percolation amounts and storage changes as the water flux in the lysimeters is mainly influenced by the flux across the upper boundary (Zurmühl, 1998). In the case that evapotranspiration is moderately over- or underestimated by the model, percolation corresponds in nearly the same amounts (Haude (mrH) LM 1 and 3 and PM grass

LM 2 and 3). If evapotranspiration or percolation is strongly overestimated by the model, discrepancies also occur between the simulated and measured storage terms. This is a consequence of the non-linear relation between soil water contents and unsaturated hydraulic conductivities. Percolation data are easier to measure and unaffected by errors in lysimeter weight measurements, which frequently occur due to soil measurements, tillage, animal activity and wind pressure (Zenker, 2003). The simulated percolation fluxes clearly discriminate between the used evapotranspiration methods. The indirect evaluation approach is useful for the evaluation of cumulative evapotranspiration and percolation amounts. As the correlation between evapotranspiration and percolation is non-linear and percolation occurs with time delay, the indirect approach is not useful for the discrimination of daily evapotranspiration flux rates and for the estimation of the goodness of fit for daily evapotranspiration models. Therefore, the percolation data were used for the indirect evaluation of evapotranspiration on the basis of cumulative water balance estimation necessary for the water transport simulation for the investigated period 1999 to 2003, when direct evapotranspiration measurements were afflicted with inaccuracies.

3.3.2 Percolation and water flow simulations

3.3.2.1 Soil hydraulic properties

Water retention curves were calculated for all lysimeters using the ptf's of Scheinost and Campbell and were compared with data measured in 2001 during the cropped and non cropped periods at the respective lysimeter soils. Fig. 3.4 exemplarily shows the estimated ptf's together with measured data for LM 1 and LM 2 at 30 and 80 cm depth. A sensitivity study of Hupet et al. (2002) shows for soils with different textures that soil water content is quite insensitive to crop parameters, in particular to root water uptake parameters, at least as compared to soil hydraulic parameters. Moreover, results of Musters et al. (2000) illustrate that uncertainties in measured soil water contents were far higher than uncertainties in root water uptake parameters and that uncertainties in uptake parameters hardly affect simulated soil water dynamics. Similar results were observed in the measured water retention curves in the present study. In the course of the measured data no obvious differences can be seen in Fig. 3.4 between the cropped and non cropped season.

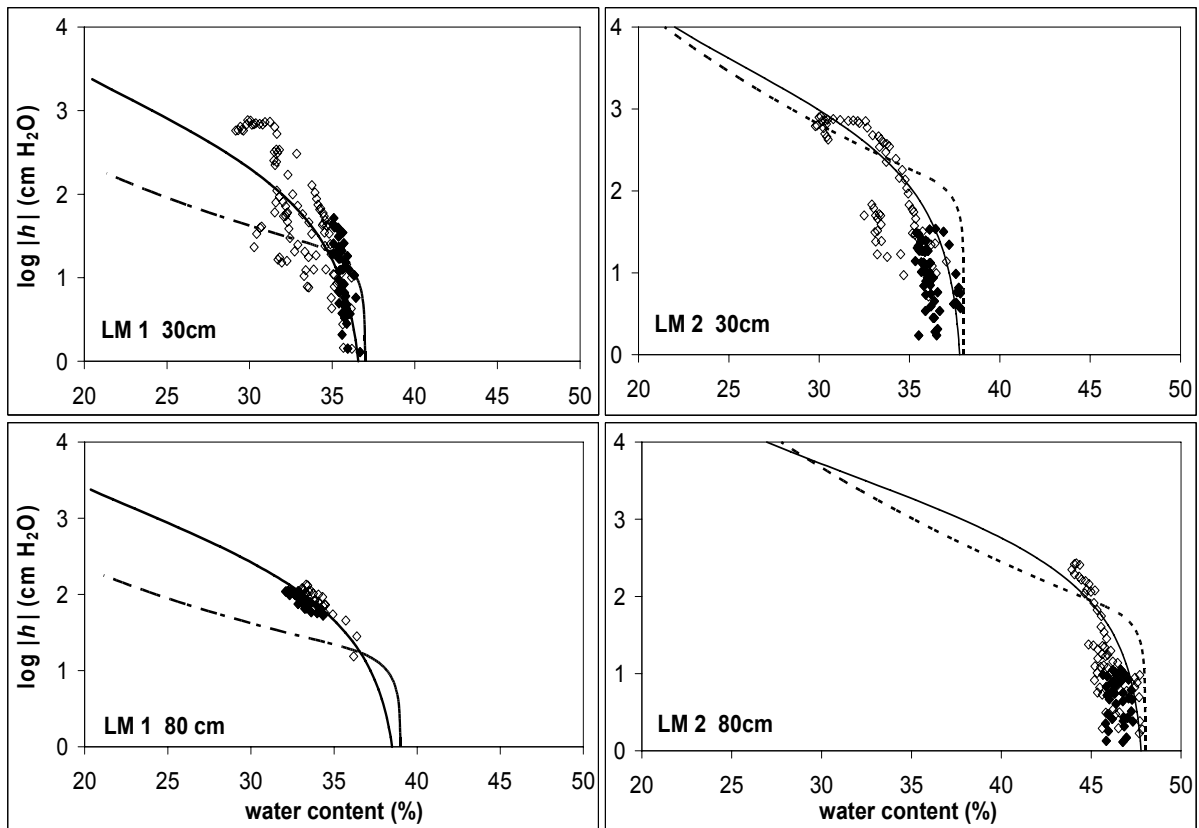


Fig. 3.4: Water retention curves estimated and measured for LM 1 and LM 2 in the year 2001; closed symbols: period of bare soil; open symbols: vegetation period ; solid line: simulated with ptf Scheinost; dotted line: simulated with ptf Campbell.

Fig. 3.4 also shows that the retention curves estimated by the ptf of Scheinost agree reasonable well with the measured retention characteristics. Also for the sandy lysimeter (LM 1) the ptf of Scheinost (e.g. 30 cm RMSE = 139.4) leads to a better representation of the retention data than the Campbell ptf (e.g. 30 cm RMSE = 182.5). This was to be expected as Scheinost developed the ptf in the same geographical area from which the lysimeter soils were taken, since ptf's perform best if calibration data originate from the same area as the evaluation data set (Cornelis et al., 2001). The different parameterisation of the soil hydraulic characteristics has a strong effect on the simulation of water content and percolation dynamics particularly for the loamy soil of LM 2. This is shown for the year 2001 in Fig. 3.5. Here, not only the simulated level between the approaches is different but also the water content dynamics differ considerably (Fig. 3.5a). The water flow simulations using the Brutsaert-Gardner and Hutson & Cass-Burdine functions predicted the measured contents quite well. Only for the time between day 140 and day 162 the simulation underestimated the water content strongly at 30 cm depth for both approaches. The Brutsaert-Gardner approach gave the best agreement with the measured values. For the total annual outflow the simulated results show no difference between the two methods applied for the sandy and the loamy soil

(Table 3.4), whereas the observed high percolation peaks are only reproduced by using the Brutsaert-Gardner method (Fig. 3.5b). For the sandy soil the differences were negligible small and resulted in a slight increase of percolation peaks with Brutsaert-Gardner (results not shown).

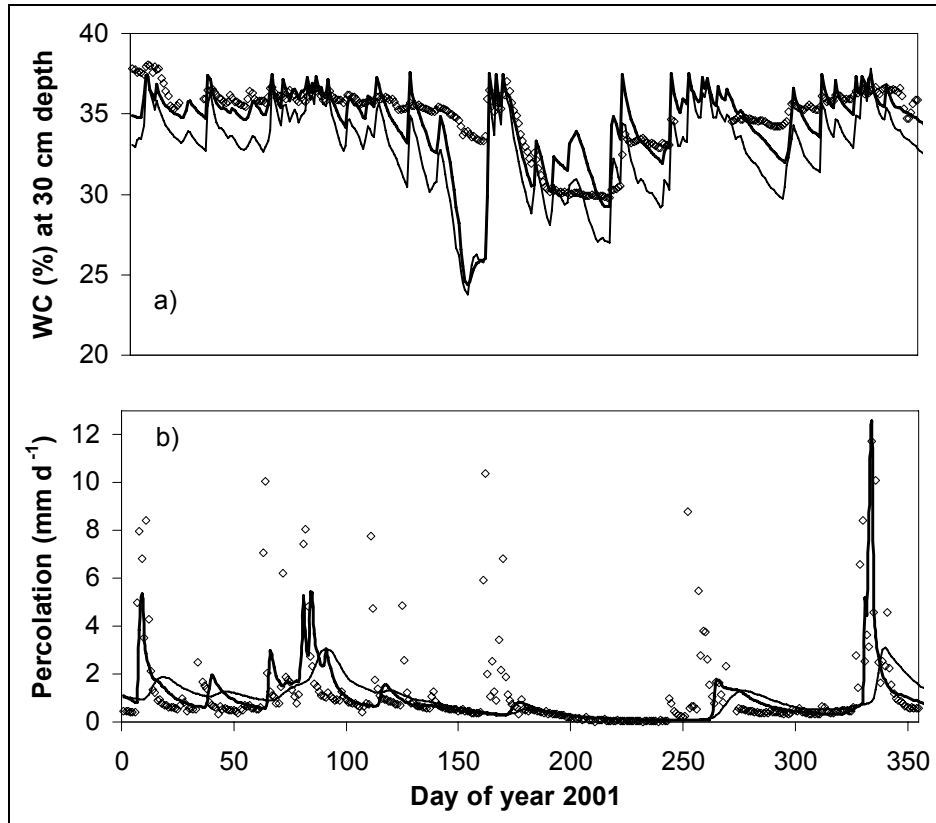


Fig. 3.5: Water content (a) measured (symbols; TDR, daily values) and simulated (lines) and percolation amounts (b) measured (symbols; daily values) and simulated (lines) for LM 2 in 2001; soil hydraulic characteristics are calculated by approaches of Brutsaert-Gardner (thick lines) and Hutson & Cass-Burdine (thin lines) (ET_p by PM grass).

It can be pointed out that the simulated, annual percolation amount is insensitive to the choice of the proposed soil hydraulic characteristics under the prescribed boundary conditions. As described in the work of Zurmühl (1998) a constant water flux is influenced mainly by the flux across the upper boundary and not so much by the form of the water retention curve, because a quasi steady-state water flux is rapidly established. However, the percolation dynamics during the year are highly sensitive to the soil hydraulic characteristics.

Table 3.4: Percolation amounts measured as well as simulated with different hydraulic characteristics in percentages of measured amounts in the year 2001 (ET_p by PM grass approach)

Percolation	LM 1	LM 2
Measured (mm)	506.1	518.2
Simulated (%):		
Brutsaert-Gardner	65.0	67.1
Hutson & Cass-Burdine	70.7	65.7

As is demonstrated in Table 3.4 the simulated percolation amounts were underestimated by both approaches up to 35 % of the measured percolation. Therefore, in the next section it was focused on a detailed analysis of single infiltration and drying cycles and in the subsequent sections on the evaluation of ET_p approaches. For all following water flow simulations the Brutsaert–Gardner hydraulic functions were applied and special attention was given to the year 2001, because in 2001 the data set for plant growth on the lysimeters was most complete.

3.3.2.2 Detailed analysis of infiltration and drying cycles

As already pointed out soil hydraulic functions have highest influence on soil water dynamics while soil water dynamics also show the influence of the applied evapotranspiration method. For detailed analysis of the observed and simulated data single infiltration and drying cycles were studied for LM 1 and 2. For the sandy lysimeter (LM 1) changes in water storage (cp. section 3.2.1.3) were calculated for infiltration and drying cycles between days 159 to 166 in the year 2001. In this simulation period ET_a was mainly governed by transpiration. For the loamy lysimeter (LM 2) the changes were calculated for the time between days 109 to 132, whereas in this simulation period ET_a was mainly governed by evaporation. Figs. 3.6 and 3.7 show simulated changes in soil water content where ET_p was calculated by the PM grass and the Haude (mrH) approach respectively, together with measured changes in lysimeter weight. It can be seen that the simulated changes in water content match the measured changes of lysimeter weight for both lysimeters. Only small differences between the two modelling approaches exist.

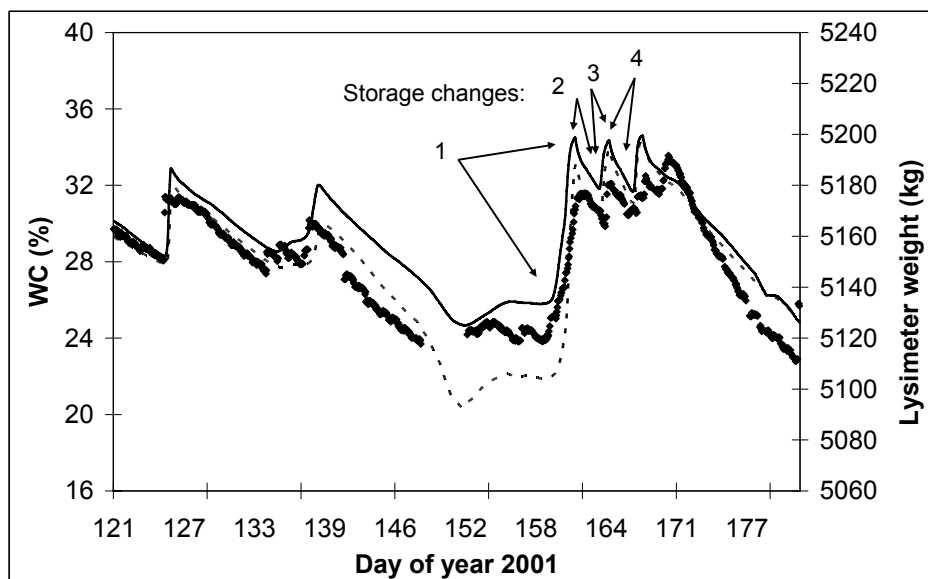


Fig. 3.6: Water content simulated in 30 cm depth with ET_p calculated by PM grass (dotted line) and Haude (mrH; solid line) and measured (symbols) lysimeter weight (LM 1, 2001).

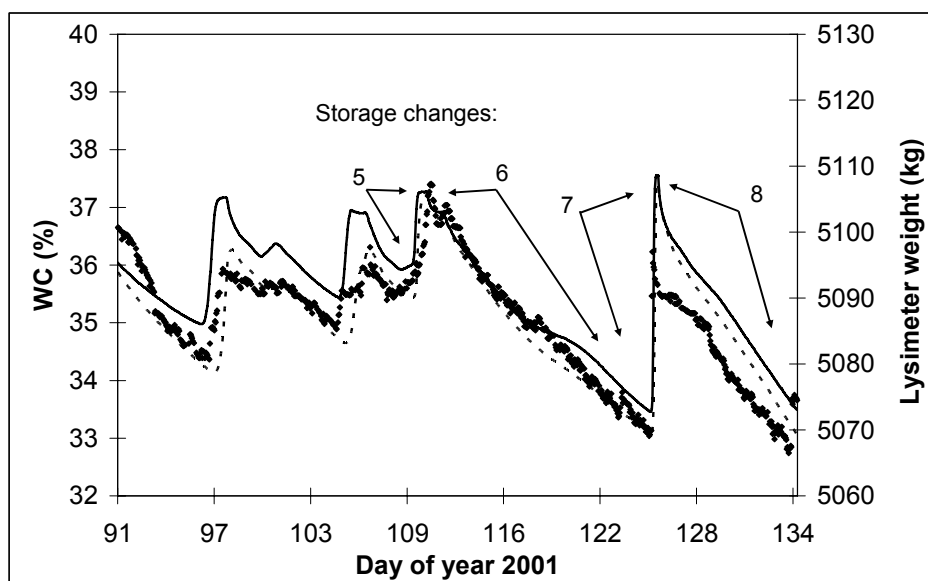


Fig. 3.7: Water content simulated in 30 cm depth with ET_p calculated by PM grass (dotted line) and Haude (mrH; solid line) and measured (symbols) lysimeter weight (LM 2, 2001).

The calculation of evapotranspiration in Table 3.5 includes infiltration (e.g. storage change 1; Fig. 3.6) as well as drying (e.g. storage change 2; Fig. 3.6), thus, evapotranspiration during rain events was also regarded. The time periods specified in Table 3.5 are indicated in Figs. 3.6 and 3.7.

In Table 3.5 the storage changes as infiltration and evapotranspiration (ET) in mm are listed. In the case of the sandy soil (LM 1) an overestimation of water storage change occurs for infiltration 1, when applying both evapotranspiration models, while the Haude (mrH) model leads to a correct simulation of the observed water storage change for infiltration 2. By use of the PM grass approach the simulation again overestimates the observed water storage change for infiltration 2. With the PM grass approach the soil is dried up more in the simulation than it was observed (compare ET 1 observed and simulated). Therefore, infiltration 2 can be higher in the simulation because more storage space can be filled up. For ET 1 the observed storage change is slightly underestimated by the Haude (mrH) approach, but strongly overestimated by the PM grass approach. For ET 2 an underestimation can be found by the Haude (mrH) approach, while the PM grass approach predicts the amounts correctly.

Table 3.5: Lysimeter storage changes measured and simulated in the top 30 cm at infiltration and drying cycles for the sandy (LM 1) and loamy soil type (LM 2); time periods are described in Figs. 3.6 and 3.7 in further detail

Soil	Cycle	Storage change	Measurement (mm)	Simulation (mm)	
				PM grass	Haude (mrH)
LM 1	Infiltration 1	1	21.08	33.15	26.13
LM 1	ET 1	1 + 2	-8.94	-12.83	-6.91
LM 1	Infiltration 2	3	7.30	10.71	7.50
LM 1	ET 2	3 + 4	-12.00	-12.24	-10.10
LM 2	Infiltration 3	5	1.32	5.46	3.81
LM 2	ET 3	5 + 6	-17.11	-29.37	-23.96
LM 2	Infiltration 4	7	1.40	13.26	11.58
LM 2	ET 4	7 + 8	-14.52	-22.47	-18.83

For the loamy soil (LM 2) similar results as for the sandy soil are obtained for infiltration 3. Infiltration 4 is strongly overestimated by the models, but the storage change measured by TDR is unrealistically low after an intense rain event of 30 mm after a drought of 14 days. Preferential flow processes in the loamy soil are probably the reason for this discrepancy. ET 3 and 4 are overestimated by both modelling approaches, while the Haude (mrH) approach leads to a smaller overestimation.

The simulated infiltration after a rain event corresponds to the observed data for both soil types more than the simulated evapotranspiration. As infiltration dynamics also depend on the depletion of the water storage by evapotranspiration, the assessment of infiltration simulation

remains difficult. Although soil water dynamics are subjective to type of pedotransfer function they can be used to discriminate between evapotranspiration methods and their effect on water storage changes. Inconsistencies in water content measurements by TDR probes and the complexity of this method show that percolation amounts as shown in the following sections were more useful for ET_p model comparison. The results already indicate that ET_p model choice has great influence on simulated soil water dynamics.

3.3.2.3 Evapotranspiration for the year 2001

3.3.2.3.1 Sandy and loamy soil type

In Fig. 3.8 the results of the simulated percolation amounts using different ET_p models are shown for the sandy soil (LM 1). Between the PM grass (Fig. 3.8a) and Penman (not shown) approach nearly no difference occurred in the simulation. Especially during the summer months (days 173-265) when plants grow, the percolation amounts are clearly underestimated. But also during spring (days 80-172) EV_a was overestimated and the simulated percolation amounts are far below the measurements. Small variations in spring between the PM grass and PM crop (Fig. 3.8b) method illustrate that the crop coefficient differs slightly from the value one during this period, which means that both methods result in almost the same ET_p . In autumn and winter the PM crop approach leads to less simulated percolation resulting from higher simulated ET_a during the cropping period. When applying the two Haude models a considerable difference between the simulated percolation amounts occurred only for the summer months. For this period the Haude model parameterised with 14³⁰ CET values (not shown) provided similar results as PM grass, while the modified Haude (mrH) approach clearly improved the simulation and an almost perfect match with the observed data is obtained in Fig. 3.8c. Between days 100 and 120 and between days 255 and 350 only a slight overestimation of outflow occurred.

For all ET_p models the measured and simulated water content values (not shown) reflect primarily the same mismatches as in the percolation data. Apart from this mismatches, all models give a reasonable well agreement with the measured data. In general, water contents at a specific depth were under-estimated prior to rainfall events and slightly over-estimated after the rainfall compared to the water contents measured by TDR. This difference may be explained by the high sensitivity of the modelled water content to variation in θ_{sat} and the variation of θ_{sat} in field affected by bulk density changes as discussed by Oliver and Smettem (2005).

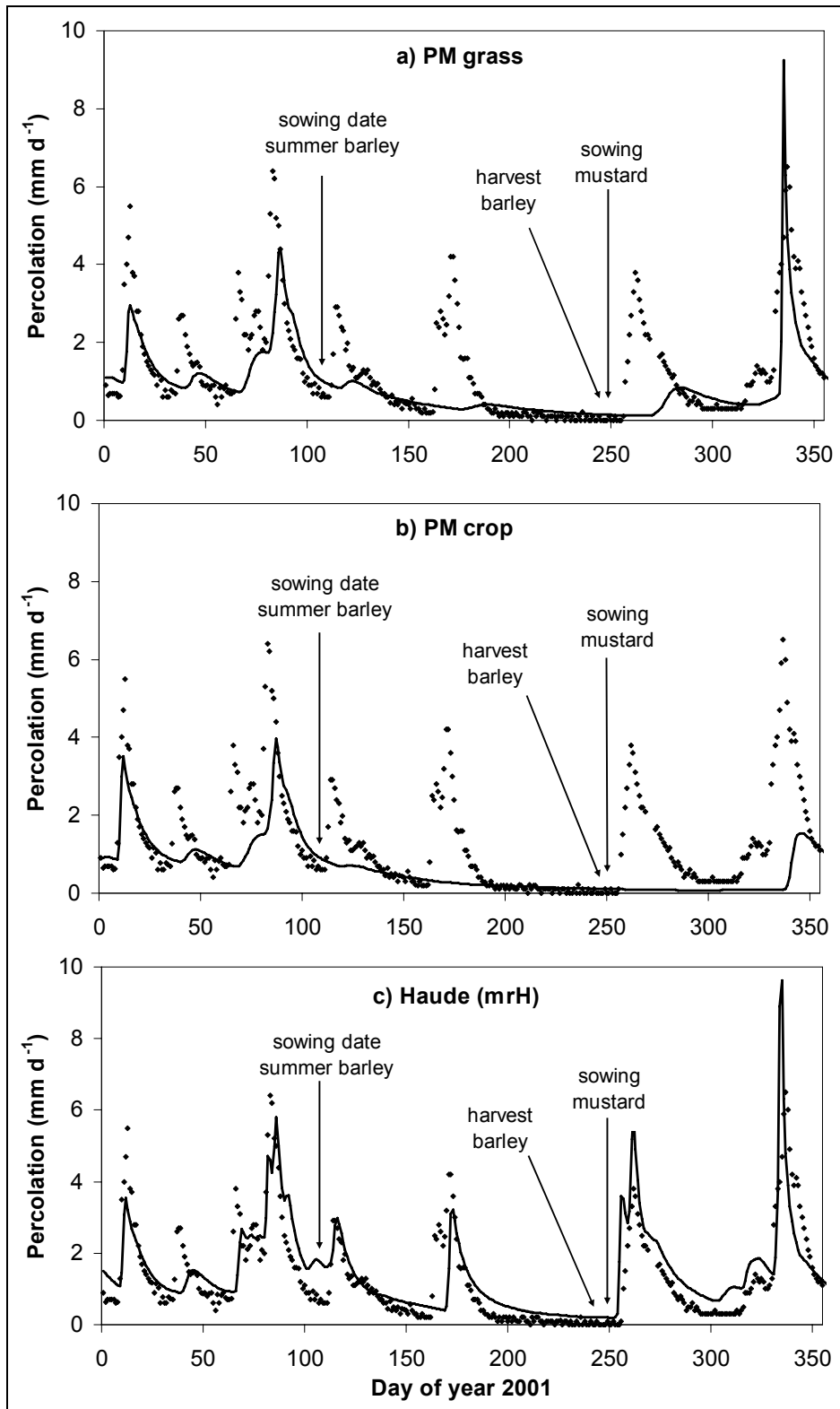


Fig. 3.8: Daily percolation amounts measured (symbols) and simulated with ET_p calculated by a) PM grass b) PM crop and c) Haude (mrH) approach (LM 1, 2001; hydraulic characteristics by Brutsaert-Gardner).

3.3.2.3.2 Transferability to other soils

In Table 3.6 the simulated outflow is shown in percentage of measured amounts for all four lysimeter soils. Applying the Penman, PM grass, PM crop and Haude (14³⁰ CET) approach a clear underestimation of the measured outflow occurred. The Haude (mrH) model provided the best simulation results with exception of LM 4 where Haude (14³⁰ CET) gave the best results. On LM 4 the highest plant biomass was measured (720 g m⁻²). This indicates that in case of increased plant growth the Haude (mrH) simulation underestimates potential TR during the summer months.

Table 3.6: Data of percolation amounts simulated with different ET_p modules in percentages of measured amounts in the year 2001 (hydraulic characteristics by Brutsaert-Gardner)

Percolation	LM 1	LM 2	LM 3	LM 4
Measured (mm)	506.1	518.2	577.6	432.6
Simulated (%):				
1. Penman (VDI)	56.7	60.4	67.4	67.7
2. Penman-Monteith:				
a) grass reference	65.0	67.1	71.4	77.5
b) crop coefficient	46.9	53.5	59.7	58.6
3. Haude:				
a) 14 ³⁰ CET	76.1	80.2	90.6	94.7
b) mrH	106.1	105.1	103.7	124.9

In Fig. 3.9 for the sandy (LM 1) and loamy (LM 2) soil type the mean and standard deviation of weekly measured percolation amounts (three lysimeter replications) are compared with simulated amounts by the Haude (mrH) approach. For the sandy soil the measured standard deviation between the replications was increased compared to the deviation in the loamy soil. Except for some mismatches the simulated percolation amounts are in good agreement with the weekly measured values for the sandy soil (Fig. 3.9a) and the total simulated percolation amounts for 2001 lie within the range of the standard deviation of the measured amounts. Discrepancies probably resulted from snow drift (days 9-15, 37-43) on the lysimeters or were caused by an overestimation of simulated plant growth (days 163-176). For the loamy soil (Fig. 3.9b) the differences between measured and simulated weekly percolation amounts are stronger. As for the sandy soil, the simulated percolation amounts between days 163 and 176 were too small, whereas in autumn (days 265-355) the simulated percolation amounts were

too high. For the loamy soil the total amounts were overestimated due to an overestimation of outflow in autumn.

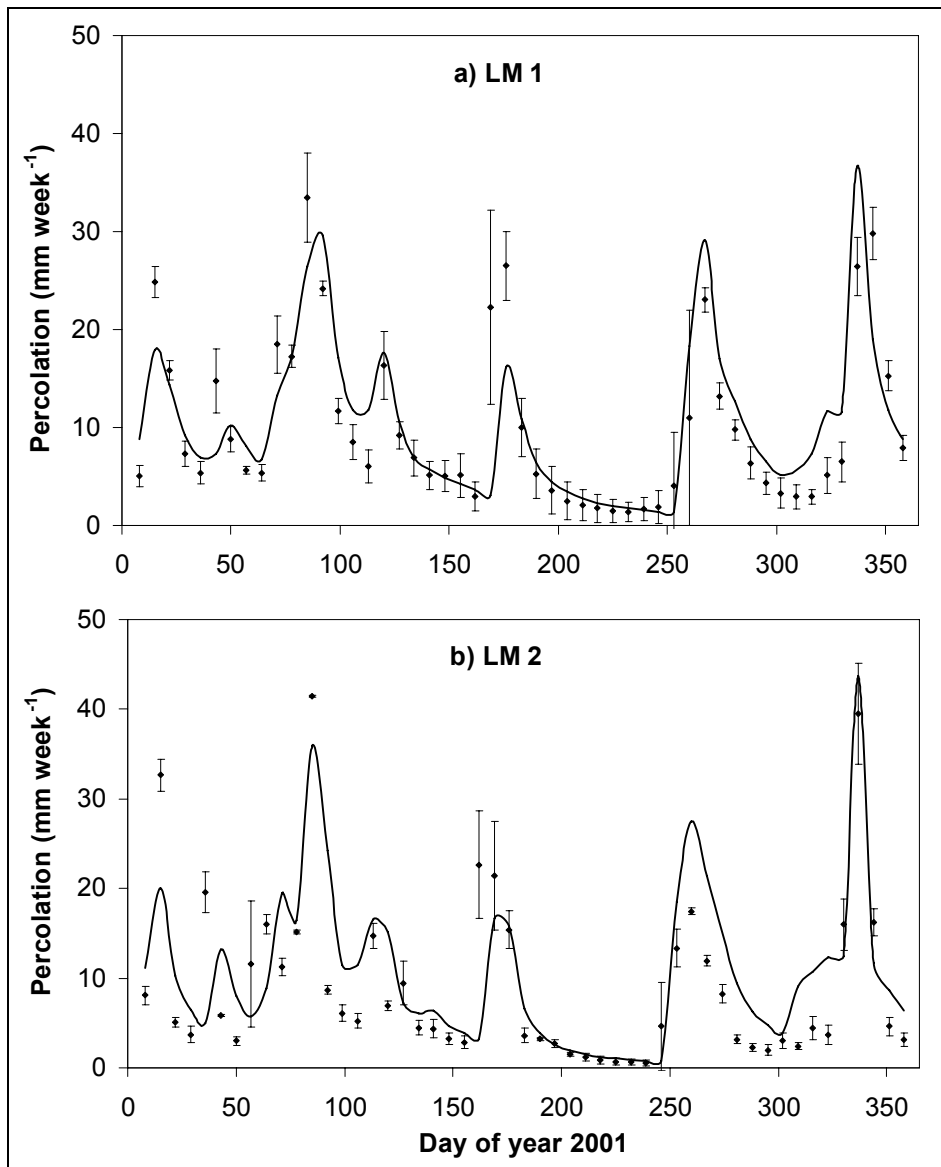


Fig. 3.9: Weekly percolation amounts measured (with standard deviation; symbols) and simulated (line) with ET_p calculated by Haude (mrH); weekly measurements were available for three replications of the soil type of a) LM 1 and b) LM 2 in the year 2001 (hydraulic characteristics by Brutsaert-Gardner).

Comparing simulated and measured percolation amounts it can be seen that both the PM crop and the PM grass approach overestimate the measured cumulative ET_a in 2001 (cp. Table 3.6). Bormann et al. (1996) investigated that due to non-linearities in the Penman-Monteith equation it is not possible to compute potential evapotranspiration from mean daily climate data. They also stress that the spatial variability of temperature, global radiation and wind velocity is low compared to the relative humidity. Liu et al. (2005) apply the Penman-Monteith approach and compare average daily with diurnal cycle simulations. They pointed

out that the use of diurnal cycles causes greatest differences for bare, sandy soils, with relatively high water tables. Regardless of these factors the application of daily average evapotranspiration consistently overestimates the actual evapotranspiration. Similar results were obtained in the present study. To calculate ET_p in 2001 hourly meteorological data for temperature and relative humidity for the aerodynamic term in the Penman-Monteith equation were used. It was also calculated that the results based on hourly measured data do not equal those based on mean daily climate data, but the difference between the two results in the simulated percolation amounts is only up to 10 % of the measured percolation in 2001. This means, that in the present case the use of hourly resolved climate data in the aerodynamic term of the Penman-Monteith approach improves the simulation results, but not markedly.

Compared with Penman-Monteith the overestimation of the measured cumulative ET_a was even increased for the Penman approach, according to VDI (1993). Crop factors were not used in case of the Penman method, since this would even more increase instead of reduce estimated ET_p . As pointed out by others (Allen et al., 1998; Sau et al., 2004) the Penman approach generally overestimates ET_p and may require local calibration of the wind function to achieve satisfactory results.

The measured percolation amounts in the lysimeters could only be correctly simulated, if the mean relative humidity was used instead of relative humidity at 14³⁰ CET in the approach of Haude. This means that actual parameterisation of reference-surface or surface-dependent approaches for calculation of ET_p which are provided in the literature are not suitable for the calculation of ET_p in the present lysimeter study for the year 2001.

In the case of the GSF-lysimeter facility, the construction of the lysimeters may slow down wind speed above ground as an exact levelling of the lysimeters to soil surface (difference of elevation up to 0.1 m, depending on tillage) is not feasible and this may contribute to lower evapotranspiration rates. Another explanation for overestimation of evapotranspiration can be that plant growth in lysimeters was sparser than under real field conditions. However, as pointed out before, the measured percolation amounts could not even be simulated in the winter term under bare soil. A reason for this might be that the evaporation fluxes were overestimated, because soil hydraulic functions may not be valid for the upper 1-3 cm of soil, which are subject to splashing rain and formation of crust or may be covered by mulch.

But it is not clear, if the overestimation of ET_p and EV_a was the only reason for the simulation of lower percolation during the winter season. An additional reason of minor importance might be that precipitation measurements are less accurate when snow was falling (e.g. snow

drift) and they can have systematic errors, which can amount of up to 6.7 % in average for the given climatic conditions (Zenker, 2003).

3.3.2.4 Evapotranspiration for the years 1999 to 2003

Finally, the results obtained for the year 2001 were transferred and used for the water flow simulations in LM 1 – 4 for the years 1999 to 2003. Only the impact of using different evapotranspiration models was investigated, because the influence of the pedotransfer functions on percolation amounts was small compared to evapotranspiration. Table 3.7 shows the precipitation and measured percolation amounts for LM 1 – 4.

Table 3.7: Precipitation and measured percolation amounts in the years 1999 to 2003 for LM 1 – LM 4

Year	1999	2000	2001	2002	2003
Precipitation (mm)	900	975	961	1016	553
Percolation measured (mm)					
LM 1	355	520	506	545	171
LM 2	374	441	518	498	147
LM 3	417	550	578	607	241
LM 4	351	423	433	534	163

For the investigated period the precipitation was between 900 and 1020 mm per year with an exception in the year 2003, which was a very dry year with only 553 mm precipitation. The percolation of the four lysimeters was between 351 and 607 mm per year between 1999 and 2002. This means 39 to 60 % of the fallen precipitation resulted in outflow. In the year 2003 amounts of only 147 to 241 mm were measured (26 – 43 % of fallen precipitation). In general the year with the highest precipitation showed the highest outflow. The Calcaric Regosol (LM 3) produced the highest percolation, followed by the Humic Cambisol (LM 1), due to its high sand fraction. Although the Aric Anthrosol (LM 4) has a similar particle size distribution as the Humic Cambisol, the lysimeter showed a significant lower percolation for the years 2000 and 2001. The outflow from the Mollic Gleysol lysimeter (LM 2) was once higher and once lower than that from the Humic Cambisol. This higher variation in the percolation tendency may be explained by preferential flow processes in some years for the Gleysol lysimeter.

Between 1999 and 2003 five different crops (maize, winter wheat, summer wheat, summer barley and mustard) were grown. As shown by Table 3.8 the Haude (mrH) approach gave the best results for LM 1 and 2, although the overestimation of the total amounts reached up to

21 % in the mean for LM 2. For LM 3 and LM 4 the results must be regarded in more detail. Although the PM grass approach had the best values for EF and r, the total outflow was underestimated up to 31 %; Haude (mrH) gave the best results for the total, simulated amounts with a mean deviation from the measurements of only 7 % for LM 3. For LM 4 the PM grass approach gave the highest value for EF and r and Haude (14³⁰ CET) had the lowest deviation from the totally measured percolation amounts.

Table 3.8: Modelling efficiency (EF), correlation coefficient (r) and mean and standard deviation (Std) of yearly simulated percolation amounts in percentages of measured amounts in the years 1999-2003 for LM 1 – LM 4 (hydraulic characteristics by Brutsaert-Gardner)

LM 1	EF	r	Mean	Std
Penman (VDI)	-0.051	0.182	59.0	17.4
PM grass reference	0.062	0.326	70.8	10.0
PM crop coefficient	-0.101	0.127	51.8	19.5
Haude (14 ³⁰ CET)	0.053	0.321	78.2	14.7
Haude (mrH)	0.326	0.581	110.9	4.7
LM 2	EF	r	Mean	Std
Penman (VDI)	0.267	0.569	63.5	15.2
PM grass reference	0.354	0.623	74.8	11.9
PM crop coefficient	0.149	0.456	62.2	12.6
Haude (14 ³⁰ CET)	0.258	0.537	81.2	9.8
Haude (mrH)	0.570	0.763	121.0	10.5
LM 3	EF	r	Mean	Std
Penman (VDI)	0.431	0.691	65.1	7.2
PM grass reference	0.432	0.697	69.1	9.2
PM crop coefficient	0.355	0.642	59.2	10.9
Haude (14 ³⁰ CET)	0.246	0.615	84.3	8.4
Haude (mrH)	0.130	0.619	106.8	9.5
LM 4	EF	r	Mean	Std
Penman (VDI)	0.510	0.745	66.9	10.2
PM grass reference	0.597	0.786	77.6	9.8
PM crop coefficient	0.338	0.638	60.8	11.6
Haude (14 ³⁰ CET)	0.490	0.723	87.6	11.4
Haude (mrH)	0.279	0.725	125.5	20.8

Summarising, from an operational point of view the modified Haude (mrH) approach seems to be more useful to predict the lysimeter water balance correctly than the other four ET_p models. Correlation coefficient and modelling efficiency, according to Loague and Green (1991), are in a sufficient range considering that they are compared on a daily basis over five years (Table 3.8). LM 4 is an exception compared to the other lysimeters and further research will be necessary to explain this behaviour. The choice of the empirical Haude approach seems to be justified in terms of efficiency and simplicity for the simulation of the water balance terms in the present study, as it is easily possible to adapt to the given lysimeter measurements. Nevertheless, the present evaluation concept cannot be used to show differences in daily simulated evapotranspiration rates compared to measurements. This will be discussed in the next section.

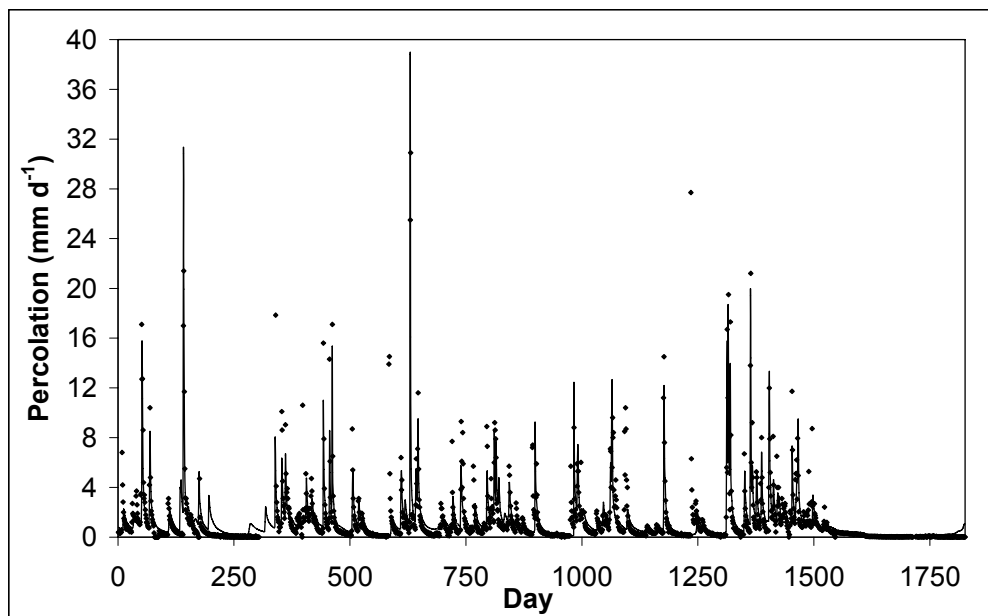


Fig. 3.10: Daily percolation amounts measured (symbols) and simulated (line) in the years 1999 to 2003 for LM 2 (ET_p by Haude (mrH); hydraulic characteristics by Brutsaert-Gardner).

In Fig. 3.10 the measured and with Haude (mrH) simulated percolation amounts are exemplarily displayed for the loamy soil (LM 2) during the years 1999 to 2003. Around day 40 and day 398 the precipitation measurement differs probably with the snow accumulated on the lysimeters because of snow drift. This is an explanation for the difference between measured and simulated percolation amounts in this period. The high measured percolation peaks around day 588 and around day 1235 may be explained by preferential flow processes after a long drought. Preferential flow was not included in the present simulations.

3.3.3 Direct evaluation of daily evapotranspiration fluxes in the year 2004

As already pointed out, the present modelling concept has the intention to discriminate between different evapotranspiration models on the basis of water balance and percolation studies. For the evaluation of daily evapotranspiration fluxes direct evapotranspiration measurements must be used. Measured and simulated evapotranspiration amounts between March and November 2004 are presented for LM 1, when mustard and summer barley were grown on the lysimeters (Fig. 3.11).

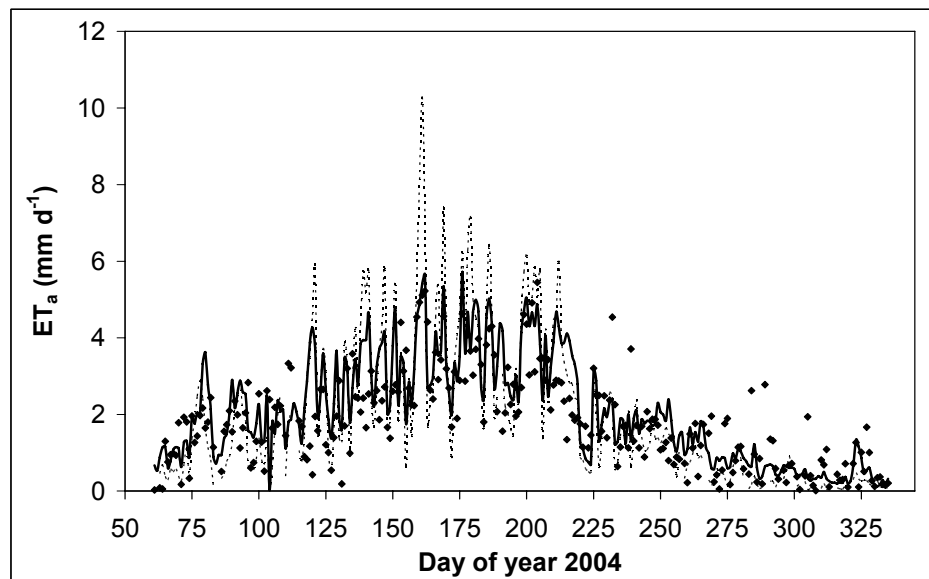


Fig. 3.11: Daily actual evapotranspiration measured (symbols) and simulated (solid line: ET_p by PM grass; dashed line: ET_p by Haude (mrH); hydraulic characteristics by Brutsaert-Gardner; LM 1, 2004).

Only PM grass and Haude (mrH) approach were compared. The direct evapotranspiration measurement in Fig. 3.11 shows that in spring (days 117-149) and autumn (days 234-313) evapotranspiration was overestimated by the model simulations with the Haude (mrH) as well as with the PM grass approach, while in summer the level of evapotranspiration was simulated correctly with the PM grass approach. The Haude (mrH) approach shows high fluctuations between single days and has thus a much lower modelling efficiency compared to the PM grass approach (Table 3.9), while the cumulative evapotranspiration amounts were predicted correctly. During the vegetation period PM grass overestimates cumulative ET_a slightly more than the Haude (mrH) approach, while cumulative percolation is underestimated in larger quantities by using PM grass.

Table 3.9: Modelling efficiency (EF), correlation coefficient (r) and cumulative percolation and evapotranspiration amounts in percentages of measured amounts in the period March to November 2004 for LM 1 (hydraulic characteristics by Brutsaert-Gardner)

Mar. - Nov. 2004			
Percolation	EF	r	Sum (%)
PM grass reference	-0.385	0.106	51.3
Haude (mrH)	-0.325	0.251	82.5
ET_a	EF	r	Sum (%)
PM grass reference	0.408	0.774	115.8
Haude (mrH)	-0.129	0.743	107.2

In conclusion it can be stated that in the simulation of daily evapotranspiration fluxes the physically based Penman-Monteith approach shows much higher correlations with measurements than the empirical Haude approach. However, the impact of inappropriate temporal sampling of the climatic input variables on the estimation of daily ET_p can reach a relative error of -27 % for the PM grass approach (Hupet and Vanclooster, 2001). In this context, appropriate sampling of the climatic input variables is essential for the exploitation of the precision of the Penman-Monteith approach.

3.4 Conclusions

The pedotransfer functions that were used for water retention and hydraulic conductivity characteristics have shown to be useful to simulate the measured percolation amounts and water contents correctly. Compared to evapotranspiration the influence of the pedotransfer functions on simulated percolation amounts was small. Therefore, the annual outflow was not very sensitive to the applied soil hydraulic characteristics under the chosen boundary conditions. However, the percolation dynamics were highly sensitive to the soil hydraulic characteristics.

The results indicate that both reference-surface and surface-dependent ET_p calculation methods overestimate the measured cumulative ET_a in the present study. The measured percolation amounts in the lysimeters could be simulated more correctly, if a pragmatic approach of simple efficiency was followed and the mean relative humidity was used instead of relative humidity at 14³⁰ CET in the surface-dependent approach of Haude. Independent from application of reference-surface or surface-dependent approaches for calculation of ET_p an overestimation of actual transpiration during the summer period occurred. While percolation during winter time was correctly predicted by the surface-dependent approach of Haude, the other approaches were not appropriate for the given lysimeter conditions. The results show

- that the present modelling concept is adequate for the discrimination between different evapotranspiration models on the basis of water balance and percolation studies,
- but that for the evaluation of daily evapotranspiration fluxes direct evapotranspiration measurements must be used.

In the simulation of daily evapotranspiration fluxes the physically based Penman-Monteith approach shows much higher correlations with measurements than the empirical Haude approach. However, appropriate sampling of the climatic input variables is essential for the exploitation of the precision of the Penman-Monteith approach.

Based on the simulation results and model analysis research demands were identified related to the question to what extent the water balance situation in lysimeters differs from real field conditions as follows:

- A detailed analysis of evaporation from bare soil under lysimeter conditions should be subject of further studies.
- Plant-growth under lysimeter conditions and the possibility of different microclimatic effects compared to large fields must be investigated in more detail.

For the tested lysimeter data it was shown that depending on ET_p model choice the simulated percolation amounts vary between 52 % and 126 % of the measured amounts. Compared to this, the influence of the parameterisation of the soil hydraulic characteristics is small with a variation of up to 5 % of the measured outflow. Thus, evapotranspiration is still the most crucial process to evaluate in water-balance modelling even if meteorological data are available in detailed temporal and spatial resolution.

4 Environmental fate of the herbicide glyphosate in the presence of genetically modified soybean

4.1 Introduction

Modelling of pesticide transport has achieved much attention in the last few decades. Widely used pesticide leaching models like LEACHP, PESTLA, WAVE use the Richards equation for water flow coupled with the convection-dispersion model for the description of solute flux under transient conditions in single-porous media. However, soil heterogeneity and macropores cause preferential flow of water and solutes on the field scale, but also in lysimeters. Preferential flow processes can dramatically increase the risk of groundwater pollution by surface-applied chemicals (e.g., see review by Flury, 1996).

At present the non-equilibrium solute transport has achieved much attention in soil and agricultural sciences and conceptually different approaches have been developed like multiple-domain transport and two-site sorption models. Models where distinct mobile and immobile flow regions were defined were developed already in the seventies (van Genuchten and Wierenga, 1976; Zurmühl, 1998). The dual-porosity concept assumes that the porous medium consists of a mobile water flow region where convective-dispersive transport of solutes occurs and an immobile water region with which the solutes exchange. During the nineties various dual-porosity and dual-permeability models – dual-permeability approaches include advective transport in both pore domains – were developed and applied (Gerke and van Genuchten, 1996; Larsson and Jarvis, 1999; Ray et al., 2004; Gärdenäs et al., 2006; Köhne et al., 2006). A comparison between different concepts to model non-equilibrium and preferential flow transport in soils was given by Simunek et al. (2003). These dual- or multiple-domain models allow the differentiation of sorption parameters between macropores and matrix domain. Also rates of pesticide degradation can vary depending upon these domains, as higher microbial activity in the more aerobic macropore is more probable than in the less-aerobic matrix domain (Ray et al., 2004). Available dual-permeability models differ mainly in the way they implement water flow between the two pore regions invoking Poiseuilles's equation, Philip infiltration models, the kinematic wave equation, and the Richards equation (Simunek et al., 2003). A proper description of water flow between the pore regions represents still the greatest challenge in the successful description of non-equilibrium flow. Solute mass transfer parameters for the validation of these dual-domain models are rare and difficult to obtain by field experimental work, since effective macropore flow parameters are often poorly identifiable (Simunek et al., 2003; Ray et al., 2004;

Gärdenäs et al., 2006). Dependencies between the numerous different model components and parameters enhance the uncertainty in model calibration of such complex models. The use of these models has therefore been restricted to theoretical and laboratory studies under controlled conditions. Moreover, dual-domain models are especially of interest for pesticides with low sorption capacity. Thus, the consideration of a single-continuum system only as applied by the model LEACHP (Hutson and Wagenet, 1992) seems to be valid and sufficient for the transport simulation of the highly sorbing herbicide glyphosate, as matrix flow is expected to be the dominant process in the sandy soil lysimeters of the present study.

Environmental fate models of pesticides are very sensitive to the parameters governing sorption and degradation. The correct determination of the parameters to simulate degradation seems to be of much greater influence than improvements in the water balance (Klein et al., 2000). But this holds only true for water flow parameters, apart from preferential flow and infiltration during application. It is important to determine uncertainty and sensitivity of parameter values describing biodegradation and adsorption to enhance the reliability of model outputs. An extensive review of the different sources of uncertainty in pesticide fate modelling was given by Dubus et al. (2003). They pointed out that traditional uncertainty analysis like Monte Carlo modelling ignores a number of key sources of uncertainty which are likely to have significant effects on the model predictions. The overall uncertainty is contributed by the different steps in the modelling process: first by the acquisition of basic data in the field or in the laboratory, then by the derivation of model input parameters and finally by the modelling itself. The overall uncertainty will therefore arise from sampling management (field) and analytical methods (laboratory), from the spatial and temporal variability of the environmental parameters themselves, from the procedures to derive model input parameters like averaging procedures, pedotransfer functions or empirical functions, and from model inadequacy and modeller subjectivity. Uncertainty in model calibration originates from the fact that multiple combinations of input parameters will provide a similar fit to the experimental data. Parameter calibration programs (e.g. CXTFIT; Toride et al., 1995) may provide good fits to observed data, but the fitted parameters represent mainly a local minimum. Comparison with the results of a generalised likelihood uncertainty estimation program shows that much wider ranges of parameter values can provide acceptable fits (Zhang et al., 2006). This results in a wider range of potential outcomes. Additionally, the conversion of the conceptual model (mathematical description) in the procedural model (computer code) includes further uncertainties. Vink et al. (1997) found that even if input data of five different pesticide leaching models were identical, the variations in the predictive

performance were high and directly attributed to the conceptual differences of the models. The uncertainty associated with pesticide fate modelling can be presented in an uncertainty iceberg (Fig. 4.1) as proposed by Dubus et al. (2003). For the reason that not all of the mentioned uncertainties can be accounted for in this work, in a first step dependencies and uncertainties in the calibration of input parameters of the biodegradation model were studied. In a second step water flow and water balance simulations were improved. Uncertainty associated with model choice was analysed by comparison of different deterministic modelling approaches. Finally, uncertainties arising from model input parameters (e.g. K_d value, dispersivity and a biodegradation parameter) were studied in a modelling approach with probability distribution of these input parameters (iceberg (b)).

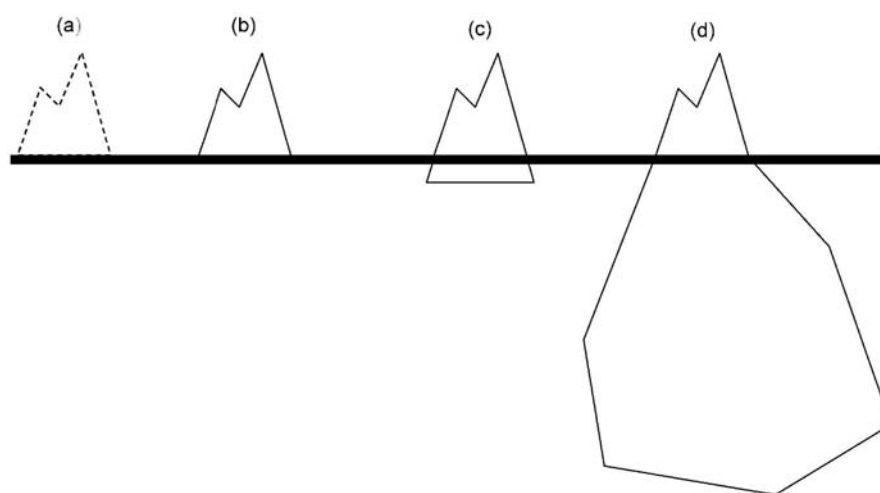


Fig. 4.1: The uncertainty iceberg. Although uncertainty in pesticide fate modelling has been ignored in the past (a), there have been a number of attempts to quantify uncertainty over the last 10 years (b). The challenge is now to ascertain whether the uncertainty, which is accounted for, represents a large (c) or small (d) proportion of the overall uncertainty in pesticide fate modelling (Dubus et al., 2003).

Due to the discussed importance of an accurate representation of biodegradation, a special task lies in the description of microbial degradation and modelling of microbial growth kinetics in the present work. In most of the cited works of multiple-domain models traditionally first-order rate reaction kinetics had been used to describe pesticide degradation. Although often soil temperature and moisture degradation dependencies are additionally applied, accurate predictions of pesticide soil residue profiles were not achieved (Dust et al., 2000) and microbial growth dynamics were still not considered. Microbial degradability and risk assessment of accumulation are prescribed in the registration procedure of new plant protection products. A pesticide can be degraded, if the soil microflora is able to mobilise an array of enzymes which can be recruited from existing biochemical pathways acting upon

naturally occurring compounds (Soulas and Lagacherie, 2001). The pesticide degrading community acts as functional entity with diverse catabolic capacities, resulting in co-metabolic or metabolic biodegradation.

Beneath the detailed analysis of biodegradation, the choice of a linear equilibrium, non-linear equilibrium (Freundlich isotherm), and linear non-equilibrium (two-site) sorption concept on the pesticide behaviour was studied. Solute movement through the vadose zone is strongly affected by the sorption capacity of the soil matrix. Non-equilibrium sorption can be caused by rate-limited sorption or by an incomplete mixing of percolation with resident waters (Vanderborght et al., 2005). The bioavailable pesticide fraction for degradation and plant uptake or the depletion by leaching depends on the shift in pesticide distribution towards the unavailable sorption state (Beulke et al., 2004b). Therefore, the distinction between the different sorption concepts follows the effects on movement and degradation.

Soil heterogeneities and resulting flow paths cause turbulence in saturated and unsaturated water flow, thus, dispersion of solutes in soil has received considerable attention beneath the analysis of degradation and sorption parameters. Proper estimates of effective solute transport parameters such as dispersivities by the use of tracer-derived breakthrough curves are essential for the description of solute movement. Breakthrough curves of conservative tracers identify the complete spectrum of solute flow paths including fingering, which must be taken into consideration in sandy soils. The influence of dispersivity characterisation was studied together with the parameterisation of soil hydraulic characteristics.

Finally, most of the mentioned pesticide transport models lack in a detailed description of the effect of crop growth on water dynamics and of the pesticide uptake by plants. Crop growth submodels like SUCROS (van Laar et al., 1997) estimate the increase in biomass and leaf area by the calculation of assimilation rates from plant specific photosynthesis parameters and radiation. The link of pesticide plant uptake models with generic plant growth models enables a detailed simulation of pesticide translocation in plants according to the special growth of the various plant tissues.

The environmental fate of the herbicide glyphosate was studied with the specific background of the presence of GM plants as described in the general introduction. The dataset of the GSF risk assessment study was used for investigation. Aim of the present part was to enhance model reliability in the simulation of the environmental fate of glyphosate with special focus on biodegradation simulations and detailed description of the herbicide translocation in GM plants. Only the fate of the parent compound and no metabolites were studied. In the analysed soil residues the main metabolite AMPA was the predominant metabolite. For simplification

it was assumed that the soil residues only consist of glyphosate, the degradation chain from glyphosate to AMPA in soil was not followed in the model. Four re-packed large weighing lysimeters (LM 5.1 – LM 5.4) were cropped with transgene soybean over two years and a conservative tracer was applied. Two of the four lysimeters were additionally treated with ^{14}C -radiolabelled glyphosate three times.

4.2 Materials and Methods

4.2.1 The dataset

4.2.1.1 Pesticide degradation and plant uptake monitoring

The pesticide degradation and plant uptake monitoring was done by the project partners. In the first project year the cultivation of non transgenic soybean under temperate climatic conditions was tested on four lysimeters (LM 5.1 – LM 5.4) of the same soil type. Lysimeter facility, lysimeter equipment and measurement of climate data were already described in section 3.2.1.1. In the second and third year, transgenic soybean was planted on all lysimeters and ^{14}C -radiolabelled glyphosate was applied on two of the lysimeters, the others were used as non-treated control (Table 4.1).

Table 4.1: Experimental design of the project

project year	2003	2004	2005
soybean variety	non transgene	transgene	transgene
period of growth	June 11 th – Sept. 30 th	May 28 th – Oct. 30 th	July 10 th – Oct. 19 th
herbicide application	–	post-emerg. July 15 th	pre-emerg. May 24 th post-emerg. Sept. 6 th

LM 5.1 and 5.4 were treated with ^{14}C -glyphosate (5 mCi; 108 mg m⁻² a.i.) and for the measurement of mineralization and volatilization of ^{14}C -glyphosate two soil chambers and one plant chamber were installed on the lysimeters respectively as explained for the herbicide isoproturon by Schroll and Kühn (2004). The soil chambers were equipped with humidity and temperature sensors in 1 cm depth as described by Ruth and Munch (2005). Additionally, further sensors were installed beneath the chambers as reference measurement. An air-flow-sensor was installed to control the air flow in the soil chamber and to provide the same wind speed as 1 cm above the soil surface on the surrounding field. Pooled soil samples consisting of three single probes were taken at 0-2, 2-5, 5-10 and 10-20 cm depth. The sampling dates of soil and plant samples for pesticide content measurements are shown in Table 4.2.

Table 4.2: Sampling scheme for pesticide measurements of soil and plant samples

project year	2004	2005
Soil samples (days after first application)	4, 8, 14, 29, 60 and 126	8, 16, 57 and 97
Plant samples (days after sowing)	33, 66, 95 and 118	101 (at harvest)

Additionally, the nodulation of the soybeans was controlled and quantified in both years. Thus, all pesticide concentrations in lysimeter soil and plant samples presented in the subsequent graphics were measured by Grundmann et al. (unpublished results).

4.2.1.2 Measurement of plant growth parameters

Various plant growth parameters are necessary as input data and for the validation of the plant growth model. The plant biomass, plant height and leaf area index (LAI) were measured 33, 66, 95 and 118 days after the sowing date of the soybeans in the year 2004. In the year 2005 various attempts were necessary for the successful germination of the plants (sowings June 6th, June 23rd, and July 10th), hence plant parameters were only measured 51 and 101 days after the last sowing date. The dry weight (drying at 105 °C, 24 h) of the plant biomass was measured gravimetrically and separately for shoots and leaves (fruits had not developed) for LM 5.2 and 5.3. Root biomass was not measured as roots were needed for the experiments of other groups and complete root biomass could not be extracted in the lysimeters due to the great perturbation of the soil system. Between two and ten plants were sampled depending on the available amount. For the LAI measurement the leaves of the single plants were scanned and the leaf area was determined by image analysis with the program *Sigma Scan Pro* (Version 5.0.0).

4.2.1.3 Soil properties

The four lysimeters of the experiment were filled with the same sandy soil type (Table 4.3) in the year 2002 and represent a worst case for desiccation and the associated leaching risk. LM 5.1 to 5.4 are re-packed soil cores.

Table 4.3: Soil properties and some hydraulic characteristics of LM 5.1 to LM 5.4

Soil Type	Horizon depth	C _{org}	Clay	Silt	Sand	θ _{sat}	K _{sat}
Site	(cm)	(kg dm ⁻³)	(%)	(%)	(%)	(mm ³ mm ⁻³)	(mm d ⁻¹)
LM 5.1 to LM 5.4	0-30	0.95	4	8	88	0.25	1653
Haplic Arenosol	30-50	0.60	4	8	88	0.25	1653
Neumarkt	50-80	0.30	3	5	92	0.25	1573
	80-200	0.09	1	1	98	0.25	2313

θ_{sat} saturated vol. water content according to gravimetric measurements

K_{sat} saturated hydraulic conductivity calculated by Hutson & Cass-Burdine approach (Vereecken et al., 1990)

Unfortunately, the soil bulk density was not determined when the lysimeters were filled. Therefore, an overall soil bulk density of 1.5 kg dm⁻³ was estimated from lysimeter weight and water content measurements. The soil is classified as Haplic Arenosol and soil origin was Neumarkt in middle Bavaria.

4.2.1.4 Tracer experiment and ¹⁴C-radioactivity in the leachate

For the determination of the dispersivity coefficient a conservative tracer (δD, 81 %) was applied on LM 5.1 to LM 5.4 two days before the application of the ¹⁴C-labelled pesticide in the year 2004. 25 mL δD in form of ²H₂O mixed with 5 L deionised water (similar composition as rain water) were dispensed by a watering can on the lysimeters. The leachate was weekly sampled and radioactivity, ²H and ¹⁸O were measured. The stable isotope measurement and interpretation was done by the Stable Isotopes Group, Institute of Groundwater Ecology, GSF.

For the radioactivity measurement of the leachate, aliquots of 10 mL were mixed with 10 mL scintillation cocktail (Ultima Gold XR) and measured in the liquid scintillation counter. To prove whether the measured radioactivity results from glyphosate and its metabolites or from ¹⁴CO₂, aliquots of 300 mL leachate were acidified with H₃PO₄ to pH 1.9 and aerated for 10 min under agitation. The evolved ¹⁴CO₂ was trapped in 15 mL 0.1 M NaOH solution. Aliquots of 2 mL of the NaOH solution were mixed with 3 mL scintillation cocktail (Ultima Flo AF) and measured in the liquid scintillation counter (Tricarb 1900 TR, Packard, Dreieich, Germany).

4.2.2 Solute transport model

The modelling approaches described in this theoretical part are also valid for other xenobiotics than pesticides. But to keep conformity with the model application the term pesticides was used in the following sections instead. LEACHM (Leaching Estimation And CHemistry Model, version 3.1) is a modular package for calculating one-dimensional water flux and solute movement in vertically layered soils under transient conditions. The complete package is described in detail by Hutson and Wagenet (1992). For this study, a modified version of the submodel for the fate of pesticides in soils, LEACHP, which is based on the convection-dispersion equation, was implemented and linked to the water flow modules of *Expert-N*. In order to consider microbial population dynamics, the original biodegradation model was modified. Additionally, the model PLANTX of Trapp (1992) was used to simulate the uptake of pesticides by plants.

4.2.2.1 Model configuration and modelling strategy

In the glyphosate transport study soil water transport was simulated according to the model HYDRUS 6.0 (Simunek et al., 1998). Beneath the Hutson & Cass-Burdine parameterisation already applied in the water balance study (see section 3.2.2.2), also the van Genuchten-Mualem parameterisation of the hydraulic characteristics was used for water flow simulations. For a detailed description of the parameterisation see the *Expert-N* documentation (Priesack, 2006). The bottom boundary condition used in this application considers free drainage (Hutson and Wagenet, 1992). Potential evapotranspiration was calculated according to Haude (mrH) and the PM grass approach as described in section 3.2.2.3. Heat transfer, N-transport and N-turnover were simulated following the approaches of the model LEACHM (Hutson and Wagenet, 1992). Run-off was not considered and snow processes were regarded according to Schulla and Jasper (2000). For the simulation of crop development and crop growth the generic plant model SUCROS (van Laar et al., 1997) was applied. Model calibration and model input parameters are described in section 4.3.1.

The modelling strategy adopted was first to calibrate the glyphosate biodegradation parameters with data of the laboratory experiments. Then measurements of lysimeter weight, water content, outflow (see section 3.2.1.1) and tracer amounts in the leachate were used to choose the appropriate water flow and evapotranspiration model and to fit the effective solute transport parameters for the lysimeters. The fact that tracer and glyphosate were applied nearly simultaneously avoids the problem of different water flow characteristics during the calibration and application process.

The depth of the soil profile was set to 2.0 m, comprising 40 equidistant numerical layers of 5 cm for the glyphosate and tracer transport analysis. For the biodegradation simulations the soil profile was set to 0.9 m, comprising 90 equidistant numerical layers of 1 cm, to recognise a thin surface layer for the homogeneous distribution of the pesticide after application. The reason of this distinction was the maximum amount of numerical layers in *Expert-N*, which is limited to hundred layers. The numerical influence of taking smaller spatial steps on the glyphosate transport simulations was found to be small, as a numerical dispersion correction was applied.

4.2.2.2 Governing equations

The LEACHP model assumes that solutes partition between the sorbed, the liquid, and the gas phase. Interactions between the liquid and solid or liquid and gaseous phases are proposed to be linear and instantaneous, additional interactions between liquid and solid phases were also described by non-linear and non-equilibrium equations. The total concentration C_t (mg dm^{-3}) of a substance is then defined as:

$$C_t = (\theta + \rho_s K_d + \varepsilon K_H) C_l \quad (4.1)$$

with C_l (mg dm^{-3}) the concentration in solution, ρ_s (kg dm^{-3}) the soil bulk density, K_d the partition coefficient between solid and liquid phase ($\text{dm}^3 \text{kg}^{-1}$), ε ($\text{mm}^3 \text{mm}^{-3}$) the gas filled soil porosity ($\varepsilon = \theta_{sat} - \theta$) and K_H (-) the dimensionless Henry's Law constant defined as the saturated vapour density (mg dm^{-3}) of the compound divided by the aqueous solubility (mg dm^{-3}).

The movement of solutes through soil can take place due to macroscopic convection and hydrodynamic dispersion in the liquid phase:

$$J_{Cl} = -\theta D_m(q) \frac{dC_l}{dz} + q C_l \quad (4.2)$$

where J_{Cl} ($\text{mg m}^{-2} \text{d}^{-1}$) is the convective flux in the liquid phase, q (mm d^{-1}) the water flux density and $D_m(q)$ ($\text{mm}^2 \text{d}^{-1}$) the mechanical dispersion coefficient in dependence of q . Further movement is possible due to the diffusion flux $J_{Dl,g}$ ($\text{mg m}^{-2} \text{d}^{-1}$) in the liquid and gaseous phase according to Fick's law:

$$J_{Dl,g} = -D_0 \frac{dC}{dz} \quad (4.3)$$

where D_0 ($\text{mm}^2 \text{d}^{-1}$) is the appropriate molecular diffusion coefficient in water or in air and C (mg dm^{-3}) the pesticide concentration. For the diffusion in porous media, tortuosity and water content adjustments were done following Millington and Quirk:

$$\tau(\theta) = \frac{\theta^{10/3}}{\theta_{sat}^2} \quad (4.4)$$

with $\tau(\theta)$ (-) the tortuosity factor. In the previous version of LEACHP that is reported in Hutson and Wagenet (1992) the effective diffusion coefficient for the liquid phase was calculated according to Kemper and Van Schaik (1966). Eq. (4.4) is also applied for the air filled volume in soil with $\tau(\varepsilon)$. The effective diffusion coefficient in soil water $D_l(\theta)$ or air $D_g(\varepsilon)$ ($\text{mm}^2 \text{d}^{-1}$) can then be described by

$$D_l(\theta) = D_0 \tau(\theta) \quad (4.5)$$

$$D_g(\varepsilon) = D_0 \tau(\varepsilon). \quad (4.6)$$

A gas diffusion coefficient enhancement term due to barometric pressure fluctuations through soil as described in the original version of LEACHP was not specified in the present implementation.

The mechanical dispersion coefficient describes mixing due to different flow velocities between pores and can be estimated from:

$$D_m(q) = \lambda |v| \quad (4.7)$$

where $v = q/\theta$ (mm d^{-1}) is the pore water velocity and λ (mm) the dispersivity.

The diffusion-dispersion coefficients are generally combined to $D(\theta, q)$ ($\text{mm}^2 \text{d}^{-1}$) the effective diffusion coefficient:

$$D(\theta, q) = \frac{D_l(\theta)}{\theta} + D_m(q) + \frac{D_g(\varepsilon)K_H}{\theta}. \quad (4.8)$$

The effective transport parameters $D(\theta, q)$ and v were estimated using an analytical solution of the convection-dispersion equation (CDE) without sink-source terms proposed by Ogata and Banks (1961; cited in van Genuchten and Alves, 1982) and an inverse estimation procedure (cp. section 4.3.1.3).

Finally, the continuity relationship of mass over space and time results in the CDE for the transport of pesticides or tracer:

$$\frac{\partial C_l}{\partial t} (\theta + \rho_s K_d + \varepsilon K_H) = \frac{\partial}{\partial z} \left[\theta D(\theta, q) \frac{\partial C_l}{\partial z} - q C_l \right] \pm \phi \quad (4.9)$$

assuming local equilibrium between liquid and sorbed phases and the sink-source term ϕ ($\text{mg dm}^{-3} \text{ d}^{-1}$) composed of volatilisation ϕ_v , kinetic sorption ϕ_{sorb} , biodegradation ϕ_{deg} and plant uptake ϕ_{plant} .

Numerical procedures

The finite central differencing procedure was set up according to the implicit method of Bresler with the modification for unequal depth according to Tillotson et al. (1980). Second-order terms were ignored. In HYDRUS (Simunek et al., 1998) the definition of grid nodes differs from that of LEACHP (Fig. 4.2). The first nodal is placed at the soil surface in HYDRUS, which means that the discretisation of the upper and lower boundary conditions is different to LEACHP. The use of different numerical methods to solve flow and transport equations was compared with analytical solutions and studied in detail by Vanderborght et al. (2005). They found that both the spatial discretization of the pressure head profile close to the soil surface and the methods of averaging the hydraulic conductivities in the first grid layer influence the numerical solutions.

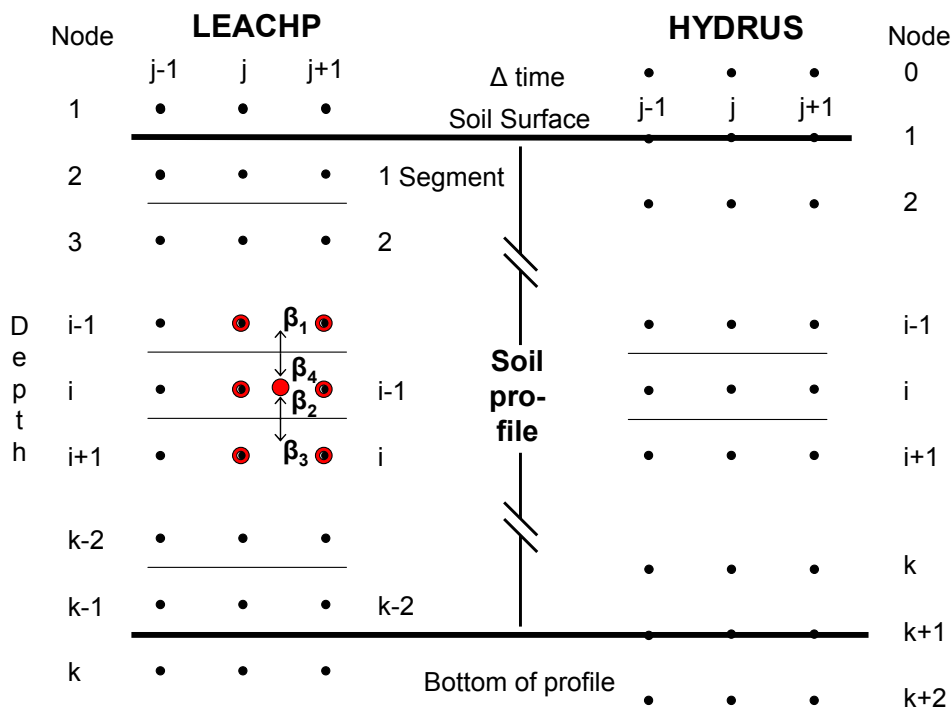


Fig. 4.2: Definition of nodes in the original LEACHP version compared to HYDRUS and water flux direction (arrows: water fluxes; red-black points: specific nodal concentrations; red point: nodal concentration $(C)_i^{j+1/2}$; $i = 1, \dots, k$ soil layer; $j = t_0, \dots, t_e$ simulation time, β see Eq. (4.10)).

The differencing procedure is exemplary shown in Eq. (4.10) for the convective transport of the solute in segment i . For the complete differencing scheme for the CDE see Hutson and Wagenet (1992). In Fig. 4.2 the nodal concentrations and water fluxes included for the calculation of solute accumulation or loss in segment i due to convection are shown. The convection term is consequently discretised considering the direction of water flux.

$$\frac{\partial}{\partial z}(qC_i)^{j+1/2} = \frac{\beta_1 q_{i-1/2}(C_{i-1}^j + C_{i-1}^{j+1})}{2\Delta z} - \frac{\beta_2 q_{i+1/2}(C_i^j + C_i^{j+1})}{2\Delta z} - \frac{\beta_3 q_{i+1/2}(C_{i+1}^j + C_{i+1}^{j+1})}{2\Delta z} + \frac{\beta_4 q_{i-1/2}(C_i^j + C_i^{j+1})}{2\Delta z} \quad (4.10)$$

According to the flux direction the values for β (Fig. 4.2) are defined as:

$$\begin{aligned} \beta_1 = 1 \quad \text{and} \quad \beta_4 = 0 \quad \text{when} \quad q_{i-1/2} > 0 \\ \beta_1 = 0 \quad \text{and} \quad \beta_4 = 1 \quad \text{when} \quad q_{i-1/2} < 0 \\ \beta_2 = 1 \quad \text{and} \quad \beta_3 = 0 \quad \text{when} \quad q_{i+1/2} > 0 \\ \beta_2 = 0 \quad \text{and} \quad \beta_3 = 1 \quad \text{when} \quad q_{i+1/2} < 0 \end{aligned}$$

Finally, the complete finite difference scheme of the CDE is solved using the Thomas tridiagonal matrix (Remson et al., 1971).

Hutson and Wagenet (1992) pointed out that because water fluxes are small in relation to total water content, the Freundlich isotherm is not incorporated into the CDE solver in LEACHP. Instead, the distribution between solved and sorbed solute concentration is calculated by a linear adsorption term. After solving the CDE with the linear adsorption isotherm, an additional sink term is called, where the partitioning of the solute according to the Freundlich isotherm is done iteratively by a bisection procedure. This procedure is usually sufficiently accurate, because water fluxes and thus as well mass balance errors are small.

Second order terms in the finite difference solution mainly were assumed to represent numerical dispersion. Simulation results of the finite difference solution of the CDE according to the LEACHP model showed to be in good agreement with the analytical solution of the CDE if numerical dispersion correction is only applied to the dispersivity coefficient (Hutson and Wagenet, 1992). Second-order terms and numerical dispersion correction for the diffusion processes were therefore ignored. The correction factor f_{corr} (mm) for the dispersivity coefficient is mainly influenced by the choice of segment thickness Δz (mm) (the correction is equivalent to a dispersivity increase of $f_{corr} = 0.16 \Delta z/\theta$). The influence of the time step length Δt (d) is negligibly small, if $\Delta t < 0.1$ day.

Upper and lower boundary conditions

It was assumed that no diffusion of the pesticide out of the soil profile is possible, therefore, at the upper and lower boundary of the soil profile the diffusion coefficients of the liquid and gaseous phase were set to zero. At the upper boundary three different Neumann conditions can be assumed: zero flux, infiltration and evaporation. Infiltration was not realised for substances, as the pesticides were applied by homogeneous mixing of the substances into the first soil horizon and they are naturally not contained in rain water. The evaporation flux for volatile substances is described apart in the section 4.2.2.4 ‘surface volatilization’. To consider that non-volatile substances accumulate in the upper soil horizon, the upper boundary condition has to assume no transport during water evaporation in the pesticide subroutine. The following upper boundary condition was assumed:

$$C_0^j = 0, \quad D_{1-1/2}^{j+1/2} = 0 \quad (4.11)$$

In *Expert-N* a free-draining profile was applied for the water flow at the lower boundary, where the hydraulic potential gradient is approximately unity. This results in a lower boundary condition of the pesticide transport equation:

$$C_{k+1}^j = const., \quad D_{k+1/2}^{j+1/2} = 0 \quad (4.12)$$

while the water flux density remains as in the water flow subroutine. Lysimeter may be simulated using a combination of constant potential and zero flux condition as proposed by Hutson and Wagenet (1992), but as described in Flury et al. (1999) a free-draining lower boundary is often applied, too.

4.2.2.3 Sorption processes ϕ_{sorb}

Solute sorption to soil can either be described by equilibrium sorption with a linear or non-linear isotherm or by kinetic two-site sorption. In the equilibrium approaches the time scale of sorption and desorption are assumed to be much smaller than the time scale of the transport processes and therefore sorption is handled as an equilibrium reaction. For the simplest case when a linear sorption isotherm is used, the adsorbed concentration C_s (mg kg⁻¹) of the solute is given by

$$C_s = K_d C_l . \quad (4.13)$$

Non-linear sorption was described by the Freundlich isotherm:

$$C_s = K_f C_l^{n_f} \quad (4.14)$$

where K_f (dm³ kg⁻¹) is the Freundlich coefficient and n_f (-) the Freundlich exponent. Additional to the original LEACHP model a Freundlich desorption isotherm was implemented. Thus, equilibrium adsorption-desorption reactions can be considered simultaneously according to van Genuchten et al. (1974). The Freundlich desorption coefficient K_{f-de} (dm³ kg⁻¹) can be expressed as

$$K_{f-de} = K_f^N C_{smax}^{(1-N)} \quad (4.15)$$

where $N = n_{f-ad}/n_{f-de}$ (-) is the proportion between Freundlich adsorption and desorption exponent and C_{smax} (mg kg⁻¹) is the adsorbed concentration prior to the initiation of desorption.

The non-equilibrium two-site sorption concept (van Genuchten and Wagenet, 1989) assumes that sorption sites can be divided into two linear fractions. The adsorbed concentration C_{s1} (mg kg⁻¹) on the equilibrium sites f (-) displays local chemical equilibrium:

$$C_{s1} = fK_d C_l \quad (4.16)$$

and on the remaining kinetic sites $(1-f)$ sorption is considered to be time-dependent. The concentration of solute at the kinetic sites C_{s2} (mg kg⁻¹) is assumed to depend upon the current degree of non-equilibrium between the kinetic sites and the solution phase C_l :

$$\frac{\partial C_{s2}}{\partial t} = \alpha((1-f)K_d C_l - C_{s2}) \quad (4.17)$$

with α (d⁻¹) the phase transfer coefficient and where $(1-f)K_d C_l$ describes the potential and C_{s2} the actual adsorption. This results in the following CDE:

$$\frac{\partial C_l}{\partial t} (\theta + f\rho_s K_d + \varepsilon K_H) = \frac{\partial}{\partial z} \left[\theta D(\theta, q) \frac{\partial C_l}{\partial z} - q C_l \right] - \alpha \rho_s ((1-f)K_d C_l - C_{s2}) \pm \phi \quad (4.18)$$

where the kinetic sites are treated as an additional source or sink term ϕ_{sorb} ($\text{mg dm}^{-3} \text{d}^{-1}$), which has to be added to the general sink term ϕ .

4.2.2.4 Surface volatilisation ϕ_v

To describe pesticide volatilisation an air-water interface consisting of a stagnant atmospheric film of thickness Δz_a (mm) where pesticide concentration is zero and a surface soil film of thickness Δz_s (mm) with a liquid pesticide concentration C_{l1} (mg dm^{-3}) was defined. The diffusive flux J_v ($\text{mg m}^{-2} \text{d}^{-1}$) through this interface is:

$$J_v = -K_{soil} C_{l1} \quad (4.19)$$

where K_{soil} (mm d^{-1}) is a diffusion mass transfer coefficient:

$$K_{soil} = \frac{D_{soil} D_{air} K_H}{D_{soil} + D_{air} K_H}. \quad (4.20)$$

For zero and upward surface water flux and for flux controlled water infiltration the effective diffusion D_{soil} (mm d^{-1}) in this surface soil segment is:

$$D_{soil} = \frac{D_l(\theta) + D_g(\varepsilon) K_H}{\Delta z_s} \quad (4.21)$$

and the diffusion D_{air} (mm d^{-1}) in the air film is:

$$D_{air} = \frac{D_{0a}}{\Delta z_a} \quad (4.22)$$

with D_{0a} ($\text{mm}^2 \text{d}^{-1}$) the molecular diffusion coefficient in air.

The sink term ϕ_v ($\text{mg dm}^{-3} \text{d}^{-1}$) for surface volatilization in the case of zero and upward water flux can be then described by

$$\phi_v = \frac{\min(C_{l1} \theta \Delta z, K_{soil} C_{l1} \Delta t)}{\Delta t \Delta z} \quad (4.23)$$

and in the case of flux controlled infiltration by

$$\phi_v = \frac{\min(C_{l1} q \Delta t, K_{soil} C_{l1} \Delta t)}{\Delta t \Delta z}. \quad (4.24)$$

This sink term is, just as the sink term for the kinetic site concentration, an additional term in the mass balance and volatilization and sorption rates are included at each time step in the CDE solver subroutine.

4.2.2.5 Microbial degradation ϕ_{deg}

Biodegradation of pesticides is controlled by the microbial activity and also by the bioavailability of the substrate (Fig. 4.3). The microbial activity is directly coupled to the solute concentration, if microorganisms use the pesticide as sole source of carbon and energy for growth. Solute transfer to the microorganisms compared to intrinsic microbial activity is in most cases the critical factor in bioremediation (Bosma et al., 1997). Up to now an important influence of degradation from the sorbed phase was not presented in literature or degradation was found to be much slower than from pesticide solution (Guo et al., 2000). Therefore, it was assumed that degradation occurs only in the liquid phase.

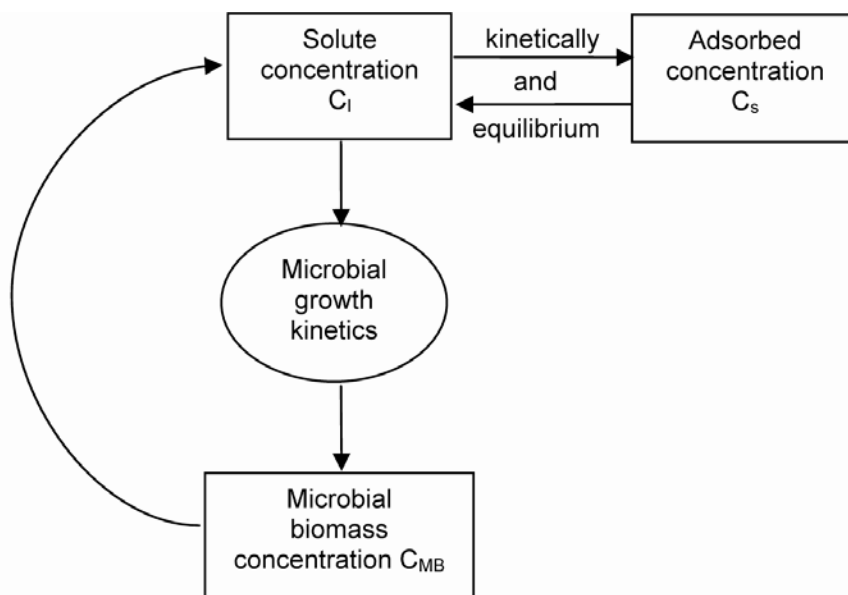


Fig. 4.3: Schematic representation of biodegradation capacities.

The microbial degradation subroutine provides optional modules for the microbial degradation processes and offers first-order degradation rate constants or Monod kinetics. Additionally, temperature and humidity response functions were implemented to account for the environmental conditions for microbial growth and degradation.

At present model structure allows to simulate up to four solutes simultaneously which can be either coupled in a unidirectional chain or may move independently of each other (Fig. 4.4).

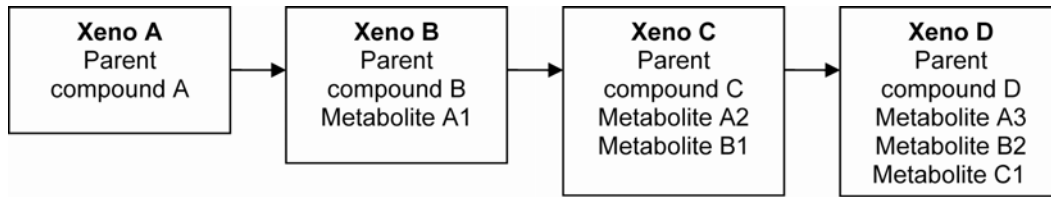


Fig. 4.4: Schematic representation of the pesticide degradation pathway.

Because it is assumed that degradation only takes place in the liquid phase the microbial degradation rate constant k_{mic} (d^{-1}) has to be multiplied by the water content. This results in an equation for the sink term ϕ_{deg} ($mg\ dm^{-3}\ d^{-1}$) assuming first-order degradation:

$$\phi_{deg} = -(k_{mic} + k_{phot})C_l\theta. \quad (4.25)$$

Additionally, the abiotic photolytic degradation rate k_{phot} (d^{-1}) is recognised for the first numerical layer.

Considering microbial population dynamics, Monod's classical approach was used, which couples the degradation of a substrate with microbial growth kinetics (Simkins and Alexander, 1984; Priesack and Kisser-Priesack, 1993; Blagodatsky and Richter, 1998; Bause and Merz, 2005):

$$\frac{dC_l}{dt} = -\frac{1}{\gamma} \frac{\mu C_l}{C_l + K_M} C_{MB} \quad (4.26\ a)$$

$$\frac{dC_{MB}}{dt} = \frac{\mu C_l}{C_l + K_M} C_{MB} - \sigma C_{MB} \quad (4.26\ b)$$

where C_l ($mg\ dm^{-3}$) is the concentration of the pesticide in solution, C_{MB} ($mg-C\ dm^{-3}$) the microbial biomass concentration, K_M ($mg\ dm^{-3}$) the half-saturation growth constant or Michaelis constant (which was assumed to be $K_M = 1/2\ C_{lmax}$ with C_{lmax} ($mg\ dm^{-3}$) the maximum concentration of the pesticide in solution), μ (d^{-1}) the specific growth rate of biomass, σ (d^{-1}) the microbial mortality rate and γ (-) the yield coefficient. γ describes the partitioning of the substrate consumption into growth and maintenance respiration and into microbial growth and is therefore the proportion of g-biomass C to g-substrate C.

The kinetic model in Eq. (4.27) is a possible mechanism to limit microbial concentrations to an upper boundary C_{MBmax} ($mg-C\ dm^{-3}$) by the logistic growth function. Simultaneously, the concentration can not fall below the lower boundary C_{MBmin} ($mg-C\ dm^{-3}$).

$$\frac{dC_{MB}}{dt} = \frac{\mu(\theta, T)C_l}{C_l + K_M} C_{MB} \left(1 - \frac{C_{MB}}{C_{MBmax}}\right) - \sigma(C_{MB} - C_{MBmin}) \quad (4.27)$$

The specific microbial growth rate μ is a function of humidity and temperature here (cp. Eqs. (4.30) and (4.31)).

This model can be used to account for the accelerated degradation behaviour of microorganisms which were adapted to the pesticide after several applications.

Microbial activity is dependent on the bioavailability of all substrates utilized by microorganisms. The upper approaches describe the consumption of a single growth-supporting substrate, e.g. a pesticide by a specialized microbial community. If it is assumed that the whole microbial biomass is able to degrade the pesticide, which means mainly co-metabolic degradation, an additional C-source must be added into the model:

$$\frac{dC_{MB}}{dt} = \left(\frac{\mu_{org} C_{org}}{C_{org} + K_{Morg}} C_{MB} + \frac{\mu(\theta, T) C_l}{C_l + K_M} C_{MB} \right) \left(1 - \frac{C_{MB}}{C_{MB \max}} \right) - \sigma(C_{MB} - C_{MB \min}) \quad (4.28)$$

where C_{org} (mg-C dm⁻³) is the concentration of bioavailable organic carbon, μ_{org} (d⁻¹) the growth rate on the bioavailable carbon substrate and K_{Morg} (mg-C dm⁻³) the respective Michaelis constant.

To get an estimation of the amount of bioavailable carbon in soil, the actual CO₂ emission from the soil surface, which is calculated in the carbon-cycle submodule in *Expert-N* and presents an indicator of microbial activity, can be equated to available carbon substrate C_{org} . According to the model SOILN (Johnsson et al., 1987) the amount of C_{CO_2} (mg m⁻²) released from soil surface can be calculated by

$$\frac{dC_{CO_2}}{dt} = ((1 - f_e) k_{avail} C_{avail}) e(\theta) e(T) \quad (4.29)$$

with C_{avail} (mg m⁻²) the available carbon amount (consisting of fresh organic substance, organic fertiliser, and humus), k_{avail} (d⁻¹) the mineralization rate of the available carbon, f_e (-) an effectivity constant and $e(\theta)$ (-) and $e(T)$ (-) reduction functions considering water content and temperature.

Two approaches were implemented, which describe temperature and soil moisture dependency of the actual microbial growth rate μ . Additionally, humidity and temperature response functions can be directly applied on the first-order degradation rate k_{mic} . The important influence of water potential on soil microorganisms responsible for pesticide degradation (Sommers et al., 1978), was described by a Gauss type humidity response function according to Richter et al. (1996). To account for the existence of optimal temperature conditions for bacterial growth the O'Neill function was used (von Götze and Richter, 1999). The combined influence of temperature and humidity on the actual microbial growth rate – called environmental response surface – was then simulated by:

$$\mu(\theta, T) = \mu_{\max} \left(\frac{\theta}{\theta_{crit}} \right)^{b_w} \exp \left(\left(1 - \frac{\theta}{\theta_{crit}} \right)^{b_w} \right) \left(\frac{T_{\max} - T}{T_{\max} - T_{opt}} \right)^x \exp \left(\frac{x(T - T_{opt})}{T_{\max} - T_{opt}} \right) \quad (4.30)$$

where μ_{\max} (d^{-1}) is the maximum specific growth rate of biomass at optimum water content, θ_{crit} ($mm^3 \text{ mm}^{-3}$) the threshold water content, b_w (-) a form parameter, T ($^{\circ}C$) is the actual temperature, T_{\max} ($^{\circ}C$) the lethal temperature for microorganisms, T_{opt} ($^{\circ}C$) the optimal temperature, and x (-) a parameter describing the sensitivity to temperature increase, similar to the Q_{10} -value. Additionally, a second humidity response function on the basis of a Weibull type function was applied:

$$\mu(\theta, T) = \mu_{\max} \left(1 - \exp \left(- \frac{\theta}{\theta_{crit1}} \right)^{b1} \right) \exp \left(\left(- \frac{\theta}{\theta_{crit2}} \right)^{b2} \right) \left(\frac{T_{\max} - T}{T_{\max} - T_{opt}} \right)^x \exp \left(\frac{x(T - T_{opt})}{T_{\max} - T_{opt}} \right) \quad (4.31)$$

where θ_{crit1} and θ_{crit2} ($mm^3 \text{ mm}^{-3}$) are the critical minimum and maximum water content, $b1$ and $b2$ (-) are form parameters.

Biodegradation rates vary with depth, as available nutrients and microbial biomass commonly decrease by more than 10-fold in the top 1m of soil (Willems et al., 1996). According to Jury et al. (1987) the initial distribution of microbial biomass concentration with depth C_{MB0} ($mg-C \text{ dm}^{-3}$) was described by

$$C_{MB0}(z) = C_{MBz(L)} \exp(-\eta(z-l)) \quad (4.32)$$

with $C_{MBz(L)}$ ($mg-C \text{ dm}^{-3}$) the initial biomass concentration in the surface zone, l (mm) the depth of this zone and η (mm^{-1}) the depth constant. The surface zone is defined as the zone within the microbial biomass is constant.

For the estimation of the microbial degradation parameters the results of the laboratory batch experiment described in section 2.3.1 were used. For the batch experiments a homogeneous distribution of the pesticide in soil without transport processes can be postulated. Here pesticide concentration in the liquid phase was calculated as follows:

$$C_l = \frac{C_{app}}{\Delta z(K_d \rho + K_H \varepsilon + \theta)} \quad (4.33)$$

where C_{app} ($mg \text{ m}^{-2}$) is the applied pesticide amount. Concentration in solution was calculated only once after application of the pesticide.

linked with the plant uptake model by the existing variable structures. In the original plant uptake model of Trapp only a linear volume growth of the plant parts with time can be simulated. The coupled simulation of plant growth and uptake also enables to include the fact that plant biomass has a death rate as well. The pesticide amount in the dead plant biomass can be added to the pesticide amount in the soil compartment and is available for microbial degradation there.

Following the pesticide uptake by roots from soil, the allocation in the whole plant is mainly governed by the transpiration stream from the roots via the stems to the leaves, whereas the reverse transport process with the phloem from leaves via stems to fruits, to roots and nodules was also suggested (Fig. 4.5). The allocation in the plant following foliar application occurs only with the phloem flux. In the following equations W (kg) denotes weight of plant tissue, C (mg kg^{-1}) concentration in the various plant parts, C_l (mg dm^{-3}) concentration in soil solution, λ (d^{-1}) first-order metabolism rate coefficient. The respective subscripts denote the single plant compartments with R for roots, St for stems, L for leaves, F for fruits and Nod for nodules. For all four original compartments pesticide metabolism in the plant tissues can be considered.

The uptake of the solute into the plant roots takes place passively with the transpiration flux into the xylem sap and by diffusion into the plant roots. Considering metabolic degradation and the phloem flux $q_{phloem,R}$ (kg d^{-1}) (cp. Eq. 4.43) in and out of the compartment as well, the daily flux into the root compartment can be written as:

$$\begin{aligned} \frac{\partial(W_R C_R)}{\partial t} = & \frac{2L_R \pi}{\ln R_2/R_1} D_{eff} \left(C_l - \frac{C_R}{K_{RW}} \right) + \frac{q_t (1-TSCF) C_l}{\rho_{plants}} \\ & + q_{phloem,R} \left(\frac{C_L}{K_L} - \frac{C_R}{K_R} \right) - \lambda_R W_R C_R \end{aligned} \quad (4.34)$$

where q_t (mm d^{-1}) is the transpiration flux and L_R (mm) the total root length for the respective simulation layer. In *Expert-N* the pesticide uptake from soil can be calculated for single spatial numerical layers, which means that both pesticide concentration and root density distribution with depth are of importance. In Eq. (4.34) R_l (mm) is the root radius and R_2 (mm) the radius of a zone of pesticide depletion around the root. K_{RW} ($\text{dm}^3 \text{ kg}$) is a partitioning coefficient between the plant tissue and water and K_R (-) and K_L (-) are partitioning coefficients between the plant tissue and phloem sap. They describe the adsorption of the pesticide to the plant material (cp. Eqs. 4.41 and 4.42). ρ_{plants} (plants m^{-2}) is the plant density and therefore accounts that q_t is an area value and has to be calculated for the single plant simulated in the plant growth model.

The effective diffusion coefficient D_{eff} ($\text{mm}^2 \text{d}^{-1}$) in soil is depth dependent as well and is calculated for each numerical spatial layer by (cp. Eqs. (4.5) and (4.6) in section 4.2.2.2):

$$D_{eff} = D_l(\theta) + D_g(\varepsilon)K_H . \quad (4.35)$$

The transpiration stream concentration factor $TSCF$ (-) for non-ionized compounds is related to the octanol-water partitioning coefficient. Eq. (4.34) reflects the theory that hydrophilic xenobiotics are not able to penetrate roots because of hydrophobic membranes and that lipophilic xenobiotics are not transported because they are removed within the root by partitioning onto the lipid-like phase (Severinsen and Jager, 1998). Therefore, the translocation in the xylem is best for medium polar substances. In the empirical approach in Eq. (4.36) the $TSCF$ was calculated in dependence on the octanol-water partitioning coefficient K_{OW} (-):

$$TSCF = 0.784 \exp\left(\frac{-(\log K_{OW} - 1.78)^2}{2.44}\right). \quad (4.36)$$

The transfer from roots to stems further takes place via the transpiration flow in the xylem. The reverse process of pesticide transport with the assimilate flow in the phloem from foliage to stem was also considered (Trapp, 1992):

$$\frac{\partial(W_{St}C_{St})}{\partial t} = \frac{q_t \left(TSCF C_l - \frac{C_{St}}{K_{StW}} \right)}{\rho_{plants}} + q_{phloem.St} \frac{C_L}{K_L} - \lambda_{St} W_{St} C_{St} \quad (4.37)$$

where $q_{phloem.St}$ (kg d^{-1}) is the flux of the assimilates partitioned from the leaves to the stems and K_{StW} ($\text{dm}^3 \text{kg}^{-1}$) (cp. Eq. 4.42) is the respective adsorption coefficient stem tissue to xylem sap. The movement into the leaves also follows the transpiration flow. The diffusive exchange between air and plant leaves as proposed by Trapp was not implemented in the present approach. The pesticide flux into the plant leaves via xylem and out of the leaves via phloem can be written as:

$$\frac{\partial(W_L C_L)}{\partial t} = \frac{q_t C_{St}}{\rho_{plants} K_{StW}} - \frac{C_L}{K_L} (q_{phloem.St} + q_{phloem.R} + q_{phloem.F}) - \lambda_L W_L C_L + J_L \quad (4.38)$$

where J_L (mg d^{-1}) considers the penetration flux through the cuticular membrane into the internal leaf tissue of a foliar applied pesticide and is described in more detail below. The pesticide transport into the fruits and nodules results from the co-transport with the assimilate flux:

$$\frac{\partial(W_F C_F)}{\partial t} = q_{phloem.F} \frac{C_L}{K_L} - \lambda_F W_F C_F \quad (4.39)$$

$$\frac{\partial(W_{Nod}C_{Nod})}{\partial t} = q_{phloem.R} \frac{C_R}{K_R} \quad (4.40)$$

For the special application of the simulation of glyphosate in soybean a transformation of the herbicide in the nodules is not considered, as glyphosate is not metabolised in plants.

The partitioning coefficients K_L and K_R (-) between plant tissue and phloem sap can be calculated by

$$K = \left(\theta_{pl.tissue} + L_{pl.tissue} K_{OW}^{b_{1/o}} \right) \frac{\rho_{pl.tissue}}{\rho_w} \quad (4.41)$$

according to Trapp (1992) and the coefficients between plant tissue and water (or xylem sap) K_{RW} , K_{StW} and K_{LW} ($\text{dm}^3 \text{kg}^{-1}$) by

$$K = \frac{\theta_{pl.tissue}}{\rho_{pl.tissue}} + \frac{L_{pl.tissue} K_{OW}^{b_{1/o}}}{\rho_w} \quad (4.42)$$

with $\theta_{pl.tissue}$ (kg kg^{-1}) the water content of plant tissue, $L_{pl.tissue}$ (kg kg^{-1}) the lipid content of plant tissue, $\rho_{pl.tissue}$ (kg dm^{-3}) the density of the dry plant tissue, ρ_w (kg dm^{-3}) the water density and $b_{1/o}$ (-) a correction exponent for the difference between plant lipid material and octanol.

The phloem flux q_{phloem} (kg d^{-1}) is partitioned according to the assimilate allocation in the plant growth model:

$$q_{phloem.R} = f_{fract.R} (\Delta W_{Bio} - \Delta W_L) / \rho_{plant} \quad (4.43)$$

$$q_{phloem.St} = f_{fract.St} (\Delta W_{Bio} - \Delta W_L) / \rho_{plant} \quad (4.44)$$

$$q_{phloem.F} = f_{fract.F} (\Delta W_{Bio} - \Delta W_L) / \rho_{plant} \quad (4.45)$$

where f_{fract} (-) denotes the respective partitioning factor, ΔW_{Bio} ($\text{kg ha}^{-1} \text{d}^{-1}$) the total biomass growth rate and ΔW_L ($\text{kg ha}^{-1} \text{d}^{-1}$) the leaf biomass growth rate.

The pesticide amount accumulated in the dead plant material W_{dead} (kg) is given by

$$\frac{\partial(W_{dead}C_{dead})}{\partial t} = \frac{\partial(W_{old}C)}{\partial t} \left(\frac{W_{old} - W}{W_{old}} \right) \quad (4.46)$$

with W_{old} (kg) the plant weight at the previous time step.

The sink term ϕ_{plant} ($\text{mg dm}^{-3} \text{d}^{-1}$) in the convection-dispersion equation must then be calculated by

$$\phi_{plant} = - \frac{\partial(W_R C_R)}{\partial t} \frac{\rho_{plants}}{\Delta z} \quad (4.47)$$

for the pesticide uptake by the plant roots in the respective numerical layer with layer thickness Δz (mm). The implementation of pesticide uptake by plant roots was exemplarily tested for the herbicide isoproturon in a test run (results are not shown).

Cuticular penetration of pesticides

The penetration of a foliar-applied pesticide through the cuticular membrane into internal plant tissues is governed by three main factors: a) the chemical structure of the pesticide itself b) properties of the leaf cuticle and c) the environmental conditions at the application date (Satchivi et al., 2000). Diffusion is considered to be the most important process for transport of pesticides across the cuticle, and the concentration gradient between the spray deposit and the inside of the plant was believed to govern the rate of uptake.

$$J_L = rHF \frac{f_{sc}}{\rho_{plants}} P \left(C_{surf} - \frac{C_L}{K_{LW}} \right) \quad (4.48)$$

The surface concentration C_{surf} (mg dm⁻³) is the amount (mg) applied per m² leaf surface divided through the thickness dx_{film} (mm) of the solution film on the plant leaves. The permeance P (mm d⁻¹) of the pesticide depends on the thickness dx_{cut} (mm) of the cuticula barrier and on k (d⁻¹) the rate constant of penetration:

$$P = k dx_{cut} . \quad (4.49)$$

According to Schönherr (2002) penetration can be completely described by the rate constant k and k is given by the fraction M_t penetrated into the leaf over time t (d) to the fraction M_0 applied on the leaf:

$$\frac{M_t}{M_0} = 1 - \exp(-kt) \quad (4.50)$$

and thus can be calculated from measured M_t/M_0 (-) for a given time interval [0,t]. The penetration rate is strongly reduced after the first day after application. The relative humidity rH (%) at the time of application has an important impact on the foliar absorption and penetration. Satchivi et al. (2000) suggested the introduction of a relative humidity factor rHF (-) based on the empirical equation

$$rHF = 0.1642 \cdot 10^{(1.4419 rH/100\%)} . \quad (4.51)$$

Because temperature effects are less consistent they are not considered in the present work. Additionally, the covering of the ground with leaves must be considered in the factor f_{sc} (-):

$$f_{sc} = 1 - \exp(-0.45LAI) \quad (4.52)$$

where LAI (m² m⁻²) is the leaf area index.

The surface concentration must be then reduced by the following equation at each time step Δt (d):

$$C_{surf} = C_{surf} - \frac{J_L \cdot \Delta t \cdot \rho_{plants}}{\Delta x_{film}} . \quad (4.53)$$

After a strong rain event the surface concentration is assumed to be zero because the pesticide is washed down.

4.2.2.7 Statistical analysis

The same statistical measures and similar model evaluation methods were used for the solute transport study as for the water flow study (see section 3.2.2.4) and are not explained again. Additionally, partial and multiple correlation coefficients according to Sachs (1984) were introduced. Partial and multiple correlation coefficients can be written in terms of the simple correlation coefficients r_{12} , r_{13} and r_{23} . The partial correlation coefficient $r_{12.3}$ describes the correlation between the dependent variable 1 and the independent variable 2 under exclusion of the influence of variable 3.

$$r_{12.3} = \frac{r_{12} - r_{13}r_{23}}{\sqrt{(1 - r_{13}^2)(1 - r_{23}^2)}} \quad (4.54)$$

The multiple correlation coefficient $r_{1.23}$ is a measure of the strength of the association between the independent variables 2 and 3 and the dependent variable 1.

$$r_{1.23} = \sqrt{\frac{r_{12}^2 + r_{13}^2 - 2r_{12}r_{13}r_{23}}{1 - r_{23}^2}} \quad (4.55)$$

Unlike the partial, the multiple correlation coefficient is always greater than zero.

4.3 Results and Discussion

4.3.1 Model calibration and model input parameters

Model input parameters were derived from literature data or were measured in laboratory batch experiments or at the lysimeter facility. The main model input parameters for the glyphosate study are listed in Table 4.4. The basic physicochemical properties of glyphosate were taken from the Review Report Glyphosate (Bruno and Schaper, 2002) and sorption parameters were derived from the laboratory batch experiments.

Table 4.4: Main model input parameters for the glyphosate study

<i>General Parameters</i>	<i>Molecular diffusion coefficient</i> ^a
Profile depth: 900/2000 mm	in water: 75.19 mm ² d ⁻¹
Segment thickness: 10/50 mm	in air: 72.45 · 10 ⁴ mm ² d ⁻¹
Lower boundary condition: free drainage	
<i>Initial profile chemical data</i> – set to zero	<i>Sorption parameters</i>
	Linear Isotherm:
	K _{OC} : 1287.4 dm ³ kg ⁻¹
<i>Chemical applications</i>	non-equilibrium α: 2.76 d ⁻¹ ^b f: 0.3 ^b
Application rates: 0.9 – 1.1 kg ha ⁻¹	Freundlich Isotherm:
	K _{fOC} : 2600.0 dm ³ kg ⁻¹
<i>Chemical properties</i>	n _f : 0.943 n: 0.538
Molecular weight: 169.0 g mol ⁻¹	
Water solubility: 1.1 · 10 ⁴ mg dm ⁻³	<i>Crop data</i>
Vapour density: 1.31 · 10 ⁻⁵ Pa	Permeability coefficient leaf ^c :
Henry constant: 8.66 · 10 ⁻¹¹	first day 1.01 · 10 ⁻⁵ m d ⁻¹
Log K _{OW} : -3.2	afterwards 2.92 · 10 ⁻⁷ m d ⁻¹

^a Calculated values according to Trapp and Matthies (1996)

^b Estimated values (see section 4.3.2.2)

^c Calculated values (see section 4.3.4)

K_{fOC} Freundlich carbon distribution coefficient

Table 4.5: Soybean input parameters for the plant uptake model (Penning de Vries et al., 1989; Trapp, 1992)

<i>Water – lipid content in %</i>	<i>Correction exponent b (lipid/octanol)</i>
Root 94.2 – 0.3	Root 0.77
Stem 76.7 – 0.5	Stem 0.77
Leaf 76.7 – 0.5	Leaf 0.95
Fruit 72.3 – 0.3	
Root radius ^a	Solution film thickness ^b
2.0 mm	0.039 mm

^a Derived from soybean measurements

^b Estimated value from the applied herbicide solution

The parameterisation of the plant growth model SUCROS was done according to the parameter values for soybean listed by Penning de Vries et al. (1989). The phenological parameters of soybean were calibrated for the present lysimeter study under usage of the measured plant parameters. The input parameters which are necessary for the simulation of herbicide uptake by soybean are listed in Table 4.5.

For the simulation of potential evapotranspiration with the Haude (mrH) approach the soybean specific Haude factors were calibrated for the year 2004 (Table 4.6) and validated with the lysimeter data of the year 2005.

Table 4.6: Haude factors calibrated for soybean in 2004 in the lysimeter study

Jan	Feb	Mar	Apr	May	June	July	Aug	Sep	Oct	Nov	Dec
0.11	0.11	0.11	0.11	0.11	0.17	0.28	0.37	0.28	0.24	0.11	0.11

Meteorological driving parameters used by the model were measured at the automatic weather station at the lysimeter facility as described in section 3.2.1.1. Further calibrations of model input parameters using measured data are shown below in detail.

4.3.1.1 Calibration of degradation parameters with laboratory results

The model parameterisation strategy adopted for the biodegradation approach was to estimate a first-order degradation rate constant using data of the laboratory experiments including parameterisation of humidity and temperature dependencies as a first step. In a second step, parameter estimation problems in kinetic models were analysed and discussed under usage of correlation coefficients and matrix scatter plots for the parameters of the Monod approach. Finally, the parameters of the Monod approach were fitted to the laboratory data.

4.3.1.1.1 First-order degradation including humidity and temperature dependencies

The degradation of glyphosate in the biodegradation batch experiments was first fitted by a first-order degradation rate for the liquid phase with the software package *Mathematica*® (version 5.0). The initial concentration of the pesticide in the liquid phase was calculated (cp. Eq. 4.33) by use of the parameters listed in Table 4.7. The soil bulk density of the sieved soil samples used in the laboratory experiments was assumed to be 1.0 kg dm^{-3} . In the case of the laboratory study, the K_d value describes the potential bioavailable pesticide amount, which includes the potentially desorbable amount of the pesticide (see Fig. 2.9 in section 2.3.2).

Table 4.7: Parameter values in the laboratory experiment for calculation of the initial concentration of glyphosate in the liquid phase

Parameters for initial distribution			
Chemical application		Soil and profile parameters	
C_t :	108.0 mg m ⁻²	θ_{sat} :	0.288
		Δz :	10 mm
Distribution parameters		ρ_s :	1.0 kg dm ⁻³
K_d value:	2.9 dm ³ kg ⁻¹		
K_H value:	$8.655 \cdot 10^{-11}$		

Initially, the first-order degradation rate k_{mic} was fitted at the optimum water content (40 % of max. WHC). Fig. 4.6a shows the decrease of the solute concentration of glyphosate in soil under the assumption that only the dissolved fraction was bioavailable for degradation and under the assumption of linear equilibrium sorption. A degradation rate constant of $k_{mic} = 2.31 \text{ d}^{-1}$ ($r^2 = 0.973$) was achieved in the fit with the *NMinimize* function in *Mathematica*®. For the $DT_{50\text{lab}}$ value this results in 10 days for the biodegradation of the dissolved fraction. In Fig. 4.6b a sensitivity analysis for k_{mic} was carried out. The analysis shows that especially for small k_{mic} values the sensitivity is high. A variation of k_{mic} of $\pm 100 \%$ results in a variation of degradation after sixteen days between - 99 % and + 45 % of the degraded concentration instead of using $k_{mic} = 2.31 \text{ d}^{-1}$.

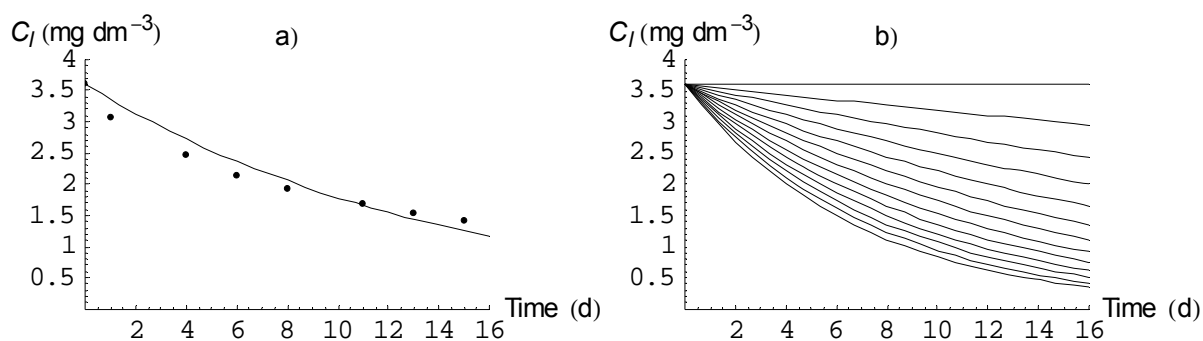


Fig. 4.6: Concentration of glyphosate in the liquid phase in the batch degradation study at a water content of 40 % of max. WHC (LM 5; part a) symbols: measurement, line: fitted model simulation with $k_{mic} = 2.31 \text{ d}^{-1}$ and part b) sensitivity analysis for k_{mic} with $2.31 \text{ d}^{-1} \pm 100 \%$ with step size 0.4 d^{-1}).

In the laboratory batch experiments reported by Schroll et al. (2006) it was shown that the degradation of glyphosate was strongly dependent on the water content in soil. The cumulative degradation amount after 15 days at different water contents (5-20 % and 70-100 % max. WHC results of Schroll et al. (2006), 30-60 % max. WHC own measurements) was used for the calibration of the humidity response function. Regarding the work of Schroll et al. it has to be discussed, whether water content or water potential is the proper variable to

use in humidity related degradation rates. The generalisation that optimum degradation occurs at a water potential of -0.015 MPa (Schroll et al., 2006) seems to be very useful for mathematical descriptions, if humidity-dependent degradation rates cannot be fitted to experimental conditions like in the present study.

Fig. 4.7a shows the Gauss type humidity response function and Fig. 4.7b the Weibull type humidity response function for the first-order degradation rate. For the goodness of fit function b ($r^2 = 0.910$) gives a better result compared to function a ($r^2 = 0.858$). For the evaluation of the experimental results it must be considered that the mixing of the soil at water contents of 70 and up to 100 % of the max. WHC (equivalent water content (WC) = 0.160 to 0.228 $\text{m}^3 \text{m}^{-3}$) is difficult and the experimental results may be inaccurate. As given by the Weibull type function a strong decrease in degradation due to a lack of oxygen in the soil at water contents of more than 80 % of the max. WHC (equivalent WC = 0.182 $\text{m}^3 \text{m}^{-3}$) is therefore more likely to occur. The sensitivity analysis in Fig. 4.6b shows that the sensitivity of the glyphosate degradation is high for small values of k_{mic} . Small values for k_{mic} are achieved for low and high water contents (Fig. 4.7). This shows that small changes in the low and high water content ranges will have strong influence on the degradation of the herbicide.

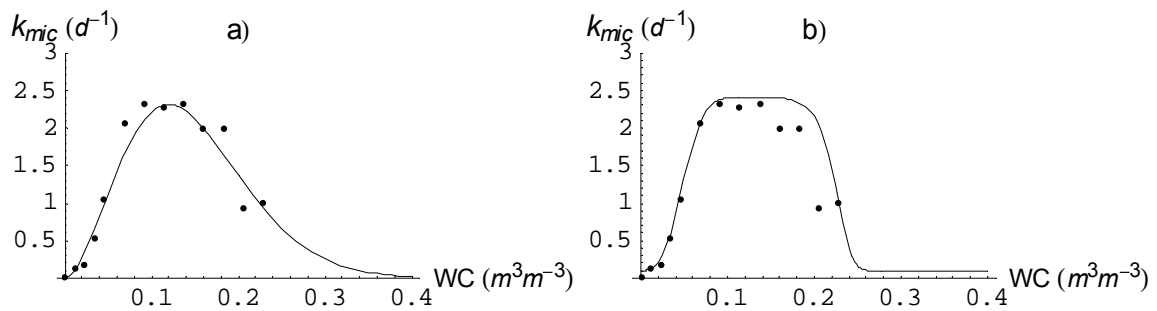


Fig. 4.7: Humidity response functions for k_{mic} (symbols: measurements, line: part a) Gauss type function with $\theta_{crit} = 0.12 \text{ m}^3 \text{m}^{-3}$, $b_w = 1.71$, $k_{max} = 2.31 \text{ d}^{-1}$ and part b) Weibull type function $\theta_{crit1} = 0.055 \text{ m}^3 \text{m}^{-3}$, $\theta_{crit2} = 0.23 \text{ m}^3 \text{m}^{-3}$, $b1 = 3$ and $b2 = 15$).

The comparison of the simulated degradation curves with the laboratory measurements indicates that the Weibull type humidity response function ($r^2 = 0.943$) achieves better results at different water contents than the Gauss type humidity response function ($r^2 = 0.913$) (Fig. 4.8).

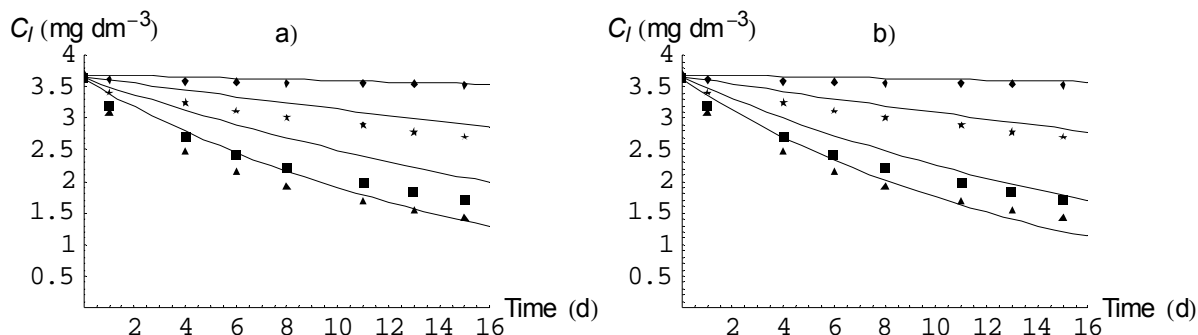


Fig. 4.8: Liquid concentration of glyphosate in the batch degradation studies at water contents of 10, 20, 30 and 40 % of max. WHC (symbols: measurements at 10 (diamonds), 20 (stars), 30 (squares) and 40 (triangles) % of max. WHC; line: model simulation with humidity response according to a) Gauss type and b) Weibull type function; LM 5).

The O'Neill function was used as temperature response function (Fig. 4.9a) for k_{mic} to account for the temperature conditions at bacterial growth. Because the effect of variable temperatures on the biodegradation of glyphosate was not examined in laboratory studies, optimum and maximum temperature were adopted from the values cited by Richter et al. (1996) for the chlorinated phenoxy-carboxylic acid herbicide 2,4 D. The combined effect of temperature and humidity is shown in Fig. 4.9b in the response surface for k_{mic} .

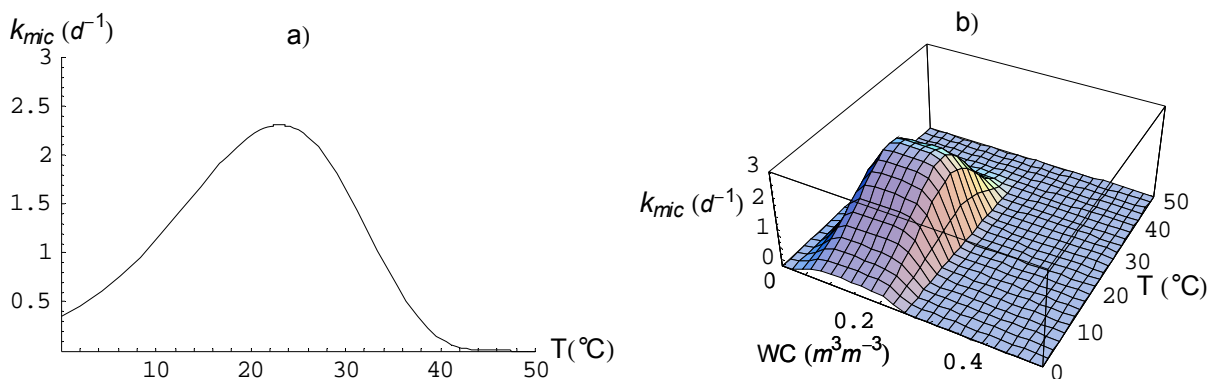


Fig. 4.9: k_{mic} in dependence of temperature (part a: O'Neill function with $T_{opt} = 23$ °C, $T_{max} = 50$ °C, $x = 8$) and of the combination of humidity and temperature (part b: Weibull type (parameters as in Fig. 4.7 b) and O'Neill function).

Temperature has diurnal cyclical variations especially in the upper soil. The heat transfer model in *Expert-N*, following the approach of Tillotson et al. (reported in the model description of LEACHM by Hutson and Wagenet, 1992), calculates mean soil temperatures without diurnal variations. In the investigated field study the application time of the pesticide was generally in summer time, when diurnal variations should be less important. Therefore, the present modelling approach of heat transfer seems to be precise enough.

4.3.1.1.2 Parameter estimation problems in Monod degradation characteristics

It was clearly shown by the biodegradation experiments (see section 2.3.1) that glyphosate degradation occurs mainly due to microbial activity. Beneath the microbial activity, biodegradation of pesticides is controlled by the bioavailability of degradable organic substrates. Applying Monod degradation characteristics, where the relation between substrate concentration and microbial biomass is described, highly correlated estimates of some of the parameters occur (Simkins and Alexander, 1984). As a consequence, multiple combinations of input parameters will provide a similar good fit to the experimental data. Thus, the link between models and data should include the application of advanced statistical and numerical methods to regression problems, to answer the problems of parameter estimation in kinetic models (Richter et al., 1996). The application of Monod degradation characteristics would necessitate the execution of various laboratory experiments with a wide range of experimental conditions. Due to the lack of such extensive experimental results, the sensitivities and correlations of model results and various independent variables were studied. First it was assumed in the simulation model that biodegradation of glyphosate occurs only by a specialized microbial community. Then it was considered that the total microbial biomass in soil is able to degrade glyphosate.

Correlation coefficients and matrix scatter plots

Partial and multiple correlation coefficients are a measure of the strength of the association between the independent and dependent variables (cp. section 4.2.2.7). The partial correlation coefficients in Table 4.8 show that the microbial growth rate has the highest effect on the simulated solute pesticide concentration in soil (cp. Eq. (4.26 a) and 4.27), while the maximum microbial biomass has the weakest effect on the concentration (cp. also Fig. 4.10). On the first and on the fifteenth day after application the yield factor is of secondary importance, but is replaced from this position by the microbial death rate in the middle of the experimental time. Beneath the maximum microbial biomass the association between minimum microbial biomass and pesticide concentration is also moderate and gets more important after degradation of most of the pesticide (day 15). The association between solute pesticide concentration and half saturation is higher than the association of concentration and minimum microbial biomass, but also moderate. The influence of K_M and γ on pesticide concentration is comparable (Table 4.8) and with time changes from a higher influence of γ at the beginning to a higher influence of K_M later.

Table 4.9 shows that K_M together with γ determines the pesticide concentration less than the growth rate together with any other parameter.

Table 4.8: Partial correlation coefficients in the Monod degradation approach

time (days)	1	4	8	15
$r_{\mu \text{ Cl.CMBmax}}$	-0.917	-0.974	-0.983	-0.962
$r_{\mu \text{ Cl.CMBmin}}$	-0.895	-0.953	-0.972	-0.971
$r_{\mu \text{ Cl. } \sigma}$	-0.735	-0.862	-0.911	-0.922
$r_{\mu \text{ Cl.Km}}$	-0.744	-0.941	-0.956	-0.941
$r_{\mu \text{ Cl.}\gamma}$	-0.688	-0.934	-0.963	-0.964
$r_{\text{CMBmax Cl.}\mu}$	-0.208	-0.356	-0.247	-0.091
$r_{\text{CMBmin Cl.}\mu}$	-0.421	-0.399	-0.610	-0.721
$r_{\sigma \text{ Cl.}\mu}$	0.575	0.803	0.819	0.744
$r_{\text{Km Cl.}\mu}$	0.557	0.766	0.779	0.691
$r_{\gamma \text{ Cl.}\mu}$	0.577	0.681	0.748	0.773
$r_{\text{Km Cl. } \gamma}$	0.513	0.688	0.824	0.884
$r_{\gamma \text{ Cl.Km}}$	0.746	0.739	0.818	0.864

Table 4.9: Multiple correlation coefficients in the Monod degradation approach

time (days)	1	4	8	15
$r_{\text{Cl. } \mu \text{ CMBmax}}$	0.918	0.974	0.983	0.962
$r_{\text{Cl. } \mu \text{ CMBmin}}$	0.900	0.954	0.973	0.973
$r_{\text{Cl. } \mu \sigma}$	0.791	0.908	0.935	0.935
$r_{\text{Cl. } \mu \text{ Km}}$	0.792	0.949	0.961	0.947
$r_{\text{Cl. } \mu \gamma}$	0.763	0.941	0.966	0.967
$r_{\text{Cl. Km } \gamma}$	0.785	0.823	0.897	0.931

Scatter plots can help to visualize the relationship between the variation in model input parameters and the related pesticide concentration. A matrix of scatter plots forms the columns of a multivariate data set plotted against each other. The matrix scatter plot of Fig. 4.10 concerns the relationship between microbial growth rate and maximum microbial biomass in soil and the sensitivity of the degraded pesticide concentration. Fig. 4.10 shows that the simulated pesticide concentration is highly sensitive to the change of μ . This does not

change with time, only for smaller values the influence increases with time, for high values the influence decreases with time. A weak association between C_{MBmax} and pesticide concentration only becomes obvious, if the microbial growth rate is high.

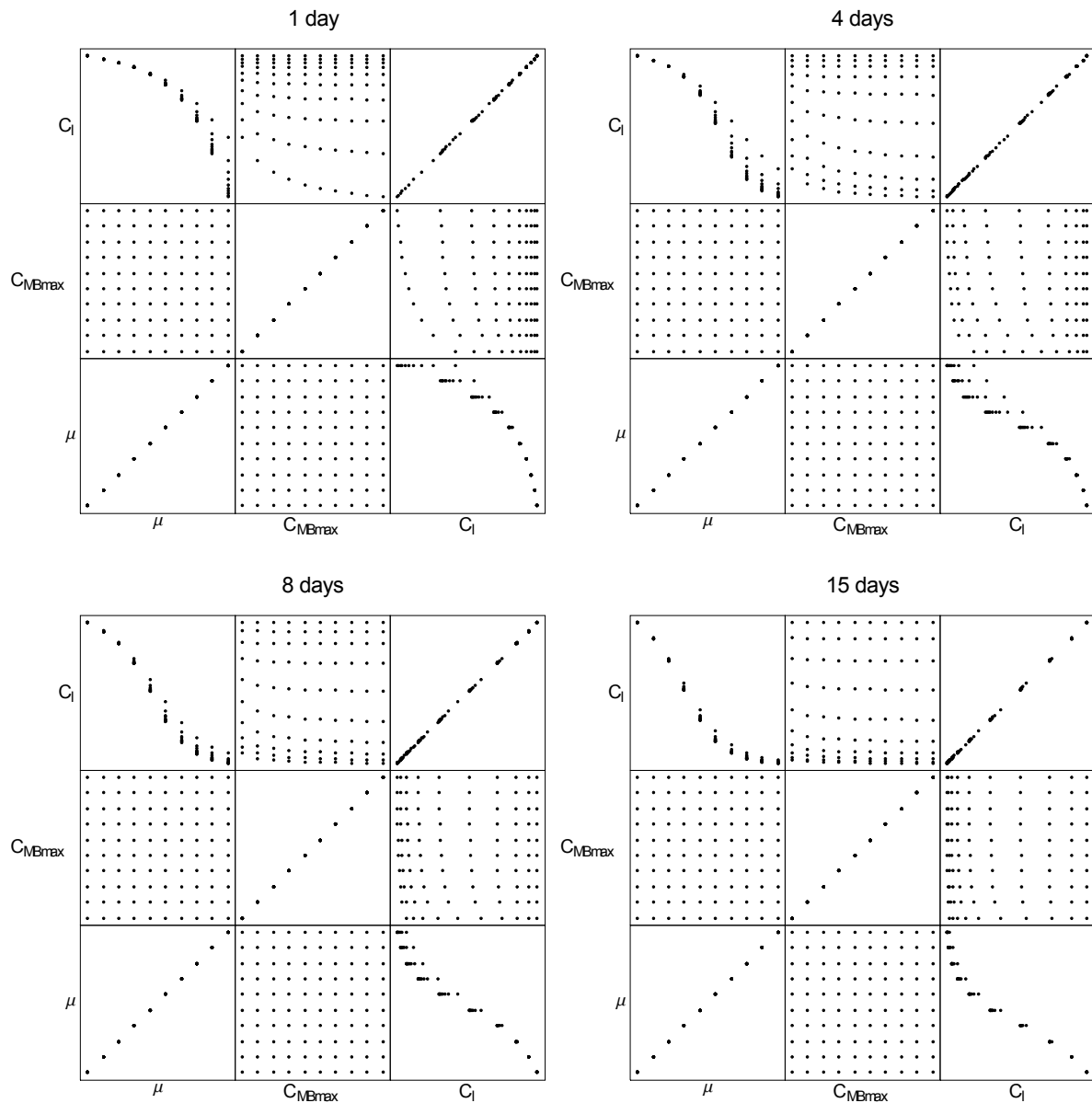


Fig. 4.10: Matrix scatter plot of μ (range 1-10 d^{-1} , step size 1 d^{-1}), C_{MBmax} (range 3-30 $mg-C dm^{-3}$, step size 3 $mg-C dm^{-3}$) and resulting C_l concentration at 1, 4, 8 and 15 days after application date; graphics predetermined in *Mathematica*®.

Fig. 4.11 shows that the influence of the death rate σ increases as expected with increasing growth rates at the beginning of degradation and decreases with increasing growth rates at the end of the observed time period. A negative correlation of both parameters is obvious. The influence of the microbial growth rate increases constantly with time.

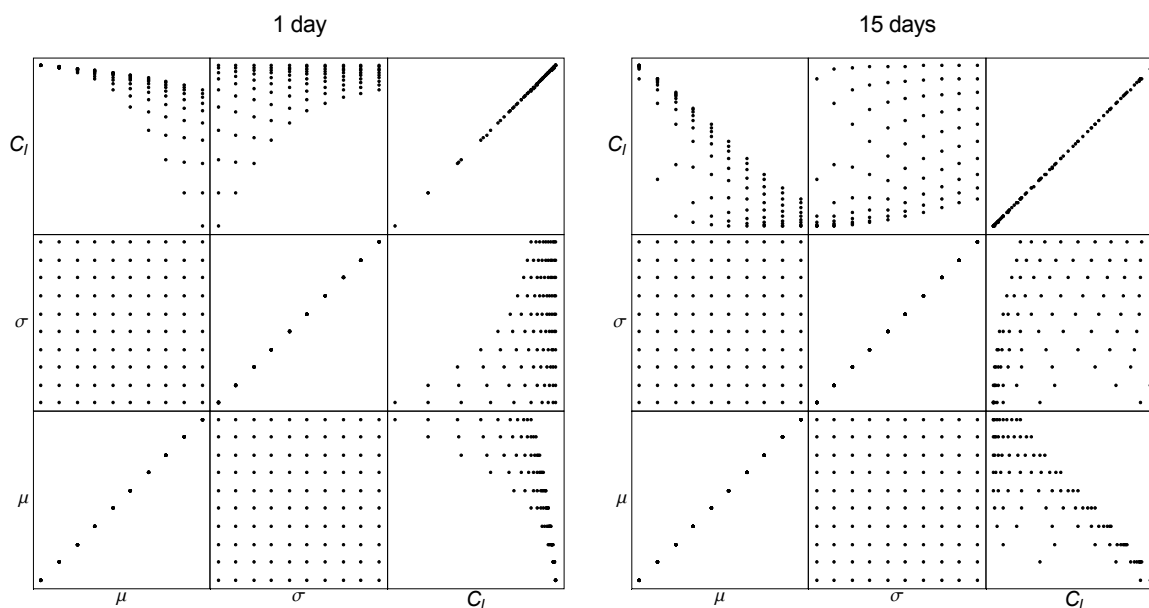


Fig. 4.11: Matrix scatter plot of μ (range 1-10 d^{-1} , step size 1 d^{-1}), σ (range 1-10 d^{-1} , step size 1 d^{-1}) and resulting C_l concentration at 1 and 15 days after application date; graphics predetermined in *Mathematica*®.

Fig. 4.12 shows that the degradation is higher the smaller K_M or γ are. At the end of the period under consideration the association between K_M (for very small γ values) and the pesticide concentration gets even linear. The same linear association gets obvious between γ and the pesticide concentration for very small K_M values.

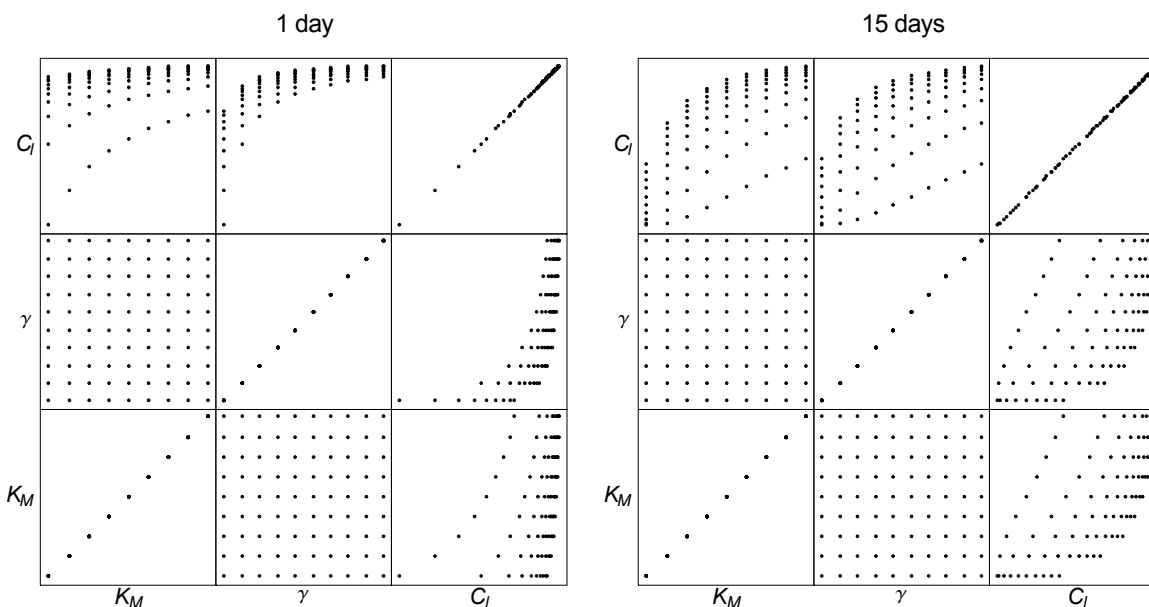


Fig. 4.12: Matrix scatter plot of γ (range 0.1-1.0 $\text{mg-C mg}^{-1}\text{-C}_{\text{substrate}}$, step size 0.1 mg mg^{-1}), K_M (range 0.4-3.6 mg dm^{-3} , step size 0.4 mg dm^{-3}) and resulting C_l concentration at 1 and 15 days after application date; graphics predetermined in *Mathematica*®.

Correlation coefficients and matrix scatter plot demonstrate that uncertainties in model calibration arise from the fact that multiple combinations of input parameters will provide a similar fit to the experimental data. This indicates that the model is overparameterised with respect to the data structure. Thus, as far as possible initial parameter settings were estimated from laboratory measurements, to minimize the discussed estimation problems. The analysis also shows that the microbial growth rate is the parameter with the highest influence on the solute pesticide concentration in the simulation.

Modelling of growth-linked biodegradation

Pesticide degradation and microbial growth are directly linked as shown in Fig. 4.13 for the degradation of glyphosate in the batch experiment at optimum soil moisture content, if pesticide degradation is restricted to a small community of specialized microbes (Eq. (4.27)). The microbial biomass increases to a level of up to 0.5 mg-C dm^{-3} between 2 and 3 days after application and thereafter decreases with substrate concentration.

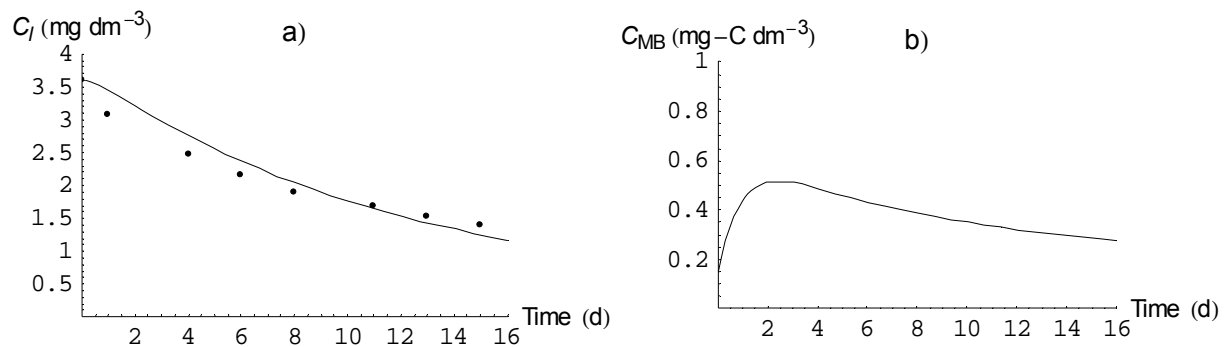


Fig. 4.13: Degradation of glyphosate in soil solution by a specialized microbial community in the batch degradation study at a water content of 40 % of max. WHC (part a: symbols – measurement, line – fitted model simulation; part b: simulated microbial biomass concentration; $r^2 = 0.966$).

As worked out in section 2.3.1, microbial carbon biomass in the topsoil of LM 5.1 to LM 5.4 was in mean $202.53 \mu\text{g-C g}^{-1}$ dry soil. Under consideration of soil density the total microbial community C_{MB} was calculated at the beginning of the experiment t_0 (Table 4.10). It was assumed that 0.05 % of the total microbial biomass was associated with the degradation. C_{MBmin} of specialized microbes was set in the model on the same value as the start value of the microbial biomass, because glyphosate has no toxicological influence on microorganisms (see also Figs. 2.2 and 2.6 and Rueppel et al.(1977)). C_{MBmax} of specialists in soil was set to the tenfold amount. The parameter values used in the simulation are listed in Table 4.10.

Table 4.10: Microbial community settings for glyphosate degradation at optimum soil moisture content

parameter	$C_{MB}(t_0)$ (mg-C dm ⁻³)	C_{MBmin} (mg-C dm ⁻³)	C_{MBmax} (mg-C dm ⁻³)
specialized microbes	0.15	0.15	15
total community	303	303	3030

Maximum microbial growth rate and related death rate of microorganisms were fitted with the *NMinimize* function in *Mathematica*® (Table 4.11, Fig. 4.13).

Table 4.11: Parameter settings in the Monod approach with growth linked and co-metabolic biodegradation at optimum soil moisture content

parameter	μ_{max} (d ⁻¹)	σ (d ⁻¹)	γ (-)	K_m (mg dm ⁻³)
specialized microbes	4.76	4.11	0.20	1.80
total community	0.007	0.080	0.23	1.87

The yield factor was set according to the proportion between molar weight of the substance and molar weight of the included C-atoms in the glyphosate molecule and the half saturation coefficient was set to half of the value for C_{lmax} (Table 4.11). In the laboratory experiments it was observed that glyphosate degradation kinetics did not change when the initial pesticide concentration was halved. To determine the sensitivity of the half saturation coefficient, further experiments with different magnitudes of initial pesticide concentrations would be necessary.

Modelling of co-metabolic biodegradation

To test the assumption that the total microbial community participates in the glyphosate degradation an easily available carbon source was considered in the model. This mainly co-metabolic approach reflects the situation that the size of the microbial community is dependent on the degradation of carbon substrate from indigenous sources. Fig. 4.14 represents that the simulated microbial biomass concentrations are hardly increased by pesticide degradation, using Eq. (4.28) under the assumption that the indigenous substrate concentration was steady during the experiment. The fit of the co-metabolic approach is less accurate than what is achieved by the application of a growth-linked biodegradation approach (cp. correlation coefficients in Figs. 4.13 and 4.14).

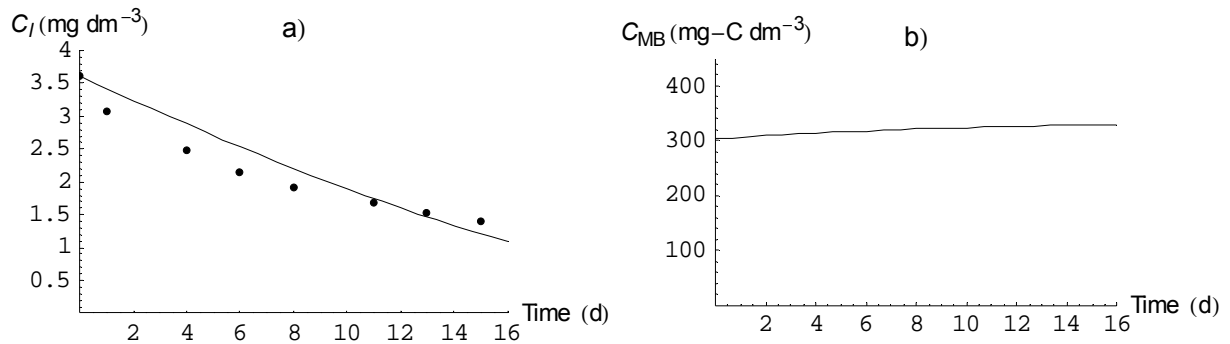


Fig. 4.14: Degradation of glyphosate in soil solution by total microbial community in the batch degradation study at a water content of 40 % of WHC (part a: symbols – measurement, line – fitted model simulation; part b: simulated microbial biomass concentration; $r^2 = 0.940$).

According to microbial biomass measurements an initial and minimum microbial biomass concentration of 303 mg-C dm^{-3} was used in the model simulation (Table 4.10), which is in good accordance with the values for microbial carbon biomass of $81\text{-}591 \text{ mg-C dm}^{-3}$ cited in Sung et al. (2006) for sandy soils with low pH. A maximum specific growth rate of 0.007 d^{-1} , a decay rate of 0.080 d^{-1} , a yield coefficient for pesticide degradation of 0.23 and a half saturation coefficient of 1.87 mg dm^{-3} were fitted for the batch experiment (Table 4.11). The half saturation coefficient K_{Morg} and the parameter μ_{org} fitted for the data of the laboratory experiment are shown by the table below.

Table 4.12: Parameter settings in the Monod approach accounting for the additional indigenous carbon source of glyphosate degradation at optimum soil moisture content

parameter	μ_{org} (d^{-1})	C_{org} (mg-C dm^{-3})	K_{Morg} (mg-C dm^{-3})
total community	0.009	145.5	72.8

Consumption and production of dissolved organic carbon (DOC) by microorganisms may be a useful parameter to link carbon availability to microbial activity. Neff and Asner (2001) defined the reactive soil pool, which represents the soil C-pool that may be lost to leaching and is available for biodegradation. They cite values between 0.11 to $0.95 \text{ mg-DOC g}^{-1}$ soil for the first soil horizon of different soil types. In the present approach, as a first approximation, the bioavailable carbon content C_{org} was assumed to be 1 % of the total organic carbon content in soil (Table 4.12), although no strong correlation between biological available DOC and total organic carbon content was found in literature data (Zsolnay and Steindl, 1991; Neff and Asner, 2001).

4.3.1.2 Water flow and soil hydraulic properties

Precise fate modelling of glyphosate goes along with a correctly simulated water flow and water balance of the lysimeters, thus, the parameterisation of the water flow model is of essential importance. The influence of the parameterisation of the soil hydraulic characteristics was estimated by comparison of the parameterisation according to the Hutson & Cass-Burdine with the van Genuchten-Mualem parameterisation. Simultaneously, the PM grass approach was compared with the Haude (mrH) approach. The measurements used for model validation were daily water content measurements by Ruth et al. (unpublished results) in 1 and 5 cm depth by the capacitance sensor with a flat sensitive volume (Ruth and Munch, 2005) in LM 5.1 and 5.4 and measurements by TDR sensors in 30 cm depth in LM 5.2 and 5.3. Daily and weekly outflow measurements of LM 5.1 to LM 5.4 were regarded and also daily ET_a fluxes. The fluxes were calculated from water balance by usage of lysimeter weight, outflow (LM 5.2 and 5.3) and the precipitation measured at the climate station.

The van Genuchten parameters α and n were fitted to the water retention curve measured in LM 5.2 in the year 2004 (Fig. 4.15). For simplicity the parameter θ_{res} was assumed to be zero and θ_{sat} was set to the value 0.25 for the whole soil profile according to the gravimetric water content measurements at saturation in the top 30 cm of the lysimeters.

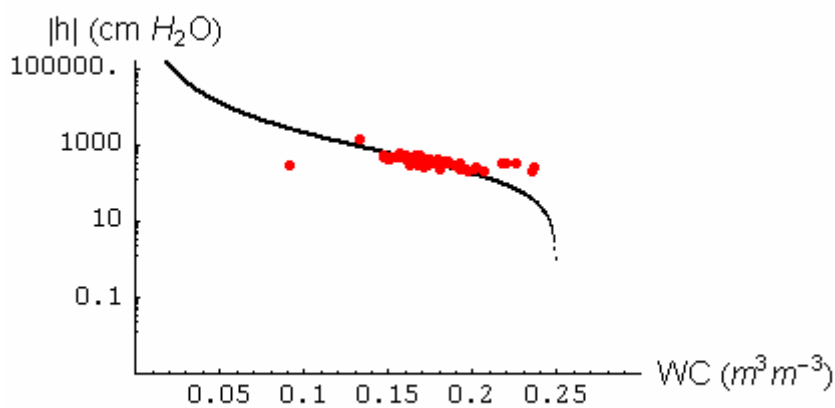


Fig. 4.15: Water retention curve measured (symbols) and fitted (line) for LM 5.2 in the year 2004 ($\theta_{sat} = 0.25 \text{ m}^3 \text{ m}^{-3}$, $\theta_{res} = 0.0 \text{ m}^3 \text{ m}^{-3}$, fitted van Genuchten parameters: $\alpha = 0.004$, $n = 1.404$).

Besides the soil hydraulic characteristics, the potential evapotranspiration model has also strong influence on water balance and flow simulations as discussed in sections 3.3.2.3 and 3.3.2.4. For the year 2004 the actual evapotranspiration can be calculated from the water balance.

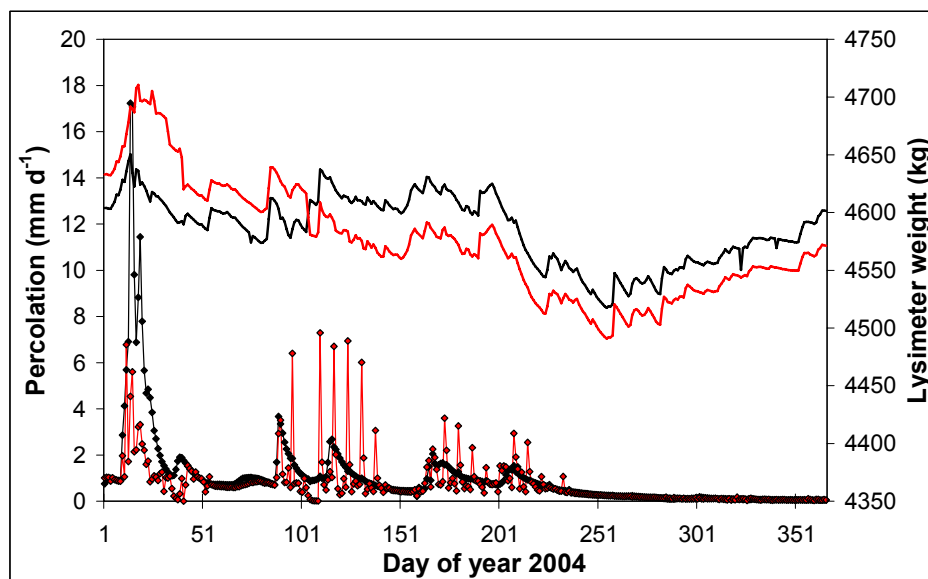


Fig. 4.16: Percolation amounts (line with symbols) and lysimeter weight measurements (line) for LM 5.2 (black) and LM 5.3 (red) in the year 2004.

Fig. 4.16 shows the time course of lysimeter weight and percolation data for LM 5.2 and 5.3. The weight at the beginning of the year is the same (± 5 kg) as at the end of the year for LM 5.2, which means that the water deficit of the summer was completely filled up by precipitation in autumn and winter. For LM 5.3 a storage deficit of about 60 kg still exists at the end of the year 2004. The main part of this deficit must be explained by the removal of soil samples around day 104. The remaining part was caused by the fact that the two lysimeters had slightly different evapotranspiration behaviour which can be explained by the differences of plant growth on the lysimeters. In the year 2004 the plant growth on LM 5.2 was sparser compared to LM 5.3. Also, the outflow of the two lysimeters was different. LM 5.2 shows the expected form of the outflow peaks while LM 5.3 shows single high peaks. The percolation amounts were comparable, but the outflow behaviour of LM 5.3 seems to be disordered. Up to now the reason for this behaviour could not be identified, a possible explanation would be the occurrence of trapped air at the lysimeter bottom.

Despite these differences in percolation behaviour, the calculated ET_a amounts were comparable and in good agreement between the two lysimeters (Figs. 4.17 and 4.18). Fig. 4.17 shows that especially in winter also negative ET_a amounts were calculated, which is certainly not realistic. Because for both lysimeters these negative values occur at the same days, the explanation for this might be an incorrect precipitation measurement when snow was falling. In summer, an explanation could not be found because single disruptions due to tillage and experimental work were corrected.

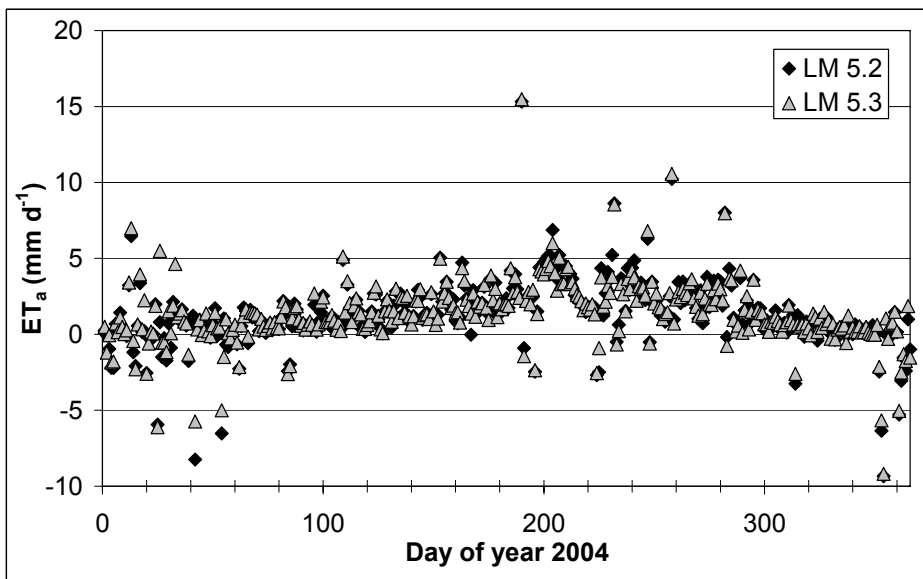


Fig. 4.17: Measured daily ET_a amounts for LM 5.2 and LM 5.3 in the year 2004.

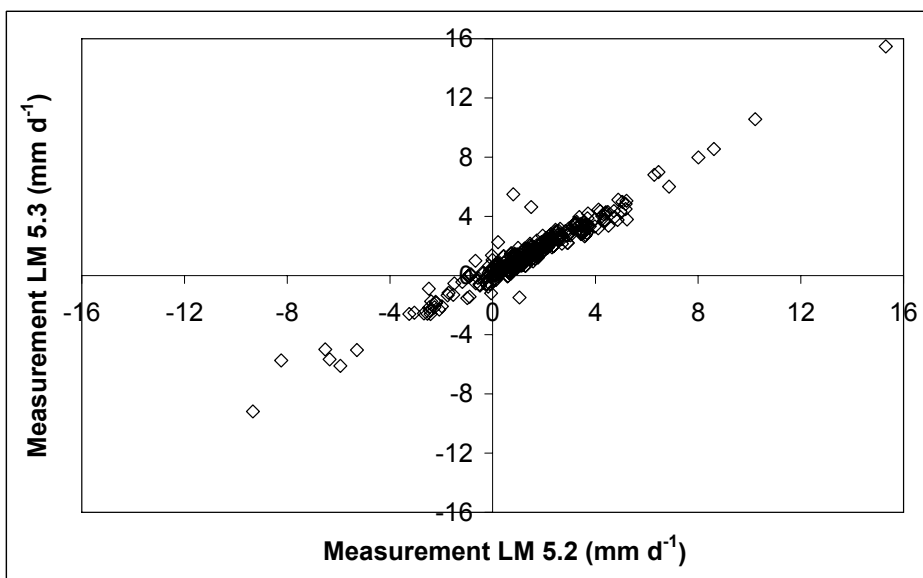


Fig. 4.18: Scatter plot of measured daily ET_a amounts for LM 5.2 and LM 5.3 in the year 2004.

The scatter plot (Fig. 4.18) shows that for small ET_a amounts as well as for high ET_a amounts the difference between the two measurements averages 0.35 mm d⁻¹. Daily actual evapotranspiration was the most variable parameter (Fig. 4.17) and a daily prediction of the precise value by the model was hardly possible. Fig. 4.19 shows scatter plots of simulated and measured ET_a amounts. The hydraulic characteristics were described by Hutson & Cass-Burdine or van Genuchten-Mualem parameterisations and ET_p was simulated using the Haude (mrH) model or the PM grass approach.

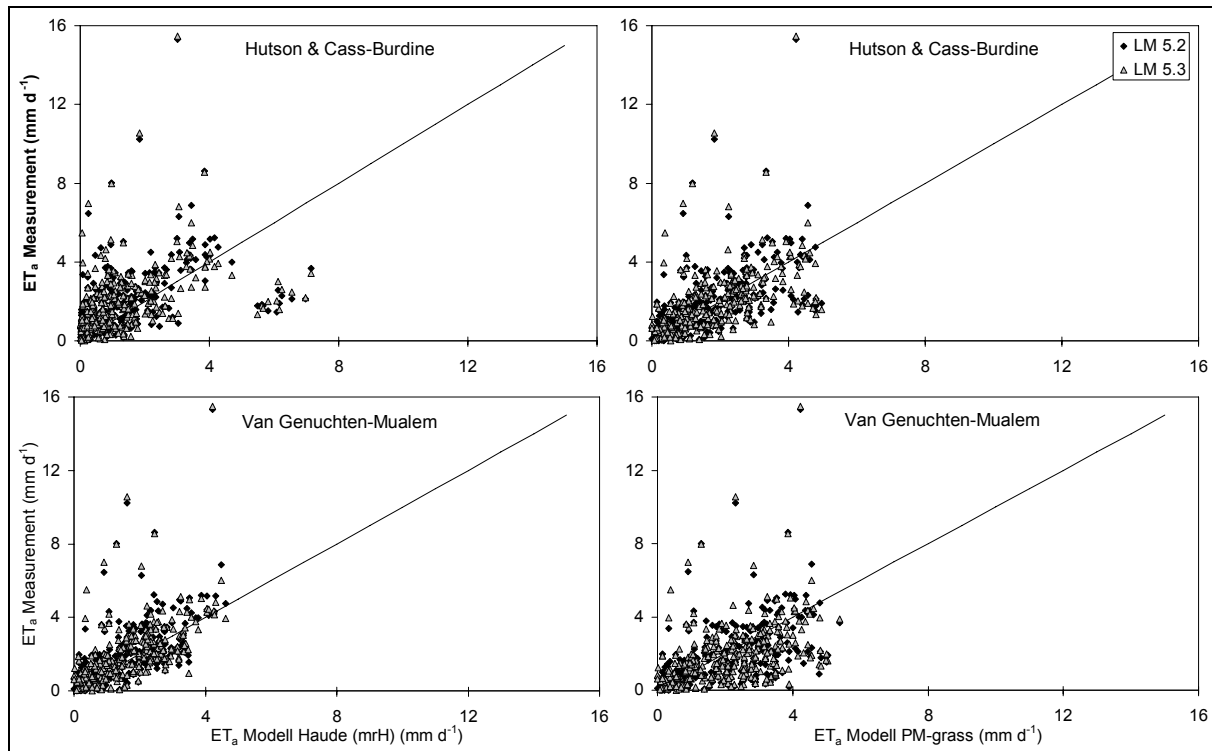


Fig. 4.19: Scatter plot of modelled and measured daily ET_a amounts for the year 2004.

Fig. 4.19 and Table 4.13 show that the best results were achieved by the van Genuchten-Mualem parameterisation combined with the Haude (mrH) evapotranspiration model. The daily variations in ET_a were sufficiently described by this approach considering the high variability in the measured amounts. The Hutson & Cass-Burdine parameterisation combined with PM grass ET_p model also results in an acceptable correlation between measured and modelled values. The combination of Hutson & Cass-Burdine with Haude (mrH) shows the tendency of underestimation of the measured ET_a by the model and modelling efficiency even becomes negative. The combination of van Genuchten-Mualem with PM grass shows the model's tendency to overestimation (Table 4.13).

Table 4.13: Modelling efficiency (EF), correlation coefficient (r) and cumulative evapotranspiration amount in percentage of measured amount in the period March to April 2004 from the mean of LM 5.2 and 5.3

ET_a	EF	r	Sum (%)
PM grass + Hutson & Cass	0.260	0.524	93.7
PM grass + van Genuchten	0.080	0.423	112.84
Haude (mrH) + Hutson & Cass	-0.131	0.393	71.1
Haude (mrH) + van Genuchten	0.340	0.596	82.8

The analysis of the weekly percolation amounts for the whole simulation period shows the same effects in r and EF values (Table 4.14 and 4.15) and gives further confidence in the good applicability of the combination van Genuchten-Mualem parameterisation and the Haude (mrH) ET_p model.

Table 4.14: Correlation coefficients (r) between simulated (with various model combinations) and measured weekly percolation amounts in 2003 to 2005

Modell	Haude (mrH)	PM-grass
Hutson & Cass-Burdine	0.773	0.645
van Genuchten-Mualem	0.841	0.639

Table 4.15: Modelling efficiency (EF) for weekly leachate amounts in 2003 to 2005

Modell	Haude (mrH)	PM-grass
Hutson & Cass-Burdine	0.519	0.379
van Genuchten-Mualem	0.720	0.466

Because of the higher values of r and EF for the Haude (mrH) model only this approach was used for further simulations. The data in Fig. 4.20 show that the percolation amounts could be predicted by both hydraulic parameterisations quite well.

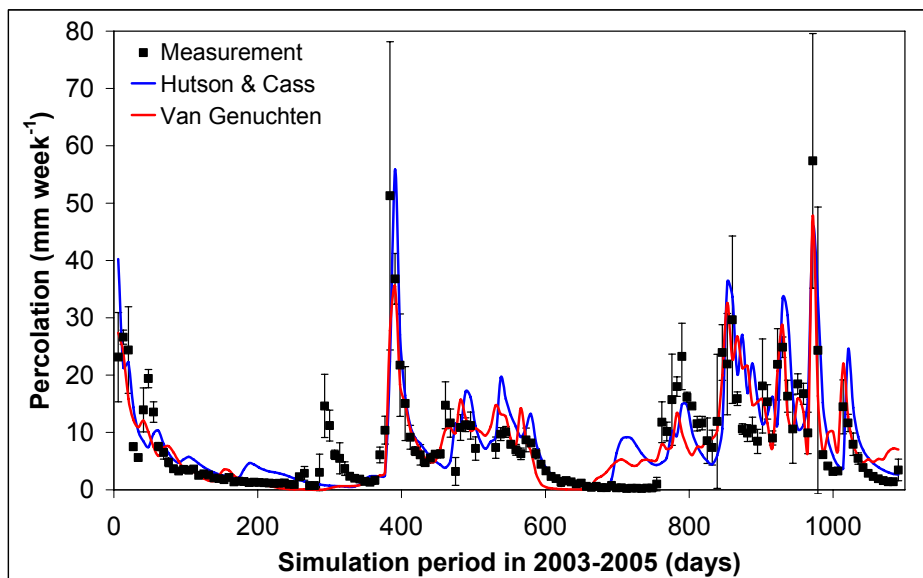


Fig. 4.20: Weekly percolation amounts measured (symbols, LM 5.1 to LM 5.4) and simulated with ET_p calculated by Haude (mrH) approach and hydraulic characteristics by Hutson & Cass-Burdine and van Genuchten-Mualem for the period 2003 to 2005.

Only between day 280 to 335 the model underestimates the outflow for both parameterisations and between day 680 to 755 the model overestimates the outflow in both

cases. These discrepancies between model simulation and measurements could be explained for the first period by an overestimation of transpiration in autumn by the model and for the second period by snow drift from the lysimeters. In Fig. 4.20 the mean of the four lysimeters and the standard deviation are shown. Although the daily percolation behaviour differs between the lysimeters (see Fig. 4.16) the weekly percolation amounts are in good agreement, on average, between the lysimeters.

Fig. 4.21 shows water content measurements (TDR) at 30 cm depth for LM 5.2 and 5.3, beginning three months before the first pesticide application. The absolute value of the water content measurements differed between the two lysimeters of about 4 %. Thus, from the measurements for LM 5.2 constantly 4 % of the volumetric water content were subtracted.

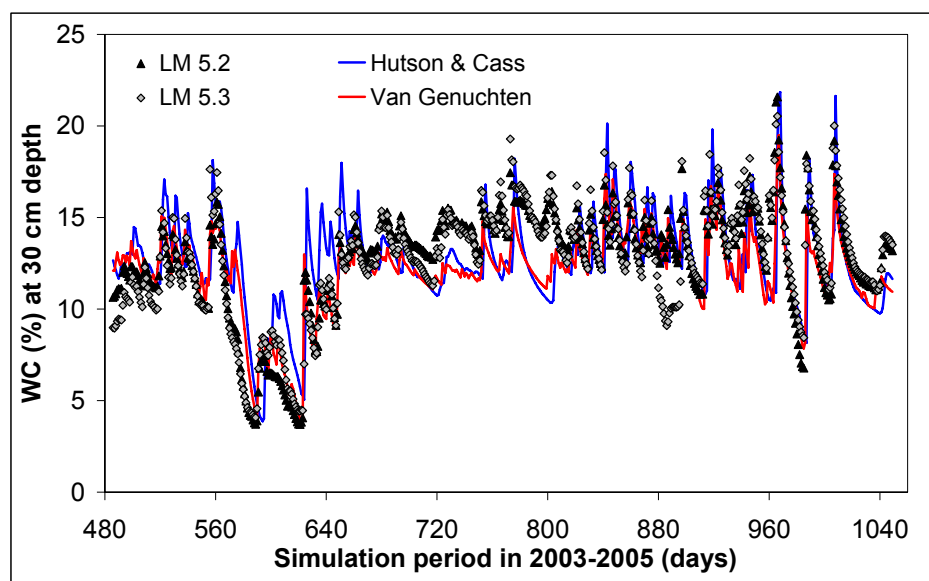


Fig. 4.21: Water content measured (symbols) and simulated (lines) at 30 cm depth in the year 2004 to 2005 (ET_p calculated by Haude (mrH) approach).

The two TDR probes agree very well in the water content fluctuations, but a calibration of the absolute value becomes necessary after installation of the probes in the soil and after comparison with the gravimetric water content (personal communication with UMS GmbH, Munich, Germany), although reports on similar problems could not be found in the literature. The model simulations agree very well with the measurements for both hydraulic parameterisations except for the period between days 720 to 810 where the measured water contents are underestimated, probably caused by an overestimation of evaporation by the model during winter. The agreement between the van Genuchten-Mualem parameterisation and the measurements is better than with the Hutson & Cass-Burdine parameterisation. Possible variations of water content measurements between the two lysimeters of the same soil type become obvious from the fact that once the measurement of the TDR probe in LM

5.2 agrees better with the simulations (days 880 to 896) and once the measurement of the TDR probe in LM 5.3 agrees better (days 596 to 612 and 698 to 720) with the simulation. For the biodegradation the water content in the top centimetres of the soil profile is of great importance. Fig. 4.22 shows that especially the high water content fluctuations in the first soil centimetre were well described by the Hutson & Cass-Burdine parameterisation at the time before and after the pesticide application in the year 2005.

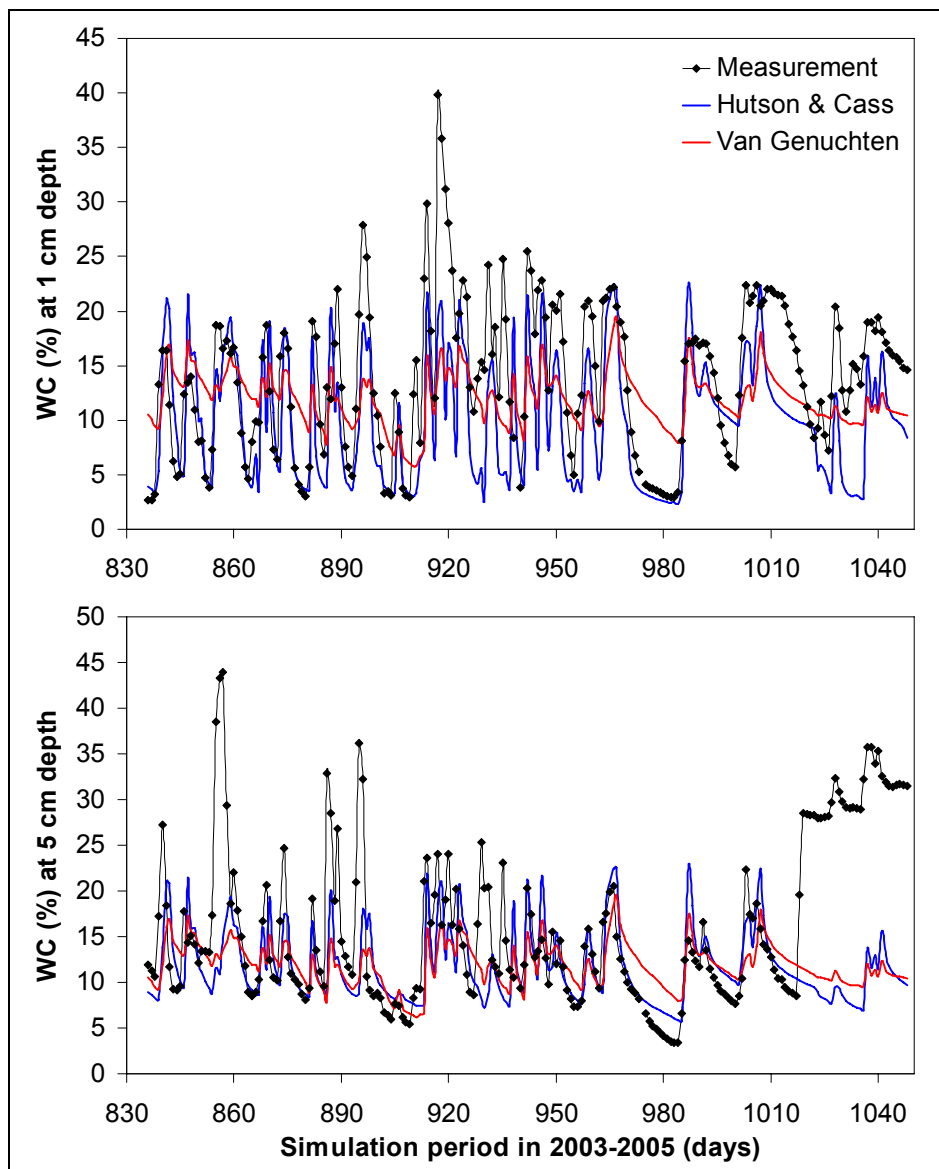


Fig. 4.22: Water content measured (line with symbols) and simulated (lines) at 1 cm and 5 cm depth in the year 2005 (ET_p calculated by Haude (mrH) approach).

The van Genuchten-Mualem parameterisation results in much smoother water content fluctuations than observed in the first centimetre. The same occurs at 5 cm depth. Water contents over 25 % measured by the humidity capacitance sensor seem unrealistically high in this case as θ_{sat} measured in the laboratory was 22.8 % and θ_{sat} measured in the field by

gravimetric methods was about 25 %. This indicates that the measurements at 5 cm depth after day 1017 and at single days before were not reliable. The water content measurements with the capacitance sensor were conducted in LM 5.1 and LM 5.4 accompanying the biodegradation experiments. Because the standard deviation between measured water contents of the two sensors in the biodegradation soil chamber and the one outside the chamber on the lysimeters was high, the standard deviation was not shown in Fig. 4.22. The influence of the simulated water content differences in the first few centimetres on the biodegradation simulations will be discussed in section 4.3.2.1.1.

4.3.1.3 Determination of the dispersivity coefficient

The results of weekly measurements of deuterium and radioactivity loads in the leachate are shown in Fig. 4.23. Deuterium and radioactivity measurements were not possible simultaneously on the same lysimeter because of the potential contamination with radioactivity of the stable isotope analyser. Therefore, the deuterium breakthrough curve (BTC) is only shown for LM 5.2 and 5.3.

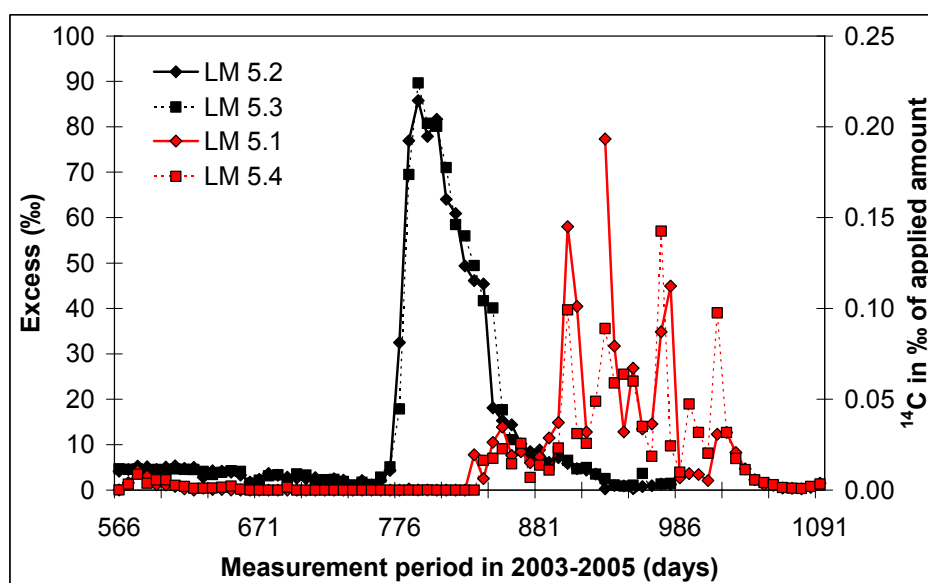


Fig. 4.23: Deuterium (LM 5.2 and 5.3) and radioactivity (LM 5.1 and 5.4) loads in the weekly leachate from July 2004 to the end of 2005.

In Fig. 4.24 the excess shows the remaining deuterium amount in the leachate after subtraction of the naturally deuterium background. The deuterium BTCs coincide very well between both lysimeters. It must be assumed that the glyphosate amount in the leachate was below the detection limit and the measured radioactivity in the leachate was in form of $^{14}\text{CO}_2$, resulting from biodegradation of glyphosate. The radioactivity load begins at the end of the tracer breakthrough and also shows good agreement in the course of the leachate amount

between both lysimeters. The deuterium BTCs were used to fit the effective transport parameters for the lysimeters because water isotopes are attractive choices for conservative tracers in that they closely resemble water behaviour both physically and chemically (Becker and Coplen, 2001). The fit of the deuterium breakthrough curves in *Mathematica*® by the inverse analytical solution (Ogata and Banks, 1961; cited in van Genuchten and Alves, 1982) results in $103.6 \text{ mm}^2 \text{ d}^{-1}$ for the effective diffusion coefficient $D(\theta, q)$ and in 8.2 mm d^{-1} for the mean pore water velocity v . When the effective diffusion coefficient is small with respect to the advective velocity the breakthrough curves of a non-reactive tracer will be symmetrical, reflecting equilibrium solute transport. When the effective diffusion coefficient is high (e.g. macropore flow) the BTCs obtained will be asymmetric, showing early breakthrough and tailing (Ersahin et al., 2002). Fig. 4.24 shows that the symmetrical form of the BTC confirms that matrix flow within a single continuum system is the dominant process in the sandy soil lysimeters.

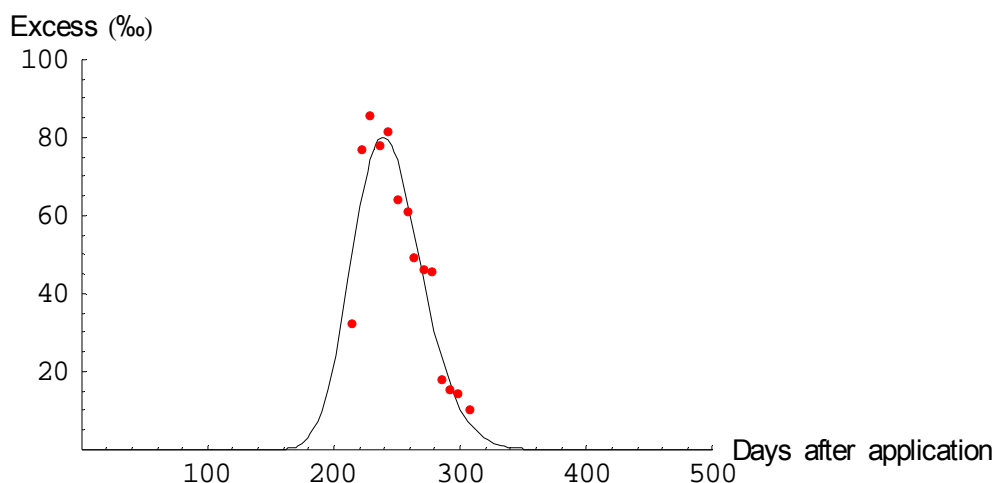


Fig. 4.24: Fitted deuterium breakthrough curve by the inverse analytical solution.

Assuming an average field water content of $0.11 \text{ mm}^3 \text{ mm}^{-3}$ and a molecular diffusion coefficient for deuterium of $198.72 \text{ mm}^2 \text{ d}^{-1}$, the dispersivity coefficient in the lysimeters reaches 10.39 mm . This relatively low dispersivity value is in agreement with the order of magnitude for other controlled unsaturated field transport studies reported by Thomasson and Wierenga (2003). Applying the numerical dispersion correction proposed by Hutson and Wagenet (1992), the dispersivity reaches a value of $\lambda_{10} = 14.55 \text{ mm}$ for a simulation layer depth of 10 mm and $\lambda_{50} = 83.12 \text{ mm}$ for a layer depth of 50 mm .

4.3.2 Model choice by comparison of deterministic modelling approaches

After the successful parameterisation of biodegradation, water flow and solute transport input parameters, different deterministic modelling approaches for the simulation of glyphosate behaviour in soil are compared. Traditionally, deterministic approaches have been applied where a single combination of model input parameters is used to predict a single time series of concentrations in the leachate (Beulke et al., 2004a). A model is termed deterministic if all the variables are viewed as free from random variations (Loague and Green, 1991). Therefore, deterministic approaches do not account for the uncertainty in the simulations which arise from uncertainty associated with the measurement, calculation or estimation of input parameters and spatial and temporal variability in factors influencing pesticide behaviour. The choice of modelling approaches for water and pesticide transport, as well as for degradation and sorption modules also has great effects on the simulation results. The aim of this section was to evaluate the effects of model selection on the prediction of the environmental fate of glyphosate in the lysimeter soils using a deterministic parameter selection. A short tabular survey of the model approaches compared, measurements and model configurations are given at the beginning of each part in this section. All the rest of the model configurations were already described in section 4.2.2.1. Uncertainties which arise from input parameters are addressed in the section 4.3.3.

4.3.2.1 Microbial degradation of glyphosate in the field lysimeters

4.3.2.1.1 First-order degradation influenced by water flow simulations

The effect of water flow simulations on degradation rates is studied with special focus on the functions describing the dependence of biodegradation on soil moisture.

Model approaches compared

Water flow	Hutson & Cass versus van Genuchten-Mualem
Degradation: humidity response function	Gauss versus Weibull type

Measurements used for model validation

Biodegradation in the field lysimeters	application 2004 and first application 2005 (soil chambers on LM 5.1 and 5.4)
Water content measurements	1 cm depth (capacitance sensor) LM 5.1 and 5.4

Model configurations

Water:

hydraulic characteristics	compared
ET_p	Haude (mrH) (Eq. (3.21))

Pesticide:

Sorption	linear equilibrium sorption (Eq. (4.13))
degradation:	first-order (Eq. (4.25) without photolytic degradation)
humidity dependencies	compared
temperature dependencies	O'Neill (Eq. (4.31))
biodegradation-depth relationships	no
volatilisation	yes (Eq. (4.23) and (4.24))

In Fig. 4.25 the cumulative degradation curves for the applications of the year 2004 and 2005 are plotted together with the data observed by Grundmann (personal communication) in the four soil chambers which were installed on the lysimeters as explained in section 4.2.1.1. The results of the second glyphosate application on the lysimeters in the year 2005 are not shown, because of the high standard deviation between the degradation measurements in the different soil chambers. The high standard deviations were caused by the fact, that glyphosate was applied when the soybeans were already near maturity and soil cover fractions of the plants differ widely in the lysimeters. The measured data in Fig. 4.25 show the mean and the resulting standard deviation of four soil chambers, two at LM 5.1 and another two at LM 5.4. Between 38.62 % (2004, $DT_{50} = 62$ d) and 56.26 % (2005, $DT_{50} = 52$ d) of the applied ^{14}C -glyphosate was completely mineralized within 48 and 58 days under the given environmental conditions. As discussed in section 4.3.1.2, the van Genuchten-Mualem parameterisation describes ET_a , outflow and water content in the deeper soil horizons best, while the Hutson & Cass-Burdine parameterisation agrees best with the water content measurements in the important upper soil horizon. Therefore, both parameterisations are discussed in this section. The environmental response surface, which describes the humidity and temperature dependence of k_{mic} was once derived from the Gauss type response surface (Eq. (4.30)) and once from the Weibull type response surface (Eq. (4.31)). Fig. 4.25 shows that for the Hutson & Cass-Burdine parameterisation of the hydraulic characteristics almost no difference can be seen in case of application of two different humidity response functions. This is caused by the high fluctuations in the simulated water content. High variations in simulated water content in the first soil centimetres over the whole range soil moisture result in high variations in the degradation rates for both humidity response functions. For the van Genuchten-Mualem

parameterisation a clear difference between the two humidity dependencies exists. The water content variation is much smaller in this approach in the first soil centimetres, but the sensitivity of the humidity response is higher. Although the water content simulations with the Hutson & Cass-Burdine parameterisation in the first soil centimetres agree much better with the measurements, better results in the simulation of the cumulative degraded pesticide amount were achieved by the van Genuchten-Mualem parameterisation.

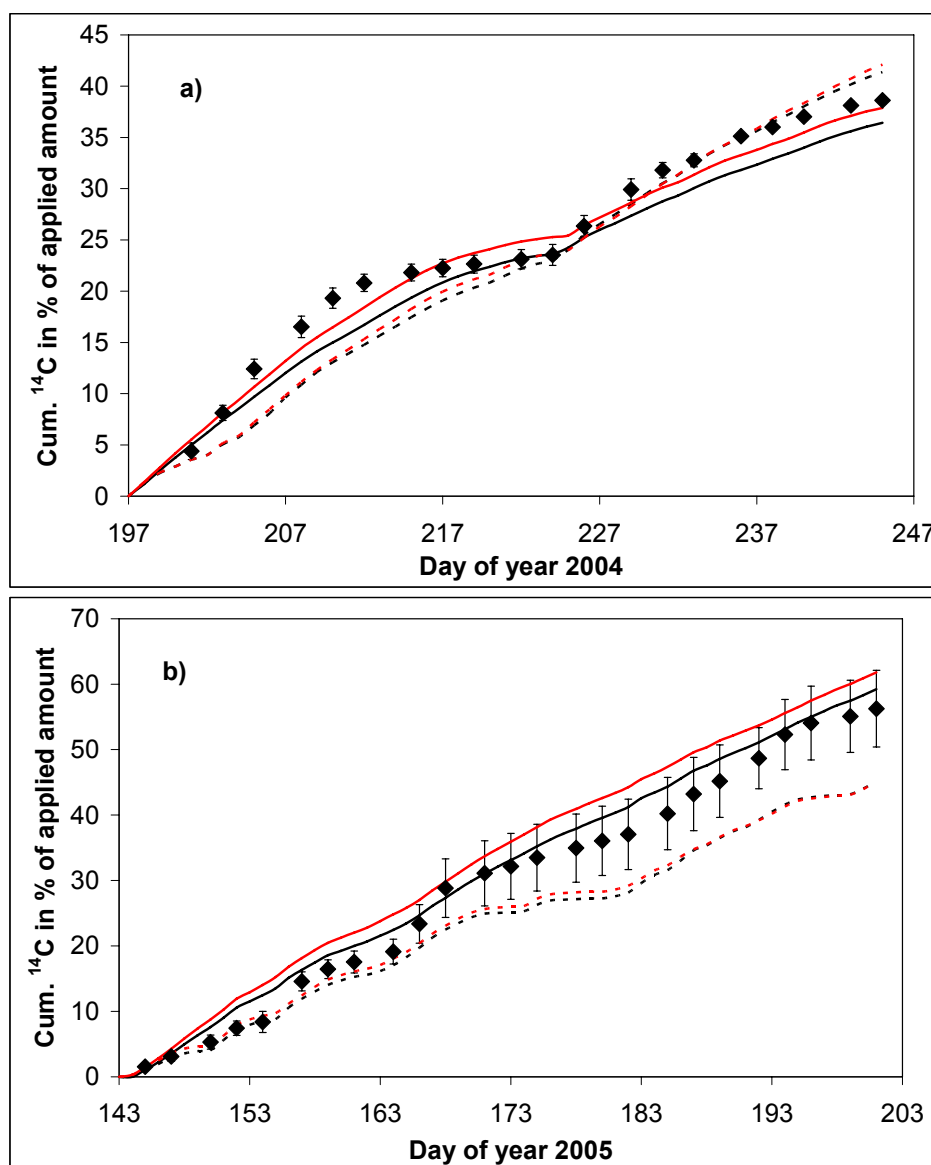


Fig. 4.25: Cumulative degradation curve measured (symbols, bars denote standard deviation between soil chambers) and simulated (dashed line: Hutson & Cass-Burdine, solid line: van Genuchten-Mualem parameterisation, red lines: response surface Gauss type, black lines: response surface Weibull type) in the years a) 2004 and b) 2005 ($k_{mic} = 2.31 \text{ d}^{-1}$).

The measured and simulated degradation rates obtained by using the environmental response surface of the Weibull type are shown in Fig. 4.26. Especially for high degradation rates the standard deviations between the four soil chambers were high. The effect of rain events can clearly be seen in an increase of the degradation rates in the measurements as well as in the simulations. The Hutson & Cass-Burdine parameterisation has a clear advantage in the simulation of the degradation fluctuation, while the van Genuchten-Mualem parameterisation agrees better in the simulation of the average degradation rates for both years. If the Hutson & Cass-Burdine parameterisation shows a good simulation of the degradation fluctuation, expectedly, the agreement in the cumulative degradation should be high as well.

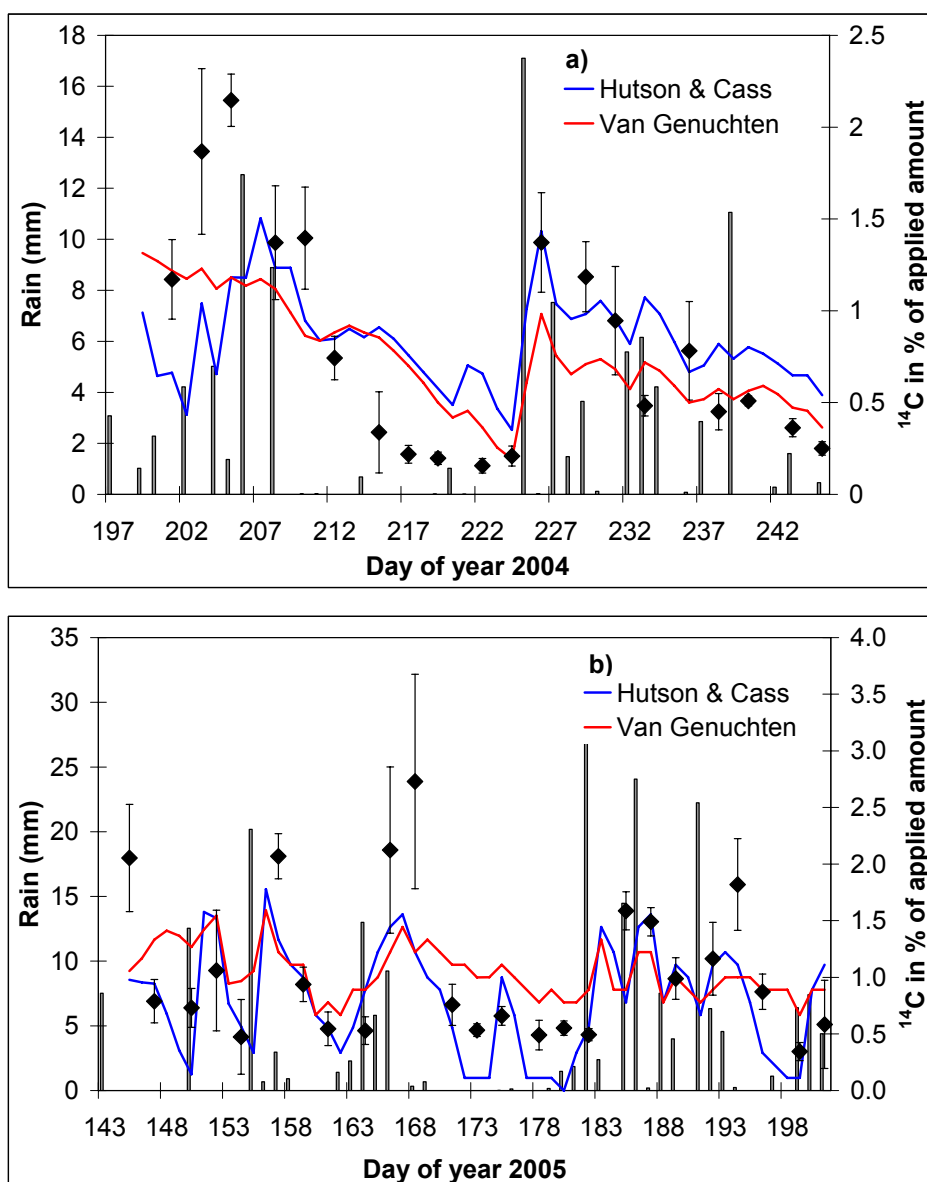


Fig. 4.26: Measured (symbols; bars denote standard deviation) and simulated (lines) degradation rates obtained by using the environmental response surface of the Weibull type and two different hydraulic parameterisations for the years a) 2004 and b) 2005; grey bars document rain events ($k_{mic} = 2.31 \text{ d}^{-1}$).

However, the measured daily degradation rates cannot be explained by the daily fluctuations in the soil moisture contents alone. Moisture changes during the course of the day, which are not reproduced in the simulation model, seem to be of high importance for the degradation in the lysimeters. Thus, the integration effect of the van Genuchten-Mualem parameterisation by smoother soil moisture dynamics can result in a better agreement with the average degradation rates. In Table 4.16 the RMSE values for the different simulations are listed.

Table 4.16: RMSE for the simulation of the degradation rates with different hydraulic characteristics and environmental response surface of the Weibull type

Hydraulic characteristics	2004	2005
Hutson & Cass-Burdine	1.98	2.78
van Genuchten-Mualem	1.72	2.90

In the year 2004 the van Genuchten-Mualem approach archives better results, while in the year 2005 the Hutson & Cass-Burdine parameterisation has a smaller RMSE. The results show that a clear advantage of one model approach cannot be found. For the Hutson & Cass-Burdine parameterisation there was a good agreement between measurement and simulation in single degradation rates, while for the van Genuchten-Mualem parameterisation the agreement was best in the average degradation rate.

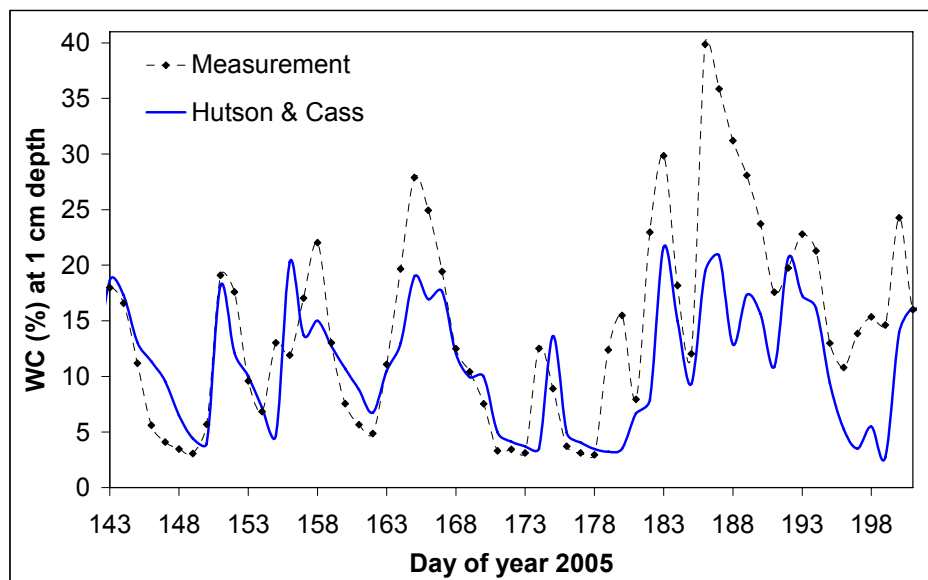


Fig. 4.27: Water content measured (humidity capacitance sensor; dashed line with symbols) and simulated (line) at 1 cm depth in the year 2005 (ET_p calculated by Haude (mrH) approach).

For a detailed comparison between water content and degradation rate simulations in Fig. 4.27 the measured and simulated water contents at 1 cm depth are shown for the simulation with

the Hutson & Cass-Burdine parameterisation. Between days 164 and 167 water content as well as degradation rates were underestimated by the model. Otherwise, between days 173 and 176 the measured water content increase seems to be correctly predicted by the model, while the measured water content increase does not become obvious in the measured degradation rate. This may result from discrepancies between irrigation in the soil chambers and natural rain events in the lysimeters. Further on, it must be stressed that a measured water content of more than 25 % must result from pond water at the soil surface or around the capacitance sensor.

The results show that by the choice of single modelling approaches the differences in the simulations are high. On the one hand the measured cumulative degradation of glyphosate in 2005 is underestimated about 19.7 % (Hutson & Cass-Burdine with Gauss type response surface) and on the other hand overestimated about 9.9 % (van Genuchten-Mualem with Gauss type response surface). It must also be pointed out that between highly dependent state variables – like water content and degradation rates in this case – error propagation is an important factor of uncertainty.

4.3.2.1.2 Microbial growth kinetics and microbial communities

The modelling concepts of co-metabolic and growth-linked biodegradation are compared and possible acceleration of pesticide degradation and response to organic amendments are discussed.

Model approaches compared	
Monod biodegradation approaches	specialized versus total microbial community
Measurements used for model validation	
Biodegradation in the field lysimeters	application 2004 and applications 2005 (soil chambers on LM 5.1 and 5.4)
Model configurations	
Water:	
hydraulic characteristics	van Genuchten-Mualem (Priesack, 2006)
ET _p	Haude (mrH) (Eq. (3.21))
Pesticide:	
Sorption	linear equilibrium sorption (Eq. (4.13))
degradation:	compared
humidity and temp. dependencies	Weibull and O'Neill (Eq. (4.31))
biodegradation-depth relationships	micro. biomass, avail. carbon substrate (Eq. (4.32))
volatilisation	yes (Eq. (4.23) and (4.24))

For the comparison of daily simulated degradation rates with measurements the RMSE values for the different modelling concepts are listed in Table 4.17. At the first day after application in the year 2005 the measured cumulative degradation amounts in Figs. 4.28 and 4.31 are set to the simulated cumulative amounts, due to the lack of continuous degradation measurement during the whole period. For the initial distribution of microbial biomass and available carbon substrate with depth it was assumed that both concentrations were constant in the first ten soil centimetres. The depth constant in Eq. (4.32) was set to $\eta = 0.003 \text{ mm}^{-1}$ with the result that at 30 cm depth still half of the initial microbial biomass concentration remains.

Table 4.17: RMSE values for the simulation of degradation rates with microbial growth kinetics of different degradation community approaches and parameterisation

RMSE values	2004	2005
specialized microbial community	1.77	2.82
total microbial community:		
– not calibrated 1 % C _{org}	2.71	3.80
– calibrated CO ₂ emission	1.69	2.98
– calibrated 1 % C _{org}	3.38	3.87
– calibrated 0.3 % C _{org}	1.81	2.81

For the simulation of glyphosate behaviour in the field lysimeters with the assumption that only a specialized microbial community is responsible for degradation, the parameters of the Monod approach (Eq. (4.27)) were directly adopted from the calibration with laboratory data (Table 4.10 and 4.11).

Fig. 4.28 shows that the glyphosate degrading community increases and dies very fast in high correlation to glyphosate availability. Accelerated degradation occurs, if pesticide applications take place in short time intervals when the size of the degrading community is still high from the application before. If mainly metabolic degradation occurs the pesticide degradation can be accelerated by multiple pesticide applications as the degrading microbial community continuously increases. The simulated degradation rates are in good accordance with the measurements (see Fig. 4.28 and RMSE in Table 4.17).

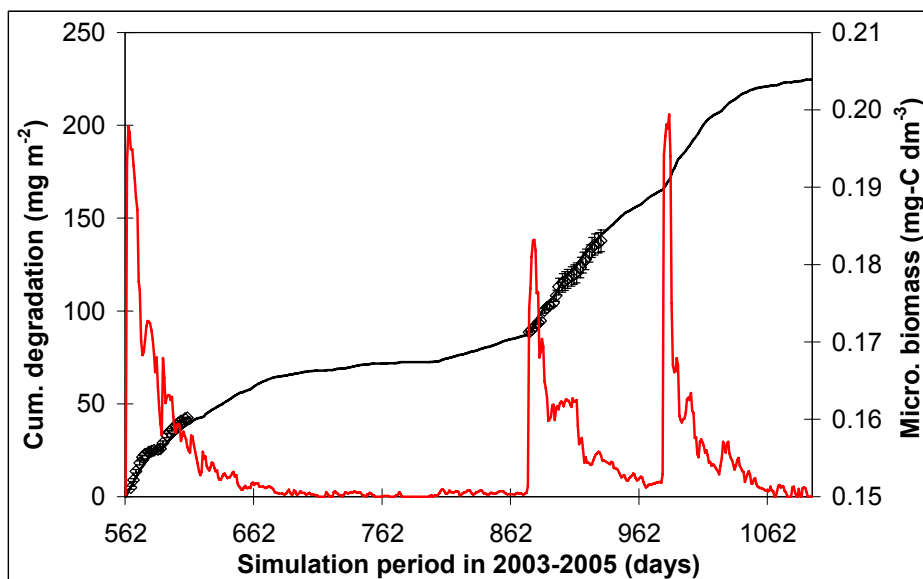


Fig. 4.28: Measurement (symbols; bars denote standard deviation) and simulation of cumulative amounts of degraded pesticide (black line) and simulated biomass concentration of specialized microbes (red line) ($C_{MB}(t_0) = C_{MBmin} = 0.15 \text{ mg-C dm}^{-3}$, $C_{MBmax} = 15.0 \text{ mg-C dm}^{-3}$, $\mu_{max} = 4.76 \text{ d}^{-1}$, $\sigma = 4.11 \text{ d}^{-1}$, $\gamma = 0.2$, $K_m = 1.80 \text{ mg dm}^{-3}$).

For the Monod approach with participation of the total microbial community and additional indigenous carbon source further calibrations were necessary. Compared to the approach with specialized microbes the fit of the degradation curve measured in the laboratory was less successful with the total community approach (cp. Figs. 4.13 and 4.14). As result, the degradation in the field lysimeters was overestimated by the modelling approach (Fig. 4.29b, dashed line; Table 4.17), when the input parameter values were directly adopted from the laboratory results. Additionally, as the total microbial biomass concentration remains nearly constant in the simulation with this parameter setting (Fig. 4.29a, dashed line), the sensitivity of the microbial growth to water content and temperature fluctuations in the soil were small and degradation rates hardly changed with environmental parameters. Due to this, the microbial growth rate was increased from 0.007 to 0.207 d^{-1} and an additional yield coefficient α_{org} for the primary substrate was applied, as the consumption of the additional C component – the pesticide – depends on the ratio of the indigenous substrate to the pesticide ($\alpha_{org} = C_{org}/C_l \text{ (mg-C mg}^{-1}\text{)}$). The gain factor of the pesticide must be multiplied by this ratio (Richter et al., 1996). The growth rate μ_{org} of the microbial community on the indigenous carbon substrate was also coupled to temperature and humidity dependencies. The availability of the carbon substrate was set constant to 1 % of the total carbon content in soil, as already assumed for the laboratory experiments.

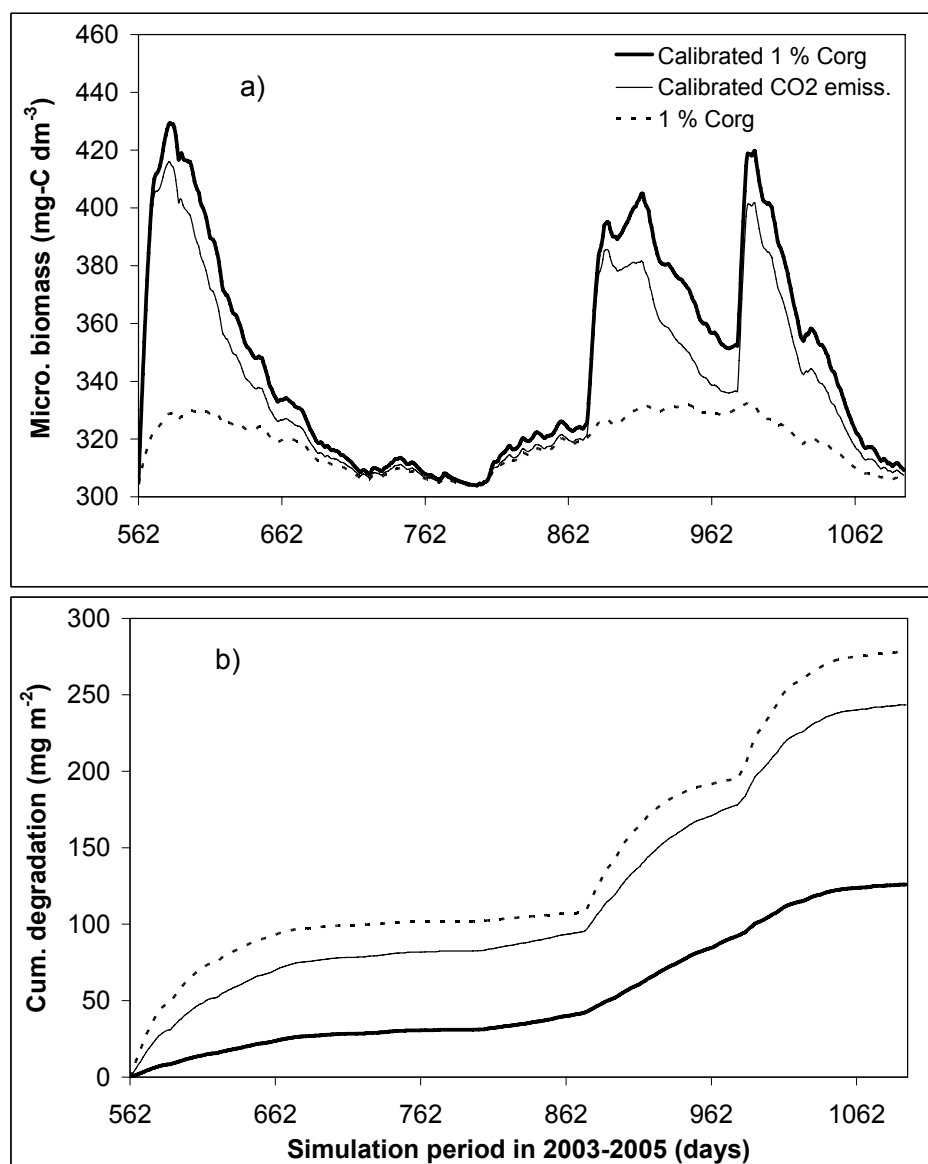


Fig. 4.29: Simulation of concentration of total microbial biomass (a) and of cumulative amounts of degraded pesticide (b) ($C_{MB}(t_0) = C_{MBmin} = 303 \text{ mg-C dm}^{-3}$, $C_{MBmax} = 3030 \text{ mg-C dm}^{-3}$, $\sigma = 0.080 \text{ d}^{-1}$, $\gamma = 0.23$, $K_m = 1.87 \text{ mg dm}^{-3}$).

In this approach the total microbial biomass is balanced between growth on indigenous substrate and die back to a minimum microbial community size, if no pesticide as additional carbon source is available. The degradation was now clearly underestimated by the model with calibrated model parameters (Fig. 4.29b, thick solid line and RMSE in Table 4.17), although microbial growth was clearly increased (Fig. 4.29a, thick solid line), if it is assumed that the available carbon substrate amounts 1 % of the total organic carbon content in soil. Therefore, carbon availability was linked to another parameter in the model, which describes microbial activity in soil. In the carbon-cycle submodel in *Expert-N* the CO₂ emission from the soil surface is calculated. This parameter was used to determine available carbon substrate in the first centimetre below soil surface. The degradation of glyphosate can be described very

well by this linked modelling approach (Fig. 4.29b, thin solid line and RMSE in Table 4.17), although simulated microbial biomass fluctuations in growth and decrease and simulated CO₂ emission had no direct correlation, as shown by Fig. 4.30.

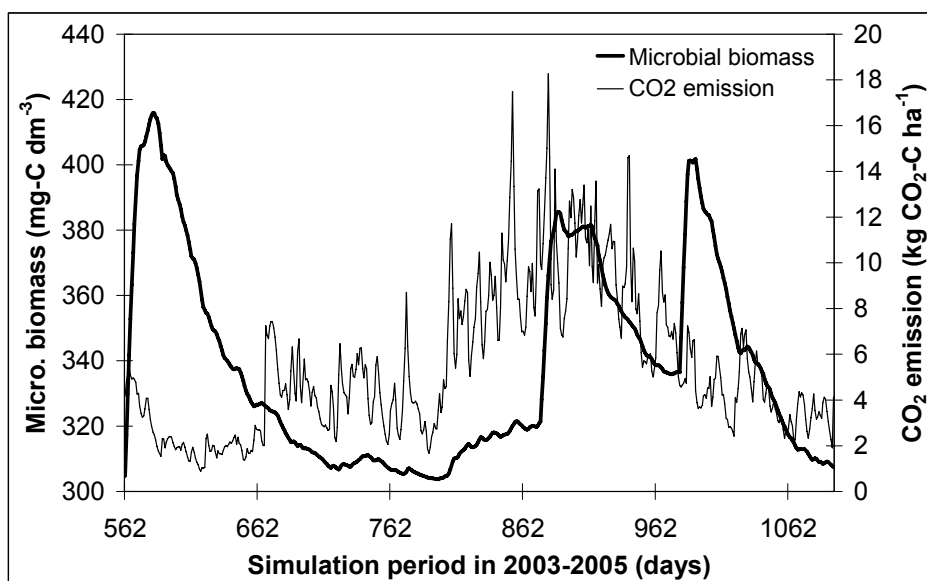


Fig. 4.30: Simulations of concentration of total microbial biomass and CO₂ emission from soil.

For different pesticides it was reported that the degrading potential of the microbial consortium does not correlate with the total soil respiration (Kühn, 2004; Schroll et al., 2004; Stenrød et al., 2006). In other works a decisive influence of soil moisture on N₂O production by nitrification and denitrification can be observed, although CO₂ emissions were not influenced by different soil moisture levels (40-90 % water filled pore space; Ruser et al., 2006). High fluxes of N₂O and CO₂ were only measured after rewetting of dry soil. The results of Ruser et al. (2006) show that even for soil processes that cause the turnover of much higher amounts of substrate like nitrification and denitrification microbial activity can be hardly correlated to soil respiration. The same effect gets obvious from the simulation results of pesticide degradation. The CO₂ emission rate is an appropriate parameter for representation of bioavailable carbon in the soil surface, but a linear correlation between CO₂ emissions and pesticide degradation does not exist, because the relation is particularly complex.

The modelling concept of co-metabolic degradation expects that the degrading community depends mainly on the amount of other easily available carbon substrate. Thus, degradation depends on different initial levels of other carbon sources. The size of the degrading community may increase in response to organic inputs like root exudates. This is shown in Fig. 4.31 where the microbial biomass concentration is clearly increased when the available carbon substrate is increased from 0.3 % to 1 % of total organic carbon.

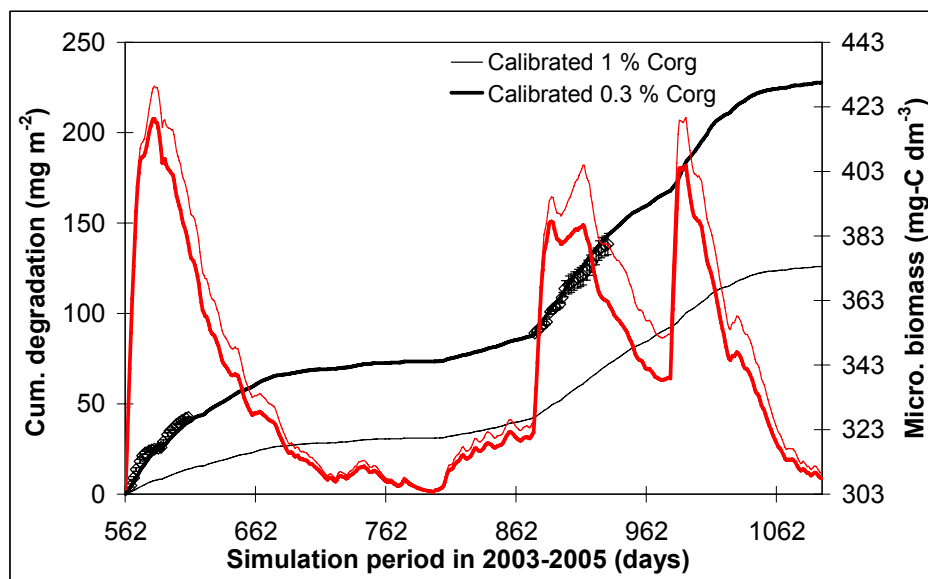


Fig. 4.31: Measurement (symbols, bars denote standard deviation) and simulation of cumulative amounts of degraded pesticide (black lines) and biomass concentration of total microbial biomass (red lines) ($C_{MB}(t_0) = C_{MBmin} = 303 \text{ mg-C dm}^{-3}$, $C_{MBmax} = 3030 \text{ mg-C dm}^{-3}$, $\mu_{max} = 0.207 \text{ d}^{-1}$, $\sigma = 0.080 \text{ d}^{-1}$, $\gamma = 0.23$, $K_m = 1.87 \text{ mg dm}^{-3}$ and $C_{org} = 145.50$ or $43.65 \text{ mg-C dm}^{-3}$).

Fig. 4.31 shows that pesticide degradation is not accelerated together with an increase in total microbial biomass. In this case the pesticide is less used as carbon source, if other easily available carbon substrate is abundant. The assumption that 0.3 % of the total carbon content in soil is bioavailable seems to be a good estimation, as simulation results and measurements are in rather good agreement (Fig. 4.31 and RMSE in Table 4.17). Therefore, the simulation results confirm that mainly co-metabolic glyphosate degradation occurs in soil, even though this approach was more difficult to parameterise.

A further aspect discussed in literature concerning pesticide degradation (Soulas and Lagacherie, 2001; Schlöter and Karl, personal communication) is the involvement of plasmids in the information transfer of degradative genes between soil microorganisms. At the moment, the long-term prediction of accelerated degradation in soils based on gene exchange is almost impossible (Soulas and Lagacherie, 2001) and only probability based approaches, modelling the potentiality of horizontal gene transfer, are discussed in literature (Nielsen and Townsend, 2004). Additionally, modelling approaches accounting for metabolic and co-metabolic degradation have to be discussed as well, because both degradation processes seem to occur simultaneously in varying fractions.

4.3.2.2 Adsorption of glyphosate to soil matrix

A linear equilibrium, non-linear equilibrium (Freundlich isotherm) and linear non-equilibrium (two-site) approach were compared for the mathematical description of the sorption processes in the lysimeter experiment.

Model approaches compared

Sorption approaches	linear equilibrium versus non-linear equilibrium versus linear non-equilibrium
---------------------	---

Measurements used for model validation

Pesticide residues in the field lysimeters	mixed soil samples after application in 2004 and applications in 2005 (LM 5.1 and LM 5.4)
--	---

Model configurations

Water:

hydraulic characteristics	van Genuchten-Mualem (Priesack, 2006)
---------------------------	---------------------------------------

ET _p	Haude (mrH) (Eq. (3.21))
-----------------	--------------------------

Pesticide:

Sorption	compared
----------	----------

degradation:	Monod – specialized microbes (Eq.(4.27))
--------------	--

humidity and temp. dependencies	Weibull and O'Neill (Eq. (4.31))
---------------------------------	----------------------------------

Biodegradation-depth relationships	micro. biomass (Eq. (4.32))
------------------------------------	-----------------------------

volatilisation	yes (Eq. (4.23) and (4.24))
----------------	-----------------------------

The phase-transfer coefficient α in the two-site sorption model (Eq. (4.17)) was calculated from the effective diffusion coefficient, the effective diffusion path length and a shape factor β , which depends on the geometry of the soil aggregates, according to the first-order solute mass transfer coefficient reported in Gärdenäs et al. (2006). Results of Gerke and van Genuchten (1996) showed that the geometry dependent factor β is closely related to the ratio of the effective surface area available for mass transfer and the soil matrix volume normalized by the effective characteristic length of the matrix system. It was assumed that the normalized surface-to-volume ratio equals 1.0 in the present study, which results according to Gerke and van Genuchten in $\beta = 3.0$. With a mean value of $D = 92.14 \text{ mm}^2 \text{ d}^{-1}$ for glyphosate in the soil profile and an effective diffusion path length of 10 mm (according to Jarvis et al., 1997; Table 8), α gets 2.76 d^{-1} . If $\alpha > 0.1 \text{ d}^{-1}$, the influence on the simulation results is small (Ma, 2003) and the fraction f of the equilibrium sites has more importance. The fraction of equilibrium sites was first assumed to be 0.7 and was then minimized to 0.3, to enhance the distinction between the linear equilibrium and non-equilibrium approach.

The only difference between a single-site and a two-site equilibrium model is that the kinetic site concentration is an additional term in the mass balance, and the effective K_d value employed for the equilibrium sites is fK_d (Hutson and Wagenet, 1992). This has the result that the two-site sorption approach has nearly no effect on glyphosate degradation (224.6 compared to 223.9 mg m^{-2} with the linear equilibrium approach at the end of simulation) and displacement of glyphosate in the lysimeters (Fig. 4.32).

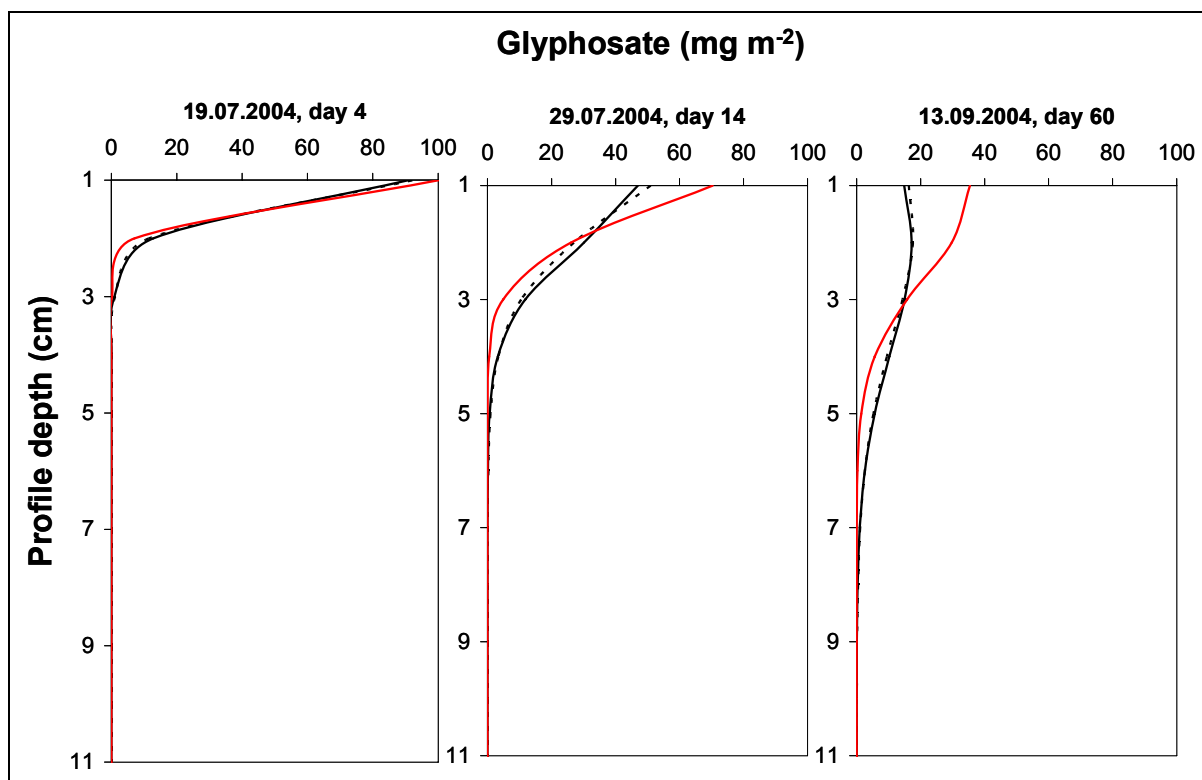


Fig. 4.32: Simulated profiles of glyphosate movement with linear equilibrium (black solid lines) and non-linear equilibrium (red solid lines) approach and two-site kinetic sorption model (black dashed lines) at 4, 14 and 60 days after application.

The only effect on the simulations occurs in time (first residual amounts were simulated 118 days after first application compared to 245 days with the linear equilibrium approach) and amount of leaching ($3.09 \cdot 10^{-17}$ compared to $2.23 \cdot 10^{-21}$ mg m^{-2} with the linear equilibrium approach at the end of simulation), due to the reduced sorption coefficient for the equilibrium sites in the two-site model.

As an alternative to the single-site linear sorption isotherm, the non-linear Freundlich isotherm with simultaneous consideration of adsorption-desorption reactions was applied (Eq. (4.14) and (4.15)). According to the laboratory batch sorption study a Freundlich coefficient of $24.7 \text{ dm}^3 \text{ kg}^{-1}$ with adjustment for deeper soil horizons according to their organic carbon content and a Freundlich exponent of 0.943 were used. The adsorption-desorption ratio of 0.538 was applied. Expectedly, the movement of glyphosate was slower

than with the linear equilibrium approach and higher amounts of glyphosate remain in the first soil centimetres (Fig. 4.32). A RMSE of 65.930 was achieved with the Freundlich sorption approach for the glyphosate movement in the years 2004 and 2005, which compared to the linear equilibrium approach (RMSE = 40.981) is less accurate. The simulated cumulative degradation of glyphosate at the end of the simulation period was about 7.97 % smaller than the amount calculated using the linear approach.

Glyphosate adsorption to the soil matrix is usually described by the Freundlich sorption isotherm (Vereecken, 2005). For compounds with non-linear sorption isotherms the ratio of sorbed to dissolved pesticide is shifted towards the sorbed state at lower concentrations. Hydrophilic compounds like glyphosate are often more strongly sorbed at high soil moisture content due to their higher affinity for hydrophilic regions of humus (Beulke et al., 2004b). If it is assumed that high soil moisture contents have a dilution effect and result in lower pesticide concentration, the ratio of sorbed to dissolved pesticide would be shifted towards the sorbed state at high soil moisture contents. But sorption behaviour in field differs from sorption in laboratory batch experiments. High soil moisture contents are often related to high water flow conditions. As a lack of equilibrium exists in soil adsorption compared with the time-scale of the flow rate, sorption sites were not reached by the pesticides and also hydrophilic compounds were less sorbed. In consequence the linear equilibrium concept reproduces the observed glyphosate movement in field better than the approach with the Freundlich sorption isotherm. Glyphosate degradation was underestimated with the Freundlich approach because pesticide fractions which are sorbed in micropores are inaccessible for the degrading microbes until direction of diffusion is reversed to the larger pores due to concentration gradients. But this process is relatively slow compared to the movement of mobile soil water between soil aggregates during intense water transport in the field (Scow and Alexander, 1992). Therefore, the linear equilibrium sorption concept seems to be more appropriate for the glyphosate transport and degradation description.

The distinction between an one-site equilibrium and a two-site non-equilibrium sorption concept cannot be seen from measurements because only radioactivity amounts and not the parent compound glyphosate could be detected in the leachate. Due to the uncertainties arising from the parameterisation of the two-site sorption approach, the linear equilibrium concept was used for further simulations.

The relation between biodegradation and sorption is a complex process and high values of the K_d in laboratory batch experiments cannot be directly used to indicate that the pesticide is

resistant to microbial degradation. Furthermore higher degradation amounts at higher water contents cannot only be related to an enhanced microbial activity, also mass-transfer including diffusion and desorption of the pesticides must be expected to be higher in wet soils. Diffusion and desorption are processes which are governed beneath the soil sorption capacities and soil structure from soil moisture conditions and pesticide properties. First-order and Monod degradation models were developed to describe metabolic processes occurring in solutions in which microorganisms and degradable substrates are well mixed. Indeed in soils, after an initial phase of unlimited availability of the chemical to the microorganisms, local degradation of the pesticide generates a concentration gradient with diffusion becoming the limiting factor (Soulas and Lagacherie, 2001). This is mostly observable in the decelerated degradation rates. Also spatial distribution of soil microorganisms has influence and patterns of spatial distribution of microbes suggest that degradation occurs mainly at surfaces or in outer layers of soil aggregates (Priesack, 1991; Scow and Hutson, 1992), which also has influence on desorption and diffusion processes due to concentration gradients. Moreover, the sorption of glyphosate to the mobile humus fraction in soil (DOM) is an additional issue as the co-transport with colloidal matter forces rapid and preferential transport of glyphosate as discussed in the next section.

4.3.2.3 Movement and leaching of glyphosate in the lysimeters

Beneath the effect of the parameterisation of the hydraulic characteristics on simulated movement and leaching of glyphosate, the important influence of the dispersivity coefficient is studied.

Model approaches compared	
Water flow	Hutson & Cass versus van Genuchten-Mualem
Measurements used for model validation	
Pesticide residues in the field lysimeters	mixed soil samples after application in 2004 and applications in 2005 (LM 5.1 and LM 5.4)
Radioactivity in the leachate	weekly leachate measurements (LM 5.1 and LM 5.4)

Model configurations

Water:

hydraulic characteristics	compared
ET_p	Haude (mrH) (Eq. (3.21))

Pesticide:

Sorption	linear equilibrium sorption (Eq. (4.13))
degradation:	Monod – specialized microbes (Eq.(4.27))
humidity and temp. dependencies	Weibull and O'Neill (Eq. (4.31))
biodegradation-depth relationships	micro. biomass (Eq. (4.32))
volatilisation	yes (Eq. (4.23) and (4.24))

The movement of glyphosate in the soil profile is shown in Fig. 4.33 in dependence of the numerical dispersion correction. Although the simulation layer depth was set to 10 mm the dispersivity coefficients λ_{50} and λ_{10} were used for the simulations. Additionally, the influence of the parameterisation of the hydraulic characteristics was examined. Fig. 4.33 shows that the influence of the parameterisation of the hydraulic characteristics is small compared to the influence of the magnitude of the dispersivity coefficient. Expectedly, a smaller value for the dispersivity results in a slower movement of glyphosate in the soil profile.

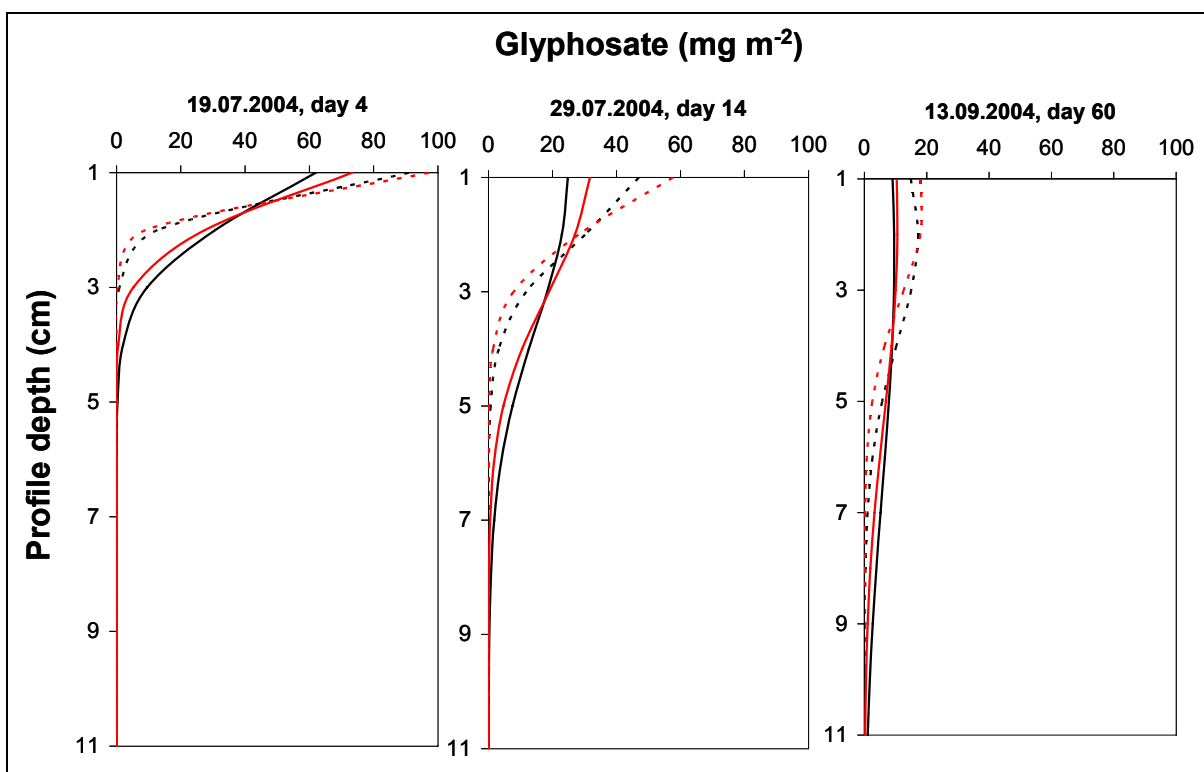


Fig. 4.33: Simulated profiles of glyphosate movement with two different parameterisations of the hydraulic characteristics and two different dispersivities (Hutson & Cass-Burdine (red lines) and van Genuchten-Mualem (black lines); λ_{50} solid lines, λ_{10} dashed lines) at 4, 14 and 60 days after application.

The comparison of the simulated glyphosate transport with measurements in LM 5.1 and LM 5.4 (mean values of both lysimeters) shows that the effect of the dispersivity coefficient on simulation results is less with the van Genuchten-Mualem parameterisation (Table 4.18). The best results were obtained for the Hutson & Cass-Burdine parameterisation combined with the higher dispersivity coefficient. This is contrary to the results obtained by the parameter fit with the deuterium breakthrough curve. Thus, the better applicability of the van Genuchten-Mualem parameterisation of the hydraulic characteristics using the fitted dispersivity coefficient λ_{10} was shown once more and applied for further simulations.

Table 4.18: Statistical criterion (RMSE) for model performance of the movement of glyphosate in the lysimeters

Hydraulic characteristics	λ_{50}	λ_{10}
Hutson & Cass-Burdine	37.368	43.634
van Genuchten-Mualem	39.999	40.981

Simulated glyphosate leaching cannot be directly compared with measurements, as the measurements show only ^{14}C -radioactivity amounts (Fig. 4.34). But the time-scales of the beginning of leaching are comparable.

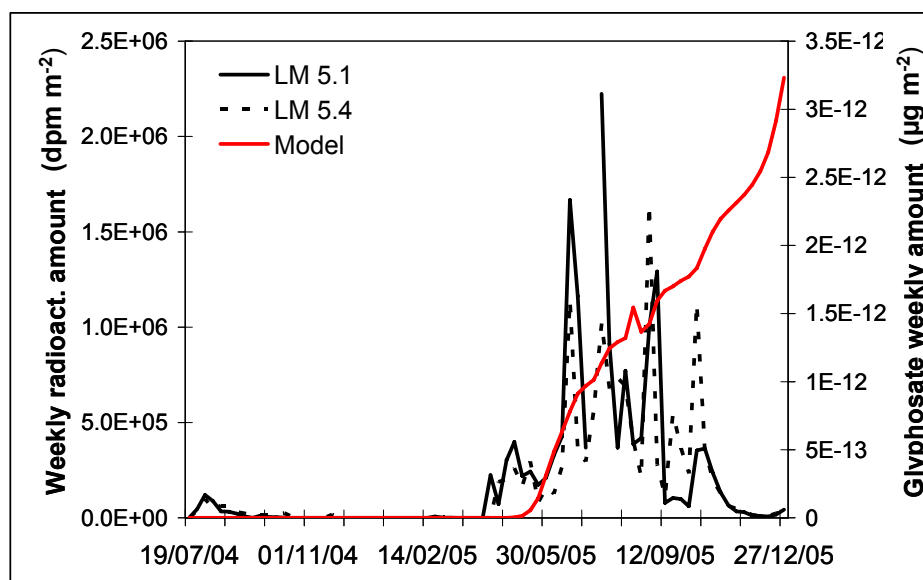


Fig. 4.34: Weekly measured ^{14}C -radioactivity amounts and simulated glyphosate leaching.

One and a half years after the first glyphosate application, glyphosate concentrations above the detection limit could not be measured in the leachate. Correspondingly, the simulated leachate concentrations were far below the threshold value for drinking water of $0.1 \mu\text{g L}^{-1}$, although the tracer breakthrough was already finished. Since there occurred no strong rainfall events after each of the three pesticide applications on the lysimeters (within five days), no

glyphosate leaching in amounts above the detection limit could be measured. An increased mobility of glyphosate could be mainly observed if there existed a lack of equilibrium in soil adsorption compared with the time-scale of the flow rate.

According to the work of de Jonge et al. (2000) high glyphosate leaching rates will be only probable due to macropore flow which occurs shortly after application. They found relatively high concentrations of glyphosate in structured sandy loam topsoil columns (20 cm depth × 20 cm diameter), leaching rates from structureless sandy soils were very low, and less than 0.3 % of the ¹⁴C applied was recovered in the effluent solution after 100 mm irrigation. The role of phosphorous, which is often discussed to occupy possible glyphosate binding sites, was found to be relatively unimportant for glyphosate leaching. Leaching studies of glyphosate in agricultural fields are sparse. Detections of glyphosate are mainly reported for drainage water rather than for ground water, especially if water saturation of the soil profile was already high and strong rain events follow (Vereecken, 2005). Glyphosate was detected in surface water samples from many streams in the Midwestern United States, but other herbicides with similar or less total use, such as acetochlor, atrazine and metolachlor were often detected more frequently and at higher concentrations (Battaglin et al., 2005). Data from glyphosate monitoring in the USA and Europe indicate a low occurrence in groundwater (Vereecken, 2005). However, the rapid increase in glyphosate use in agricultural practices indicates additional monitoring for glyphosate as other researchers suggest that the occurrence and persistence of glyphosate could be similar to that of atrazine. In conclusion, due to the high sorption of glyphosate to the soil matrix and the high microbial capacities for glyphosate degradation in most agricultural soils, leaching risk is generally regarded to be low, but cannot be entirely excluded.

4.3.3 Modelling approach considering probability distribution of substrate availability, sorption and dispersivity

Probabilistic modelling approaches can be achieved by running a deterministic model many times for a large number of different input values or modelling scenarios (Beulke et al., 2004a). This means that probability distributions are used for the input parameters of a deterministic modelling approach. In this study Latin Hypercube Sampling (LHS) from distributions of model input parameters was used which allows the number of model runs to be kept to a minimum. LHS is a stratified sampling technique based on a subdivision of the probability distribution of each input parameter in N disjunct equiprobable intervals. Random sampling of one value in each interval is performed and one obtains N samples for each parameter. Random sampling into statistical distributions was performed using the *Random* function of the *Mathematica*® software package (version 5.0). The sampled values of the first parameter were then randomly paired with the sampled values of the second parameter and furthermore randomly paired with combinations resulting in N combinations of p parameters. This set of p -tuples is the Latin Hypercube sample and according to Janssen et al. (1994) the choice of $N > 4/3 p$ usually gives satisfactory results. A modelling exercise was carried out where the probability distribution of three input parameters was analysed and a value of $N = 25$ was chosen. Model configurations were used as described for section 4.3.2.1.2 with the assumption that the total microbial community participates in glyphosate degradation.

A number of sensitivity analyses have demonstrated that predictions of leaching are mainly influenced by sorption and degradation parameters beneath the large sensitivity to hydrological parameters (Dubus et al., 2003). On the basis of these results, the variability of the K_d value in the present modelling approach, the available carbon substrate and the dispersivity coefficient were incorporated. Probability distributions of these variables were specified by the means and the standard deviation assuming normal distributions. The use of a normal distribution seems to be justified for the K_d value as in most modelling studies accounting the variability in sorption a normal distribution was hypothesised (Di and Aylmore, 1997; Dubus et al., 2003). This was also considered for the probability distributions of dispersivity and available carbon substrate on the fact of insufficient data for a distribution assessment. A pragmatic approach was followed instead. The coefficient of variation (CV) for the K_d value was set according to Wauchope et al. (2002) to 40 % and CV for the dispersivity coefficient was set according to the work of Thomasson and Wierenga (2003) to 30 %. Only a small variability (CV = 10 %) was assigned to the available carbon substrate in soil as in agricultural soils the seasonal variation in the total organic carbon content is small.

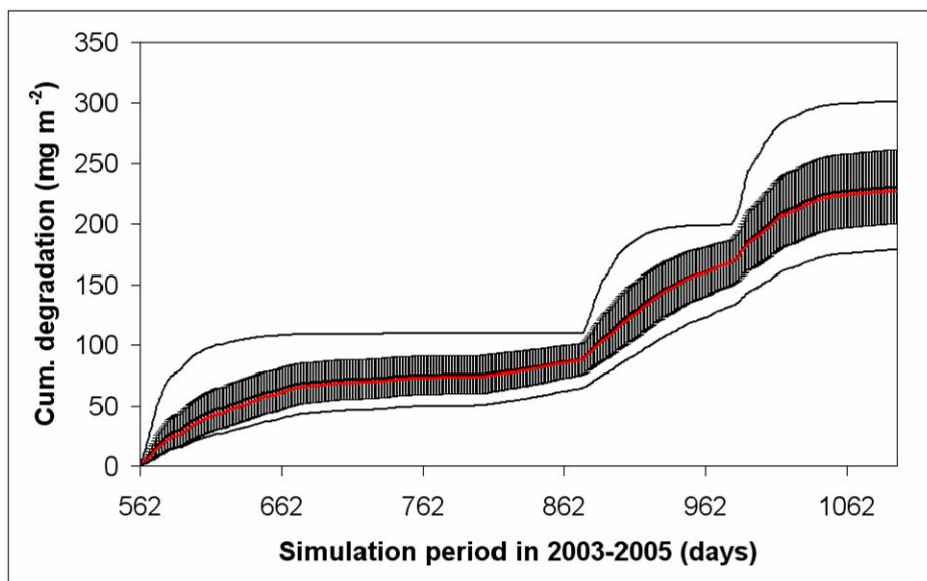


Fig. 4.35: Simulation of cumulative amounts of degraded pesticide following variation ($N = 25$) of pesticide input parameters K_d , available carbon substrate and dispersivity (top line: maximum, bottom line: minimum, black line and grey bars: mean of 25 simulation runs with standard deviation, red line: reference run with average parameters).

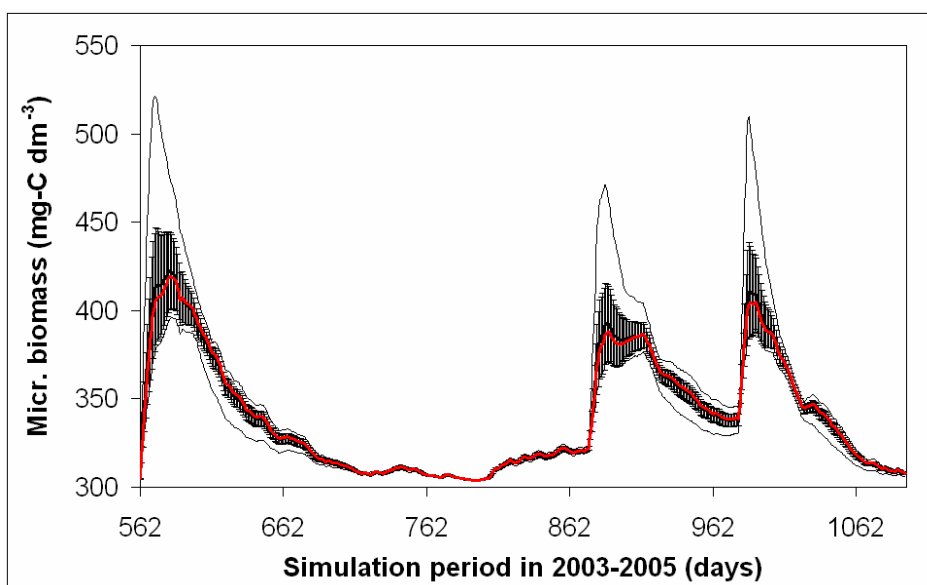


Fig. 4.36: Simulation of concentration of total microbial biomass following variation ($N = 25$) of pesticide input parameters K_d , available carbon substrate and dispersivity (top line: maximum, bottom line: minimum, black line and grey bars: mean of 25 simulation runs with standard deviation, red line: reference run with average parameters).

Expectedly, both figures (Figs. 4.35 and 4.36) show that between the reference run with the parameter values set at their average values and the mean of the 25 simulation runs nearly no difference occurs. The adoption of a normal distribution implies that the most frequent value of a specific parameter is the mean of the range of values. The degraded amount of glyphosate

was simulated to be maximal if sorption was very low ($K_d = 2.19$) and the available carbon substrate was in the upper range of values ($C_{org} = 48.98$), while the dispersivity ranges near the fitted value ($\lambda = 13.83$). Almost the whole amount applied in three applications was degradable with this parameter setting (Fig. 4.35). In the simulation with minimal degradation only some more than half of the applied amount was degraded because sorption was very strong ($K_d = 21.59$), although available carbon substrate and dispersivity ranged near the normal values. Also the parameter setting of maximum degradation results in maximum microbial biomass with 27.10 % more microbial biomass than with the mean value (Fig. 4.36, day 572). Despite the high degradation rates this parameter setting resulted also in the maximum leaching amount ($3.53 \cdot 10^{-14}$ mg glyphosate m^{-2}), due to the low sorption of glyphosate to the soil matrix. No leaching occurs if sorption is high ($K_d = 20.17$) and dispersivity is in the lowest range of values ($\lambda = 6.34$). The results confirm that the simulation of glyphosate behaviour is more sensitive to changes in the K_d value than in the dispersivity coefficient.

Box-and-whisker plots in Fig. 4.37 show that the variability in the input parameters (CV = 10-40 %) caused a smaller variability in the output parameters with a coefficient of variation of 13.14 % in the cumulative degradation amounts at the end of the simulation period and a maximum coefficient of variation for the microbial biomass of 8.16 % (day 572). The coefficient of variation for the leachate amounts at the end of the simulation period was 500.71 %, due to the very small leaching amounts ($3.53 \cdot 10^{-14} - 2.69 \cdot 10^{-40}$ mg glyphosate m^{-2}).

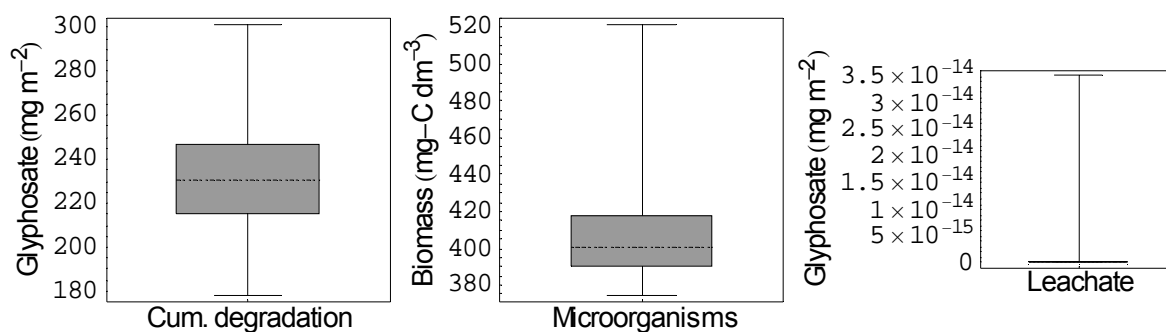


Fig. 4.37: Box-and-whisker plots for cumulative amounts of degradation and leachate amounts at the end of the simulation period 2003-2005 and maximum microbial biomass (day 572) for variation (N = 25) of pesticide input parameters (dashed lines: median, “whiskers” lines: full data, boxes: values between 25th and 75th percentile).

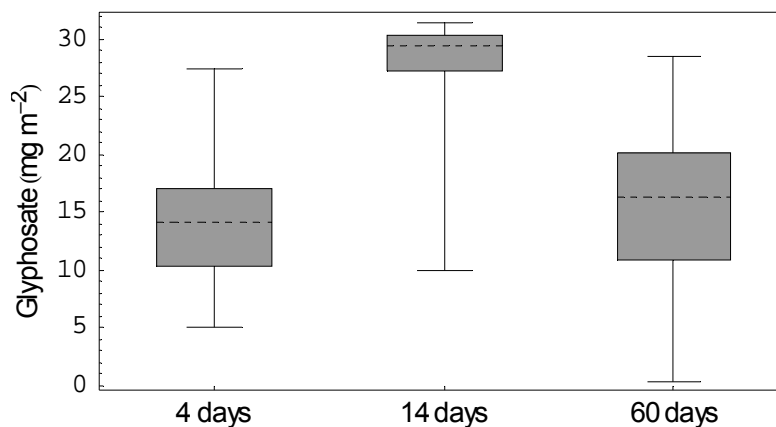


Fig. 4.38: Box-and-whisker plots for glyphosate movement in 2 cm depth at 4, 14 and 60 days after application in 2004 for variation (N = 25) of pesticide input parameters (dashed lines: median, “whiskers” lines: full data, boxes: values between 25th and 75th percentile).

Fig. 4.38 compares box-and whisker plots for glyphosate movement in 2 cm depth and shows that the variability in the glyphosate amount first decreases and then increases with time. The variability in the output of all LHS samples is high and ranges after 60 days between 28.48 and 0.36 mg m⁻².

The measurement in Figs. 4.39 and 4.40 show that glyphosate remains almost immobile in the top soil centimetres (1-2 cm) even after more than 100 days after the first application in both years. In 2004 a clear reduction of the residues in the course of time from 47.53 to 13.99 mg m⁻² was observable in the first sampling depth, while the residues in the second sampling depth range between 1.30 and 2.94 mg m⁻². In 2005 the first sampling depth contained 33.69 mg m⁻² at day 8 after application and then a fast decrease occurred from day 8 to day 16 to 23.48 mg m⁻², due to mixing of the soil at the first sowing of the soybeans. This amount remained nearly constant until the last sampling date 97 days after application. By contrast, in the second sampling depth glyphosate residues increased fast from day 8 to 16 from 0.93 to 7.59 mg m⁻² and then remain constant on this amount.

Soil solution samplers were not installed in the lysimeters because of the small probability of glyphosate transport to deeper soil horizons due to its high K_d value. Additionally, the solution samplers measure the concentration only at the cup location and usually cannot provide a complete spectrum of solute flow paths (Thomasson and Wierenga, 2003).

Glyphosate residues were accurately predicted at the first sampling date in 2004 by the mean of the LHS sample (Fig. 4.39). Afterwards the residues in the top sampling depth were slightly overestimated by the mean value until day 60 after application. At sampling dates 60 and 126 days after application the remaining glyphosate residues in the top sampling depth

were slightly underestimated by the model and penetration depths of the residues in the deeper sampling depth were overestimated.

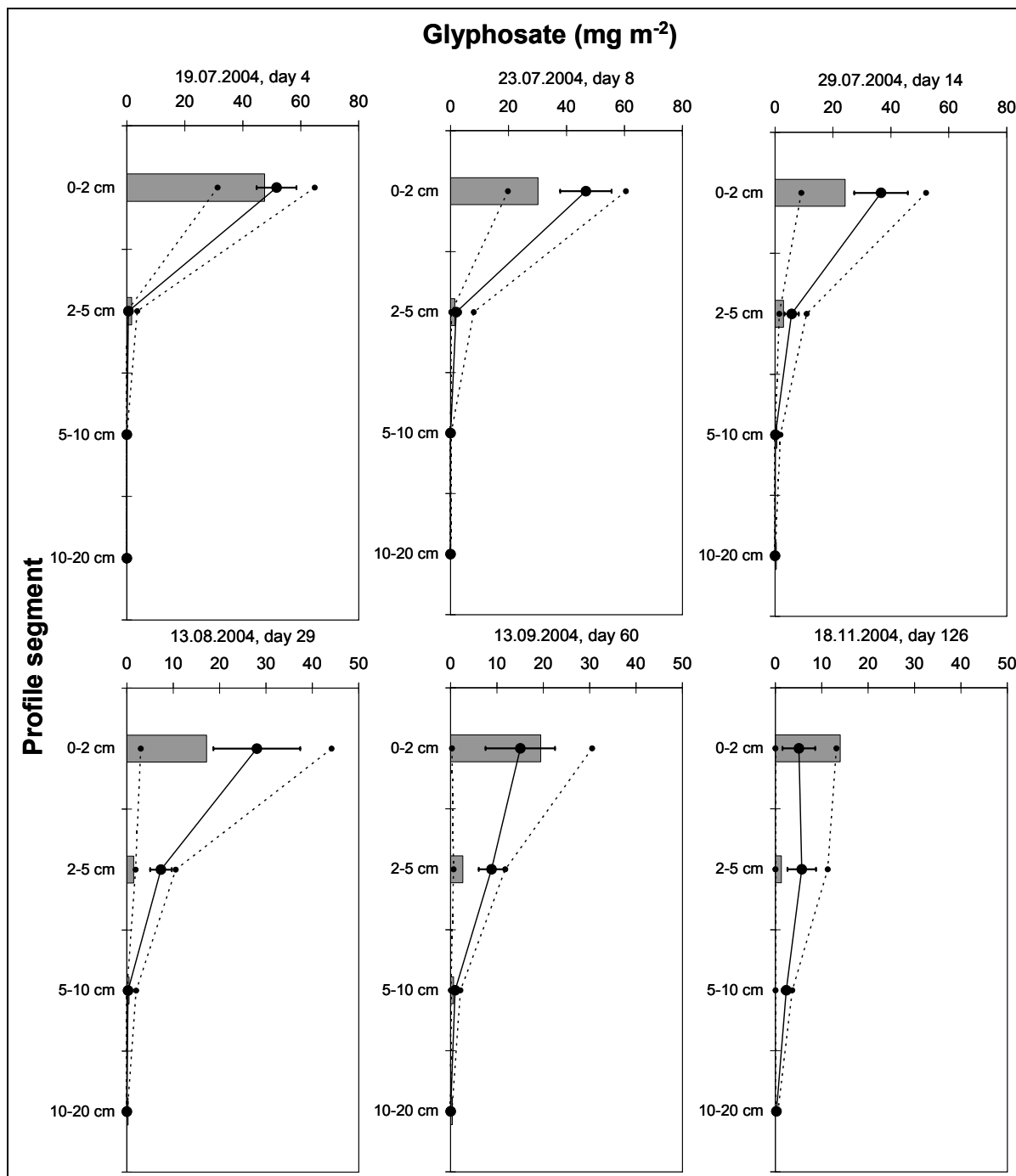


Fig. 4.39: Measured profile (grey bars) of glyphosate movement and model simulation following variation ($N = 25$) of pesticide input parameters K_d , available carbon substrate, and dispersivity (dashed lines: maximum and minimum, black line with bars: mean of 25 simulation runs with standard deviation) in 2004. Note the different amount scale from day 29.

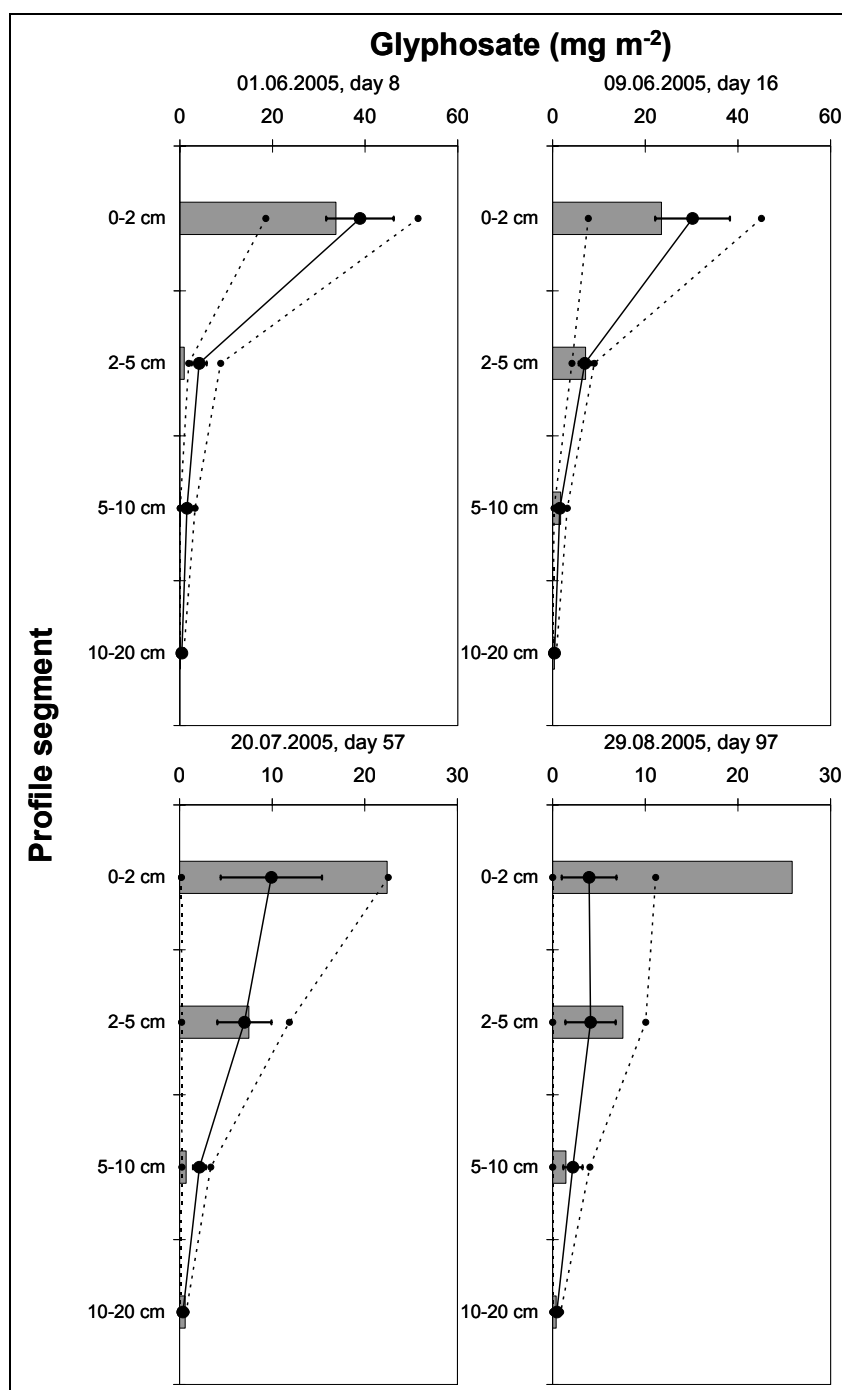


Fig. 4.40: Measured profile (grey bars) of glyphosate movement and model simulation following variation ($N = 25$) of pesticide input parameters K_d , available carbon substrate and dispersivity (dashed lines: maximum and minimum, black line with bars: mean of 25 simulation runs with standard deviation) in 2005. Note the different amount scale from day 57.

In the year 2005 glyphosate profiles were simulated reasonably well until day 57 (Fig. 4.40). Afterwards, glyphosate and residues in the top sampling depth were underestimated by the mean of the LHS sample and especially at day 97 penetration of glyphosate was overestimated by model simulations. The degraded glyphosate amounts in the years 2004 and

2005 were comparable (2004: $DT_{50} = 62$ d and 2005: $DT_{50} = 52$ d), although the measurements of the glyphosate residues show no decrease from day 16 to day 97 in 2005. Thus, probably a representative sampling was not obtained in 2005 because of the application conditions. The pesticide application on the lysimeters in 2005 was more inhomogeneous. The variation in the minimum and maximum glyphosate penetration predicted by the LHS sample is high and seems to be overestimated especially for the maximum movement, due to the low K_d value used in this input parameter set. This shows that the coefficient of variation of 40 % for the K_d value is probably too high.

The modelling results showed that the incorporation of uncertainty in sorption, dispersivity and degradation parameters resulted in a considerable variability in model output (Figs. 4.39 and 4.40). The variability in the output was smaller than the variability in the input parameters. The results suggest that the incorporation of variability helps to improve the simulation of the variability in glyphosate movement in the soil profile. Unfortunately, experimental information of only two lysimeter replicates was available and therefore, no uncertainty analyses for the experimental results exist for comparison. As already discussed, inhomogeneous pesticide application or not representative sampling seems to have a higher contribution to the uncertainty in the movement of glyphosate in the year 2005 than the uncertainties arising from the pesticide input parameters.

It should be noted that the range and distribution of model output strongly depends on the assignment of plausible ranges and distributions to each of the input parameters (Beulke et al., 2004a). For example the coefficient of variation for the available carbon substrate was chosen to be smaller than for the sorption and dispersivity coefficients. As described by Dubus et al. (2003) it is somewhat awkward that the selection and implementation of techniques designed to account for uncertainties are themselves subject to significant uncertainty. Nevertheless, in conclusion the variability of simulated glyphosate behaviour in the present study seems to be well described by the consideration of the uncertainties arising from the variability of the selected input parameters.

4.3.4 Uptake and translocation of glyphosate in transgene soybeans

Modelling of pesticide uptake by plants depends on a correct simulation of plant growth carried out in *Expert-N* by applying the plant submodule. In case of applying the generic crop growth model SUCROS (van Laar et al., 1997) a constant specific leaf weight is needed as model input parameter that cannot be given in dependence of the development stage of the plants. The specific leaf weight is calculated from measurements by the ratio of leaf biomass to LAI. Field measurements of leaf biomass and LAI showed that the specific leaf weight of the soybeans changed from 1130 kg ha⁻¹ (66 days after sowing) to 405 kg ha⁻¹ (118 days after sowing). A constant specific leaf weight of 405 kg ha⁻¹ was used for the simulations at last, because of the good accordance of the simulated plant biomass with the measurements over the whole growing season. Further on the influence of a correctly simulated LAI on related simulation results (e.g. pesticide concentrations) is small compared to a correctly predicted leaf biomass. In the plant growth model SUCROS soybean nodules were not considered. The root weight to nodule weight ratio measured in the lysimeters was 1:3. Thus for the pesticide uptake submodule the nodule weight was assumed to be 30 % of the simulated root weight.

A number of studies have reported no evidence of metabolic degradation of glyphosate in a variety of susceptible and resistant plant species (Duke, 1988; Franz et al., 1997; Lorraine-Colwill et al., 2003). According to the statement of the manufacturer of GR (glyphosate resistant) soybean, Monsanto (personal communication Norbert Mülleder, Monsanto, Düsseldorf), and according to the results of the GSF-lysimeter study (Grundmann, unpublished results) no degradation of glyphosate occurs in GR soybean and no metabolites were identified. Less than 2 % was determined to be converted to ¹⁴CO₂ in the lysimeter study 2004. This small amount of 2 % may be explained by the uptake of ¹⁴C-metabolites by the plant roots from soil and metabolisation in the plants to ¹⁴CO₂. No volatilisation from plants after foliar application was measured.

The development of the soybeans under the given climatic conditions in 2004 and 2005 was restricted. As already documented, even various attempts were necessary for the successful germination of the plants in the year 2005, resulting in a short growing season and sparse growth (Fig. 4.41). In both vegetation years no beans were developed. Simulation of the sparse growth of the soybeans was considered in the simulation study by the adjustment of the development parameters and by minimizing of the photosynthesis response in the SUCROS model. Fig. 4.41 shows that in 2004 the soybean biomass could be adequately described by the model and only at the end of vegetation period the model shows a slight trend to

overestimate stem biomass. In 2005 plant biomass was still overestimated by the simulation results.

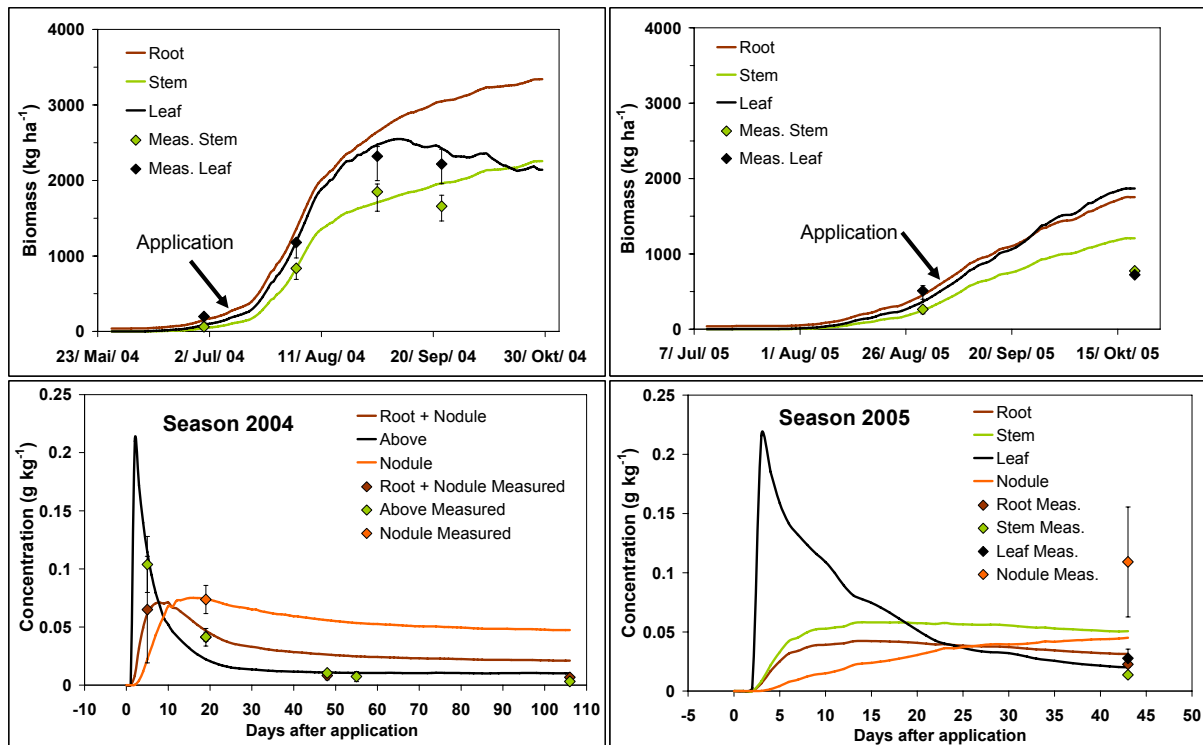


Fig. 4.41: Soybean biomass and glyphosate concentrations simulated and measured in respective plant tissues in the growing seasons 2004 and 2005 on lysimeters (for the year 2004 glyphosate was only measured in a mixed sample of leaf and stem material denoted as ‘above concentration’).

Both, simulation results of plant biomass and glyphosate concentration in 2004 are in good accordance with the measurements (Fig. 4.41). In the year 2005, especially glyphosate concentration in nodules was underestimated by the model, although glyphosate concentration in plant roots was correctly predicted. Because of the shortened growing season in 2005 and the high standard deviation in the measured glyphosate concentration in nodules, the comparison of simulation results with measurements is difficult.

After a fast herbicide uptake by the plant leaves, glyphosate was translocated rapidly from the site of application. Herbicide transport in the newly developing plant parts appears in the model by the dilution of glyphosate concentration in the course of time (Fig. 4.41). Glyphosate penetrates the cuticle of most species to enter the plant apoplast. It then slowly enters the symplast passively and is translocated primarily via the phloem to metabolic sinks (Duke, 1988). Results of the pesticide plant uptake model of Chiou et al. (2001), also based on an equilibrium approach like the approach used in the present study, indicate that for all plants with high water contents the water in the plant acts as the major reservoir for highly water-soluble contaminants. Accumulation of glyphosate in roots and meristematic regions of

treated plants has been well documented (Franz et al., 1997; Geiger et al., 1999; Lorraine-Colwill et al., 2003). Although the action of a phloem-mobile herbicide on plant tissues can inhibit assimilate translocation and thereby limit its own translocation. Geiger et al. (1999) found that glyphosate tolerant plants continued to transport glyphosate at a significant rate while susceptible plants (*Beta vulgaris*) stopped transport. Since glyphosate is not metabolised in the GR soybeans and considering the demand for photosynthate in nodules it is apparent that glyphosate also accumulates in nodules (cp. Fig. 4.41).

The soybean nitrogen fixing symbiont, *Bradyrhizobium japonicum*, possesses a glyphosate-sensitive enzyme and upon exposure to glyphosate accumulates shikimic acid and hydroxybenzoic acids (Zablotowicz and Reddy, 2004; Wagner et al., 2006). Studies of Zablotowicz and Reddy (2004) confirmed that glyphosate accumulated in nodules of field-grown GR soybean, but its effect on nitrogenase activity of GR soybean was inconsistent in their field studies. The effects of glyphosate on N₂ fixation potential of GR soybean should be especially evaluated on sandy soils with limited nitrogen availability. Yield reductions due to the reduced N₂ fixation in early stages of growth have not been demonstrated in their study. But yield reduction in GR plant systems is discussed controversial in literature. According to Raymer and Grey (2003) possible explanations for yield suppression in GR soybean would be: (i) the presence of the CP4-EPSP synthase gene reduces the fitness of the plant, (ii) normal genetic or physiological processes were disrupted by the transformation process, and (iii) the application of glyphosate causes yield suppression. Based on the results of Elmore et al. (2001), the yield suppression appears to be associated with the CP4-EPSP synthase gene or its insertion process rather than glyphosate itself.

The accumulation of glyphosate in the soybean nodules results in a selection pressure for the bacteria in the rhizosphere that are sensitive to glyphosate and therefore favours the successful establishment of a HGT (horizontal gene transfer). Mathematical modelling is a useful tool for the evaluation of herbicide application time and resulting glyphosate concentration in single plant tissues. For the simulation of a worst-case scenario with the highest selection pressure and the highest risk to accomplish a HGT, different application scenarios were simulated for the plant growth in 2004 (Table 4.19). Scenario 1 and 2 were chosen according to commonly used herbicide treatments (Duke et al., 2003), with one week delay for the first application due to the retarded development of the plants in the lysimeter study. Duke et al. (2003) found that glyphosate residues in seeds were higher, if glyphosate was used in applications later in the season. Thus, glyphosate was also assumed to be applied twice at a later stage of soybean growth (cp. Table 4.19 and 4.20).

Table 4.19: Herbicide application scenarios

Scenario	1. App. (110 mg a.i. ha⁻¹) (weeks after sowing)	2. App. (90 mg a.i. ha⁻¹) (weeks after sowing)
1	4	7
2	4	8
3	7	10
4	7	11
measurement	7	-

Table 4.20: Plant parameters of soybean growth at the date of the assumed herbicide applications in 2004

Date of application	Weeks after sowing	LAI (-)	Soil Cover (%)	Development Stage (SUCROS)
26.06.2004	4	0.2	8.6	19
15.07.2004	7	1.08	38.5	25
23.07.2004	8	1.89	57.3	29
06.08.2004	10	4.23	85.1	35
13.08.2004	11	5.23	90.5	38

In the simulation model it was assumed that after a rain event of more than 5 mm the remaining pesticide amount on the soybean leaves was washed down. In Table 4.21 therefore rain amounts within five days after the application date with more than 5 mm are given.

Table 4.21: Rain in 2004 within five days after the assumed application date and with more than 5 mm amount

Date	Rain (mm)
01.07.2004	6.6
24.07.2004	12.5
26.07.2004	8.9
14.08.2004	7.5

Glyphosate was found at highest levels in the nodules, when it was applied according to the commonly used treatment (scenario 1, Fig. 4.42) with a first application at four weeks and a second at seven weeks after sowing. Scenario 2 shows that a rain event one day after application significantly reduces the herbicide uptake by the plant leaves and the following translocation within the plants.

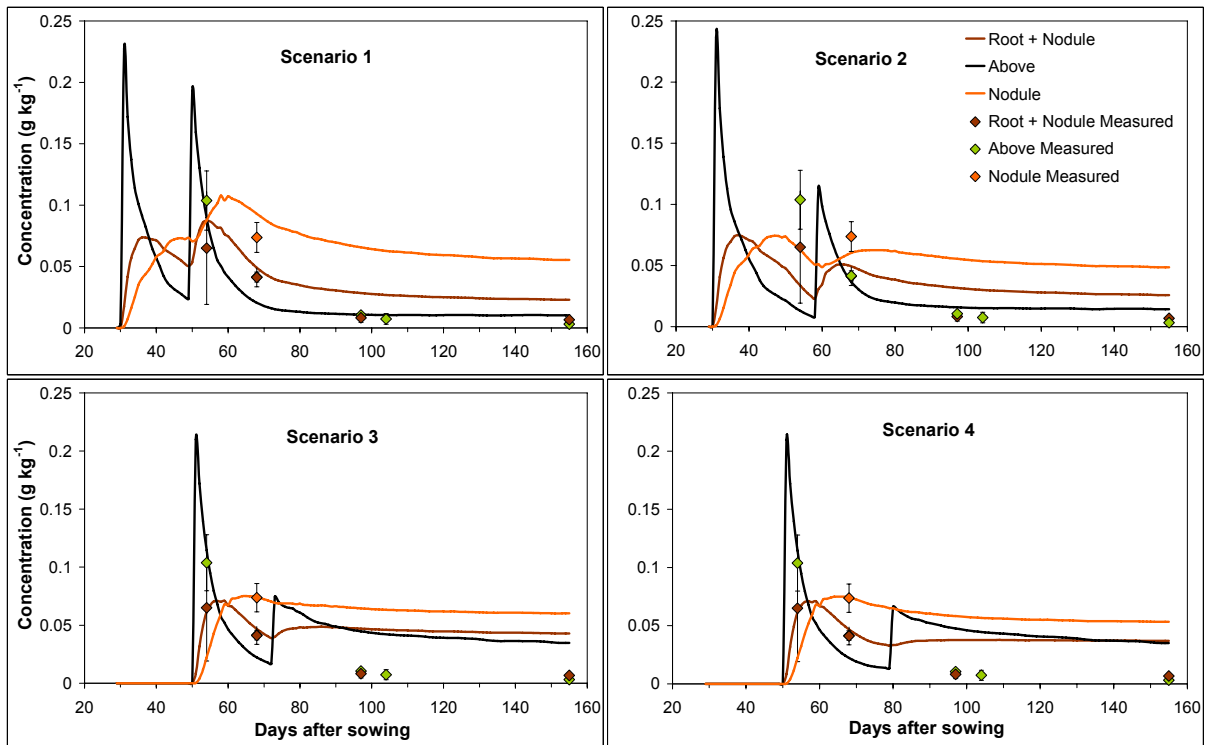


Fig. 4.42: Glyphosate concentration in plant tissues (above = leaf and stem) measurement in 2004 and simulation with different application scenarios (see Table 4.19).

Further increase of glyphosate concentration in plant nodules when used in later season applications cannot be achieved (scenario 3 and 4, Fig. 4.42). This is because the soil cover increases logarithmical with the LAI (Fig. 4.43a), while the above ground biomass increases almost linear with LAI (Fig. 4.43b). Thus, the dilution factor with growth increases compared to the earlier stage applications. Additionally, allocation of assimilation products in the plants is more towards leaf and bean in the development stage of the tenth week and less in stem and root. This effect is even increased, when the second application is shifted from ten (scenario 3) to eleven weeks (scenario 4).

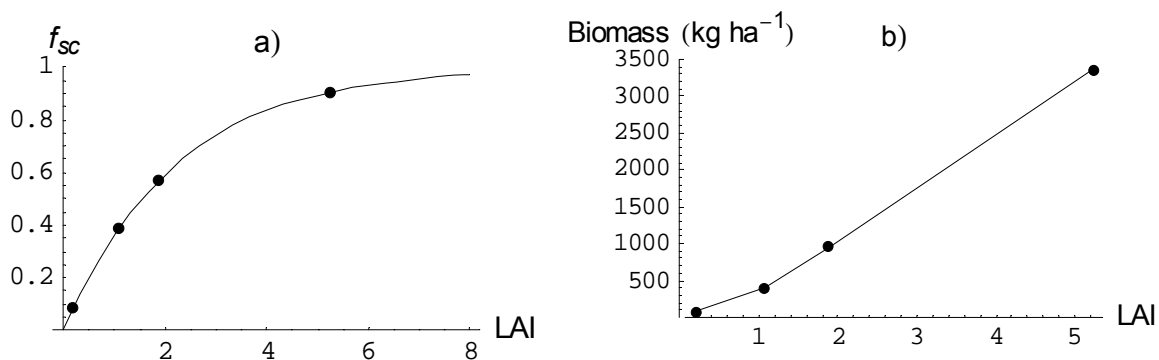


Fig. 4.43: Simulated soil cover factor (a) and above ground biomass (b) in dependence of LAI at 4, 7, 8 and 11 weeks after sowing in 2004.

The level of glyphosate residues in seeds of glyphosate-resistant soybean is of great interest for food and animal feed production. A maximum residue level (MRL) of 0.02 g kg⁻¹ glyphosate in beans of transgene soybean was proposed in the Review Report Glyphosate of the European Union (Bruno and Schaper, 2002). Only in the year 2003, when non-transgene soybean was planted on the lysimeters and growth was favoured by temperatures above average for the present climatic conditions, beans were developed by the soybean plants. For a risk assessment study of glyphosate accumulation in soybean seeds a hypothetical glyphosate application in the simulation model was again assumed for the growing season 2003.

Glyphosate is rapidly absorbed by plant foliage. According to Pline et al. (1999) 45 % (at 15 °C) to 49 % (at 35 °C) of the foliar-applied ¹⁴C-glyphosate was absorbed by GR soybeans 24 h after application. Absorption of 34 % (*Agropyron repens*) within 4 h and 19 % (*Apocynum cannabinum*) within 12 h of the applied glyphosate amount were reported by Franz et al. (1997). This shows that plant cuticles vary considerably in their permeability to glyphosate. Cuticles are solid-state lipid membranes, which are crossed by non-electrolytes by dissolving and diffusing in lipophilic domains composed of cutin and amorphous cuticular waxes (lipophilic pathway). But stomatous leaf surfaces have additional pores in cuticular ledges and permeability of these pores has been shown to depend on stomatal opening (Schönherr, 2002). These polar pores constitute the aqueous or hydrophilic pathway which is accessible for ions. Results of Schönherr (2002) indicate that IPA-glyphosate is penetrated via the aqueous pathway as hydrated ions. The relatively rapid passage of the highly polar molecule from the leaf surface into the apoplast supports this view (Franz et al., 1997). The sorption of hydrophilic compounds into cuticular membranes is significantly higher than expected from their octanol/water partition coefficients. This implies that for these compounds the transport across the cuticular wax barrier is not relevant (Popp et al., 2005).

The rate of glyphosate penetration was highest initially after application and tended to level off in the course of time (Pline et al., 1999; Schönherr, 2002). Thus, diffusion is considered to be the most likely process for transport across the cuticle (Franz et al., 1997) and the concentration gradient between the spray deposit and the inside of the plant a driving force of cuticular penetration. Seven days after application absorption only reached a height of 56 % of the applied ¹⁴C at 15 °C compared to 45 % after 24 h (Pline et al., 1999).

It was assumed that cuticular permeance can be described by the rate constant of penetration and the cuticular thickness for the hydrophilic pathway (cp. Eq. (4.49)). According to the results of Pline et al. (1999) for GR soybean, glyphosate penetration k was calculated

(Eq. (4.50)) to reach 0.672 d^{-1} for the first day after application and 0.019 d^{-1} afterwards. The cuticular thickness of the soybean leaves was estimated from the thickness of the epidermal soybean cell layers reported in the work of Sims et al. (1998). Because cuticular thickness was only roughly estimated, different values have been used and compared for the simulation model. The resulting cuticular permeance in dependence of the assumed cuticular thickness is listed in Table 4.22.

Table 4.22: Cuticular permeance in dependence of cuticular thickness for GR soybean leaves at the first day after application and afterwards

Cuticular permeance (m d^{-1})	Cuticular thickness		
	a) $3 \mu\text{m}$	b) $15 \mu\text{m}$	c) $30 \mu\text{m}$
<i>P1</i> (24 h)	$2.10 \cdot 10^{-6}$	$1.01 \cdot 10^{-5}$	$2.1 \cdot 10^{-5}$
<i>P2</i> (after 24 h)	$5.83 \cdot 10^{-8}$	$2.92 \cdot 10^{-7}$	$5.83 \cdot 10^{-7}$

As the rate of penetration of glyphosate for GR soybean is known, permeance must be faster, if the cuticular thickness is assumed to be higher. Permeances measured for solutes range from $8.64 \cdot 10^{-6} \text{ m d}^{-1}$ (*Ficus*, 2,4 D) to $7.4 \cdot 10^{-2} \text{ m d}^{-1}$ (*Citrus*, hexachlorobenzene) (Schönherr and Riederer, 1989). This is a range of almost four orders of magnitude.

For the year 2003 no measurements of plant biomass exist for comparison with simulation results, but development of beans was observed in the lysimeter study. The simulated soybean biomass development is shown in Fig. 4.44a. Simulated glyphosate concentrations in the above ground biomass and in the beans using different estimates for the cuticular permeance for the hypothetical glyphosate application in the year 2003 are shown in Fig. 4.44b. According to Duke et al. (2003) highest concentration in beans was reached, if glyphosate was applied at full bloom of the plants. Thus, time of application was chosen to be seven weeks after sowing with an amount of $110 \text{ mg a.i. ha}^{-1}$. Any factor, whether plant-related or environmental, that influences cuticula penetration and phloem transport from the site of application to other parts of the plant will similarly influence the translocation of glyphosate (Fig. 4.44b). The influence of the permeance on the concentration of glyphosate in the soybean plants is high. An increase in the order of magnitude of the cuticular permeance of one results in an increase of the maximum glyphosate concentration in the beans 36 days after application in nearly one order of magnitude as well.

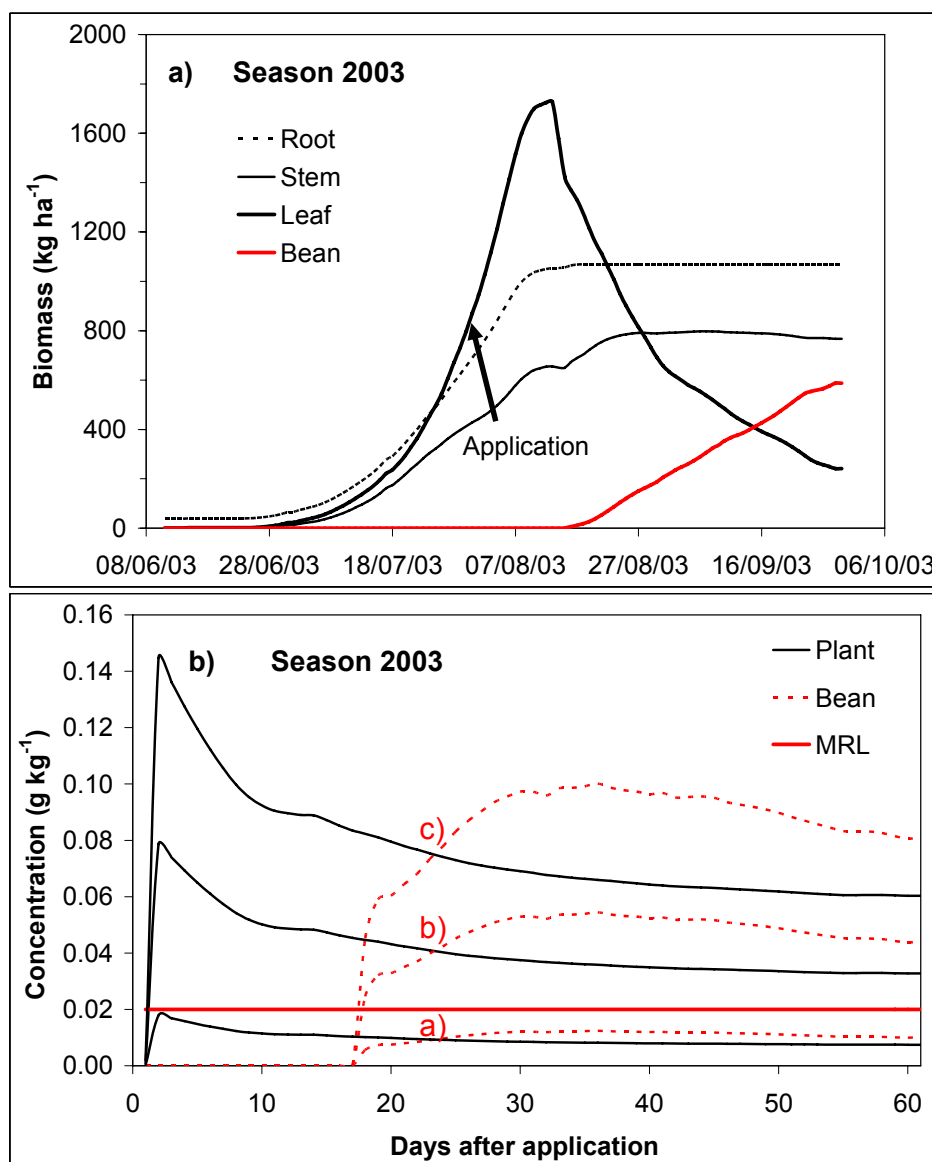


Fig. 4.44: Simulated plant biomass (a) and simulated glyphosate concentration in above ground biomass (plant) and beans and maximum residue level (MRL) (b) of glyphosate in GR beans with different permeances ($P_l =$ a) $2 \cdot 10^{-6}$ b) $1.01 \cdot 10^{-5}$ c) $2.1 \cdot 10^{-5} \text{ m d}^{-1}$) in the year 2003.

Fig. 4.44b shows that the maximum residue level recommended by the European Union is exceeded by the simulated glyphosate concentrations in the beans in 2003, if cuticula permeance is assumed to be $1.01 \cdot 10^{-5} \text{ m d}^{-1}$ and higher. The simulation results indicate that the glyphosate concentrations in beans of transgenic soybean can exceed recommended guideline values under commonly used herbicide treatments. Therefore, the aspect of a possible decrease of food quality of GR soybeans should be a subject of further experimental studies as supported by the simulation results.

4.4 Conclusions

A modelling system for the description of solute transport and pesticide behaviour was successfully implemented in the modular modelling system *Expert-N*. The newly inserted submodule was effectively coupled to the existing water flow and plant growth modules. For the simulation of pesticide degradation a first-order kinetic degradation approach and a microbial growth kinetic approach, both, including humidity and temperature dependencies, were developed. Pesticide sorption kinetics can now be described in *Expert-N* either by a linear equilibrium, by a nonlinear equilibrium (Freundlich isotherm) or by a linear non-equilibrium (two-site) sorption model. Pesticide uptake by plant leaves and roots and pesticide translocation in plants was implemented in a plant uptake submodule.

The differentiation between a deterministic parameter selection and a probabilistic distribution of model input parameters was useful to show sources of uncertainty in model output. Deterministic modelling approaches do not account for uncertainties in simulations, which for example arise from uncertainty in the acquisition of basic data in field and laboratory, then by the derivation of model input parameters and finally by the modelling itself. Aim of the comparison of different deterministic modelling approaches was to evaluate the effect of model selection on the environmental fate of glyphosate in the lysimeters. The choice of modelling approaches for water flow, as well as for degradation and sorption modules has a strong effect on the simulation results. But these differences in simulation results are difficult to quantify. A probability distribution of model input parameters describing sorption, dispersivity and degradation in a deterministic model resulted also in a considerable variability in model output. Variability in output was smaller than variability in input parameters. The results suggest that the incorporation of variability in model input helps to improve the simulation of the variability in glyphosate movement in the soil profile, but it should be noted that the range and distribution of model output strongly depends on the assignment of plausible ranges and distributions to each of the input parameters. The results demonstrate that the coefficient of variation for single input values can also be overestimated. Today it is increasingly recognised that pesticide leaching models cannot accurately simulate field data in predictive mode, partly because of variability and uncertainty aspects (Vanclooster et al., 2000).

The present study demonstrated that field lysimeters are an appropriate environment to evaluate the fate of pesticides in closed systems under natural conditions. They can reproduce real field conditions under the restriction of the observed problems like microclimatic effects

and disturbing effects of measurements. Lysimeter measurements showed that cumulative evapotranspiration amounts between the single lysimeters were slightly different. The difference averages 0.35 mm d^{-1} per day and can be explained by differences in plant growth on the lysimeters. Percolation amounts were comparable between the lysimeters, but differences could be observed in the outflow behaviour. Also deuterium BTCs coincide very well between the lysimeters. Moreover, the symmetrical form of the BTCs confirms that matrix flow within a single continuum system was the dominant process in the sandy soil lysimeters. Since there occurred no strong rainfall events (within five days) after each of the three pesticide applications on the lysimeters, no glyphosate leaching in amounts above the detection limit could be measured. The measured radioactivity in the leachate was in form of $^{14}\text{CO}_2$, resulting probably from biodegradation of glyphosate. The installed TDR probes and tensiometers were useful for the establishment of water retention curves, but a calibration of TDR probes after comparison with gravimetric water content measurements became necessary.

Water flow simulations and measurements identified that daily actual evapotranspiration was the most varying parameter in water balance and a daily prediction of precise evapotranspiration by the simulation models was hardly possible. Best simulation results were achieved by using the van Genuchten-Mualem parameterisation of the hydraulic characteristics combined with the Haude (mrH) evapotranspiration model. The daily variations in ET_a were sufficiently described by this approach considering the high variability in the measured amounts. High water content fluctuations observed by the humidity capacitance sensor in the first soil centimetres were well simulated by the Hutson & Cass-Burdine parameterisation of the hydraulic characteristics. However, the agreement between the van Genuchten-Mualem parameterisation and water content measurements (TDR) at 30 cm depth was higher than with the Hutson & Cass-Burdine parameterisation. Additionally, weekly percolation amounts gave further confidence of the good applicability of the combination of the van Genuchten-Mualem parameterisation with the Haude (mrH) evapotranspiration model. But percolation amounts could be predicted in a satisfying way by both hydraulic parameterisations. The influence of the parameterisation of hydraulic characteristics on movement of glyphosate in the soil profile was small compared to the influence of the magnitude of the dispersivity coefficient. Expectedly, a smaller value for the dispersivity resulted in a slower movement of glyphosate in the soil profile.

After the adjustment of water balance simulations and determination of the dispersivity coefficient, first the accurate representation of glyphosate biodegradation was addressed. Biodegradation batch experiments already showed that small changes at low and high water content ranges in soil have strong influence on the degradation of the herbicide. Moreover, the effect of rain events on biodegradation rates in the field lysimeters was clearly represented in an increase of measured degradation rates after rain was fallen. This humidity dependence of degradation could be best achieved in the simulations by using the environmental response surface of the Weibull type. For the Hutson & Cass-Burdine parameterisation of the hydraulic characteristics there was a good agreement between measurement and simulation in single first-order degradation rates, while for the van Genuchten-Mualem parameterisation the agreement was best in the first-order average degradation rate for both project years. The results showed that by the choice of single modelling approaches high differences in the simulated degradation rates occur. On the one hand the measured cumulative degradation of glyphosate in 2005 was underestimated about 19.7 % (Hutson & Cass-Burdine with environmental response surface of Gauss type) and on the other hand overestimated about 9.9 % (van Genuchten-Mualem with environmental response surface of Gauss type). It must be also pointed out, that between highly dependent state variables – like water content and degradation rates in this case – error propagation is an important factor of uncertainty.

More conceptual descriptions of microbial response to pesticide and nutrient additions are Monod degradation characteristics. However, if such approaches were applied, correlation coefficients and matrix scatter plot demonstrated that uncertainties in calibration of Monod models arise from the fact that multiple combinations of input parameters will provide similar fits to the experimental data. This indicates that the model was overparameterised with respect to the data structure. Correlation analysis also showed that microbial growth rate is the parameter with the highest influence on solute pesticide concentration in simulation. If it was assumed that mainly metabolic degradation occurs, the glyphosate degrading community of specialists' increases and dies very fast in high correlation to glyphosate availability. Thus, pesticide degradation can be accelerated by multiple pesticide applications as the degrading microbial community continuously increases. The modelling concept of co-metabolic degradation expects that the degrading community depends mainly on the amount of other easily available carbon substrate. Thus, degradation depends on different initial levels of other carbon sources. The size of the degrading community may increase in response to organic inputs like root exudates. But pesticide degradation is not automatically accelerated with an increase in total microbial biomass, because the pesticide is less used as carbon source, if

other easily available carbon substrate is abundant. Problems in the co-metabolic degradation concept arise from the definition of a dynamic indigenous carbon source in the modelling approach. Simulated actual CO₂ emission rates from soil are an appropriate parameter for representation of bioavailable carbon in the soil surface, but a linear correlation between CO₂ emissions and pesticide degradation does not exist, because the relation is particularly complex. The simulation results confirm that mainly co-metabolic glyphosate degradation occurs in soil, even though this approach was more difficult to parameterise.

Furthermore, different sorption concepts were discussed. Between the single-site equilibrium and two-site non-equilibrium model nearly no difference in simulated glyphosate behaviour gets obvious, only simulation results of leachate amount and time of first glyphosate appearance differ. Because only radioactivity amounts and not the parent compound glyphosate could be detected in the leachate, a distinction between single-site equilibrium and two-site non-equilibrium sorption concept based on the measurements cannot be undertaken. The simulated leachate concentrations for both concepts were far below the threshold value for drinking water of 0.1 µg L⁻¹. The linear equilibrium concept reproduces the observed glyphosate movement better than the approach with the Freundlich sorption isotherm. It must be assumed that glyphosate degradation was underestimated with the Freundlich approach, because higher pesticide fractions are sorbed. Pesticide fractions which are sorbed in micropores are inaccessible for the degrading microbes until direction of diffusion is reversed to the larger pores due to concentration gradients. But this process is slow relative to the movement of mobile soil water.

Finally, glyphosate behaviour in transgene soybean was studied for the restricted growing conditions under the climatic conditions of the years 2004 and 2005. Thus, soybean biomass could be only adequately described if model input parameters were adjusted to the lysimeter conditions. Measured and simulated results showed that after a fast uptake of the herbicide by plant leaves, glyphosate was translocated rapidly from the site of application. Herbicide transport in the newly developing plant parts appeared in the model by the dilution of glyphosate concentration with time. Both, simulation results of plant biomass and glyphosate concentration in the year 2004 were in good accordance with the measurements, while in the year 2005 due to the shortened growing season simulation results compared to measurements were difficult to evaluate. Since glyphosate is not metabolised in the GR soybeans and considering the demand for photosynthate in nodules it is apparent that glyphosate also

accumulates in nodules as simulation and measurements showed. Mathematical modelling was a useful tool for the evaluation of herbicide application time and resulting glyphosate concentration in single plant tissues. For the estimation of the date of herbicide application that facilitates glyphosate concentration in the soybean nodules and thus increases selection pressure on glyphosate sensitive microorganisms, different application scenarios were simulated. Glyphosate was found at highest levels in the nodules, when it was applied according to the commonly used treatment. Moreover, the influence of cuticular permeance on simulated glyphosate concentration in the soybean plants is high. An increase in one order of magnitude of the cuticular permeance, results in an increase of the simulated maximum glyphosate concentration in the beans in nearly one order of magnitude as well.

Summarising, due to the high sorption of glyphosate to the soil matrix and the high microbial capacities for glyphosate degradation in the lysimeter soil, leaching risk can be regarded to be low, but cannot be excluded entirely. Preferential flow or co-transport of glyphosate with dissolved organic matter or colloids was not observed in the present study, although discussed in literature. Neither a significant acceleration (adaptation) nor a deceleration (inhibition) of the degradation process by microorganisms was observable after repeated herbicide applications. This was confirmed by the modelling results. The results showed that the introduction of more conceptual descriptions of microbial response to pesticide and nutrient additions can contribute to a reduction in the uncertainty of pesticide degradation. Biodegradation was mainly influenced by soil humidity in the field study. But it must be regarded that biodegradation is not only higher due to an enhanced microbial activity in wet soils, also mass-transfer including diffusion and desorption of the pesticides must be expected to be higher. No metabolisation of glyphosate by transgene soybeans is observable and the possibility of accumulation in the plants exists. The simulation results indicate that glyphosate concentrations in beans of GR soybean can exceed recommended guideline values under commonly used herbicide treatments. Therefore, the aspect of a possible decrease of food quality of GR soybeans should be a subject of further experimental studies as supported by the simulation results. Additionally, measured and simulated accumulation of glyphosate in soybean nodules favours the selection pressure given for the glyphosate sensitive bacteria in the rhizosphere. Finally, the results showed that the implemented modelling system for the description and assessment of pesticide behaviour in various soils and plants was able to describe environmental behaviour of glyphosate in the presence of genetically modified plants.

5 Technical note: Solute transport model implementation in *Expert-N*

5.1 Introduction to *Expert-N*

The *Expert-N* model system comprises a number of modules that provide different approaches to simulate vertical one-dimensional soil water flow, evapotranspiration, soil heat transfer and nitrogen transport, soil carbon and nitrogen turnover, crop growth processes, and soil management (Fig. 5.1). The process models available in *Expert-N* have either been taken from published models or have been developed by the *Expert-N* team (Engel and Priesack, 1993; Stenger et al., 1999). The highly modular structure of *Expert-N* allows the easy implementation of newly developed submodels as in this case the solute transport model. The implementation of these modules in *Expert-N* was realized using the concept of dynamic link libraries (DLLs) of the *Microsoft C* programming environment (*Visual Studio .NET 2003*®). DLLs allow further development and verification of the submodel in the *Expert-N* environment. Besides the user friendly interface for model choice and graphical display of the simulation results, *Expert-N* comprises a menu driven database for the variable input system. For the submodels, which are under development, one's own input and output files are necessary.

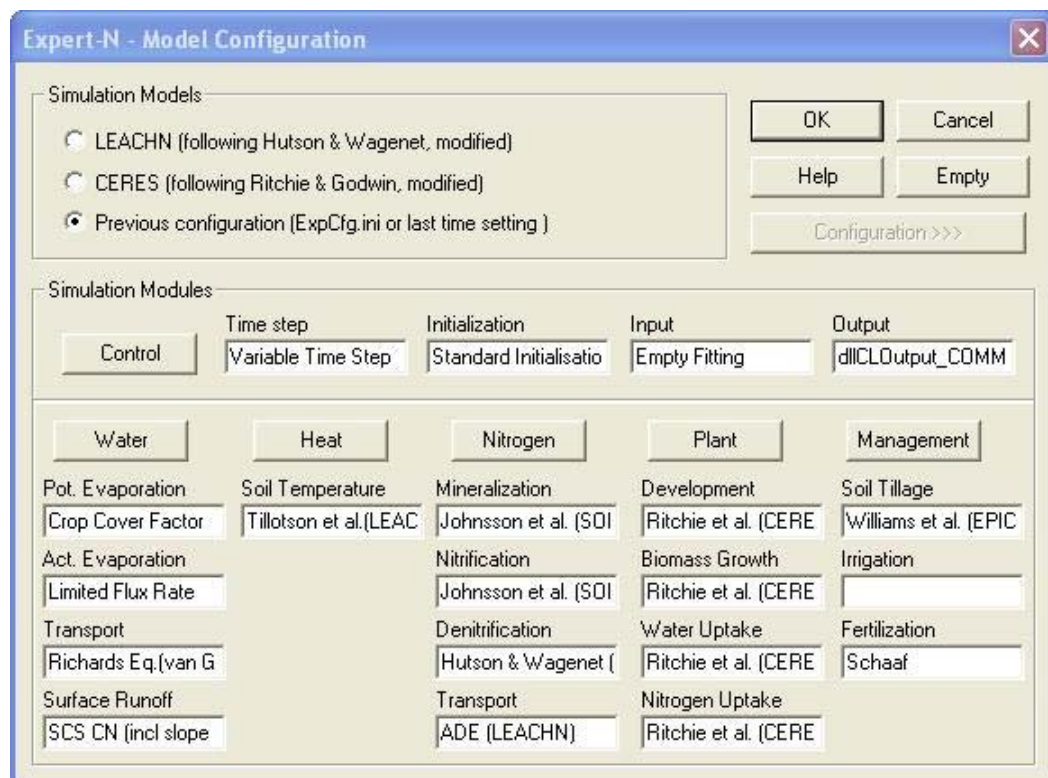


Fig. 5.1: The modular modelling system *Expert-N*.

5.2 Description of the DLL system components

DLLs are shared libraries which allow new modules and sections of source code to be integrated at run-time into pre-existing applications. Three DLLs concerning the solute transport model are called from the *Expert-N* program (Table 5.1).

Table 5.1: DLLs called from the *Expert-N* program

Dynamic link library	Address	Library description
dllCLXenoTrans_LEAHP	@2500	Xenobiotica transport
dllCLOutput_XENO	@2510	Xenobiotica transport: Output
dllCLOutput_COMMON	@2520	Xenobiotica transport: Output compilation of special common used variables
dllCLEVCropFactorFAO	@2550	Evapotranspiration: PM dual crop factor

The DLL `dllCLXenoTrans_LEAHP` is called up after the calculation of the water transport module. After the readout of the input file (C function: `Xeno_Transport_Read`) the main process function `Xeno_Transp` of the program is called in the DLL. The other two DLLs listed in Table 5.1 with the code name `dllCLOutput` are needed to generate two different output files, explained in further detail in section 5.5. The fourth DLL `dllCLEVCropFactorFAO` provides a further potential evapotranspiration module in *Expert-N* called up at the beginning of the time step and concerning the Penman-Monteith dual crop coefficient approach discussed in section 3.2.2.3.

5.3 Process functions and calling order

According to *Expert-N* the program structure of the solute transport module should supply the possibility to exchange and add on process functions and to simulate processes of various pesticides. At present, up to four pesticides can be considered. The differentiation between and parallel simulation of the four pesticides was solved in two ways. For short code sections where differentiation was necessary the `if/else` operator was used. C also allows the use of function pointers and these were used when differentiation between pesticides was necessary for whole functions. The specific parameter values of the respective pesticide were then passed to the function as pointer structure and dereferenced in the function to access the data stored. At the end of the function the newly calculated parameter values in the pointer structure were then passed back to the variables in the main menu. The second way was used

for the process functions `Get_SolutionConc` and `Get_PlantUptake`. The calling order of the C-process functions in the main program `Xeno_Transp` is shown in Fig. 5.2.

```

int Xeno_Transp (EXP_POINTER)
{
  Get_SolutionConc (& XenoX);
  Get_Diffusion_Const_Xeno (exp_p);
  Sorption_Kinetics_Xeno (exp_p);
  Surface_Volatilization_Xeno (exp_p);
  Degradation_Xeno (exp_p);
  Get_PlantUptake (& XenoXPlant);
  Solve_LGS_Xeno (exp_p);
  Get_SolutionConc (& XenoX);
}

```

Fig. 5.2: Calling order of functions in the main program source code.

The subroutine `Get_SolutionConc` partitions the pesticide between the solid, liquid and gas phase and is called in three places from `Xeno_Transp`:

- i) at the start, to partition the chemical initially in the profile
- ii) after the application of the chemical on the soil surface
- iii) after exiting the solver of the solute transport subroutine `Solve_LSG_Xeno`.

In the subroutine `Get_Diffusion_Const_Xeno` the diffusion-dispersion coefficients of the pesticides in the single numerical layers are calculated. `Sorption_Kinetics_Xeno` describes the non-equilibrium two-site sorption concept and calculates the additional source or sink ϕ_{sorb} . The pesticide volatilisation at the air-water interface (sink term ϕ_v) is determined in the subroutine `Surface_Volatilization_Xeno`. In the subroutine `Degradation_Xeno` the photolytic and microbial degradation processes are described and the sink term ϕ_{deg} is calculated. `Get_PlantUptake` includes the pesticide plant uptake submodel and the description of the sink term ϕ_{Plant} . In the subroutine `Solve_LGS_Xeno` the differencing scheme of the CDE is solved.

5.4 Function parameters and C-data structures

Function parameters are generally passed by value or by reference in the form of pointers. All the various state and rate variables used in the solute transport module are grouped into five C-data structure categories listed in Table 5.2. The superordinate C-data structure containing all pointer structures related to the solute transport model was defined as PXENO (Fig. 5.3).

```
typedef struct stXeno * PXENO;
typedef struct stXeno
{
    PXLAYER          pXLayer;
    PXPROFILE        pXProfile;
    PXPARAM          pXParam;
    PXPLANT          pXPlant;
    PSOLUTESCENARIO pSoluteScenario;
}
XENO;
```

Fig. 5.3: Organisation of the superordinate data structure PXENO of the solute transport module.

The structure names have the code P at the beginning to signal the organisation in pointers. The layer dependent variables which describe the pesticide behaviour in the single numerical layers e.g. solute and adsorbed concentrations or liquid diffusion coefficients are defined and grouped in the structure PXLAYER. Variables indicating general information like application date, boolean variables (yes/no information like pesticide uptake by plant) and balancing variables like total leachate amount over time are summed up in the structure PXPROFILE. The structure PXPARAM contains all pesticide, soil, microbial and plant properties describing variables like pesticide solubility in water, K_d value, microbial growth rate and root radius. The variables associated with the pesticide plant uptake submodule like pesticide concentrations in roots, stems, leaves or fruits are defined in the PXPLANT structure. The PSOLUTESCENARIO structure contains auxiliary variables for the output file.

Table 5.2: Information contained in the subsidiary data structures in the solute transport model

Data Type	Variable information
PXLAYER	layer dependent variables describing pesticide behaviour in soil
PXPROFILE	variables indicating general information for the whole soil profile
PXPARAM	pesticide, soil, microbial and plant properties
PXPLANT	variables describing pesticide behaviour in plants
PXSOLUTESCENARIO	variables necessary for output characterisation

The complete list of variable of the data structure PXENO and the description of the single variables is summarised in appendix B.

5.5 Input/Output files

In the simulation of pesticide processes the required input data include pesticide properties like basic physicochemical parameters, initial pesticide concentration in soil profile, application time and amount, as well as crop data. The pesticide input file (see appendix C) is stored in ASCII format as other input files in *Expert-N*. The file contains several blocks and sections. Each section has an identification code. The data items in each section are separated by one or more space characters.

To limit the size of the pesticide output file the user can choose the desired output variables in an additional file where each possible variable is specified by an identification code (appendix D). During simulation, *Expert-N* generates various output files. The selected pesticide output variables are read out in the pesticide output file (appendix E).

6 Conclusions

Biodegradation batch experiments showed that the variability in glyphosate degradation was linked to the variability in soil microbial biomass, as a clear positive correlation between measured microbial biomass and degradation of glyphosate in different soils was observed. After repeated applications of glyphosate in laboratory batch experiments no adaptation or inhibition of the degrading microbial community could be noticed. This indicates and also the high correlation of degradation and microbial biomass that a great amount of microbial communities in soil is responsible for glyphosate mineralization and not only a small community of highly specialized species. Glyphosate shows a relatively rapid degradation in soil and high adsorption to soil matrix. The recovery of glyphosate in the biodegradation experiments was lower than expected and further research to explain this discrepancy in mass balance is necessary. Pesticide fate models are highly sensitive to parameters controlling biodegradation and sorption. The conducted laboratory experiments were useful to generate appropriate input values in dependence on environmental conditions for the subsequent fate modelling of glyphosate.

Water flow in soil was investigated under various crops for data of undisturbed lysimeter monoliths filled with four different soil types. It was shown that depending on potential evapotranspiration model choice the simulated percolation amounts vary between 52 % and 126 % of the measured amounts. Compared to this, the influence of the parameterisation of the soil hydraulic characteristics is small with a variation of only up to 5 % of the measured outflow. The annual outflow was not very sensitive to the applied soil hydraulic characteristics, however percolation dynamics were highly sensitive. The results indicate that both reference-surface (Penman, Penman-Monteith grass reference) and surface-dependent (Penman-Monteith dual crop coefficient, Haude) potential evapotranspiration calculation methods overestimate the measured cumulative actual evapotranspiration in the present study. The measured percolation amounts in the lysimeters could be simulated more correctly, if a modified Haude approach of simple efficiency was followed in a pragmatic way. The results showed

- that the presented modelling concept is adequate for the discrimination between different evapotranspiration models on the basis of water balance and percolation studies,
- but that for the evaluation of daily evapotranspiration fluxes direct evapotranspiration measurements must be used.

In the simulation of daily evapotranspiration fluxes the physically based Penman-Monteith approach shows much higher correlations with measurements than the empirical Haude approach. However, appropriate sampling of the climatic input variables is essential for the exploitation of the precision of the Penman-Monteith approach.

Based on the simulation results and model analysis research demands were identified related to the question to what extent the water balance situation in lysimeters differs from real field conditions as follows:

- A detailed analysis of evaporation from bare soil under lysimeter conditions should be subject of further studies.
- Plant-growth under lysimeter conditions and the possibility of different microclimatic effects compared to large fields must be investigated in more detail.

It must be pointed out that evapotranspiration is still the most crucial process to evaluate in water-balance modelling even if meteorological data are available in detailed temporal and spatial resolution. Appropriate choice of a potential evapotranspiration model is an essential part of simulations concerning environmental behaviour of pesticides.

Glyphosate transport and behaviour in the presence of genetically modified soybean was studied in four re-packed lysimeter cores filled with the same soil type. A modelling system for the description of solute transport and pesticide behaviour was successfully implemented in the modular modelling system *Expert-N*. The present study demonstrated that field lysimeters are an appropriate environment to evaluate the fate of pesticides in a closed system under natural conditions. They can reproduce real field conditions under the restriction of the observed problems like microclimatic effects and disturbing effects of measurements.

The differentiation between a deterministic parameter selection and a probabilistic distribution of model input parameters was useful to show sources of uncertainty in model output. The choice of different deterministic modelling approaches for water flow, as well as for degradation and sorption modules has a strong effect on the simulation results. A probability distribution of model input parameters describing sorption, dispersivity and degradation in a deterministic model resulted also in a considerable variability in model output. The results suggest that the incorporation of variability in model input helps to improve the simulation of the variability in glyphosate movement in the soil profile, but it should be noted that the range and distribution of model output strongly depends on the assignment of plausible ranges and distributions to each of the input parameters.

The risk assessment study concerning the GR soybean system and the mathematical modelling results indicate that due to the high sorption of glyphosate to the soil matrix and the high microbial capacities for glyphosate degradation in the lysimeter soil, leaching risk can be considered to be low, but cannot be excluded entirely. Preferential flow or co-transport of glyphosate with dissolved organic matter or colloids was not observed.

Neither a significant acceleration (adaptation) nor a deceleration (inhibition) of the degradation process by microorganisms was observable after repeated herbicide applications in field. The introduction of more conceptual descriptions of microbial response to pesticide and nutrient additions can contribute to a reduction in the uncertainty of pesticide degradation modelling. As a result the mathematical simulation confirms the observed behaviour of the degrading microbial community and that mainly co-metabolic glyphosate degradation in soil occurs, even though this approach was more difficult to parameterise. In the field study biodegradation was mainly influenced by soil humidity. The humidity dependence of degradation could be achieved in the modelling approach very well, but the selection of the humidity response function for microbial growth and the parameterisation of the hydraulic characteristics had a strong effect on the simulation results.

Measured and simulated results showed that after a fast uptake of the herbicide by plant leaves, glyphosate was translocated rapidly from the site of application. Both, simulation results of plant biomass and glyphosate concentration were in good accordance with the measurements. Metabolisation of glyphosate by GR soybeans was not observable, thus, the possibility of herbicide accumulation in the plants exists. Mathematical modelling was a useful tool for the evaluation of herbicide application time and resulting glyphosate concentration in single plant tissues. The simulation results indicate that glyphosate concentrations in beans of GR soybean can exceed recommended guideline values under commonly used herbicide treatments. Therefore, the aspect of a possible decrease of nutritional quality of GR soybeans should be a subject of further experimental studies as supported by the simulation results. Additionally, the measured and simulated accumulation of glyphosate in soybean nodules favours the selection pressure given for the glyphosate sensitive bacteria in the rhizosphere.

Finally, the results showed that the implemented modelling system for description and assessment of pesticide behaviour in various soils and plants was able to describe environmental behaviour of glyphosate and to be a useful tool for risk assessment of GR soybean.

7 Summary

The use of genetically modified plants has become an integral part of modern agriculture. The purpose of this research work was to assess and describe by mathematical modelling the environmental fate of the herbicide glyphosate in the presence of genetically modified soybean. Therefore, in the modular modelling system *Expert-N* a new submodel for the simulation of solute transport and pesticide behaviour was implemented. The glyphosate resistant (GR) soybean system was chosen for the study “Effects of transgenic, glyphosate tolerant soybean in combination with the herbicide glyphosate on the soil ecosystem – A risk assessment study using lysimeters” of the GSF - National Research Centre for Environment and Health, due to the rapid adoption rate of the GR soybean system worldwide. The present work was an integral part of this study, where the effects of a modified agricultural practice associated with the cultivation of herbicide-resistant crops were investigated. The cultivation of herbicide-resistant, genetically modified plants can result in a repeated annual and perennial application of the non-selective, systemic herbicide glyphosate that controls a wide range of weeds, as the herbicide can be also applied post-emergence. The potential increase of glyphosate applications includes several risks such as an increased loading of the leachate with herbicide residues. As a consequence of herbicide accumulation in the upper soil horizon an increased selection pressure on glyphosate sensitive microorganisms occurs. Thus, microbial transformation processes of the herbicide as well as microbial population dynamics may change. Additionally, there is no evidence of metabolic degradation of glyphosate in GR soybean, therefore glyphosate is transported to and accumulated in metabolic sinks given as nodules and beans.

Batch biodegradation and sorption experiments were necessary for the calibration of the mathematical model system and for parameterisation of model input parameters. In this context, degradation behaviour of glyphosate in five different agricultural soils under consideration of microbial community size was investigated. Afterwards, lysimeter water flow data of a five year period from four cropped undisturbed field lysimeters were evaluated, because precise environmental fate modelling of pesticides depends on a correctly simulated water flow in soil. Soil water flow strongly depends on available water amounts, thus the influence of water retention characteristics on water balance simulations was studied together with the influence of evapotranspiration models. After uncertainties in water balance simulations were evaluated on undisturbed lysimeter monoliths, data from four re-packed field lysimeter cores filled with the same soil type were used to study the environmental

behaviour of the herbicide glyphosate. The lysimeters were cropped with transgenic soybean over two years to analyse the interaction of the factors water flow, solute transport, plant and microbial growth.

The modelling of pesticide behaviour in the soil-plant system was based on the pesticide transport model LEACHP (Hutson and Wagenet, 1992) and the pesticide plant uptake model PLANTX of Trapp (1992). The implementation of these modules in *Expert-N* was realized using the concept of dynamic link libraries (DLLs) of the *Microsoft C* programming environment (*Visual Studio .NET 2003*®).

The results indicate that the variability in glyphosate degradation was linked to the variability in soil microbial biomass, as a clear positive correlation between measured microbial biomass and degradation of glyphosate in the laboratory batch experiments was observed. Pesticide fate models are highly sensitive to parameters controlling biodegradation and sorption. The conducted laboratory experiments were useful to generate appropriate input values in dependence on environmental conditions for the subsequent fate modelling of glyphosate.

Water flow studies in the four different lysimeter monoliths under various crops show that depending on potential evapotranspiration model choice the simulated percolation amounts vary between 52 % and 126 % of the measured amounts. Compared to this, the influence of the parameterisation of the soil hydraulic characteristics is small with a variation of only up to 5 % of the measured outflow. The annual outflow was not very sensitive to the applied soil hydraulic characteristics, however percolation dynamics were highly sensitive. Percolation studies were an adequate concept for the discrimination between different evapotranspiration models on the basis of water balance studies. For the evaluation of daily evapotranspiration fluxes direct evapotranspiration measurements must be used. It must be pointed out that evapotranspiration is still the most crucial process to evaluate in water-balance modelling, even if meteorological data are available in detailed temporal and spatial resolution. Appropriate choice of a potential evapotranspiration model is an essential part of simulations concerning environmental behaviour of pesticides.

Glyphosate transport measurements in the risk assessment study and the mathematical modelling results indicate that due to the high sorption of glyphosate to the soil matrix and the high microbial capacities for glyphosate degradation in the lysimeter soil, leaching risk can be considered to be low, but cannot be excluded entirely. Neither a significant acceleration (adaptation) nor a deceleration (inhibition) of the degradation process by microorganisms was observable after repeated herbicide applications in the field lysimeters. This behaviour of the degrading microbial community was also confirmed by the modelling results. The

introduction of more conceptual descriptions of microbial response to pesticide and nutrient additions can contribute to a reduction in the uncertainty of pesticide degradation modelling. Because no metabolisation of glyphosate by GR soybeans was observable, the possibility of herbicide accumulation in the plants exists. The simulation results indicate that glyphosate concentrations in beans of GR soybean can exceed recommended guideline values under commonly used herbicide treatments. Therefore, the aspect of a possible decrease of nutritional quality of GR soybeans should be a subject of further experimental studies. Additionally, the measured and simulated accumulation of glyphosate in soybean nodules favours the selection pressure given for the glyphosate sensitive bacteria in the rhizosphere. Finally, the results showed that the implemented modelling system for description and assessment of pesticide behaviour in various soils and plants was able to describe environmental behaviour of glyphosate and to be a useful tool for risk assessment of GR soybean.

References

- Acutis, M. and Donatelli, M., 2003. *SOILPAR 2.00*: software to estimate soil hydrological parameters and functions. *European Journal of Agronomy*, 18: 373-377.
- Allen, R.G., 2000. Using the FAO-56 dual crop coefficient method over an irrigated region as part of an evapotranspiration intercomparison study. *Journal of Hydrology*, 229: 27-41.
- Allen, R.G., Pereira, L.S., Raes, D. and Smith, M., 1998. Crop evapotranspiration: Guidelines for computing crop requirements. Irrigation and Drainage Paper No. 56, FAO, Rome, Italy.
- Battaglin, W.A., Kolpin, D.W., Scribner, E.A., Kuivila, K.M. and Sandstrom, M.W., 2005. Glyphosate, Other herbicides, and Transformation Products in Midwestern Streams, 2002. *Journal of the American Water Resources Association*, 41: 323-332.
- Bause, M. and Merz, W., 2005. Higher order regularity and approximation of solutions to the Monod biodegradation model. *Applied Numerical Mathematics*, 55: 154-172.
- Becker, M.W. and Coplen, T.B., 2001. Technical Note: Use of deuterated water as a conservative artificial groundwater tracer. *Hydrogeology Journal*, 9: 512-516.
- Benbrook, C., 2001. Do GM Crops Mean Less Pesticide Use? Northwest Science and Environmental Policy Center at Sandpoint (Idaho, USA), <http://www.mindfully.org/Pesticide/More-GMOs-Less-Pesticide.htm>.
- Bergström, L., 1990. Use of Lysimeters to Estimate Leaching of Pesticides in Agricultural Soils. *Environmental Pollution*, 67: 325-347.
- Beulke, S., Brown, C.D., Dubus, I.G., Fryer, C.J. and Walker, A., 2004a. Evaluation of probabilistic modelling approaches against data on leaching of isoproturon through undisturbed lysimeters. *Ecological Modelling*, 179: 131-144.
- Beulke, S., Brown, C.D., Fryer, C.J. and van Beinum, W., 2004b. Influence of kinetic sorption and diffusion on pesticide movement through aggregated soils. *Chemosphere*, 57: 481-490.
- Blagodatsky, S.A. and Richter, O., 1998. Microbial growth in soil and nitrogen turnover: a theoretical model considering the activity state of microorganisms. *Soil Biology & Biochemistry*, 30: 1743-1755.
- Boivin, A., Cherrier, R. and Schiavon, M., 2005. A comparison of five pesticides adsorption and desorption processes in thirteen contrasting field soils. *Chemosphere*, 61: 668-676.
- Bormann, H., Diekkrüger, B. and Richter, O., 1996. Effects of data availability on estimation of evapotranspiration. *Physics and Chemistry of The Earth*, 21: 171-175.
- Bosma, T.N.P., Middeldorp, P.J.M., Schraa, G. and Zehnder, A.J.B., 1997. Mass Transfer Limitation of Biotransformation: Quantifying Bioavailability. *Environmental Science & Technology*, 31: 248-252.

- Bruno, H. and Schaper, S., 2002. Review Report Glyphosate: Legal Regulations of the European Union for Plant Protection Products and their Active Substances. Volume D 26, Federal Biological Research Centre for Agriculture and Forestry Braunschweig.
- Brutsaert, W., 1966. Probability laws for pore size distributions. *Soil Science*, 101: 85-92.
- Burdine, N.T., 1953. Relative permeability calculations from pore-size distribution data. *Trans AIME*, 198: 71-77.
- Campbell, G.S., 1985. *Soil Physics with BASIC, Transport Models for Soil-Plant Systems*. Developments in Soil Science, 14. Elsevier, Amsterdam
- Chiou, C.T., Sheng, G. and Manes, M., 2001. A Partition-Limited Model for the Plant Uptake of Organic Contaminants from Soil and Water. *Environmental Science & Technology*, 35: 1437-1444.
- Cornelis, W.M., Ronsyn, J., Van Meirvenne, M. and Hartmann, R., 2001. Evaluation of Pedotransfer Functions for Predicting the Soil Moisture Retention Curve. *Soil Science Society of America Journal*, 65: 638-648.
- Corwin, D.L., 2000. Evaluation of a simple lysimeter-design modification to minimize sidewall flow. *Journal of Contaminant Hydrology*, 42: 35-49.
- Council of the European Union, 1997. Proposal for a council directive establishing annexe VI to directive 91/414/EEC concerning the placing of the plant protection products on the market. *Official Journal of the European Communities C 240*, pp. 1-23.
- de Jonge, H., de Jonge, L.W. and Jacobsen, O.H., 2000. [¹⁴C]Glyphosate transport in undisturbed topsoil columns. *Pesticide Management Science*, 56: 909-915.
- DFG Senate commission, 2001. Threshold values for products from genetically modified plants: statement by the DFG Senate Commission for the assessment of chemicals used in agriculture. http://www.dfg.de/aktuelles_presse/reden_stellungnahmen/download/gvo_031201_e.pdf [October, 2006].
- Di, H.J. and Aylmore, L.A.G., 1997. Modeling the Probabilities of Groundwater Contamination by Pesticides. *Soil Science Society of America Journal*, 61: 17-23.
- Diekkrüger, B., Söndgerath, D., Kersebaum, K.C. and McVoy, C.W., 1995. Validity of agroecosystem models a comparison of results of different models applied to the same data set. *Ecological Modelling*, 81: 3-29.
- Dörfler, U., Cao, G., Grundmann, S. and Schroll, R., 2006. Influence of a heavy rainfall event on the leaching of [¹⁴C]isoproturon and its degradation products in outdoor lysimeters. *Environmental Pollution*, 144: 695-702.
- Dörfler, U., Haala, R., Matthies, M. and Scheunert, I., 1996. Mineralization Kinetics of Chemicals in Soils in Relation to Environmental Conditions. *Ecotoxicology and Environmental Safety*, 34: 216-222.
- Droogers, P., 2000. Estimating actual evapotranspiration using a detailed agro-hydrological model. *Journal of Hydrology*, 229: 50-58.

- Dubus, I.G., Brown, C.D. and Beulke, S., 2003. Sources of uncertainty in pesticide fate modelling. *The Science of the Total Environment*, 317: 53-72.
- Duke, S.O., 1988. Glyphosate. In: P.C. Kearney and D.D. Kaufman (Editors), *Herbicides: Chemistry, degradation, and mode of action*. Marcel Dekker, New York, pp. 1-70.
- Duke, S.O., Rimando, A.M., Pace, P.F., Reddy, K.N. and Smeda, R.J., 2003. Isoflavone, Glyphosate, and Aminomethylphosphonic Acid Levels in Seeds of Glyphosate-Treated, Glyphosate-Resistant Soybean. *Journal of Agricultural Food Chemistry*, 51: 340-344.
- Dust, M., Baran, N., Errera, G., Hutson, J.L., Mouvet, C., Schäfer, H., Verreken, H. and Walker, A., 2000. Simulation of water and solute transport in field soils with the LEACHP model. *Agricultural Water Management*, 44: 225-245.
- Eitzinger, J., Trnka, M., Hösch, J., Zalud, Z. and Dubrovský, M., 2004. Comparison of CERES, WOFOST and SWAP models in simulating soil water content during growing season under different soil conditions. *Ecological Modelling*, 171: 223-246.
- Elmore, R.W., Roeth, F.W., Nelson, L.A., Shapiro, C.A., Klein, R.N., Knezevic, S.Z. and Martin, A., 2001. Glyphosate-Resistant Soybean Cultivar Yields Compared with Sister Lines. *Agronomy Journal*, 93: 408-412.
- Engel, T. and Priesack, E., 1993. Expert-N, a building block system of nitrogen models as resource for advice, research, water management and policy. In: H.J.P. Eijsackers and T. Hamers (Editors), *Integrated Soil and Sediment Research: A Basis for Proper Protection*. Kluwer Academic Publishers, Dordrecht, Netherlands, pp. 503-507.
- Ersahin, S., Papendick, R.I., Smith, J.L., Keller, C.K. and Manoranjan, V.S., 2002. Macropore transport of bromide as influenced by soil structure differences. *Geoderma*, 108: 207-223.
- Evett, S.R., Howell, T.A., Steiner, J.L. and Cresap, J.L., 1993. Evapotranspiration by soil water balance using TDR and neutron scattering. In: R.G. Allen and C.M.U. Neale (Editors), *Management of Irrigation and Drainage Systems, Integrated Perspectives. Proceedings of the National Conference on Irrigation and Drainage Engineering*, Park City, UT, pp. 914-921.
- Fisher, J.B., DeBiase, T.A., Qi, Y., Xu, M. and Goldstein, A.H., 2005. Evapotranspiration models compared on a Sierra Nevada forest ecosystem. *Environmental Modelling & Software*, 20: 783-796.
- Flury, M., 1996. Experimental Evidence of Transport of Pesticides through Field Soils - A Review. *Journal of Environmental Quality*, 25: 25-45.
- Flury, M., Yates, M.V. and Jury, W.A., 1999. Numerical Analysis of the Effect of the Lower Boundary Condition on Solute Transport in Lysimeters. *Soil Science Society of America Journal*, 63: 1493-1499.
- FOCUS, 2000. FOCUS groundwater scenarios in the EU review of active substances. Report of the FOCUS Groundwater Scenarios Workgroup, EC Document Reference Sanco/321/2000 rev.2, pp. 202.

- Forlani, G., Mangiagalli, A., Nielsen, E. and Suardi, C.M., 1999. Degradation of the phosphonate herbicide glyphosate in soil: evidence for a possible involvement of unculturable microorganism. *Soil Biology & Biochemistry*, 31: 991-997.
- Franz, J.E., Mao, M.K. and Sikorski, J.A., 1997. *Glyphosate: A Unique Global Herbicide*, ACS Monograph 189. American Chemical Society, Washington DC
- Fresco, L.O., 2001. *Genetically Modified Organisms in Food and Agriculture*, Conference of Crop and Forest Biotechnology for the Future. Royal Swedish Academy of Agriculture and Forestry, Falkenberg, Sweden.
- Gårdenäs, A.I., Šimůnek, J., Jarvis, N. and van Genuchten, M.T., 2006. Two-dimensional modelling of preferential water flow and pesticide transport from a tile-drained field. *Journal of Hydrology*, 329: 647-660.
- Gardner, W.R., 1958. Some steady state solutions of the unsaturated moisture flow equation with application to evaporation from a water table. *Soil Science*, 85: 228-232.
- Geiger, D., R., Shieh, W.-J. and Fuchs, M.A., 1999. Causes of Self-Limited Translocation of Glyphosate in *Beta vulgaris* Plants. *Pesticide Biochemistry and Physiology*, 64: 124-133.
- Gerke, H.H. and van Genuchten, M.T., 1996. Macroscopic representation of structural geometry for simulating water and solute movement in dual-porosity media. *Advances in Water Resources*, 19: 343-357.
- Givi, J., Prasher, S.O. and Patel, R.M., 2004. Evaluation of pedotransfer functions in predicting the soil water contents at field capacity and wilting point. *Agricultural Water Management*, 70: 83-96.
- Glass, R.L., 1987. Adsorption of Glyphosate by Soils and Clay Minerals. *Journal of Agricultural and Food Chemistry*, 35: 497-500.
- Guo, L., Jury, W.A., Wagenet, R.J. and Flury, M., 2000. Dependence of pesticide degradation on sorption: nonequilibrium model and application to soil reactors. *Journal of Contaminant Hydrology*, 43: 45-62.
- Haude, W., 1955. Zur Bestimmung der Verdunstung auf möglichst einfache Weise. *Mitteilungen Deutscher Wetterdienst*, 11: 1-24.
- Herbst, M., Fialkiewicz, W., Chen, T., Pütz, T., Thiéry, D., Mouvet, C., Vachaud, G. and Vereecken, H., 2005. Intercomparison of Flow and Transport Models Applied to Vertical Drainage in Cropped Lysimeters. *Vadose Zone Journal*, 4: 240-254.
- Hupet, F., Lambot, S., Javaux, M. and Vanclooster, M., 2002. On the identification of macroscopic root water uptake parameters from soil water content observations. *Water resources research*, 38: doi:10.1029/2002WR001556.
- Hupet, F. and Vanclooster, M., 2001. Effect of the sampling frequency of meteorological variables on the estimation of the reference evapotranspiration. *Journal of Hydrology*, 243: 192-204.

- Hutson, J.L. and Cass, A., 1987. A retentivity function for use in soil-water simulation models. *Journal of Soil Science*, 38: 105-113.
- Hutson, J.L. and Wagenet, R.J., 1992. LEACHM: Leaching Estimation And Chemistry Model. Research Series No. 92-93, Version 3. Department of Soil, Crop and Atmospheric Sciences, Research Series No. 92-93, Ithaca USA
- Jacob, G.S., Garbow, J.R., Hallas, L., Kimack, N.M., Kishore, G.M. and Schaefer, J., 1988. Metabolism of Glyphosate in *Pseudomonas* sp. Strain LBr. *Applied and Environmental Microbiology*, 54: 2953-2958.
- James, C., 2005. Global Status of Commercialized Biotech/GM Crops: 2005. ISAAA International Service for the Acquisition of Agri-Biotech Applications, ISAAA Briefs, 34, pp. 1-11.
- Janssen, P.H.M., Heuberger, P.S.C. and Sanders, R., 1994. UNCSAM: a tool for automating sensitivity and uncertainty analysis. *Environmental Software*, 9: 1-11.
- Jarvis, N.J., Hollis, J.M., Nicholls, P.H., Mayr, T. and Evans, S.P., 1997. MACRO—DB: a decision-support tool for assessing pesticide fate and mobility in soils. *Environmental Modelling & Software*, 12: 251-265.
- Jarvis, N.J., Zavattaro, L., Rajkai, K., Reynolds, W.D., Olsen, P.-A., McGechan, M., Mecke, M., Mohanty, B., Leeds-Harrison, P.B. and Jacques, D., 2002. Indirect estimation of near-saturated hydraulic conductivity from readily available soil information. *Geoderma*, 108: 1-17.
- Johnsson, H., Bergström, L., Jansson, P.E. and Paustian, K., 1987. Simulated nitrogen dynamics and losses in a layered agricultural soil. *Agriculture, Ecosystems & Environment*, 18: 333-356.
- Jones, C.A. and Kiniry, J.R. (Editors), 1986. CERES-Maize. A Simulation Model of Maize Growth and Development. Texas A&M University Press, Temple, TX, USA.
- Jury, W.A., Focht, D.D. and Farmer, W.J., 1987. Evaluation of Pesticide Groundwater Pollution Potential from Standard Indices of Soil-Chemical Adsorption and Biodegradation. *Journal of Environmental Quality*, 16: 422-428.
- Kemper, W.D. and Van Schaik, J.C., 1966. Diffusion in salts in clay-water systems. *Soil Sci. Soc. Amer. Proc.*: 534-540.
- Klein, M., Hosang, J., Schäfer, H., Erzgräber, B. and Ressler, H., 2000. Comparing and evaluating pesticide leaching models - Results of simulations with PELMO. *Agricultural Water Management*, 44: 263-281.
- Köhne, J.M., Köhne, S. and Šimůnek, J., 2006. Multi-process herbicide transport in structured soil columns: Experiments and model analysis. *Journal of Hydrology*, 85: 1-32.
- Kühn, S., 2004. Bedeutung der Leistung mikrobieller Lebensgemeinschaften beim Umsatz und Abbau von Isoproturon in Böden und Möglichkeiten zur Steuerung des in-situ-Pestizidabbaus, Dissertation Technische Universität München, 171 pp.

- Larsson, M.H. and Jarvis, N.J., 1999. Evaluation of a dual-porosity model to predict field-scale solute transport in a macroporous soil. *Journal of Hydrology*, 215: 153-171.
- Liu, C.M., McLean, P.A., Sookdeo, C.C. and Cannon, F.C., 1991. Degradation of the Herbicide Glyphosate by Members of the Family Rhizobiaceae. *Applied and Environmental Microbiology*, 57: 1799-1804.
- Liu, S., Graham, W.D. and Jacobs, J.M., 2005. Daily potential evapotranspiration and diurnal climate forcings: influence on the numerical modelling of soil water dynamics and evapotranspiration. *Journal of Hydrology*, 309: 39-52.
- Loague, K. and Green, R.E., 1991. Statistical and graphical methods for evaluating solute transport models: Overview and application. *Journal of Contaminant Hydrology*, 7: 51-73.
- Loos, C., Gayler, S. and Priesack, E., 2007. Assessment of water balance simulations for large-scale weighing lysimeters. *Journal of Hydrology*, 335: 259-270.
- Loos, C., Seppelt, R., Meier-Bethke, S., Schiemann, J. and Richter, O., 2003. Spatially explicit modelling of transgenic maize pollen dispersal and cross-pollination. *Journal of Theoretical Biology*, 225: 241-255.
- Lorraine-Colwill, D.F., Powles, S.B., Hawkes, T.R., Hollinshead, P.H., Warner, S.A.J. and Preston, C., 2003. Investigations into the mechanism of glyphosate resistance in *Lolium rigidum*. *Pesticide Biochemistry and Physiology*, 74: 62-72.
- Ma, K., 2003. Simulation des Pestizidverhaltens im System Boden-Pflanze-Atmosphäre, Dissertation Universität Göttingen, 118 pp.
- Miles, C.J. and Moye, H.A., 1988. Extraction of Glyphosate Herbicide from Soil and Clay Minerals and Determination of Residues in Soils. *Journal of Agricultural and Food Chemistry*, 36: 486-491.
- Monsanto, 2005. Formaldehyde is not a major degradate of glyphosate in the environment. Monsanto Company, St. Louis, USA;
http://www.monsanto.com/monsanto/content/products/productivity/roundup/gly_formald_bkg.pdf.
- Musters, P.A.D., Bouten, W. and Verstraten, J.M., 2000. Potentials and limitations of modelling vertical distributions of root water uptake of an Austrian pine forest on a sandy soil. *Hydrological Processes*, 14: 103-115.
- National Agricultural Statistics Service, 2006. Acreage [online]. Agric. Stat. Board, NASS, USDA, U.S. Gov. Print. Office, Washington, DC.
- Neff, J.C. and Asner, G.P., 2001. Dissolved Organic Carbon in Terrestrial Ecosystems: Synthesis and a Model. *Ecosystems*, 4: 29-48.
- Nehring, K., 1960. Agrikulturchemische Untersuchungsmethoden für Dünge- und Futtermittel, Böden und Milch. Verlag Paul Parey, Hamburg-Berlin
- Nielsen, K.M. and Townsend, J.P., 2004. Monitoring and modeling horizontal gene transfer. *Nature Biotechnology*, 22: 1110-1114.

- OECD, 1981. OECD-Guideline for testing chemicals (106): "Adsorption/Desorption", Organisation for Economic Cooperation and Development, Paris.
- Oliver, Y.M. and Smettem, K.R.J., 2005. Predicting water balance in a sandy soil: model sensitivity to the variability of measured saturated and near saturated hydraulic properties. *Australian Journal of Soil Research*, 43: 87-96.
- Penaloza-Vazquez, A., Mena, G.L., Herrera-Estrella, L. and Bailey, A.M., 1995. Cloning and Sequencing of the Genes Involved in Glyphosate Utilization by *Pseudomonas pseudomallei*. *Applied and Environmental Microbiology*, 61: 538-543.
- Penman, H.L., 1948. Natural evaporation from open water. *Proceedings of the Royal Meteorological Society A*, 193: 120-145.
- Penning de Vries, F.W.T., Jansen, D.M., ten Berge, H.F.M. and Bakema, A., 1989. Simulation of ecophysiological processes of growth in several annual crops. Centre for Agricultural Publishing and Documentation, Wageningen, the Netherlands, 271 pp.
- Piccolo, A., Celano, G. and Conte, P., 1996. Adsorption of Glyphosate by Humic Substances. *Journal of Agricultural and Food Chemistry*, 44: 2442-2446.
- Pline, W.A., Wu, J. and Hatzios, K.K., 1999. Effects of Temperature and Chemical Additives on the Response of Transgenic Herbicide-Resistant Soybeans to Glufosinate and Glyphosate Applications. *Pesticide Biochemistry and Physiology*, 65: 119-131.
- Popp, C., Burghardt, M., Friedmann, A. and Riederer, M., 2005. Characterization of hydrophilic and lipophilic pathways of *Hedera helix* L. cuticular membranes: permeation of water and uncharged organic compounds. *Journal of Experimental Botany*, 56: 2797-2806.
- Priesack, E., 1991. Analytical Solution of Solute Diffusion and Biodegradation in Spherical Aggregates. *Soil Science Society of America Journal*, 55: 1227-1230.
- Priesack, E., 2006. Expert-N: Dokumentation der Modell Bibliothek. FAM-Bericht 60. Hieronymus, München, 308 pp.
- Priesack, E., Achatz, S. and Stenger, R., 2001. Parameterisation of soil nitrogen transport models by use of laboratory and field data. In: M.J. Shaffer, L. MaandS. Hansen (Editors), *Modelling carbon and nitrogen dynamics for soil management*. CRC Press, Boca Raton, USA, pp. 461-484.
- Priesack, E. and Kisser-Priesack, G.M., 1993. Modelling diffusion and microbial uptake of ¹³C-glucose in soil aggregates. *Geoderma*, 56: 561-573.
- Rana, G. and Katerji, N., 2000. Measurement and estimation of actual evapotranspiration in the field under Mediterranean climate: a review. *European Journal of Agronomy*, 13: 125-153.
- Ray, C., Vogel, T. and Dusek, J., 2004. Modeling depth-variant and domain-specific sorption and biodegradation in dual-permeability media. *Journal of Contaminant Hydrology*, 70: 63-87.

- Raymer, P.L. and Grey, T.L., 2003. Challenges in Comparing Transgenic and Nontransgenic Soybean Cultivars. *Crop Science*, 43: 1584-1589.
- Remson, I., Hornberger, G.M. and Molz, F.J., 1971. *Numerical Methods in Subsurface Hydrology with an introduction to the finite element method*. John Wiley & Sons, New York
- Richter, O., Diekkrüger, B. and Nörtersheuser, P., 1996. *Environmental Fate Modelling of Pesticides*. VCH Verlagsgesellschaft mbH, Weinheim
- Ritchie, J.T., 1991. Wheat phasic development. In: J. Hanks and J.T. Ritchie (Editors), *Modelling plant and soil systems*. Agronomy Monograph 31, ASA-CSSA-SSSA, Madison, WI, USA, pp. 31-54.
- Rueppel, M.L., Brightwell, B.B., Schaefer, J. and Marvel, J.T., 1977. Metabolism and Degradation of Glyphosate in Soil and Water. *Journal of Agricultural and Food Chemistry*, 25: 517-528.
- Ruser, R., Flessa, H., Russow, R., Schmidt, G., Buegger, F. and Munch, J.C., 2006. Emission of N₂O, N₂ and CO₂ from soil fertilized with nitrate: effect of compaction, soil moisture and rewetting. *Soil Biology & Biochemistry*, 38: 263-274.
- Ruth, B. and Munch, J.C., 2005. Field measurements of the water content in the top soil using a new capacitance sensor with a flat sensitive volume. *Journal of Plant Nutrition and Soil Science*, 168: 169-175.
- Sachs, L., 1984. *Angewandte Statistik*. Springer-Verlag, Berlin
- Satchivi, N.M., Stoller, E.W., Wax, L.M. and Briskin, D.P., 2000. A Nonlinear Dynamic Simulation Model for Xenobiotic Transport and Whole Plant Allocation Following Foliar Application I. Conceptual Foundation for Model Development. *Pesticide Biochemistry and Physiology*, 68: 67-84.
- Sau, F., Boote, K.J., Bostick, W.M., Jones, J.W. and Minguetz, M.I., 2004. Testing and improving evapotranspiration and soil water balance of the DSSAT crop models. *Agronomy Journal*, 96: 1243-1257.
- Scheinost, A.C., Sinowski, W. and Auerswald, K., 1997. Regionalization of soil water retention curves in a highly variable soilscape, I. Developing a new pedotransfer function. *Geoderma*, 78: 129-143.
- Schierholz, I., Schäfer, H. and Kollé, H., 2000. The Weiherbach data set: An experimental data set for pesticide model testing on the field scale. *Agricultural Water Management*, 44: 43-61.
- Schönherr, J., 2002. A mechanistic analysis of penetration of glyphosate salts across stomatous cuticular membranes. *Pest Management Science*, 58: 343-351.
- Schönherr, J. and Riederer, M., 1989. Foliar penetration and accumulation of organic chemicals in plant cuticles. *Reviews of Environmental Contamination and Toxicology*, 108: 1-70.

- Schröder, P., Huber, B., Olazabal, U., Kämmerer, A. and Munch, J.C., 2002. Land use and sustainability: FAM research network on agroecosystems. *Geoderma*, 105: 155-166.
- Schroll, R., Becher, H.H., Dörfler, U., Gayler, S., Grundmann, S., Hartmann, H.P. and Ruoss, J., 2006. Quantifying the Effect of Soil Moisture on the Aerobic Microbial Mineralization of Selected Pesticides in Different Soils. *Environmental Science & Technology*, 40: 3305-3312.
- Schroll, R., Brahushi, F., Dörfler, U., Kühn, S., Fekete, J. and Munch, J.C., 2004. Biomineralisation of 1,2,4-trichlorobenzene in soils by an adapted microbial population. *Environmental Pollution*, 127: 395-401.
- Schroll, R. and Kühn, S., 2004. Test System To Establish Mass Balances for ¹⁴C-Labeled Substances in Soil-Plant-Atmosphere Systems under Field Conditions. *Environmental Science & Technology*, 38: 1537-1544.
- Schulla, J. and Jasper, K., 2000. Model Description WaSiM-ETH. Institute for Climate Research, ETH, Zürich, 166 pp.
- Scow, K.M. and Alexander, M., 1992. Effect of Diffusion on the Kinetics of Biodegradation: Experimental Results with Synthetic Aggregates. *Soil Science Society of America Journal*, 56: 128-134.
- Scow, K.M. and Hutson, J., 1992. Effect of Diffusion and Sorption on the Kinetics of Biodegradation: Theoretical Considerations. *Soil Science Society of America Journal*, 56: 119-127.
- Severinsen, M. and Jager, T., 1998. Modelling the influence of terrestrial vegetation on the environmental fate of xenobiotics. *Chemosphere*, 37: 41-62.
- Shirazi, M.A. and Boersma, L., 1984. A unifying quantitative analysis of soil texture. *Soil Science Society of America Journal*, 48: 142-147.
- Shirazi, M.A., Boersma, L. and Hart, J.W., 1988. A unifying quantitative analysis of soil texture: improvement of precision and extension of scale. *Soil Science Society of America Journal*, 52: 181-190.
- Simkins, S. and Alexander, M., 1984. Models for mineralization kinetics with the variables of substrate concentration and population density. *Applied and Environmental Microbiology*, 47: 1299-1306.
- Sims, D.A., Seemann, J.R. and Luo, Y., 1998. Elevated CO₂ concentration has independent effects on expansion rates and thickness of soybean leaves across light and nitrogen gradients. *Journal of Experimental Botany*, 49: 583-591.
- Simunek, J., Huang, K. and van Genuchten, M.T., 1998. The HYDRUS code for simulating the one-dimensional movement of water, heat and multiple solutes in variably-saturated media. Version 6.0. U.S. Salinity Laboratory, Riverside USA
- Simunek, J., Jarvis, N.J., van Genuchten, M.T. and Gärdenäs, A., 2003. Review and comparison of models for describing non-equilibrium and preferential flow and transport in the vadose zone. *Journal of Hydrology*, 272: 14-35.

- Sommers, L.E., Gilmour, C.M., Wildung, R.E. and Beck, S.M., 1978. The Effect of Water Potential on Decomposition Processes in Soils. In: J.F. Parr, W.R. Gardner and L.F. Elliott (Editors), Proceedings: Water Potential Relations in Soil Microbiology. Soil Science Society of America, Chicago, Illinois, USA, pp. 97-117.
- Soulas, G. and Lagacherie, B., 2001. Modelling of microbial degradation of pesticides in soils. *Biology and Fertility of Soils*, 33: 551-557.
- Sparling, G.P., 1981. Microcalorimetry and other methods to assess biomass and activity in soil. *Soil Biology & Biochemistry*, 13: 93-98.
- Sparling, G.P., 1983. Estimation of microbial biomass and activity in soil using microcalorimetry. *European Journal of Soil Science*, 34: 381-390.
- Stenger, R., Priesack, E., Barkle, G. and Sperr, C., 1999. Expert-N. A tool for simulating nitrogen and carbon dynamics in the soil-plant-atmosphere system. In: M. Tomer, M. Robinson and G. Gielen (Editors), Modelling of Land Treatment Systems. NZ Land Treatment Collective Proceedings Technical Session 20, New Plymouth New Zealand, pp. 19-28.
- Stenrød, M., Charnay, M.-P., Benoit, P. and Eklo, O.M., 2006. Spatial variability of glyphosate mineralization and soil microbial characteristics in two Norwegian sandy loam soils as affected by surface topographical features. *Soil Biology & Biochemistry*, 38: 962-971.
- Sung, K., Kim, J., Munster, C.L., Corapcioglu, M.Y., Park, S., Drew, M.C. and Chang, Y.Y., 2006. A simple approach to modeling microbial biomass in the rhizosphere. *Ecological Modelling*, 190: 277-286.
- Thomasson, M.J. and Wierenga, P.J., 2003. Spatial variability of the effective retardation factor in an unsaturated field soil. *Journal of Hydrology*, 272: 213-225.
- Tillotson, W.R., Robbins, C.W., Wagenet, R.J. and Hanks, R.J., 1980. Soil water, solute, and plant growth simulation. Bulletin 502. Logan, UT.: Utah State Agr. Exp. Stn.
- Toride, N., Leij, F.J. and van Genuchten, M.T., 1995. The CXTFIT Code for Estimating Transport Parameters from Laboratory or Field Tracer Experiments, Version 2.0, Research Report No. 137, U. S. Salinity Laboratory, USDA, ARS, Riverside, CA.
- Trapp, S., 1992. Modellierung der Aufnahme anthropogener organischer Chemikalien in Pflanzen, Dissertation Technische Universität München, 135 pp.
- Trapp, S. and Matthies, M., 1996. Dynamik von Schadstoffen - Umweltmodellierung mit Chemos. Springer-Verlag, Berlin Heidelberg
- van Genuchten, M.T., 1980. A closed-form equation for predicting the hydraulic conductivity of unsaturated soils. *Soil Science Society of America Journal*, 44: 892-898.
- van Genuchten, M.T. and Alves, W.J., 1982. Analytical Solutions of the One-Dimensional Convective-Dispersive Solute Transport Equation. Technical Bulletin No. 1661. U.S. Department of Agriculture, 151 pp.

- van Genuchten, M.T., Davidson, J.M. and Wierenga, P.J., 1974. An Evaluation of Kinetic and Equilibrium Equations for the Prediction of Pesticide Movement Through Porous Media. *Proceedings of the Soil Science Society of America*, 38: 29-35.
- van Genuchten, M.T. and Wagenet, R.J., 1989. Two-site/two region models for pesticide transport and degradation: theoretical development and analytical solutions. *Soil Science Society of America Journal*, 53: 1303-1310.
- van Genuchten, M.T. and Wierenga, P.J., 1976. Mass transfer studies in sorbing porous media. 1. Analytical solutions. *Soil Science Society of America Journal*, 40: 473-480.
- van Laar, H.H., Goudriaan, J. and van Keulen, H., 1997. SUCROS97: Simulation of crop growth for potential and water-limited production situations 14, *Quantitative Approaches in System Analysis*. C.T. de Wit Graduate School for Production Ecology and Resource Conservation, Wageningen, the Netherlands.
- Vanclooster, M., Boesten, J.J.T.I., Trevisan, M., Brown, C.D., Capri, E., Eklo, O.M., Gottesbüren, B., Gouy, V. and van der Linden, A.M.A., 2000. A European test of pesticide-leaching models: methodology and major recommendations. *Agricultural Water Management*, 44: 1-19.
- Vanderborght, J., Kasteel, R., Herbst, M., Javaux, M., Thiéry, D., Vanclooster, M., Mouvet, C. and Vereecken, H., 2005. A Set of Analytical Benchmarks to Test Numerical Models of Flow and Transport in Soils. *Vadose Zone Journal*, 4: 206-221.
- VDI, 1993. Meteorologische Messungen. Agrarmeteorologische Meßstation mit rechnergestütztem Datenbetrieb - Richtlinie 3786 Blatt 13. In: K.R.d.L.i.V.u. DIN-Normenausschuss (Editor), *VDI/DIN-Handbuch Reinhaltung der Luft Band 1A - Maximale Immissions-Werte*. Beuth Verlag GmbH, Berlin.
- Vereecken, H., 2005. Mobility and leaching of glyphosate: a review. *Pesticide Management Science*, 61: 1139-1151.
- Vereecken, H., Maes, J. and Feyen, J., 1990. Estimating unsaturated hydraulic conductivity from easily measured soil properties. *Soil Science*, 149: 1-11.
- Vink, J.P.M., Gottesbüren, B., Diekkrüger, B. and van der Zee, S.E.A.T.M., 1997. Simulation and model comparison of unsaturated movement of pesticides from a large clay lysimeter. *Ecological Modelling*, 105: 113-127.
- von Götze, N. and Richter, O., 1999. Simulation of herbicide degradation in different soils by use of pedo-transfer functions (PTF) and non-linear kinetics. *Chemosphere*, 38: 1401-1407.
- von Wiren-Lehr, S., Komoßa, D., Gläßgen, W.E., Sandermann, H. and Scheunert, I., 1997. Mineralization of [¹⁴C]Glyphosate and its Plant-Associated Residues in Arable Soils Originating from Different Farming Systems. *Pesticide Science*, 51: 436-442.
- Wagner, T., Arango, L. and Ernst, D., 2006. The Probability of a Horizontal Gene Transfer from Roundup Ready Soybean to Microorganisms - A risk assessment Study on the GSF Lysimeter Station. In: J.C. Munch (Editor), *Conference on Lysimeters for Global Change Research: Biological Processes and the Environmental Fate of Pollutants*, Neuherberg, Germany.

- Wauchope, R.D., Yeh, S., Linders, J.B.H.J., Kloskowski, R., Tanaka, K., Rubin, B., Katayama, A., Kördel, W., Gerstl, Z., Lane, M. and Unsworth, J.B., 2002. Review - Pesticide soil sorption parameters: theory, measurement, uses, limitations and reliability. *Pesticide Management Science*, 58: 419-445.
- Willems, H.P.L., Lewis, K.J., Dyson, J.S. and Lewis, F.J., 1996. Mineralization of 2,4-D and atrazine in the unsaturated zone of a sandy loam soil. *Soil Biology & Biochemistry*, 28: 989-996.
- Zablotowicz, R.M. and Reddy, K.N., 2004. Impact of Glyphosate on the *Bradyrhizobium japonicum* Symbiosis with Glyphosate-Resistant Transgenic Soybean: A Minireview. *Journal of Environmental Quality*, 33: 825-831.
- Zenker, T., 2003. Verdunstungswiderstände und Gras-Referenzverdunstung, Technische Universität Berlin, 161 pp.
- Zhang, D., Beven, K. and Mermoud, A., 2006. A comparison of non-linear least square and GLUE for model calibration and uncertainty estimation for pesticide transport in soils. *Advances in Water Resources*, 29: 1924-1933.
- Zsolnay, A. and Steindl, H., 1991. Geovariability and biodegradability of the water-extractable organic material in an agricultural soil. *Soil Biology & Biochemistry*, 23: 1077-1082.
- Zurmühl, T., 1998. Capability of convection-dispersion transport models to predict transient water and solute movement in undisturbed soil columns. *Journal of Contaminant Hydrology*, 30: 101-128.

Appendix A – List of Symbols

A	(mm ⁻¹)	empirical parameter of the hydraulic conductivity function according to Gardner (1958)
a	(mm)	matric potential at the air entry value
B	(-)	empirical parameter of the hydraulic conductivity function according to Gardner (1958)
b	(-)	empirical parameter of the water retention function according to Hutson & Cass (1987)
$b_{l/o}$	(-)	correction exponent for difference between plant lipid material and octanol
b_w	(-)	form parameter describing humidity response of microbial growth
$b1$	(-)	form parameter Weibull humidity function
$b2$	(-)	form parameter Weibull humidity function
C	(mg dm ⁻³)	pesticide concentration
C	(mg kg ⁻¹)	pesticide concentration in various plant compartments differentiated by subscripts
C_{app}	(mg m ⁻²)	applied pesticide amount
C_{avail}	(mg m ⁻²)	available carbon amount
C_{CO_2}	(mg m ⁻²)	actual CO ₂ emission from the soil surface
C_{MB}	(mg-C dm ⁻³)	microbial biomass concentration
C_{MBmax}	(mg-C dm ⁻³)	maximum microbial biomass concentration
C_{MBmin}	(mg-C dm ⁻³)	minimum microbial biomass concentration
$C_{MB0}(z)$	(mg-C dm ⁻³)	initial distribution of microbial biomass concentration in dependence of depth
$C_{MB z(L)}$	(mg-C dm ⁻³)	initial biomass concentration in the surface zone
C_{bio-C}	(μg-C g ⁻¹ dry soil)	biomass-C concentration in measurements
C_l	(mg dm ⁻³)	pesticide concentration in soil solution
C_{l1}	(mg dm ⁻³)	liquid pesticide concentration in surface soil film
C_{lmax}	(mg dm ⁻³)	maximum concentration of the pesticide in solution
C_{org}	(mg-C dm ⁻³)	concentration of bioavailable organic carbon
C_s	(mg kg ⁻¹)	adsorbed pesticide concentration
C_{smax}	(mg kg ⁻¹)	adsorbed concentration prior to initiation of desorption
C_{s1}	(mg kg ⁻¹)	adsorbed concentration on the equilibrium sites
C_{s2}	(mg kg ⁻¹)	adsorbed concentration on the kinetic sites
C_{surf}	(mg dm ⁻³)	pesticide concentration on plant surface
C_t	(mg dm ⁻³)	total pesticide concentration
C_W	(mm ⁻¹)	water capacity
DR	(mm)	percolation amount
$D(\theta, q)$	(mm ² d ⁻¹)	effective diffusion coefficient in dependence of θ and q
D_{air}	(mm d ⁻¹)	effective diffusion coefficient in air film of surface-interface

Appendix A – List of Symbols

D_{eff}	(mm ² d ⁻¹)	diffusion coefficient for plant model (without dispersion)
$D_g(\varepsilon)$	(mm ² d ⁻¹)	diffusion coefficient in gaseous phase in dependence of gas filled soil porosity
$D_l(\theta)$	(mm ² d ⁻¹)	diffusion coefficient in liquid phase in dependence of soil water content
$D_m(q)$	(mm ² d ⁻¹)	mechanical dispersion coefficient in dependence of q
D_{soil}	(mm d ⁻¹)	effective diffusion in liquid film of surface-interface
D_0	(mm ² d ⁻¹)	molecular diffusion coefficient in water or in air
d_g	(mm)	geometric mean particle diameter
dx_{cut}	(mm)	thickness of cuticula barrier
dx_{film}	(mm)	thickness of solution film on plant leaves
E_H	(μ W g ⁻¹ dry soil)	heat production
ET_a	(mm)	actual evapotranspiration
ET_p^{day}	(mm d ⁻¹)	daily potential evapotranspiration
EV_p^{day}	(mm d ⁻¹)	daily potential evaporation
e_a	(hPa)	actual vapour pressure
$e_s(T)$	(hPa)	saturated vapour pressure as a function of temperature
$e(\theta)$	(-)	reduction function water
$e(T)$	(-)	reduction function temperature
f	(-)	fraction of equilibrium sites
f_{clay}	(-)	fraction of clay
f_{Corg}	(-)	fraction of organic carbon
f_{corr}	(mm)	correction factor dispersivity coefficient
f_e	(-)	effectivity constant of carbon utilization
f_{fract}	(-)	partitioning factor of assimilates
f_{Haude}	(mm d ⁻¹ hPa ⁻¹)	monthly, crop dependent factor
f_{sand}	(-)	fraction of sand
f_{silt}	(-)	fraction of silt
f_{sc}	(-)	soil cover fraction
$f(v)$	(mm d ⁻¹ hPa ⁻¹)	function describing dependency of evaporation on wind
G	(MJ m ⁻² d ⁻¹)	soil heat flux density
h	(mm)	matric potential
h_i	(mm)	matric potential at the inflexion point
J_{Cl}	(mg m ⁻² d ⁻¹)	convective flux in the liquid phase
$J_{Dl,g}$	(mg m ⁻² d ⁻¹)	diffusion flux in the liquid and gaseous phase
J_L	(mg d ⁻¹)	penetration flux through the cuticular plant membrane
J_v	(mg m ⁻² d ⁻¹)	diffusive flux through the interface at the soil surface
K	(mm d ⁻¹)	unsaturated hydraulic conductivity
K_c	(-)	specific crop coefficient

Appendix A – List of Symbols

K_{Cb}	(-)	basal crop coefficient
K_{Cmax}	(-)	maximum crop coefficient
K_d	($\text{dm}^3 \text{kg}^{-1}$)	distribution coefficient between solid and liquid phase
K_e	(-)	soil water evaporation coefficient
K_f	($\text{dm}^3 \text{kg}^{-1}$)	Freundlich coefficient
K_{f-de}	($\text{dm}^3 \text{kg}^{-1}$)	Freundlich desorption coefficient
K_{fOC}	($\text{dm}^3 \text{kg}^{-1}$)	Freundlich carbon distribution coefficient
K_H	(-)	dimensionless Henry's Law constant
K_L	(-)	partitioning coefficient leaf tissue and phloem sap
K_{LW}	($\text{dm}^3 \text{kg}^{-1}$)	partitioning coefficient leaf tissue and water (xylem sap)
K_M	(mg dm^{-3})	Michaelis constant
K_{Morg}	(mg-C dm^{-3})	Michaelis constant for bioavailable organic carbon
K_{OC}	($\text{dm}^3 \text{kg}^{-1}$)	soil organic carbon distribution coefficient
K_{OW}	(-)	octanol-water partitioning coefficient
K_R	(-)	partitioning coefficient root tissue and phloem sap
K_{RW}	($\text{dm}^3 \text{kg}$)	partitioning coefficient root tissue and water
K_{sat}	(mm d^{-1})	saturated hydraulic conductivity
K_{soil}	(mm d^{-1})	diffusion mass transfer coefficient
K_{StW}	($\text{dm}^3 \text{kg}^{-1}$)	partitioning coefficient stem tissue and water (xylem sap)
k	(d^{-1})	rate constant of penetration
k_{avail}	(d^{-1})	mineralization rate of available carbon
k_{mic}	(d^{-1})	microbial degradation rate
k_{phot}	(d^{-1})	abiotic photolytic degradation rate
L	($\text{MJ m}^{-2} \text{mm}^{-1}$)	specific heat of evaporation
l	(mm)	depth of surface zone
LAI	($\text{m}^2 \text{m}^{-2}$)	leaf area index
$L_{pl.tissue}$	(kg kg^{-1})	lipid content of plant tissue
L_R	(mm)	total root length
M_t/M_0	(-)	pesticide fraction penetrated into the leaf to fraction applied on the leaf
m	(-)	empirical parameter of water retention function according to Brutsaert (1966)
n	(-)	empirical parameter of water retention function according to Brutsaert (1966)
N	(-)	n_{f-ad}/n_{f-de} proportion between Freundlich adsorption and desorption exponent
n_f	(-)	Freundlich exponent
PR	(mm)	precipitation
P	(mm d^{-1})	permeance
R_n	($\text{MJ m}^{-2} \text{d}^{-1}$)	net radiation at crop surface
R_{ns}	($\text{MJ m}^{-2} \text{d}^{-1}$)	short-wave radiation

Appendix A – List of Symbols

R_{nl}	(MJ m ⁻² d ⁻¹)	long-wave radiation
R_p^{day}	(mm d ⁻¹)	daily potential root water uptake
R_1	(mm)	root radius
R_2	(mm)	radius of zone of pesticide depletion around the root
rH	(%)	relative humidity
rHF	(-)	relative humidity factor
q	(mm d ⁻¹)	water flux density
q_{max}	(mm d ⁻¹)	maximal water flux from the top soil segment
q_{phloem}	(kg d ⁻¹)	phloem flux differentiated by subscripts
q_t	(mm d ⁻¹)	transpiration flux
τ	(-)	tortuosity factor
T	(°C)	actual temperature
T_{max}	(°C)	lethal temperature for microorganisms
T_{opt}	(°C)	optimal temperature of microbial growth
$\tau(\theta)$	(-)	tortuosity factor in water filled pore space
$\tau(\varepsilon)$	(-)	tortuosity factor in air filled pore space
TR_p^{day}	(mm d ⁻¹)	daily potential transpiration
$TSCF$	(-)	transpiration stream concentration factor
t	(d)	time
Δt	(d)	time step length
u_2	(m d ⁻¹)	wind speed at 2 m height
W	(kg)	weight of various plant tissues differentiated by subscripts
W_{dead}	(kg)	dead plant material
W_{old}	(kg)	plant weight at previous time step
ΔW	(mm)	change in soil water and interception storage
ΔW_{Bio}	(kg ha ⁻¹ d ⁻¹)	growth rate of total biomass
ΔW_L	(kg ha ⁻¹ d ⁻¹)	growth rate of leaf biomass
X	(µg-C µW ⁻¹)	coefficient of regression equation of Sparling (1981)
x	(-)	parameter describing microbial sensitivity to temperature increase
z	(mm)	vertical coordinate taken positively upward
Δz	(mm)	segment thickness
Δz_a	(mm)	thickness of stagnant atmospheric film
Δz_s	(mm)	thickness of surface soil film

Greek letters

α	(d ⁻¹)	phase transfer coefficient
α_w	(mm ⁻¹)	empirical parameter of the water retention function according to Brutsaert (1966)

Appendix A – List of Symbols

β	(-)	parameter describing flux direction
Γ	(hPa K ⁻¹)	psychometric constant
γ	(-)	yield coefficient
Δ	(hPa K ⁻¹)	derivative of saturated vapour pressure versus temperature
ε	(mm ³ mm ⁻³)	gas filled soil porosity
η	(mm ⁻¹)	depth constant
θ	(mm ³ mm ⁻³)	volumetric water content
θ_{crit}	(mm ³ mm ⁻³)	threshold water content of microbial growth
θ_{crit1}	(mm ³ mm ⁻³)	critical minimum water content of Weibull type function
θ_{crit2}	(mm ³ mm ⁻³)	critical maximum water content of Weibull type function
$\theta_{pl.tissue}$	(kg kg ⁻¹)	water content of plant tissue
θ_{res}	(mm ³ mm ⁻³)	residual water content
θ_{sat}	(mm ³ mm ⁻³)	saturated water content
λ	(mm)	dispersivity
λ	(d ⁻¹)	first-order metabolism rate coefficient in various plant compartments differentiated by subscripts
μ	(d ⁻¹)	specific growth rate of microbial biomass
μ_{max}	(d ⁻¹)	maximum specific growth rate of microbial biomass
μ_{org}	(d ⁻¹)	microbial growth rate on bioavailable carbon substrate
v	(mm d ⁻¹)	pore water velocity
ρ_{plants}	(plants m ⁻²)	plant density
$\rho_{pl.tissue}$	(kg dm ⁻³)	density of dry plant tissue
ρ_s	(kg dm ⁻³)	soil bulk density
ρ_w	(kg dm ⁻³)	water density
σ	(d ⁻¹)	microbial mortality rate
σ_g	(mm)	standard deviation of the geometric mean particle diameter
ϕ	(mg dm ⁻³ d ⁻¹)	sink-source term
ϕ_{deg}	(mg dm ⁻³ d ⁻¹)	sink term biodegradation
ϕ_{plant}	(mg dm ⁻³ d ⁻¹)	sink term plant uptake
ϕ_{sorb}	(mg dm ⁻³ d ⁻¹)	sink-source term kinetic sorption
ϕ_v	(mg dm ⁻³ d ⁻¹)	sink-term volatilisation
ϕ_w	(mm ³ mm ⁻³ d ⁻¹)	soil water extraction rate by plant roots

Subscripts

i, j, k		subscript index notations (with values of 1, 2, 3)
<i>F</i>		fruits
<i>L</i>		leaves
<i>Nod</i>		nodules
<i>R</i>		roots
<i>St</i>		stems

Appendix B – List of Variables

Xenobiotica.h				
X		means Xenobiotica and accordingly pesticide A,B,C,D or metabolites		
fXenoXFlux	float	solute flux accross soil segment at time step	mg m ⁻²	PXLAYER
fXenoXTotalConc	float	total pesticide amount in soil segment	mg m ⁻²	PXLAYER
fXenoXConc	float	pesticide concentration in soil solution of soil segment	g m ⁻³	PXLAYER
fXenoXConcOld	float	pesticide concentration in soil solution of soil segment at previous time step	g m ⁻³	PXLAYER
fXenoXAdsConc	float	pesticide concentration adsorbed to soil matrix in soil segment	mg kg ⁻¹	PXLAYER
fXenoXAdsConc2	float	pesticide concentration adsorbed to kinetic sites of soil matrix in soil segment	mg kg ⁻¹	PXLAYER
fXenoXGasConc	float	pesticide concentration in soil air of soil segment	g m ⁻³	PXLAYER
fXenoXPrecipConc	float	precipitated amount of pesticide in soil segment	mg m ⁻²	PXLAYER
fXenoXSinkAds	float	sink-source term kinetic sorption in soil segment	g m ⁻³ d ⁻¹	PXLAYER
fXenoXSinkDegr	float	sink term degradation in soil segment	g m ⁻³ d ⁻¹	PXLAYER
fXenoXSinkVola	float	sink term volatilisation in soilsegment	g m ⁻³ d ⁻¹	PXLAYER
fXenoXSinkPlant	float	sink term plant uptake in soil segment	g m ⁻³ d ⁻¹	PXLAYER
fXenoXVolaFlux	float	volatilisation flux of pesticide accross soil surface at time step	mg m ⁻²	PXLAYER
fXenoXConAdDes	float	flag for ad- or desorption Freundlich isotherm in soil segment dependent on solute flux at time step	mg m ⁻²	PXLAYER
fXenoXGasDiffCoef	float	diffusion coefficient in gaseous phase of soil segment	mm ² d ⁻¹	PXLAYER
fXenoXLiqDiffCoef	float	diffusion coefficient in liquid phase of soil segment	mm ² d ⁻¹	PXLAYER
fXenoXLiqDiffus	float	effective diffusion coefficient for plant model (without dispersion)	mm ² d ⁻¹	PXLAYER
fXenoXMicBioConc	float	microbial biomass concentration in soil segment	g m ⁻³	PXLAYER
fDOC	float	concentration of bioavailable dissolved organic carbon in soil segment	g m ⁻³	PXLAYER
iAppl	int	number of pesticide applications	-	PXPROFILE
fTime	float	time flag	day	PXPROFILE
fTimeDummy1,2,3	float	time flags for output	day	PXPROFILE
fDayAfterAppl	float	day after pesticide application	day	PXPROFILE
iOutputCommon	int	variable for numbering of common output variables	-	PXPROFILE

Appendix B – List of Variables

iOutputSolute	int	variable for numbering of pesticide output variables	-	PXPROFILE
abSolute_Out[]	Bool	flag for output of pesticide related variables	TRUE/ FALSE	PXPROFILE
abSolute_OutCommon[]	Bool	flag for output of common variables	TRUE/ FALSE	PXPROFILE
IStopPlantMeasurement	long	end time of import of plant measurements	DDMMYY	PXPROFILE
IStopWaterMeasurement	long	end time of import of water measurements	DDMMYY	PXPROFILE
ITimeAppl[]	long	date of pesticide application	DDMMYY	PXPROFILE
bApplication	Bool	flag for pesticide application	TRUE/ FALSE	PXPROFILE
bDegradationXenoX	Bool	flag for pesticide degradation	TRUE/ FALSE	PXPROFILE
bPlantUptakeRootXenoX	Bool	flag for pesticide uptake by plant roots	TRUE/ FALSE	PXPROFILE
bPlantUptakeLeavesXenoX	Bool	flag for pesticide uptake by plant leaves	TRUE/ FALSE	PXPROFILE
fXenoXDummySurf[]	float	applied pesticide amount at application day i	kg ha ⁻¹	PXPROFILE
fXenoXSurf	float	applied pesticide amount on soil/plant surface	kg ha ⁻¹	PXPROFILE
fXenoXLeachDay	float	amount of pesticide leachate per day	mg m ⁻²	PXPROFILE
fXenoXLeachCum	float	cumulative amount of pesticide leachate	mg m ⁻²	PXPROFILE
fXenoXSinkSumDegr	float	cumulative pesticide degradation amount	mg m ⁻²	PXPROFILE
fXenoXSinkSumVola	float	cumulative volatilisation amount	mg m ⁻²	PXPROFILE
fXenoXSinkSumPlant	float	cumulative pesticide uptake by plant root	mg m ⁻²	PXPROFILE
fXenoXBalancePlant	float	mass balance plant for pesticide uptake from soil	mg m ⁻²	PXPROFILE
afXenoGDIF[]	float	molecular diffusion coefficient in air	mm ² d ⁻¹	PXPARAM
afXenoMolDiffCoef[]	float	molecular diffusion coefficient in water	mm ² d ⁻¹	PXPARAM
afXenoMolWeight[]	float	molar weight	g mol ⁻¹	PXPARAM
ilsothermX	int	coefficient of Linear (1) or Freundlich (2) adsorption isotherm	-	PXPARAM
fKhXenoX	float	dimensionless Henry's Law constant	-	PXPARAM
afKdXenoX[]	float	Kd-value of pesticide X in layer i (linear adsorption)	dm ³ kg ⁻¹	PXPARAM
afScFrac[]	float	fraction of equilibrium sites	-	PXPARAM
afFreundKdXenoX[]	float	Kf-value of pesticide X in layer i (Freundlich isotherm)	dm ³ kg ⁻¹	PXPARAM
afFreundExpXenoX[]	float	Freundlich exponent of pesticide X in layer i	-	PXPARAM
afAdsDesRatioXenoX[]	float	proportion between Freundlich adsorption and desorption exponent in layer i	-	PXPARAM

Appendix B – List of Variables

fXenoXSolub	float	solubility of pesticide X in water	g m^{-3}	PXPARAM
afLogOctWatCoef[]	float	log of octanol-water partitioning coefficient	-	PXPARAM
fXenoXPhotoDegR	float	abiotic photolytic degradation rate of pesticide X	d^{-1}	PXPARAM
fXenoBioMaxGrowR	float	maximum specific growth rate of microbial biomass	d^{-1}	PXPARAM
fXenoBioGrowR	float	specific growth rate of microbial biomass	d^{-1}	PXPARAM
fXenoMicBioMin	float	minimum microbial biomass concentration	g m^{-3}	PXPARAM
fXenoMicBioMax	float	maximum microbial biomass concentration	g m^{-3}	PXPARAM
fXenoMicBioIni	float	initial microbial biomass concentration	g m^{-3}	PXPARAM
fXenoHalfSat	float	half-saturation growth constant or Michaelis constant	g m^{-3}	PXPARAM
fXenoMaintCoeff	float	microbial mortality rate	d^{-1}	PXPARAM
fXenoXYieldCoeff	float	pesticide yield coefficient	-	PXPARAM
iXenoALinkXenoB	int	link between transformation chain	-	PXPARAM
fRootRadius	float	root radius	mm	PXPARAM
fStemDensity	float	density of dry stem tissue	kg m^{-3}	PXPARAM
fLeafDensity	float	density of dry leaf tissue	kg m^{-3}	PXPARAM
fRootWaterCont	float	water content of root biomass	-	PXPARAM
fStemWaterCont	float	water content of stem biomass	-	PXPARAM
fLeafWaterCont	float	water content of leaf biomass	-	PXPARAM
fFruitWaterCont	float	water content of fruit biomass	-	PXPARAM
fRootLipidCont	float	lipid content of root biomass	-	PXPARAM
fStemLipidCont	float	lipid content of stem biomass	-	PXPARAM
fLeafLipidCont	float	lipid content of leaf biomass	-	PXPARAM
fFruitLipidCont	float	lipid content of fruit biomass	-	PXPARAM
afPermCoefXenoX[]	float	permeance	m d^{-1}	PXPARAM
fDispersivity	float	dispersivity	mm	PXPARAM
fXenoXPlantSurfaceConc	float	pesticide concentration on plant surface	g m^{-3}	PXPLANT
fXenoXAvailSurfaceConc	float	available pesticide concentration for plant uptake	g m^{-3}	PXPLANT
fRootLengthTotal	float	total root length per plant	mm	PXPLANT

Appendix B – List of Variables

fCanopyClosure	float	soil cover fraction	–	PXPLANT
fRootXenoXConc	float	pesticide concentration in root biomass	g kg ⁻¹	PXPLANT
fNoduleXenoXConc	float	pesticide concentration in nodule biomass	g kg ⁻¹	PXPLANT
fStemXenoXConc	float	pesticide concentration in stem biomass	g kg ⁻¹	PXPLANT
fLeafXenoXConc	float	pesticide concentration in leaf biomass	g kg ⁻¹	PXPLANT
fFruitXenoXConc	float	pesticide concentration in fruit biomass	g kg ⁻¹	PXPLANT
fAirXenoXConc	float	pesticide concentration in air-plant interface	g m ⁻³	PXPLANT
fRootXenoXInc	float	incorporated pesticide amount by plant root (per plant)	g d ⁻¹	PXPLANT
fDeadRootXenoXInc	float	cumulative pesticide amount incorporated in dead root biomass per area	g m ⁻²	PXPLANT
fRootXenoXIncTotal	float	cumulative incorporated pesticide amount in root biomass (per plant)	g	PXPLANT
fRootXenoXIncMax	float	maximum possible pesticide uptake by plant root (per plant)	g d ⁻¹	PXPLANT
fNoduleXenoXIncTotal	float	cumulative incorporated pesticide amount in nodule biomass (per plant)	g	PXPLANT
fStemXenoXInc	float	incorporated pesticide amount in stem biomass (per plant)	g d ⁻¹	PXPLANT
fDeadStemXenoXInc	float	cumulative pesticide amount incorporated in dead stem biomass per area	g m ⁻²	PXPLANT
fStemXenoXIncTotal	float	cumulative incorporated pesticide amount in stem biomass (per plant)	g	PXPLANT
fLeafXenoXInc	float	incorporated pesticide amount in leaf biomass (per plant)	g d ⁻¹	PXPLANT
fDeadLeafXenoXInc	float	cumulative pesticide amount incorporated in dead leaf biomass per area	g m ⁻²	PXPLANT
fLeafXenoXIncTotal	float	cumulative incorporated pesticide amount in leaf biomass (per plant)	g	PXPLANT
fFruitXenoXIncTotal	float	cumulative incorporated pesticide amount in fruit biomass (per plant)	g	PXPLANT
fDeadFruitXenoXInc	float	cumulative pesticide amount incorporated in dead fruit biomass per area	g m ⁻²	PXPLANT
fXenoXPlantDegradR	float	first-order metabolism rate in plants	d ⁻¹	PXPLANT
fRootWeightOld	float	root weight at previous time step	kg ha ⁻¹	PXPLANT
fStemWeightOld	float	stem weight at previous time step	kg ha ⁻¹	PXPLANT
fLeafWeightOld	float	leaf weight at previous time step	kg ha ⁻¹	PXPLANT
fFruitWeightOld	float	fruit weight at previous time step	kg ha ⁻¹	PXPLANT
fNoduleWeight	float	nodule weight	kg ha ⁻¹	PXPLANT
bRoot	Bool	flag for root growth	TRUE/ FALSE	PXPLANT
fXenoXSinkSumCultivar	float	cumulative pesticide uptake by plant root in actual crop	mg m ⁻²	PXPLANT
fPermeabilityXenoX	float	actual permeance	m d ⁻¹	PXPLANT

Appendix B – List of Variables

acSolute_OutCommonText	char	text variable for legend of common output	PSOLUTESCENARIO
acSolute_OutSolText[]	char	text variable for legend of pesticide output	PSOLUTESCENARIO

Appendix C – Pesticide input file

```

*****
XENOBIOTICA (PESTICIDE) INPUT DATA FILE
*****

*****
INITIAL PROFILE XENOBIOTICA DATA
*****
-----
Soil      XenoA      XenoB      XenoC      XenoD
layer
-----
          ----- mg/m^2 -----
-----
1000001 18
1         0.0         0.0         0.0         0.0
2         0.0         0.0         0.0         0.0
3         0.0         0.0         0.0         0.0
4         0.0         0.0         0.0         0.0
5         0.0         0.0         0.0         0.0
6         0.0         0.0         0.0         0.0
7         0.0         0.0         0.0         0.0
8         0.0         0.0         0.0         0.0
9         0.0         0.0         0.0         0.0
10        0.0         0.0         0.0         0.0
11        0.0         0.0         0.0         0.0
12        0.0         0.0         0.0         0.0
13        0.0         0.0         0.0         0.0
14        0.0         0.0         0.0         0.0
15        0.0         0.0         0.0         0.0
16        0.0         0.0         0.0         0.0
17        0.0         0.0         0.0         0.0
18        0.0         0.0         0.0         0.0
19        0.0         0.0         0.0         0.0
20        0.0         0.0         0.0         0.0
-----
Concentration (mg/l) below profile
1000002 1
1         0.0         0.0         0.0         0.0

*****
XENOBIOTICA PROPERTIES
*****
-----
Xeno  Name      Mol.weight  log Kow    Solubility  Vapour.Dens.
      (g/mol)   (-)        (g/m^3)    (Pa)
-----
1000003 3
A 'Isoproturon' 206.3      2.5        0.702e02   0.28e-05
B 'Glyphosate'  169.0      -3.2       0.105e05   1.31e-05
C 'Tracer D20'  18.015     0.0        10.000e05  0.0
D 'Not specified' 0.0        0.0        0.0        0.0

      Degradation      Plant Uptake
      1(yes),0(no)     Root  Leaves 1(yes),0(no)
-----
A         1           1      0
B         1           0      1
C         0           0      0
D         0           0      0

```

Appendix C – Pesticide input file

Xeno	Molecular diffusion coefficient		Henry constant
	in water (mm ² /day)	in air (mm ² /day)	(~VapourDensity/Solubility) (-)
1000004	3		
A	68.056	0.6558e06	3.378e-09
B	75.193	0.7245e06	8.655e-11
C	198.72	0.7245e06	1.856e-05
D	0.0	0.0	0.0

Xeno	Adsorption		Linear isotherm two-site model	
	Linear(1) or Freundlich(2)		f	alpha
1000005	2			
A	2		1.0	0.0
B	1		1.0	0.693
C	1		1.0	0.0
D	1		1.0	0.0

Soil horizon	Kd-Value linear adsorption (dm ³ /kg)				Ad-/Desorption ratio Freundlich (-)			
	A	B	C	D	A	B	C	D
1000006	4							
1	0.0	12.40	0.0	0.0	0.538	0.0	0.0	0.0
2	0.0	7.83	0.0	0.0	0.538	0.0	0.0	0.0
3	0.0	3.92	0.0	0.0	0.538	0.0	0.0	0.0
4	0.0	1.17	0.0	0.0	0.538	0.0	0.0	0.0

Soil horizon	Kf-Value Freundlich (dm ³ /kg)				Freundlich exponent (-)			
	A	B	C	D	A	B	C	D
1000007	4							
1	1.71	0.0	0.0	0.0	0.91	0.0	0.0	0.0
2	1.71	0.0	0.0	0.0	0.91	0.0	0.0	0.0
3	1.71	0.0	0.0	0.0	0.91	0.0	0.0	0.0
4	1.71	0.0	0.0	0.0	0.91	0.0	0.0	0.0

XENOBIOTICA APPLICATIONS

Date	Incorporation segments	XenoA	XenoB	XenoC	XenoD
(kg/ha)					
1000008	3				
150704	1	0.0	1.10	0.0	0.0
240505	1	0.0	0.90	0.0	0.0
060905	1	0.0	1.10	0.0	0.0

Appendix C – Pesticide input file

XENOBIOTICA DEGRADATION

Parameters for microbial biomass and biodegradation

	initial biom. (g-C/m ³)	max.biom. (g-C/m ³)	min.biom. (g-C/m ³)	max.growthrate (day ⁻¹)
--	--	------------------------------------	------------------------------------	--

1000009 1	303	3030	303	0.207
-----------	-----	------	-----	-------

maintenance coeff.
(day⁻¹)

0.080

	yield coefficient (-)(must be >0)				half saturation (g/m ³)
	XenoA	XenoB	XenoC	XenoD	

1000010 1	1.0	0.23	1.0	1.0	1.87
-----------	-----	------	-----	-----	------

Transformation Chain (link)
XenoA-XenoB XenoB-XenoC XenoC-XenoD

1000011 1		0	0	0
-----------	--	---	---	---

The values above determine which species form a transformation chain.
Setting link = 0 breaks the pathway, link = 1 restores it.

Parameter for soil photolysis (only used in first layer)

layer no.	photolytic degradation rate (day ⁻¹)			
	XenoA	XenoB	XenoC	XenoD

1000012 1	0.0	0.0	0.0	0.0
-----------	-----	-----	-----	-----

CROP DATA

Plant	Root radius (mm)	Stem density (kg/m ³)	Leaf density (kg/m ³)
-------	---------------------	--------------------------------------	--------------------------------------

1000013 1	2.0	920.0	750.0
-----------	-----	-------	-------

Content (%)	Root	Stem	Leaf	Fruit
-------------	------	------	------	-------

1000014 1				
Water	94.2	76.7	76.7	72.3
Lipid	0.3	0.5	0.5	0.3

Appendix C – Pesticide input file

```
-----  
                          Permeability coefficient leaf  
                          (m/d)  
-----  
1000015 2                XenoA      XenoB      XenoC      XenoD  
1stday                   0.0        1.01e-05   0.0        0.0  
dayafter1st              0.0        2.92e-07   0.0        0.0  
  
*****  
*****
```

Appendix D – Input file for variable selection

List of variables: XENO OUTPUT

x Or X denotes variable output

- denotes no output

Caution: if no variable name is given no variable output is possible

```
1000001 (-) XenoA:Total_Amount(layerdependent)[mg/m2]
1000002 (-) XenoA:Solute_Concentration(layerdependent)[g/m3]
1000003 (-) XenoA:Adsorbed_Concentration(layerdependent)[g/m3]
1000004 (-) XenoA:Kinetically_Adsorbed_Concentration(layerdependent)[g/m3]
1000005 (-) XenoA:Gaseous_Concentration(layerdependent)[g/m3]
1000006 (-) XenoA:Leachate_Amount[mg/m2]
1000007 (-) XenoA:Sink_Biodegradation[mg/m2]
1000008 (-) XenoA:Sink_Volatilisation[mg/m2]
1000009 (-) XenoA:Sink_Plant[mg/m2]
1000010 (-) XenoA:Root_Concentration[g/kg]
1000011 (-) XenoA:Stem_Concentration[g/kg]
1000012 (-) XenoA:Leaf_Concentration[g/kg]
1000013 (-) XenoA:Fruit_Concentration[g/kg]
1000014 (x) Plant_RootWeight[kg/ha]
1000015 (x) Plant_StemWeight[kg/ha]
1000016 (x) Plant_LeafWeight[kg/ha]
1000017 (-) Plant_FruitWeight[kg/ha]
1000018 (-) Plant_Water_uptake(layerdependent)[mm/day]
1000019 (-) PlantHeight[cm]
1000020 (-) XenoA:BalancePlant[mg/m2]
1000021 (-) XenoB:Total_Amount(layerdependent)[mg/m2]
1000022 (-) XenoB:Solute_Concentration(layerdependent)[g/m3]
1000023 (-) XenoB:Adsorbed_Concentration(layerdependent)[g/m3]
1000024 (-) XenoB:Kinetically_Adsorbed_Concentration(layerdependent)[g/m3]
1000025 (-) XenoB:Gaseous_Concentration(layerdependent)[g/m3]
1000026 (x) XenoB:Leachate_Amount[mg/m2]
1000027 (x) XenoB:Sink_Biodegradation[mg/m2]
1000028 (x) XenoB:Sink_Volatilisation[mg/m2]
1000029 (-) XenoB:Sink_Plant[mg/m2]
1000030 (x) XenoB:Root_Concentration[g/kg]
1000031 (x) XenoB:Stem_Concentration[g/kg]
1000032 (x) XenoB:Leaf_Concentration[g/kg]
1000033 (-) XenoB:Fruit_Concentration[g/kg]
1000034 (x) XenoB:Microbial_Biomass_Concentration[g/m3]
1000035 (-) XenoB:LeafIncorporation[g/d]
1000036 (x) XenoB:Nodule_Concentration[g/kg]
1000037 (x) NoduleWeight[Kg/ha]
1000038 (-)
1000039 (-)
1000040 (-)
1000041 (-) XenoC:Total_Amount(layerdependent)[mg/m2]
1000042 (-) XenoC:Solute_Concentration(layerdependent)[g/m3]
1000043 (-) XenoC:Adsorbed_Concentration(layerdependent)[g/m3]
1000044 (-) XenoC:Kinetically_Adsorbed_Concentration(layerdependent)[g/m3]
1000045 (-) XenoC:Gaseous_Concentration(layerdependent)[g/m3]
1000046 (-) XenoC:Leachate_Amount[mg/m2]
1000047 (-) XenoC:Sink_Biodegradation[mg/m2]
1000048 (-) XenoC:Sink_Volatilisation[mg/m2]
1000049 (-) XenoC:Sink_Plant[mg/m2]
1000050 (-) XenoC:Root_Concentration[g/kg]
1000051 (-) XenoC:Stem_Concentration[g/kg]
1000052 (-) XenoC:Leaf_Concentration[g/kg]
1000053 (-) XenoC:Fruit_Concentration[g/kg]
```

Appendix D – Input file for variable selection

1000054 (-)
1000055 (-)
1000056 (-)
1000057 (-)
1000058 (-)
1000059 (-)
1000060 (-)
1000061 (-) XenoD:Total_Amount(layerdependent)[mg/m2]
1000062 (-) XenoD:Solute_Concentration(layerdependent)[g/m3]
1000063 (-) XenoD:Adsorbed_Concentration(layerdependent)[g/m3]
1000064 (-) XenoD:Kinetically_Adsorbed_Concentration(layerdependent)[g/m3]
1000065 (-) XenoD:Gaseous_Concentration(layerdependent)[g/m3]
1000066 (-) XenoD:Leachate_Amount[mg/m2]
1000067 (-) XenoD:Sink_Biodegradation[mg/m2]
1000068 (-) XenoD:Sink_Volatilisation[mg/m2]
1000069 (-) XenoD:Sink_Plant[mg/m2]
1000070 (-) XenoD:Root_Concentration[g/kg]
1000071 (-) XenoD:Stem_Concentration[g/kg]
1000072 (-) XenoD:Leaf_Concentration[g/kg]
1000073 (-) XenoD:Fruit_Concentration[g/kg]
1000074 (-)
1000075 (-)
1000076 (-)
1000077 (-)
1000078 (-)
1000079 (-)
1000080 (-)

Appendix E – Pesticide output file

EXPERT-N : XENO Result File.

----> userdefined <----

Date: 11/15/06

Time: 16:36:24

- (1) Plant_RootWeight[kg/ha]
- (2) Plant_StemWeight[kg/ha]
- (3) Plant_LeafWeight[kg/ha]
- (4) XenoB:Leachate_Amount[mg/m2]
- (5) XenoB:Sink_Biodegradation[mg/m2]
- (6) XenoB:Sink_Volatilisation[mg/m2]
- (7) XenoB:Root_Concentration[g/kg]
- (8) XenoB:Stem_Concentration[g/kg]
- (9) XenoB:Leaf_Concentration[g/kg]
- (10) XenoB:Microbial_Biomass_Concentration[g/m3]
- (11) XenoB:Nodule_Concentration[g/kg]
- (12) NoduleWeight[Kg/ha]

SimDay	Date	(1)	(2)	(3)	(4)	(5)	(6)	(7)	(8)	(9)	(10)	(11)	(12)
563.	160704	606.4	273.3	458.4	0.	1.028	0.	6.935e-003	8.452e-003	0.2235	317.2	3.011e-004	181.9
564.	170704	669.3	308.7	511.8	0.	2.126	0.	2.45e-002	3.05e-002	0.1666	329.9	3.896e-003	200.8
565.	180704	736.9	347.5	569.8	0.	3.241	0.	3.49e-002	4.457e-002	0.1252	342.	1.028e-002	221.1
566.	190704	803.2	386.7	627.4	0.	4.366	0.	4.051e-002	5.32e-002	9.632e-002	353.	1.781e-002	241.
567.	200704	876.7	431.2	692.	0.	5.491	0.	4.228e-002	5.682e-002	7.632e-002	363.6	2.441e-002	263.
568.	210704	952.2	478.	759.1	0.	6.718	0.	4.261e-002	5.88e-002	6.099e-002	373.6	3.106e-002	285.6
569.	220704	1030	527.7	829.3	0.	7.869	0.	4.171e-002	5.896e-002	4.997e-002	382.5	3.662e-002	309.1
570.	230704	1104	576.	896.5	0.	9.123	0.	4.032e-002	5.846e-002	3.888e-002	390.7	4.162e-002	331.2
571.	240704	1138	598.5	927.4	0.	10.36	0.	3.979e-002	5.952e-002	3.227e-002	398.	4.694e-002	341.3
572.	250704	1213	650.	997.5	0.	11.69	0.	3.746e-002	5.602e-002	2.802e-002	402.4	4.678e-002	363.9
573.	260704	1258	681.3	1040	0.	12.97	0.	3.621e-002	5.565e-002	2.332e-002	406.1	5.066e-002	377.4
574.	270704	1322	726.1	1099	0.	14.12	0.	3.441e-002	5.331e-002	2.03e-002	407.3	5.13e-002	396.5
575.	280704	1392	776.3	1166	0.	15.13	0.	3.248e-002	5.11e-002	1.715e-002	407.5	5.256e-002	417.6
576.	290704	1466	829.5	1237	0.	16.12	0.	3.056e-002	4.891e-002	1.441e-002	407.9	5.375e-002	439.8